ZooKeys 830: 1–31 (2019)
doi: 10.3897/zookeys.830.31433
http://zookeys.pensoft.net

RESEARCH ARTICLE

A peer-reviewed open-access journal
ZooKeys
Launched to accelerate biodiversity research

The first Paratropididae (Araneae, Mygalomorphae) from Colombia: new genus, species and records

Carlos Perafán[1], William Galvis[2], Fernando Pérez-Miles[1]

1 *Sección Entomología, Facultad de Ciencias, Universidad de La República, Iguá 4225, Montevideo, Uruguay*
2 *Laboratorio de Aracnología & Miriapodología (LAM-UN), Instituto de Ciencias Naturales, Universidad Nacional de Colombia, Bogotá, Colombia*

Corresponding author: *Carlos Perafán* (caperafanl@gmail.com)

Academic editor: *C. Hamilton* | Received 6 November 2018 | Accepted 19 January 2019 | Published 14 March 2019

http://zoobank.org/2A84BECF-E531-4942-AA5C-2E476BBE310E

Citation: Perafán C, Galvis W, Pérez-Miles F (2019) The first Paratropididae (Araneae, Mygalomorphae) from Colombia: new genus, species and records. ZooKeys 830: 1–31. https://doi.org/10.3897/zookeys.830.31433

Abstract

The family of mygalomorph spiders Paratropididae Simon, 1889 is here reported for the first time for Colombia, where it is represented by three genera (*Anisaspis*, *Paratropis*, *Stormtropis* **gen. n.**) and eight species. One genus, *Stormtropis*, and six species constitute new taxa that are here diagnosed, described and illustrated. The geographical distribution of *Paratropis papilligera* FO Pickard-Cambridge, 1896 and *Paratropis elicioi* Dupérré, 2015 are also redescribed and expanded on the basis of new material examined. The diagnosis of the subfamily Paratropidinae, *Paratropis* Simon, 1889 and *Anisaspis* Simon, 1892 are emended including the variations of the new species. Likewise, a geographic distribution map for the entire family and a taxonomic key for the males of Paratropidinae are included. Other biogeographic, morphological, and taxonomic aspects are discussed.

Keywords

Andean Region, bald legged spiders, Ecuador, Neotropics, new genus, new species

Introduction

Paratropididae Simon, 1889, known as bald legged spiders, is one of the most enigmatic groups of Mygalomorphae due to its cryptic habits, singular biology, and controversial phylogenetic position. Paratropidids constitute a small family of spiders, currently comprising four genera and eleven species, distributed in Mexico, Central America, Lesser Antilles, and northern South America except Colombia (Raven 1985, WSC

2018). Their presence in Venezuela, Mexico, and Ecuador has been recently reported by Bertani (2013), Valdez-Mondragón et al. (2014) and Dupérré (2015), respectively. Paratropidids are cursorial, medium to small-sized mygalomorphs, which hide themselves in the surface layers of the soil (West in Raven 1999); found in leaf litter and rotten logs, under rocks, moss, and burrows in ravines (personal observations). The main paratropidid morphological characteristic is the presence of a scaly cuticle adapted to adhere to soil particles (Raven 1985, Jocqué and Dippenaar-Schoeman 2006).

Formerly, Paratropididae was considered the sister-group of Theraphosidae into Theraphosoidea, and this group was related with Barychelidae in Theraphosoidina (Raven 1985, Goloboff 1993). However, results of some molecular and total evidence studies suggest a distant phylogenetic relationship of Paratropididae with the Theraphosoidina clade, not closely related with Theraphosidae or Barychelidae (Bond and Hedin 2006, Bond et al. 2012). Conversely, in recent studies, Paratropididae was recovered as sister group of some ctenizids (Wheeler et al. 2017), or some nemesiids (Garrison et al. 2016); although, both studies pointing out this position as questionable. Likewise, in Fernandez et al. (2018) Paratropididae was resolved as a sister group of *Macrothele* (Macrothelidae), but this study focused in Araneomorphae, and mygalomorph sampling was very limited. Hamilton et al. (2016) recovered Paratropididae as the sister group to all other Avicularioidea taxa, with the exception of *Bymainiella* sp. (Hexathelidae); this grouping was followed by Hedin et al. (2018).

Paratropidids are characterized by the soil encrusted or scaly cuticle, weakly or ascopulate tarsi I and II and absence of scopulae elsewhere, maxillary lobes elongated, and the presence of labial cuspules usually arranged in an anterior rectangular group (Raven 1985). Pérez-Miles et al. (2017) found that the putative scopula of paratropidids was in fact a pseudoscopula, constituted of chemosensory not-adhesive setae. The family comprises two subfamilies, Paratropidinae Simon, 1889 and Glabropelmatinae Raven, 1985. Paratropidinae is characterized by a long single tooth on the superior tarsal claws, the steeply elevated eye tubercle, very long anterior maxillary lobes, and absence of a tibial apophysis and claw tufts, unlike Glabropelmatinae that has thin claw tufts (without scopula), a bifurcated tibial apophysis, a typical elevated eye tubercle, and shorter anterior maxillary lobes (Raven 1985).

Paratropidinae includes three genera, *Paratropis* Simon, 1889 with six species, distributed in Mexico, Venezuela, Brazil and Peru; *Anisaspis* Simon, 1892 with one species from Saint Vincent island; and *Anisaspoides* FO Pickard-Cambridge, 1896 with one species from Brazil. *Anisaspis* and *Anisaspoides* are only known by females. Glabropelmatinae includes only one genus *Melloina* Brignoli, 1985, with three species, distributed in Venezuela and Panama (WSC 2018).

Two characteristics have been important in Paratropidinae taxonomy, the number of spinnerets, four (*Paratropis*) or two (*Anisaspis*, *Anisaspoides*), and the presence of a third tarsal claw, only on leg I (most *Paratropis*), only on legs I and II (*Anisaspoides*), or absent (*Anisaspis*) (Raven 1985, Pickard-Cambridge 1896, Valdez-Mondragón et al. 2014).

The presence of Paratropididae in Colombia was informally indicated by de Mello-Leitão (1941) and in unpublished studies (Flórez-D. and Sánchez-C. 1995, Perafán et al. 2013); however, this is the first formal report for the country. A review of myga-

lomorph spiders from Colombia including field and collection data produced some important results for Paratropididae, which we present here: a new genus, *Stormtropis* gen. n., with four new species; a new species of *Anisaspis*, which represent the first male description for the genus and the first record for South America; one new species of *Paratropis*; and a new record of *P. papilligera* FO Pickard-Cambridge, 1896 and *P. elicioi* Duperré, 2015. We discuss the geographic distribution and diversity of paratropidids as well as some biological and morphological characteristics.

Materials and methods

The general description format follows Raven (1999) and Bertani (2013), with modifications. Specimens were examined using an Advanced Optical stereomicroscope. Photographs were taken with an Olympus LC30 camera adapted to a stereomicroscope. All measurements are in millimeters and were taken with an ocular micrometer. Legs and palp measurements were taken along a dorsal longitudinal line of the left side. Total body length excludes chelicerae and spinnerets. Spination: we consider as spines the thick, sclerotized setae, with acute and non-translucent apex; similar setae but with translucent apex were not counted. Male palpal bulbs (usually left) were removed from cymbium for study and illustrations. Records without geographic coordinates were determined using GoogleMaps and the gazetteers GeoLocator and GeoNames. The distribution map was produced using the Geographic Information System QGIS 'Girona' (version 3.0, QGIS team, www.qgis.org), with raster files from NaturalEarth and DivaGis. WSC means World Spider Catalog.

Abbreviations in figures or text are as follows:

ALE anterior lateral eyes;
AME anterior median eyes;
fe femur;
ITC inferior tarsal claw;
me metatarsus;
p prolateral;
pa patella;
pd prolatero-dorsal;
PME posterior median eyes;
PMS posterior median spinnerets;
PLE posterior lateral eyes;
PLS posterior lateral spinnerets;
pv prolatero-ventral;
r retrolateral;
rv retrolatero-ventral;
STC superior tarsal claw;
ta tarsus;
ti tibia.

Examined materials are deposited in the following institutions:

BMNH (NHM) Natural History Museum, London;
ICN Instituto de Ciencias Naturales, Universidad Nacional de Colombia, Bogotá;
FC-My Facultad de Ciencias, Universidad de la República, Montevideo, Uruguay;
QCAZ Quito-Católica-Zoología, Museo de Zoología, Pontificia Universidad Católica del Ecuador.

Taxonomy

Family Paratropididae Simon, 1889
Subfamily Paratropidinae Simon, 1889

Emended diagnosis. Paratropidinae spiders differ from those of Glabropelmatinae (that includes only the genus *Melloina* Brignoli, 1985) by the absence of claw tufts, presence of a single long tooth on the superior tarsal claws (STC), the steeply elevated eye tubercle, and the book lung apertures projected, oval and sclerotized. Males without tibial apophysis (*Anisaspis*, *Paratropis* and *S. muisca* sp. n.) or composed by a single prolateral branch (*Stormtropis* gen. n., except *S. muisca* sp. n.). *Anisaspoides* males are still unknown.

Included genera. *Anisaspis* Simon, 1892, *Anisaspoides* FO Pickard-Cambridge, 1896, *Paratropis* Simon, 1889 and *Stormtropis* Perafán, Galvis and Pérez-Miles gen. n.

Identification key to males of Paratropidinae species

1 One pair of spinnerets (PLS) (Figure 1B) and all legs with only two tarsal claws (only STC) ..... ***Anisaspis camarita* sp. n.**

– Two pairs of spinnerets (PMS and PLS), legs with or without inferior tarsal claw (ITC) **2**

2 Palpal bulb with embolus relatively straight, thin and elongated. Leg I without tibial apophysis ..... **3** ***Paratropis***

– Palpal bulb pyriform elongated, embolus slightly curved tapering to the apex and with a subapical triangular tooth. Leg I with or without tibial apophysis ... . **5** ***Stormtropis* gen. n.**

3 Palpal bulb with short embolus and slightly sigmoid (Valdez-Mondragón et al. 2014, figs 10–15) ..... ***Paratropis tuxtlensis***

– Palpal bulb with large embolus **4**

4 Palpal bulb with very long and straight embolus (Figure 2E, F), tibia I without basal retrolateral conic process ..... ***Paratropis elicioi***

– Palpal bulb with very thin and long embolus, distally curved (Figure 4F, G), and tibia I with a basal retrolateral conic process with spiniform setae (Figure 4D, E) ..... ***Paratropis papilligera***

5 Leg I without tibial apophysis. Palpal bulb as Figure 6D, E .... ***Stormtropis muisca* sp. n.**

– Leg I with tibial apophysis **6**

6 Discontinuous row and few cheliceral teeth on promargin (2-2-3) (Figure 9B), tibial apophysis with a long base and separated from the tibia and with few spines (Figure 9D, E) ..... ***Stormtropis parvum* sp. n.**

– Continuous row and numerous cheliceral teeth on promargin, tibial apophysis with a short base and with many spines **7**

7 Tibial apophysis with numerous spines on the proximal row (12) (Figure 7D, E); presence of a sclerotized dark mark on proximal dorsal tibia, with a slight excavation (Figure 7A) ..... ***Stormtropis paisa* sp. n.**

– Tibial apophysis with less spines on the proximal row (6) (Figure 5D, E); without sclerotized dark mark on tibia (Figure 5A) .... ***Stormtropis colima* sp. n.**

***Anisaspis* Simon, 1891**
Figure 1

Type species. *Anisaspis tuberculata* Simon, 1892, deposited in NHM, examined.

Diagnosis. *Anisaspis* differs from other paratropidid genera by the presence of only two spinnerets (PLS) (Figure 1D) and all legs with only two tarsal claws (STC), males without tibial apophysis and palpal bulb with sinuous embolus (Figure 1E, F). PLS relatively long (Figure 1A, B). Females remain unknown.

Remarks. The specimen described as holotype female of *A. tuberculata* is actually a juvenile specimen. Therefore, females of this genus remain unknown.

Included species. *Anisaspis tuberculata* Simon, 1892 and *Anisaspis camarita* Perafán, Galvis & Pérez-Miles, sp. n.

Distribution. Lesser Antilles, Saint Vincent island and Colombia, on the eastern flank of the Eastern Cordillera, Meta Department, Llanos foothills (Figure 10); from sea level to 570 m altitude.

***Anisaspis camarita* sp. n.**
http://zoobank.org/E0378E15-1F64-4F82-BE43-3305D962984C
Figure 1

Type material. ***Holotype*** male from Colombia, Meta, Villavicencio, Bosque de Bavaria, 4.18089N, 73.64800W, 570 m, 7-X-2005, col. HJ Salazar (ICN-Ar 1404).

Diagnosis. *Anisaspis camarita* sp. n. differs from *A. tuberculata* by the absence of a spine on dorsal tarsi distally, longer spinnerets (PLS) with apical segment digitiform (domed in *A. tuberculata*) (Figure 1A, B) and AME on a super-tubercle (another higher tubercle on the ocular tubercle, Figure 1D).

Description. ***Holotype male*** (ICN-Ar 1404) (Figure 1): total length 12.6; carapace length 6.0, width 6.5; abdomen length 5.8, width 3.4; chelicerae length 2.8. Color (in alcohol): body with soil particles encrusted; carapace, chelicerae, coxa, trochanter and femur dark reddish brown; abdomen dorsally and patella-tarsus brown. Carapace: glabrous, striae conspicuous, lateral margins with single line of curved setae mixed with disperse clubbed setae; caput strongly arched, separated from thoracic region by transverse shallow fovea, straight, width 1.1 (Figure 1A). Eyes and ocular tubercle: tubercle length 1.0, width 1.0, very elevated (height 0.8) and forwardly directed, with few stout

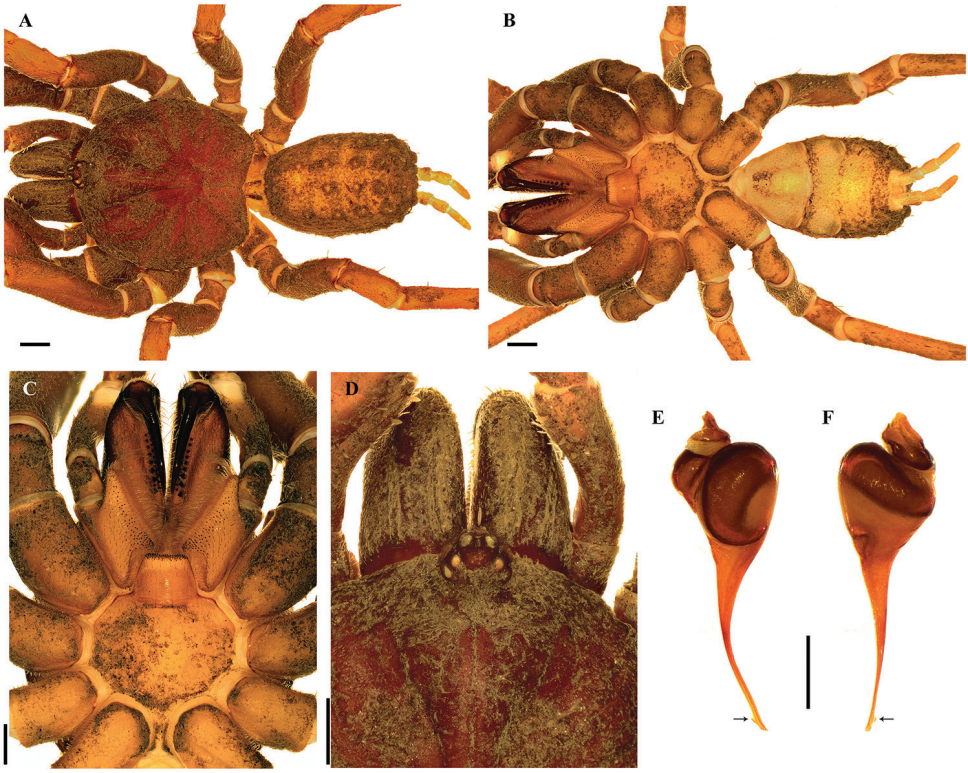

Figure 1. *Anisaspis camarita* sp. n., male. **A, B** *habitus* **A** dorsal view **B** ventral view **C** sternum, labium and maxillae **D** caput and ocular tubercle **E, F** palpal bulb **E** prolateral view **F** retrolateral view. Arrow points to the triangular tooth on the subapical region of the embolus. Scale bars: 1.0 mm (**A–D**); 0.5 mm (**E, F**).

setae. AME on a supertubercle (another higher tubercle on the ocular tubercle, Figure 1D). Clypeus absent. Anterior eye row slightly procurved, posterior recurved. Ocular sizes and interdistances: AME 0.25, ALE 0.30, PME 0.23, PLE 0.28, AME-AME 0.15, AME-ALE 0.05, PME-PME 0.48, PME-PLE 0.05, ALE-PLE 0.08, AME-PME 0.10, ALE-ALE 0.65, PLE-PLE 0.70. Chelicerae: short sparse bristles on dorsal and lateral areas, long fine bristles on ventral and anterior area. Rastellun absent. Cheliceral furrow with two rows of teeth well-developed, 12 and 9 teeth on promargin and retromargin, respectively. Fang long. Labium: length 0.7, width 0.9, with 77 cuspules on anterior edge (Figure 1C). Labio-sternal groove narrower in the middle than laterally. Maxillae longer than wide, with the anterior prolateral lobe very elongated, conical (Figure 1C); with 75/78 rounded cuspules spaced, largely spread over prolatero-ventral border from the inner edge to anterior lobe. Lyra absent. Sternum: length 2.5, width 3.4; three pairs of sigillae, anterior and median subcircular, posterior sigillae oval, all submarginal. Anterior half of sternum elevated (Figure 1C).

Legs: cuticle with soil particles encrusted. Leg and palpal segments measurements provided in Table 1. Leg I clearly thicker than the others. Bristles, plumose and thorn-like setae and spines evident. Trichobothria: filiform, on central 2/3 of tarsi, palp 5,

Table 1. Lengths (in mm) of legs and palpal segments of the holotype male *Anisaspis camarita* sp. n.

	I	II	III	IV	Palp
Femur	6.4	5.3	4.6	6.1	2.6
Patella	3.3	2.5	2.2	2.4	1.5
Tibia	6.0	4.2	3.4	5.1	1.9
Metatarsus	5.0	4.5	4.0	5.9	–
Tarsus	2.0	2.0	2.0	2.4	1.0
Total	22.7	18.5	16.2	21.9	7.0

leg I 8, II 7, III 6, IV 8; on distal 1/4 of metatarsi, legs I-III 4, IV 5; and on proximal 1/3 of tibiae, palp two rows of 3 each, legs I-III two rows of 4 each, IV two rows of 4 and 1 respectively. Scopula absent. Pseudoscopula weak and divided by conical longer setae, only present on distal tarsi I and II; tarsi III and IV with few sparse pseudoscopula setae. Claw tufts absent. Tarsal claws: ITC absent on all legs but a very small tooth present on right leg I in the same position of ITC; STC with one medial tooth on all legs. Tibial apophysis absent. Spination: principally thorn-like setae on all segments. Spines: palp and legs I-II 0; leg III, fe 0, pa 0, ti 0, me 1pd, 3v, ta 1p; leg IV, fe 0, pa 0, ti 0, me 2v, ta 1p.

Palp: cymbium with two unequal lobes separated by a sclerotized groove; tibia with shallow distoventral groove. Palpal bulb pyriform elongated; embolus curved, long, tapering to the apex, apex wide; a triangular translucent tooth on the subapical region, close to the apex (Figure 1E, F).

Abdomen: with four longitudinal dorsal rows of seven small tubercles, each emitting from its summit a plumose, bacilliform seta; lateral area finely tuberculate, with smaller plumose setae (Figure 1A). Book lung apertures projected, oval, sclerotized (Figure 1B). Spinnerets: PMS absent; PLS length 2.8, apical segment digitiform. Basal segment of PLS divided in two unequal cuticle plates (Figure 1B).

Female. Unknown.

Distribution. Only known from its type locality, in the foothills of the Eastern Cordillera of Colombian Andes (at 570 m altitude), Meta Department, Bavaria forest (Figure 10).

Etymology. The specific epithet *camarita* is a noun in apposition which means friend, in the colloquial way of the Llanos Region of Colombia, where this species is distributed.

Paratropis Simon, 1889

Figs 2–4

Type species. *Paratropis scruposa* Simon, 1889.

Diagnosis. *Paratropis* differs from other paratropidids by the combination of the following characters: presence of ITC on legs I, two pairs of spinnerets (PMS and PLS) (Figs 2B, 3B, 4B), males without tibial apophysis, and palpal bulb with embolus relatively straight, thin and very elongated (Figs 2E, F, 4F, G); females with spermathecal receptacles with multilobed fundus (Figs 2H, 3D).

Included species. *Paratropis elicioi* Dupérré, 2015, *Paratropis florezi* Perafán, Galvis & Pérez-Miles, sp. n., *Paratropis papilligera* FO Pickard-Cambridge, 1896, *Paratropis sanguinea* Mello-Leitão, 1923, *Paratropis scruposa* Simon, 1889, *Paratropis seminermis* Caporiacco, 1955, *Paratropis tuxtlensis* Valdez-Mondragón, Mendoza & Francke, 2014.

Distribution. Mexico, Lesser Antilles, and northern South America (Brazil, Colombia, Ecuador, Peru and Venezuela). In Colombia it is widely distributed in the three mountain ranges that make up the Andes, the inter-Andean valleys and lowlands of the Amazon, Llanos, and Caribbean regions (Perafán 2017) (Figure 10).

Paratropis elicioi Dupérré, 2015

Figure 2

Type material. ***Holotype*** male from Ecuador, Cotopaxi Province, Otonga Biological Reserve, near Rio Esmeraldas, 0.41941S, 78.99607W, 1717 m, 25.xi–08.xii.2014, pitfall, col. N Dupérré & E Tapia (QCAZ), not examined.

Additional material Examined. Colombia, Nariño, Barbacoas, Altaquer, Reserva Natural Río Ñambí, 1.3N, 78.08333W, 1400 m, 17-27-vii-2012, col. M Medrano, A García, Y Cifuentes, D Martínez, 1 male (ICN-Ar 11435); one female with the same data (ICN-Ar 11436); one female from the same locality, 1440 m, 17-30-vi-2011, col. A García (ICN-Ar 6974). Ecuador: Pichincha: Santo Domingo, 466 m, 1-xi-1999, col. M Rivadeneira, 1 female (QCAZ, MV-PAR-018); Nanegalito, 1500 m, 27-xii-1996, col. M Davalos, 1 female (QCAZ, MV-PAR-015); Nanegalito, 1400 m, 23-i-1993, col. C Segovia, 1 female (QCAZ, MV-PAR-07); Las Tolas, 20-iii-1989, col. V Utreras, 1 female (QCAZ, MV-PAR-031).

Emended diagnosis. Males of *P. elicioi* differ from those of other *Paratropis* species by the morphology of the palpal bulb with very long and straight embolus (Figure 2E, F). Females can be distinguished by the morphology of spermathecal receptacles with long neck, longitudinal dorsal fold and numerous apical lobes (Figure 2H).

Remarks. The examination of new material from Colombia and Ecuador allowed us to infer that both the diagnosis and the descriptions of the two sexes of *P. elicioi* were inaccurate (Dupérré 2015). Below we present an emended description.

Description. ***Male*** (ICN-Ar 11435) (Figure 2A–C, E, F): total length 13.0; carapace length 6.1, width 6.1; abdomen length 6.0, width 3.8; chelicerae length 1.9. Color (in alcohol): body with few soil particles encrusted; carapace, chelicerae and legs reddish brown; abdomen grayish brown (Figure 2A). Carapace: slightly setose, with a single line of curved setae mixed with disperse clubbed setae, striae conspicuous; caput arched, separated from thoracic region by transverse shallow fovea, straight, width 0.9 (Figure 2A). Eyes and ocular tubercle: tubercle length 0.9, width 1.1, very elevated (height 0.8) and forwardly directed, with few setae. Clypeus absent. Anterior eye row slightly procurved, posterior recurved. Ocular sizes and interdistances: AME 0.35, ALE 0.35, PME 0.20, PLE 0.25, AME-AME 0.10, AME-ALE 0.03, PME-PME 0.50, PME-PLE 0.03, ALE-PLE 0.08, AME-PME 0.03, ALE-ALE 0.65, PLE-PLE

Figure 2. *Paratropis elicioi* Dupérré, 2015. **A–C** male **A, B** *habitus* **A** dorsal view **B** ventral view **C** sternum, labium and maxillae **D** sternum, labium and maxillae female **E, F** palpal bulb **E** prolateral view **F** retrolateral view **G** *habitus* female, dorsal view **H** spermathecae. Scale bars: 1.0 mm(**A–D, G**); 0.5 mm (**E–H**).

0.70. Chelicerae: short sparse bristles on dorsal and lateral areas, long fine bristles on ventral and anterior area; basal segment with clubbed-plumose setae. Rastellum absent. Cheliceral furrow with two rows of teeth well developed, 16/14 and 11/13 teeth on promargin and retromargin, respectively. Labium: length 0.7, width 1.4, with 75

cuspules on anterior edge (Figure 2C). Labio-sternal groove with two lateral mounds. Maxillae longer than wide, with the anterior prolateral lobe very elongated, conical (Figure 2C); with 73/76 cuspules spaced, largely spread over prolatero-ventral border from the inner edge to anterior lobe. Lyra absent. Sternum: length 2.5, width 3.2; three pairs of sigillae, anterior subcircular, median and posterior sigillae oval; anterior and median sigillae marginal, posterior submarginal (Figure 2C).

Legs: cuticle normal. Leg and palpal segments measurements provided in Table 2. Leg I clearly thicker than the others. Bristles, clubbed and thorn-like setae present. Trichobothria: filiform, on central 2/3 of tarsi, palp 4, leg I 9, II 9, III 8, IV 9; on distal 1/4 of metatarsi, leg I 5, II 5, III 4, IV 4; on proximal 1/3 of tibiae, palp with two rows of 3 and 4 respectively, legs I–III two groups of 4 each, IV 2r-5p-1d (proximal/distal). Scopula absent. Pseudoscopula weak and divided by conical longer setae, only present on distal tarsi I, II and III. Claw tufts absent. Tarsi distally incrassate on anterior legs. Tarsal claws: ITC present on leg I; STC with one tooth on all legs. Spination: principally thorn-like setae on all segments. Spines: palp 0; leg I 0; leg II 0; leg III fe 0, pa 0, ti 0, me 1pv, ta 1pv; leg IV fe 0, pa 0, ti 0, me 1pv, ta 2pv.

Palp: cymbium with two unequal lobes separated by a sclerotized groove; tibia with distoventral groove. Palpal bulb pyriform very elongated; embolus as long as tibia and half patella, straight then tapering to the apex, apex stout but flattened (Figure 2E, F).

Abdomen: with four longitudinal dorsal rows of seven small tubercles, each emitting from its summit a plumose, bacilliform seta. Book lung apertures projected, oval, sclerotized (Figure 2B). Spinnerets: PMS 0.50; PLS length 1.9, apical segment digitiform. Basal segment of PLS divided in two unequal cuticle plates (Figure 2B).

Female (ICN-Ar 6974) (Figure 2D, G, H): total length 18.5, carapace length 7.2, width 7.1; abdomen length 10.0, width 7.0; chelicerae length 4.0. Color (in alcohol): body with soil particles encrusted; carapace, and legs reddish dark brown, chelicerae dark brown, abdomen grayish brown (Figure 2G). Carapace: slightly setose, lateral margins with single line of spiniform setae with a single line of curved setae mixed with disperse clubbed setae; striae conspicuous; caput arched, separated from thoracic region by transverse fovea, straight, width 1.4 (Figure 2G). Eyes and ocular tubercle: tubercle length 1.2, width 1.3, very elevated (height 0.9) and forwardly directed, with few setae. Clypeus absent. Anterior eye row slightly procurved, posterior recurved. Ocular sizes and interdistances: AME 0.35, ALE 0.38, PME 0.28, PLE 0.33, AME-AME 0.18, AME-ALE 0.05, PME-PME 0.65, PME-PLE 0.03, ALE-PLE 0.05, AME-PME 0.05, ALE-ALE 0.73, PLE-PLE 0.85. Chelicerae: short sparse bristles on dorsal and lateral areas, long fine bristles on ventral and anterior area; basal segment with clubbed plumose setae. Rastellum absent. Cheliceral furrow with two rows of teeth well-developed, 13/14 and 13/12 teeth on promargin and retromargin, respectively. Labium: length 1.1, width 1.8, with 97 cuspules on anterior edge (Figure 2D). Labio-sternal groove with two lateral mounds. Maxillae longer than wide, with the anterior prolateral lobe very elongated, conical (Figure 2D); with 91/97 cuspules spaced, largely spread over prolatero-ventral border from the inner edge to anterior

Table 2. Lengths (in mm) of legs and palpal segments of male (ICN-Ar 11435) / female (ICN-Ar 11436) *Paratropis elicioi.*

	I	II	III	IV	Palp
Femur	6.0/6.0	4.9/4.3	4.3/4.0	5.8/5.7	2.9/3.3
Patella	3.0/3.2	2.3/2.5	2.1/2.5	2.3/2.8	1.7/1.8
Tibia	5.2/5.0	3.8/3.5	2.9/3.0	5.1/5.1	2.0/2.2
Metatarsus	4.9/4.0	4.3/3.3	3.9/3.6	5.7/5.4	–
Tarsus	2.4/1.7	2.2/1.7	2.0/1.8	2.1/2.5	0.9/2.5
Total	21.5/19.9	17.5/15.3	15.2/14.9	21.0/21.5	7.5/9.8

lobe. Lyra absent. Sternum: length 2.8, width 3.9; three pairs of sigillae, anterior subcircular, median and posterior sigillae oval; anterior and median sigillae marginal, posterior submarginal. Anterior edge of sternum with a semicircular area slightly elevated (joined to labio-sternal groove) (Figure 2D).

Legs: cuticle normal. Leg and palpal segments measurements provided in Table 2. Leg I clearly thicker than the others. Bristles, thorn-like setae and spines present. Trichobothria: filiform, on central 2/3 of tarsi, palp 9, leg I 11, II 10, III 9, IV 8; on distal 1/4 of metatarsi, leg I 5, II 4, III 4, IV 5; on proximal 1/3 of tibiae, palp 7 in two groups of 4 and 3 respectively, legs I-III two groups of 4 each, IV 2r-5p-1d (proximal/distal). Scopula or pseudoscopula absent. Claw tufts absent. Tarsal claws: ITC present on leg I; STC with one tooth on all legs. Spination: principally thorn-like setae on all segments. Spines: palp fe 0, pa 0, ti 0, ta 1pv, 2rv; leg I fe 0, pa 0, ti 0, me 5pv, 10rv, ta 8pv, 7rv; leg II fe 0, pa 0, ti 0, me 1pd, 2pv, 1r, 3rv, ta 1rv; leg III fe 0, pa 0, ti 0, me 2p, 3pv, 1r, 2rv, ta 1pv, 1rv; leg IV fe 0, pa 0, ti 0, me 3pv, 1rv, ta 2pv.

Abdomen: with four longitudinal dorsal rows of seven small tubercles, each emitting from its apex a plumose, bacilliform seta. Book lung apertures projected, oval, sclerotized. Two spermathecal receptacles with a long neck, with a longitudinal dorsal fold, ended in a multilobed fundus (Figure 2H). Spinnerets: PMS length 0.60; PLS length 3.0, apical segment digitiform. Basal segment of PLS divided in two unequal cuticle plates.

Distribution. South of Colombia and north of Ecuador, on the Western Andean montane forest, between 500–1700 m altitudes. In Colombia it's distributed on Nariño Department (Barbacoas, Reserva Natural Río Ñambí) and Ecuador distributed on Cotopaxi Province (Otonga Biological Reserve) and Pichincha Province (Santo Domingo; Nanegalito; Las Tolas) (Figure 10).

***Paratropis florezi* sp. n.**
http://zoobank.org/260E4931-0972-4FB1-8BEE-68CC7A4D401B
Figure 3

Type material. ***Holotype*** female from Colombia, Valle del Cauca, km 16 road Cali-Buenaventura, 3.52519N, 76.61992W, 1800 m, 14-xii-2014, col. C Perafán (ICN-Ar 11437). ***Paratypes***: three females with the same data (ICN-Ar 11438).

Diagnosis. Females of *Paratropis florezi* sp. n. differ from those of all other species of *Paratropis* by having the abdominal tubercles not prominent (Figure 3A) and by the spermathecal receptacles with a long neck, with the base widened and apex narrow, ended in a fundus with several projected lobes (Figure 3D).

Description. ***Female*** (ICN-Ar 11437) (Figure 3): total length 15.2, carapace length 7.0, width 6.7; abdomen length 7.2, width 5.6; chelicerae length 3.4. Color (in alcohol): body with soil particles encrusted; carapace and legs reddish dark brown, chelicerae dark brown, abdomen grayish brown (Figure 3A). Carapace: scarcely setose, lateral margins with single line of spiniform setae; striae conspicuous; caput arched, separated from thoracic region by transverse fovea, slightly procurved, width 1.3 (Figure 3A). Eyes and ocular tubercle: tubercle length 0.8, width 0.7, very elevated (height 0.8) and slightly forwardly directed, with few setae. Clypeus absent. Anterior eye row slightly procurved, posterior recurved. Ocular sizes and interdistances: AME 0.38, ALE 0.35, PME 0.18, PLE 0.33, AME-AME 0.10, AME-ALE 0.08, PME-PME 0.55, PME-PLE 0.05, ALE-PLE 0.10, AME-PME 0.05, ALE-ALE 0.80, PLE-PLE 0.83. Chelicerae: short sparse bristles on dorsal and lateral areas, long fine bristles on ventral and anterior area. Rastellum absent. Cheliceral furrow with two rows of teeth well-developed, 11/13 and 9/12 teeth on promargin and retromargin, respectively. Labium: sub-rectangular, length 1.0, width 1.8, with 120 cuspules on anterior edge (Figure 3C). Labio-sternal groove with two lateral mounds. Maxillae longer than wide, with the anterior prolateral lobe very elongated, conical (Figure 3C); with 80/71 cuspules spaced, largely spread over prolateral-ventral border from the inner edge to anterior lobe. Sternum: heart shaped length 2.9, width 3.8; three pairs of sigillae, anterior subcircular, median and posterior sigillae oval; anterior and median sigillae marginal, posterior submarginal. Anterior edge of sternum with a semicircular area slightly elevated (joined to labio-sternal groove) (Figure 3C).

Legs: cuticle with soil particles encrusted. Leg and palpal segments measurements provided in Table 3. Palp, tarsi swollen. Leg I, clearly thicker than the others. Bristles, thorn-like setae, and spines present. Trichobothria: filiform, on central 2/3 of tarsi, palp 9, leg I 12, II 11, III 9, IV 13; on distal 1/4 of metatarsi, leg I 5, II 4, III 5, IV5; on proximal 1/3 of tibiae, palp and leg I two rows of 4 each, II two groups of 4 and 5 respectively, III two groups of 4 each, IV 2r-5p-1d (proximal/distal). Scopula or pseudoscopula absent. Claw tufts absent. Tarsal claws: ITC present on leg I; STC with one curved tooth on all legs. Spination: principally thorn-like setae on all segments. Spines: palp fe 0, pa 0, ti 0, ta 1pv, 4rv; leg I fe 0, pa 0, ti 0, me 10v, 5pv, 7rv, ta 10pv, 10rv; leg II fe 0, pa 0, ti 0, me 4v, 1pd, 1pv, 1rv, ta 3rv; leg III fe 0, pa 0, ti 0, me 3v, 2pd, 2pv, 1rv, ta 1pv, 1rv; leg IV fe 0, pa 0, ti 0, me 3v, 2pv, ta 5pv.

Abdomen: with four longitudinal dorsal rows of seven small tubercles, each emitting from them a plumose, bacilliform seta. Book lung apertures projected, oval, sclerotized (Figure 3B). Two spermathecal receptacles with a long neck, with the base widened and apex narrow, ended in a fundus with several projected lobes (Figure 3D). Spinnerets: PMS length 0.6; PLS length 2.7, apical segment digitiform. Basal segment of PLS divided in two unequal cuticle plates (Figure 3B).

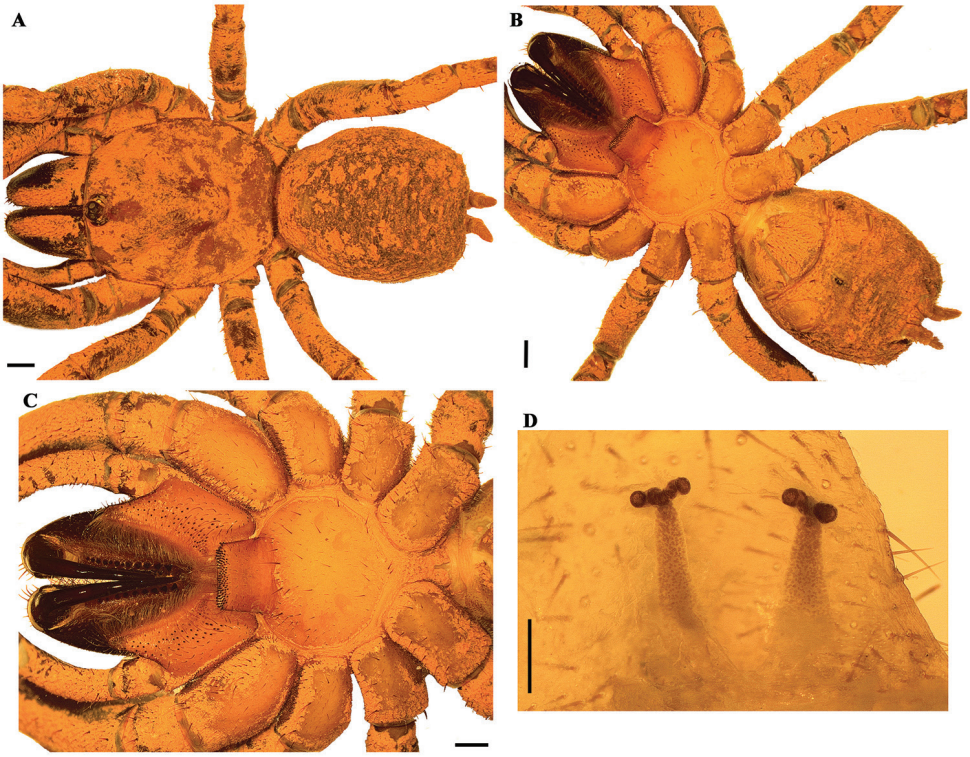

Figure 3. *Paratropis florezi* sp. n., female. **A, B** *habitus* **A** dorsal view **B** ventral view **C** sternum, labium and maxillae **D** spermathecae. Scale bars: 1.0 mm (**A–C**); 0.5 mm (**D**).

Table 3. Lengths (in mm) of legs and palpal segments of the holotype female *Paratropis florezi* sp. n.

	I	II	III	IV	Palp
Femur	5.9	4.6	3.0	5.6	3.1
Patella	3.2	2.6	2.3	2.7	1.9
Tibia	4.5	3.0	2.4	4.6	1.9
Metatarsus	3.8	3.4	3.3	5.1	–
Tarsus	2.0	1.9	2.0	2.6	2.6
Total	19.4	15.5	13.0	20.6	9.5

Male. Unknown.

Distribution. Only known from its type locality, in the western Cordillera of Colombian Andes, Valle del Cauca Department, km 16 road Cali-Buenaventura, at 1800 m altitude (Figure 10).

Natural history. The females of *Paratropis florezi* sp. n. live in shallow burrows that they dig in the substrate of the ravines of the road.

Etymology. The species epithet is a noun in genitive, in honor of Dr Eduardo Flórez Daza (ICN), in recognition of his friendship, teachings, and vast contributions to Colombian arachnology.

Paratropis papilligera **FO Pickard-Cambridge, 1896**
Figure 4

Type material. ***Holotype*** male and ***paratype*** female from Santarem, Pará, Brazil, deposited in NHM, only male examined.

Additional material examined. Colombia, Amazonas, Leticia, km 11 road to Tarapacá, 100 m, 25-iv-2002, it was collected manually in the day on leaf litter, col. G Amat and Estudiantes Introducción Sistemática Animal - Universidad Nacional de Colombia, 1 male (ICN-Ar 2315).

Emended diagnosis. Males of *P. papilligera* differ from those of other *Paratropis* species by the morphology of the palpal bulb with very thin and long embolus, distally curved (Figure 4F, G), and by the tibia I with a basal retrolateral conic process with spiniform setae (Figure 4D, E).

Redescription. ***Male*** (ICN-Ar 2315) (Figure 4): total length 12.3; carapace length 6.1, width 6.8; abdomen length 5.4, width 3.3; chelicerae length 2.7. Color (in alcohol): body with soil particles encrusted; carapace and chelicerae dark reddish brown, legs and abdomen brown (Figure 4A). Carapace slightly setose, striae conspicuous, lateral margins with single line of curved setae mixed with disperse clubbed setae; caput arched, separated from thoracic region by transverse shallow fovea, straight, width 1.0 (Figure 4A). Eyes and ocular tubercle: tubercle length 1.10, width 1.40, very elevated (height 0.9) and forwardly directed, with few stout setae. Clypeus absent. Anterior eye row slightly procurved, posterior recurved. Ocular sizes and interdistances: AME 0.45, ALE 0.35, PME 0.23, PLE 0.33, AME-AME 0.10, AME-ALE 0.08, PME-PME 0.63, PME-PLE 0.05, ALE-PLE 0.08, AME-PME 0.05, ALE-ALE 0.93, PLE-PLE 0.80. Chelicerae: short sparse bristles on dorsal and lateral areas, long fine bristles on ventral and anterior area. Rastellum absent. Cheliceral furrow with two rows of teeth well developed, 10/10 and 9/10 teeth on promargin and retromargin, respectively. Fang long. Labium: length 0.8, width 1.4, with 105 cuspules on anterior edge (Figure 4C). Labio-sternal groove narrower in the middle than laterally. Maxillae longer than wide, with the anterior prolateral lobe very elongated, conical (Figure 4C); with 73/72 rounded cuspules spaced, largely spread over prolatero-ventral border from the inner edge to anterior lobe. Lyra absent. Sternum: length 2.7, width 3.4; three pairs of sigillae, anterior subcircular, median and posterior sigillae oval; anterior and median sigillae marginal, posterior submarginal. Anterior edge of sternum with a semicircular area slightly elevated (joined to labio-sternal groove) (Figure 4C).

Legs: cuticle with soil particles encrusted. Leg and palpal segments measurements provided in Table 4. Leg I clearly thicker than the others. Bristles, plumose and thorn-like setae and spines evident. Tibia I with a basal retrolateral conic process with spiniform setae (Figure 4D, E). Trichobothria: filiform, on central 2/3 of tarsi, palp 6, leg I 9, II 8, III 7, IV 8; on distal 1/4 of metatarsi, leg I 5, II 4, III 4, IV 4; on proximal 1/3 of tibiae, palp two rows of 4 each, leg I two groups of 5 each, II-III two groups of 4 each, IV 2r-5p-1d (proximal/distal). Scopulae absent. Pseudoscopula weak and divided by conical longer setae, only present on distal tarsi I and II; tarsi III and IV with few sparse pseudoscopula setae. Claw tufts absent. Tarsal claws: ITC only present on leg I; STC with one

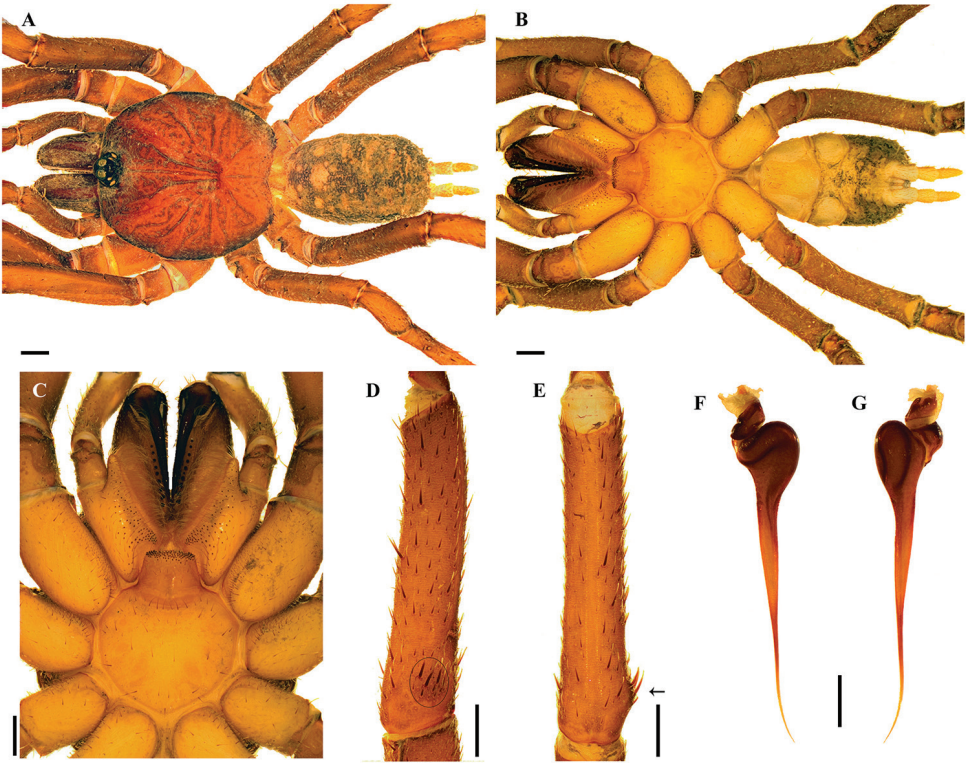

Figure 4. *Paratropis papilligera* FO Pickard-Cambridge, 1896, male. **A, B** *habitus* **A** dorsal view **B** ventral view **C** sternum, labium and maxillae **D, E** tibia I **D** retrolateral view **E** ventral view **F, G** palpal bulb **F** prolateral view **G** retrolateral view. Arrow and circle indicate the basal retrolateral conic process on tibia I. Scale bars: 1.0 mm (**A–C**); 0.5 mm (**F, G**).

Table 4. Length (in mm) of legs and palpal segments of male *Paratropis papilligera* (ICN-Ar 2315).

	I	II	III	IV	Palp
Femur	7.3	6.2	5.3	7.2	3.0
Patella	3.4	2.7	2.3	2.6	1.8
Tibia	6.5	5.0	4.0	6.1	2.7
Metatarsus	6.2	5.8	5.2	7.2	–
Tarsus	2.2	2.5	2.3	2.9	1.0
Total	25.6	22.2	19.1	26.0	8.5

tooth on all legs. Spination: principally thorn-like setae on all segments. Spines: palp 0; leg I 0; leg II 0; leg III, fe 0, pa 0, ti 0, me 1p 1v, ta 1p; leg IV, fe 0, pa 0, ti 0, me 1p, ta 1p.

Palp: cymbium with two unequal lobes separated by a sclerotized groove; tibia with shallow distoventral groove. Palpal bulb elongated; embolus very thin and long (longer than tibia), distally curved, tapering to the apex (Figure 4F, G).

Abdomen: with four longitudinal dorsal rows of seven small tubercles, each emitting from its summit a plumose, bacilliform seta; lateral area finely tuberculate, with smaller plumose setae. Book lung apertures projected, oval, sclerotized (Figure 4B).

Spinnerets: PMS length 0.50; PLS length 3.00, apical segment digitiform. Basal segment of PLS divided in two unequal cuticle plates (Figure 4B).

Distribution. Amazonas of Brazil and Colombia. Brazil, Santarem (Pará); Colombia, Amazonas (Leticia) (Figure 10).

***Stormtropis* gen. n.**

http://zoobank.org/F0DD1290-6D25-40A3-B9AF-430A4316F24A
Figs 5–9

Type species. *Stormtropis parvum* Perafán, Galvis & Pérez-Miles, sp. n.

Diagnosis. *Stormtropis* gen. n. males differ from those of all other paratropidids by the combination of the following characteristics: absence of spines on all segments of legs, lack third claw (ITC) on all tarsi and by the morphology of palpal bulb; pyriform, elongated, with embolus slightly curved tapering to the apex and a subapical triangular tooth (Figs 5F–G, 6D–E, 7F–G, 9F–G). Excepting *S. muisca* sp. n. the other species have a tibial prolateral apophysis, constituted by a single spur and a group of about 15 spines in two parallel rows (Figs 5D–E, 7D–E, 9D–E); it differs from *Melloina* males by the absence of claw tufts and the different morphology of tibial apophysis (two branches and few megaspines in *Melloina*: Schenkel 1953: fig. 4C, D; Raven 1999: fig. 2F; Bertani 2013: figs 12, 13). Females differ from all other paratropidids by the morphology of the spermathecal receptacles with a tubular neck and a wide globose fundus (mushroom shaped) (Figure 8D), and few spines on all legs. Additionally, *Stormtropis* gen. n. has few labial and maxillary elongated cuspules (less than 70), four spinnerets (PMS and PLS), and fewer tricobothriae on each article.

Included species. *Stormtropis colima* Perafán, Galvis and Pérez-Miles sp. n., *Stormtropis muisca* Perafán, Galvis and Pérez-Miles sp. n., *Stormtropis paisa* Perafán, Galvis and Pérez-Miles sp. n. and *Stormtropis parvum* Perafán, Galvis and Pérez-Miles sp. n.

Description. Carapace round, almost glabrous, light to dark brown. Caput arched. Fovea shallow, transverse, straight to slightly procurved. Eye group subquadrate, wider than long, tubercle well defined, elevated. Clypeus absent. Chelicerae without rastellum, cheliceral furrow narrow with teeth on both margins: promargin 7–13, retromargin 6–13, fangs long. Labium subquadrate with 20–70 cuspules restricted to anterior edge. Maxillae longer than wide with the anterior prolateral lobe very elongated, conical; few cuspules (24–77) throughout the prolateral diagonal half of the maxillae. Labio-sternal groove narrow in the middle and wider laterally. Sternum heart shaped, slightly wider than long, sigillae oval, submarginal. Legs, thin and long, pair I slightly stouter than II-IV; clubbed setae present. Few filiform tricobothria on tarsus, metatarsus, and tibia in males. Long paired claws (STC) with one medial long tooth ventrally; third unpaired claw (ITS) absent on all legs of males; ITS present on leg I of females. Claw tufts absent, tarsal scopula absent, pseudoscopula setae generally present on the distal third of anterior tarsi. Males with spinose apophysis (similar to Avicularinae) on prolateral distal tibiae I (except *S. muisca*). Abdomen oval, glabrous, with clubbed

setae present on dorsum. Four spinnerets; PLS well developed, PMS small (half of the basal segment of PLS). All body encrusted by soil particles. Males without spines, and females with few spines on all legs. Males with cymbium with two unequal lobes separated by a sclerotized groove; palpal tibia with shallow distoventral groove; and palpal bulb pyriform elongated, with embolus slightly curved tapering to the apex, and a subapical triangular tooth. Females with spermathecal receptacles with a tubular neck and globose fundus.

Distribution. *Stormtropis* gen. n. is distributed in the central and eastern Cordilleras of Colombia, on the montane forests of the Magdalena Valley and Cauca Valley, between 1400–3400 m altitudes, in the Departments of Antioquia (Santa Elena), Boyacá (Sotaquirá and Santuario de Fauna y Flora Iguaque), Caldas (Pensilvania) and Cundinamarca (Topaipí) (Figure 10).

Etymology. The name *Stormtropis* is a Latin declension (neuter) of the noun Stormtrooper from the fictional universe of the Star Wars films**.** The stormtroopers are the soldiers of the main ground force of the Galactic Empire. These soldiers are very similar to each other, with some capacity for camouflage but with unskillful movements, like this group of spiders.

***Stormtropis colima* sp. n.**
http://zoobank.org/B0A52980-1C2D-4CA5-A813-B0BCC6806314
Figure 5

Type material. ***Holotype*** male from Colombia, Cundinamarca, Río Negro Province, Topaipí, 1377 m, 18-23-x-2012, col. M Medrano, A García, E Martínez (ICN-Ar 11439).

Diagnosis. *Stormtropis colima* sp. n. differs from the other species of the genus by the presence of a tibial apophysis with shorter base and not so much separated from the tibia as in the other species (Figure 5D, E). Additionally, *S. colima* sp. n. differs from *S. parvum* sp. n. by the presence of a continuous row and more numerous cheliceral teeth on promargin (13–11) (7 in *S. parvum* sp. n.) and from *S. paisa* sp. n. by the absence of a sclerotized dark mark on proximal dorsal tibia, without a slight excavation.

In addition, *S. colima* sp. n. is larger (8.4 mm) and lives at lower elevation (1377m) than *S. parvum* sp. n. (6 mm; 2750 m) and *S. paisa* sp. n. (8.5 mm; 2400 m).

Description. ***Holotype male*** (ICN-Ar 11439) (Figure 5): total length 8.4, carapace length 4.2, width 4.2; abdomen length 3.3, width 2.7; chelicerae length 1.7. Color (in alcohol): body with soil particles encrusted; carapace, chelicerae, coxa, trochanter and femur dark brown; abdomen dorsally and patella-tarsus brown. Carapace: glabrous, striae conspicuous, lateral margins with single line of curved setae mixed with disperse clubbed setae; caput arched, separated from thoracic region by transverse shallow fovea, straight, width 0.4 (Figure 5A). Eyes and ocular tubercle: tubercle length 0.6, width 0.7, very elevated (height 0.5) and forwardly directed, with few stout setae. Clypeus absent. Anterior eye row slightly procurved, posterior recurved. Ocular sizes and interdistances: AME 0.23, ALE 0.25, PME 0.15, PLE 0.18, AME-AME 0.08,

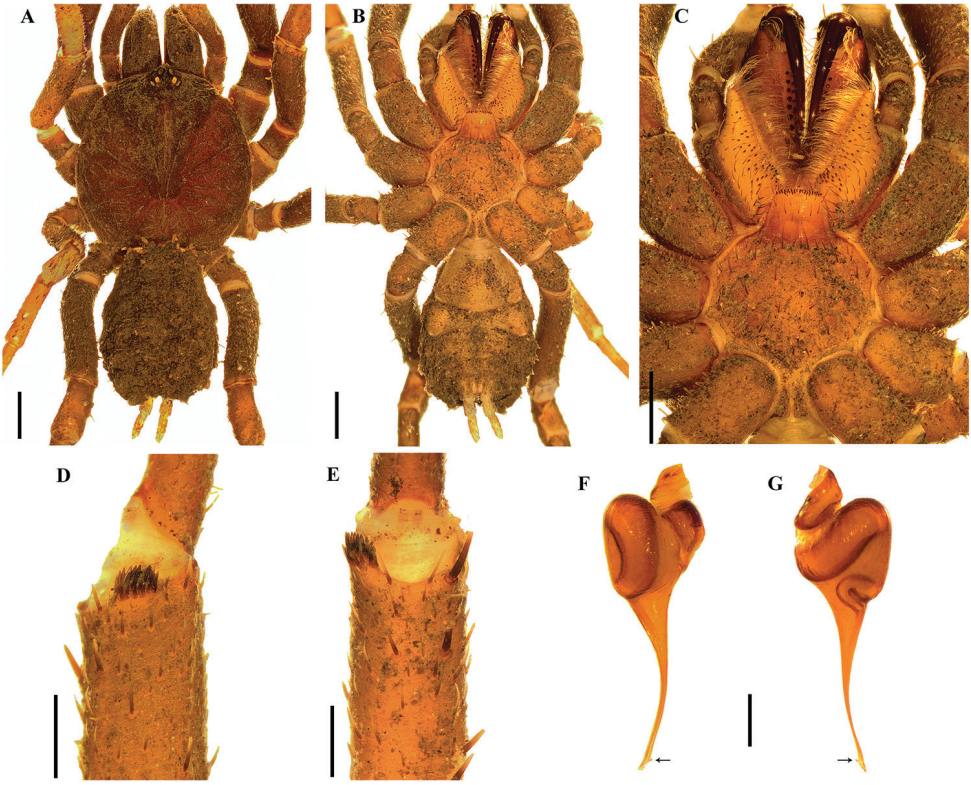

Figure 5. *Stormtropis colima* gen. n., sp. n., male. **A, B** *habitus* **A** dorsal view **B** ventral view **C** sternum, labium and maxillae **D, E** tibial apophysis on leg I **D** prolateral view **E** ventral view **F, G** palpal bulb **F** prolateral view **G** retrolateral view. Arrows point to the triangular tooth on the subapical region of the embolus. Scale bars: 1.0 mm (**A–C**); 0.5 mm (**D, E**); 0.25 mm (**F, G**).

Table 5. Length (in mm) of legs and palpal segments of the holotype male *Stormtropis colima* sp. n.

	I	II	III	IV	Palp
Femur	3.9	3.2	2.7	3.6	1.7
Patella	1.9	1.5	1.3	1.5	1.2
Tibia	3.1	2.3	1.7	3.0	1.3
Metatarsus	3.0	2.5	2.4	3.5	–
Tarsus	1.5	1.4	1.4	1.7	0.6
Total	13.4	10.9	9.5	13.3	4.8

AME-ALE 0.03, PME-PME 0.28, PME-PLE 0.03, ALE-PLE 0.05, AME-PME 0.03, ALE-ALE 0.38, PLE-PLE 0.45. Chelicerae: dorsal few plumose setae, short sparse bristles on dorsal and lateral areas, long fine bristles on ventral and anterior areas. Rastellum absent. Cheliceral furrow narrow with two rows of teeth, 13/11 teeth on promargin, and 8 teeth on retromargin. Fang long. Labium subquadrate, length 0.5, width 1.00, with 39 elongated cuspules on anterior edge (Figure 5C). Labio-sternal

groove narrower in the middle than laterally. Maxillae longer than wide, with the anterior prolateral lobe very elongated, conical; with 42/44 elongated cuspules widely distributed throughout the prolateral half of the maxillae; field of cuspules wider proximally (Figure 5C). Sternum heart shaped, length 1.73, width 2.15; three pairs of sigillae, anterior and median subcircular, posterior sigillae oval, all marginal (Figure 5C).

Legs: cuticle with soil particles encrusted. Leg and palpal segments measurements provided in Table 5. Legs I slightly stouter than II–IV. Femur IV widened. Clubbed plumose and thorn-like setae. Trichobothria: filiform, on central 2/3 of tarsi, palp, and all legs 5; on distal 1/4 of metatarsi, all legs 3; and on proximal 1/3 of tibiae, palp and legs I–III two rows of 2 each, IV 4. Scopula absent, few and sparse pseudoscopula setae on tarsi I and II. Claw tufts absent. Tarsal claws: ITC absent from all legs; STC long, with one tooth on all legs. Tibial apophysis on leg I present: a short flattened branch on distal prolateral side, with spines on two parallel rows, 10 distal and 5 proximal (Figure 5D, E). Thorn-like setae mainly present on legs III and IV. Spines absent.

Palp: cymbium with two unequal lobes separated by a sclerotized groove; tibia with shallow distoventral groove. Palpal bulb pyriform elongated; embolus curved, very long, tapering to the apex, apex wide; a triangular translucent tooth on subapical region, close to apex (Figure 5F, G).

Abdomen: oval, with small clubbed setae; lateral and dorsal areas finely tuberculate, with small plumose clubbed setae, principally on posterior area (Figure 5A). Book lung apertures projected, oval, sclerotized (Figure 5B). Spinnerets: PMS length 0.3; PLS length 1.6, apical segment digitiform (Figure 5B).

Female: unknown.

Distribution. Only known from its type locality, Topaipí in the Río Negro Province (Cundimarca), in the Eastern Cordillera of Colombian Andes, at 1300 m altitude (Figure 10).

Etymology. The species epithet *colima* is a noun in apposition which means warrior in the extinct Muisca language. The Colimas were an indigenous tribe that inhabited in the central highlands of Colombia, where the species occurs.

***Stormtropis muisca* sp. n.**
http://zoobank.org/BDD00B70-6EDF-480B-9CAA-87FE0C174A85
Figure 6

Type material. ***Holotype*** male from Colombia, Boyacá, Sotaquirá, Vereda Guaguaní, 5.80886N, 73.25063W, 3415 m, 8-10-vi-2015, col. Y Cifuentes, J Moreno (ICN-Ar 11440). ***Paratype***: 1 male from Colombia, Boyacá, Villa de Leyva, Santuario de Flora y Fauna Iguaque, 11-iv-2000, pitfall, col. C Fagua (ICN-Ar 880).

Diagnosis. Males of *Stormtropis muisca* sp. n. differ from those of all other species of *Stormtropis* gen. n. by the absence of tibial apophysis, and by the pattern of abdominal color, grayish brown with a pattern of seven pairs of lighter dots, and sub-circular carapace (Figure 6A). Also, by the palpal bulb elongated, with the embolus slightly

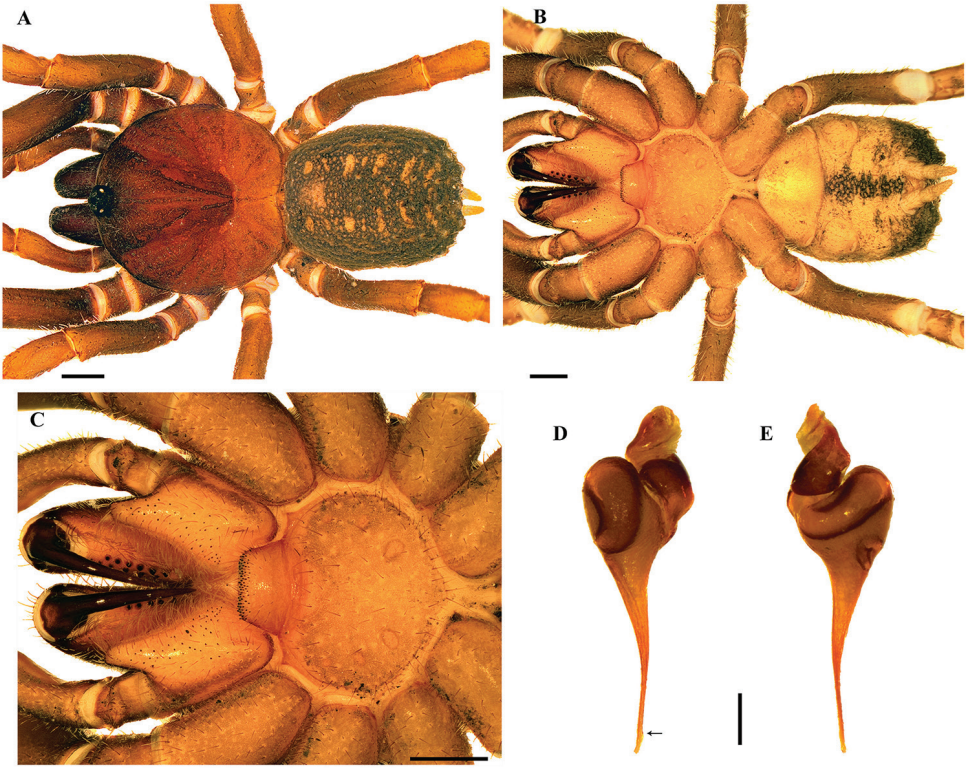

Figure 6. *Stormtropis muisca* gen. n., sp. n., male. **A, B** *habitus* **A** dorsal view **B** ventral view **C** sternum, labium and maxillae **D, E** palpal bulb **D** prolateral view **E** retrolateral view. Arrows point to the triangular tooth on the subapical region of the embolus. Scale bars: 1.0 mm (**A–C**); 0.25 mm (**D, E**).

Table 6. Length (in mm) of legs and palpal segments of the holotype male *Stormtropis muisca* sp. n.

	I	II	III	IV	Palp
Femur	4.0	3.5	3.0	3.8	1.9
Patella	2.3	1.8	1.4	1.8	1.4
Tibia	3.5	2.6	2.0	3.1	1.4
Metatarsus	3.0	2.7	2.2	3.0	–
Tarsus	1.6	1.5	1.5	1.5	0.9
Total	14.4	12.1	10.1	13.2	5.6

curved tapering to the apex, which is stout but flattened, and a very small subapical triangular tooth (Figure 6D, E).

Description. ***Male*** (ICN-Ar 11440) (Figure 6): total length 9.5; carapace length 4.6, width 4.8; abdomen length 4.6, width 3.5; chelicerae length 1.3. Color (in alcohol): body with few soil particles encrusted; carapace, chelicerae and legs dark reddish brown; abdomen grayish brown with a pattern of seven pairs of lighter dots (Figure 6A). Carapace slightly setose, striae conspicuous, lateral margins with single line of spiniform setae; caput very arched, separated from thoracic region by transverse shallow fovea, straight, width 0.9 (Figure 6A). Eyes and ocular tubercle: tubercle length

0.73, width 0.8, very elevated (height 0.5) and forwardly directed, with few stout setae. Clypeus absent. Anterior eye row slightly procurved, posterior recurved. Ocular sizes and interdistances: AME 0.25, ALE 0.25, PME 0.10, PLE 0.20, AME-AME 0.15, AME-ALE 0.25, PME-PME 0.40, PME-PLE 0.03, ALE-PLE 0.08, AME-PME 0.05, ALE-ALE 0.50, PLE-PLE 0.50. Chelicerae: short sparse bristles on dorsal and lateral areas, long fine bristles on ventral and anterior areas. Rastellum absent. Cheliceral furrow with two rows of well-developed teeth, 8/7 and 6/6 teeth on promargin and retromargin, respectively. Labium: length 0.5, width 1.2, with 69 cuspules on anterior edge (Figure 6C). Labio-sternal groove of uniform width. Maxillae longer than wide, with the anterior prolateral lobe very elongated, conical (Figure 6C); with 37/36 conical cuspules spaced, largely spread over prolatero-ventral border from the inner edge to anterior lobe. Lyra absent. Sternum: length 1.8, width 2.5; three pairs of sigillae, anterior subcircular, median and posterior sigillae oval; anterior and median sigillae marginal, posterior submarginal. Anterior edge of sternum with a semicircular area slightly elevated (joined to labio-sternal groove) (Figure 6C).

Legs: cuticle normal. Leg and palpal segments measurements provided in Table 6. Leg I clearly thicker than the others. Bristles and thorn-like setae present. Trichobothria: filiform, on central 2/3 of tarsi, palp 4, leg I 7, II 5, III 4, IV 4; on distal 1/4 of metatarsi, leg I 4, II 3, III 3, IV 3; on proximal 1/3 of tibiae, palp and legs I-III two rows of 2 each, IV a row of 3p and 1d. Scopulae absent. Pseudoscopula weak and divided by conical longer setae, only present on distal tarsi I, II and III; tarsi IV with few sparse pseudoscopula setae. Claw tufts absent. Tarsi distally incrassate, mainly on anterior legs. Tarsal claws: ITC absent on all legs, but a very small tooth present on legs I; STC with one curved tooth on all legs. Spination: principally thorn-like setae on all segments. Spines absent.

Palp: cymbium with two unequal lobes separated by a sclerotized groove; tibia with shallow distoventral groove. Palpal bulb pyriform; embolus slightly curved tapering to the apex, apex stout but flattened, a subapical triangular tooth on embolus (Figure 6D, E).

Abdomen: with four longitudinal dorsal rows of nine small tubercles, each emitting from its summit a spiniform seta. Book lung apertures projected, oval, sclerotized (Figure 6B). Spinnerets: PMS length 0.10; PLS length 1.40, apical segment digitiform (Figure 6B).

***Female*:** Unknown.

Distribution. Eastern Cordillera of Colombian Andes, at a height above 3000 m, Páramo biogeographic province. Boyacá Department, municipality of Sotaquirá (Guaguaní) and Iguaque Fauna and Flora Sanctuary (Figure 10).

Etymology. The species epithet *muisca* is a noun in apposition which refers to the indigenous tribe who inhabit in the same region where this species occur.

***Stormtropis paisa* sp. n.**
http://zoobank.org/BDCF8B14-4E67-436B-9BE8-7625D492002A
Figures 7, 8

Type material. ***Holotype*** male from Colombia, Antioquia, Santa Elena, Parque Ecoturístico Arví, Piedras Blancas, 12-iv-2017, 2400 m, col. C. Perafán, L. Montes de Oca,

F. Pérez-Miles, J. Salazar, (ICN-Ar 11441). ***Paratypes***: 3 females with the same data (ICN-Ar 11442-11443) (FC-My 1409).

Diagnosis. *Stormtropis paisa* sp. n. differs from the other species of the genus by the presence of a sclerotized dark mark on proximal dorsal tibia, with a slight excavation (Figure 7A). Males additionally differ from the other species by the presence of a tibial apophysis bearing more numerous spines on the proximal row (12) (Figure 7D, E); in the other species with tibial apophysis the number of such spines is 5–6; and by the palpal bulb with the embolus sinuous, distally twisted and more widened on the apex (Figure 7F, G). Females can be distinguished by the morphology of the spermathecal receptacles with a tubular neck and a wide globose fundus (mushroom shaped) (Figure 8D).

Description. ***Holotype male*** (ICN-Ar 11441) (Figure 7): total length 8.5; carapace length 3.9, width 4.0; abdomen length 4.7, width 2.7; chelicerae length 1.6. Color (in alcohol): body with soil particles encrusted; carapace, chelicerae, coxa, trochanter and femur reddish brown; abdomen dorsally and patella-tarsus brown, tibiae dorsally with a proximal dark brown mark. Carapace: glabrous, striae conspicuous, lateral margins with single line of curved setae mixed with dispersed clubbed setae; caput arched, with three longitudinal lines of plumose setae; caput slightly arched, separated from thoracic region by transverse shallow fovea, straight, width 0.7 (Figure 7A). Eyes and ocular tubercle: tubercle length 0.6, width 0.8, very elevated (height 0.6) and forwardly directed, with few stout setae. Clypeus absent. Anterior eye row slightly procurved, posterior slightly recurved. Ocular sizes and interdistances: AME 0.25, ALE 0.30, PME 0.20, PLE 0.25, AME-AME 0.10, AME-ALE 0.03, PME-PME 0.35, PME-PLE 0.03, ALE-PLE 0.05, AME-PME 0.03, ALE-ALE 0.50, PLE-PLE 0.48. Chelicerae: short sparse bristles on dorsal and lateral areas, long bristles on ventral and anterior area. Rastellum absent. Cheliceral furrow narrow, with two rows of teeth, 10 teeth on promargin, 10/9 teeth on retromargin. Fang long. Labium sub-trapezoid, length 0.90, width 0.50, with 33 elongated cuspules on anterior edge (Figure 7C). Labio-sternal groove wide. Maxillae longer than wide, with the anterior prolateral lobe very elongated, conical; with 35 elongated cuspules widely distributed throughout the prolateral half of the maxillae; field of cuspules wider proximally (Figure 7C). Sternum heart shaped with an anterior nodule, length 1.60, width 2.00; three pairs of sigillae, anterior and median subcircular, submarginal; posterior sigillae oval, marginal (Figure 7C). Anterior edge of sternum with a semicircular area slightly elevated (joined to labio-sternal groove) (Figure 7C).

Legs: cuticle with soil particles encrusted. Leg and palpal segments measurements provided in Table 7. Legs I slightly stouter than II-IV. Clubbed plumose and thorn-like setae. Trichobothria: filiform, on central 2/3 of tarsi, palp and all legs 5; on distal 1/4 of metatarsi, leg I 4, II–IV 3; on proximal 1/3 of tibiae, palp and legs I-III 5 in two rows (2/3 each), IV 4. Scopula absent, pseudoscopula slightly denser on tarsi I and II, sparse pseudoscopula setae on tarsi III and IV. Claw tufts absent. Tarsal claws: ITC absent on all legs; STC long, with one tooth on all legs. Tibial apophysis on leg I present: only one flattened branch on distal prolateral side, with spines on two parallel rows, 15 dis-

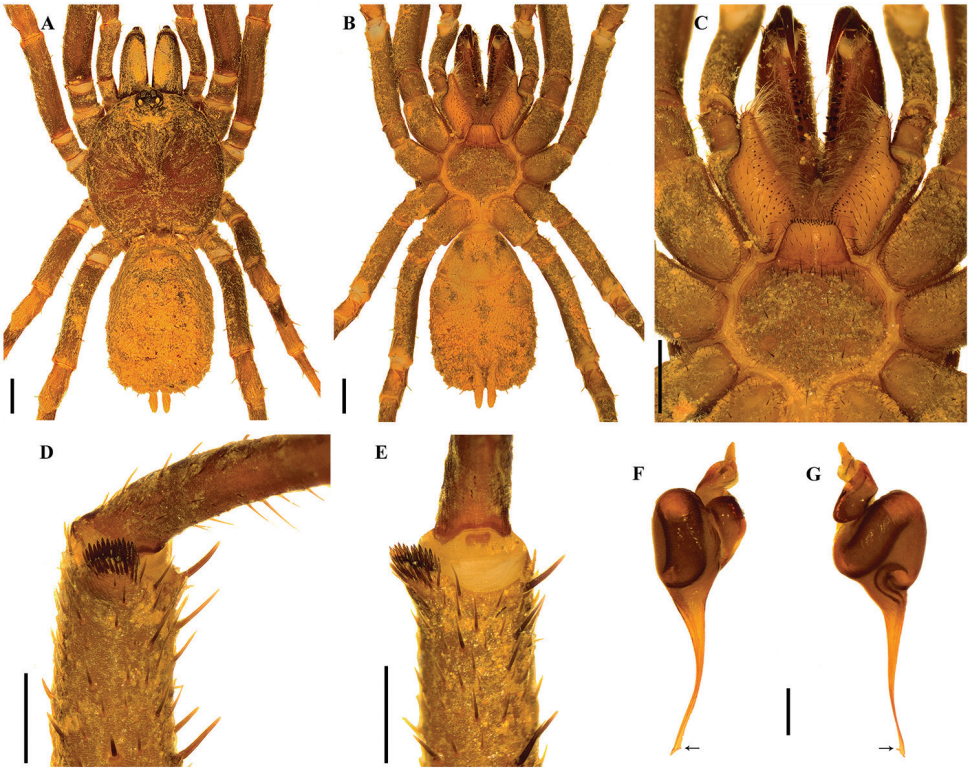

Figure 7. *Stormtropis paisa* gen. n., sp. n., male. **A, B** *habitus* **A** dorsal view **B** ventral view **C** sternum, labium and maxillae **D, E** tibial apophysis on leg I **D** prolateral view **E** ventral view **F, G** palpal bulb **F** prolateral view **G** retrolateral view. Arrows point to the triangular tooth on the subapical region of the embolus. Scale bars: 1.0 mm (**A–C**); 0.5 mm (**D, E**); 0.25 mm (**F, G**).

Table 7. Length (in mm) of legs and palpal segments of the holotype male / paratype female *Stormtropis paisa* sp. n.

	I	II	III	IV	Palp
Femur	3.8/3.8	3.1/3.0	2.6/2.7	3.5/3.7	1.8/2.2
Patella	1.8/2.2	1.5/1.6	1.3/1.5	1.4/1.6	1.1/1.3
Tibia	3.0/2.8	2.2/1.9	1.7/1.6	2.8/2.7	1.3/1.2
Metatarsus	2.8/2.3	2.4/2.0	2.1/2.0	3.1/3.1	–
Tarsus	1.6/1.3	1.5/1.3	1.3/1.3	1.7/1.7	0.8/1.9
Total	13.0/12.4	10.7/9.8	9.0/9.1	12.5/12.8	5.0/6.6

tal and 12 proximal (Figure 7D, E). Thorn-like setae on tibiae, metatarsi, and tarsi of all legs, more dense on legs III and IV. Spines absent.

Palp: cymbium with two unequal lobes separated by a sclerotized groove; tibia with a distoventral groove. Palpal bulb pyriform elongated; embolus sinuous and distally twisted, long, tapering to the apex; a triangular translucent tooth on subapical region (Figure 7F, G).

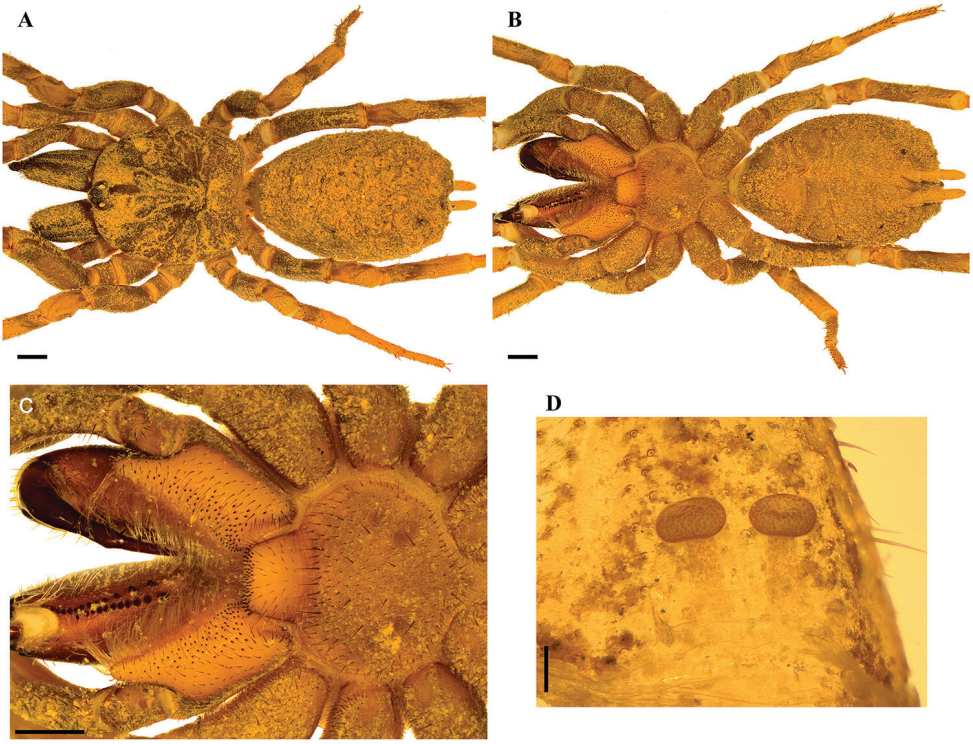

Figure 8. *Stormtropis paisa* gen. n., sp. n., female. **A, B** *habitus* **A** dorsal view **B** ventral view **C** sternum, labium and maxillae **D** spermathecae. Scale bars: 1.0 mm (**A–C**); 0.2 mm (**D**).

Abdomen: oval, with seven transverse dorsal rows of 4–6 small clubbed setae; with smaller plumose clubbed setae, principally on posterior area (Figure 7A). Book lung apertures projected, oval, and sclerotized (Figure 7B). Spinnerets: PMS length 0.30; PLS length 1.4, apical segment digitiform (Figure 7B).

Female (ICN-Ar 11442) (Figure 8): total length 11.7; carapace length 4.8, width 4.6; abdomen length 6.4, width 4.0; chelicerae length 2.4. Color, coverage, and habitus as in male (Figure 8A, B). Eyes and ocular tubercle: tubercle length 0.7, width 1.0, very elevated (height 0.7) and forwardly directed, with setae. Clypeus absent. Anterior eye row slightly procurved, posterior recurved. Ocular sizes and interdistances: AME 0.25, ALE 0.33, PME 0.23, PLE 0.25, AME-AME 0.05, AME-ALE 0.05, PME-PME 0.43, PME-PLE 0.03, ALE-PLE 0.05, AME-PME 0.05, ALE-ALE 0.55, PLE-PLE 0.60. Chelicerae as in male. Rastellum absent. Cheliceral furrow with two rows of well-developed teeth, 12/7 teeth on promargin, 11/13 teeth on retromargin. Labium sub-trapezoid, length 0.6, width 1.2, with 53 cuspules on anterior edge (Figure 8A). Labio-sternal groove wide. Maxillae longer than wide, with the anterior prolateral lobe very elongated, conical; with 75/77 cuspules spaced, largely spread over prolatero-ventral border from the inner edge to anterior lobe. Sternum and sigillae as in male; sternum length 2.0, width 2.7 (Figure 8A).

Legs: cuticle as in male. Leg and palpal segments measurements provided in Table 7. Legs I clearly thicker than the others. Bristles, clubbed, thorn-like setae, and spines present. Trichobothria: filiform, on central 2/3 of tarsi, palp 5, legs I–II 5, III 4, IV 6; on distal 1/4 of metatarsi, leg I 4, II 3, III 4, IV 2; on proximal 1/3 of tibiae, palp 4, legs I-II two rows of 2 each, III two rows of 3 and 2 each, IV 4. Scopula and pseudoscopula absent. Claw tufts absent. Tarsal claws: ITC present on leg I; STC present on all legs with one tooth. Spination: principally thorn-like setae on all segments. Spines: palp 0; leg I fe 0, pa 0, ti 0, me 2v, 2pv, 4rv,1r, ta 4pv, 5rv; leg II fe 0, pa 0, ti 0, me 1pd, 2v, 1pv, ta 0; leg III fe 0, pa 0, ti 0, me 1pv, 1pd, ta 0; leg IV fe 0, pa 0, ti 0, me 1pv, ta 0.

Abdomen: book lung apertures and spinnerets as in male (Figure 8B). Two spermathecal receptacles with a tubular neck, ended in a globose flattened fundus; spermathecal fundus with higher density of glands than the neck (mushroom shaped, Figure 8D). Spinnerets: PMS length 0.40; PLS length 2.20, apical segment digitiform (Figure 8B).

Distribution. Only known from its type locality, Central Cordillera of the Colombian Andes, Antioquia Department, Medellin (Santa Elena), at 2400 m altitude (Figure 10).

Etymology. The species epithet *paisa* is a noun in apposition which means the vernacular name given to the people of Medellín, where the species occurs.

***Stormtropis parvum* sp. n.**
http://zoobank.org/0D2EEF63-4E0D-4D0E-A067-F179CC4D45D5
Figure 9

Type material. ***Holotype*** male from Colombia, Caldas, Pensilvania, Berlín, 5.35222N, 75.18611W, 2750 m, 24-28-vii-2004, col. E Gonzáles, L Arango, JM Molina (ICN-Ar 11444).

Diagnosis. *Stormtropis parvum* sp. n. differs from the other species of the genus by the less numerous and discontinuous row of cheliceral teeth on promargin (2-2-3) (Figure 9B), and by the presence of a tibial apophysis, with a larger base, more separated from the tibia than on the other species (Figure 9D, E). Additionally, differs from *S. paisa* by the absence of a sclerotized dark mark on proximal dorsal tibia, without excavation, and lower number of spines in the spur (eleven on the distal row and six on proximal).

In addition, *S. parvum* is smaller (6mm), with lighter red and brown tones, and lives at higher elevation (2750 m) than *S. colima* (8.4 mm; 1377 m) and *S. paisa* (8.5 mm; 2400 m).

Description. ***Holotype male*** (ICN-Ar 11444) (Figure 9): total length 6.0; carapace length 2.9, width 2.8; abdomen length 2.8, width 2.3; chelicerae length 1.5. Color (in alcohol): body with soil particles encrusted; carapace, chelicerae, coxa, trochanter and femur red brown; abdomen dorsally and patella-tarsus brown. Carapace: glabrous, striae conspicuous, lateral margins with single line of curved setae mixed with disperse clubbed setae; caput arched, separated from thoracic region by trans-

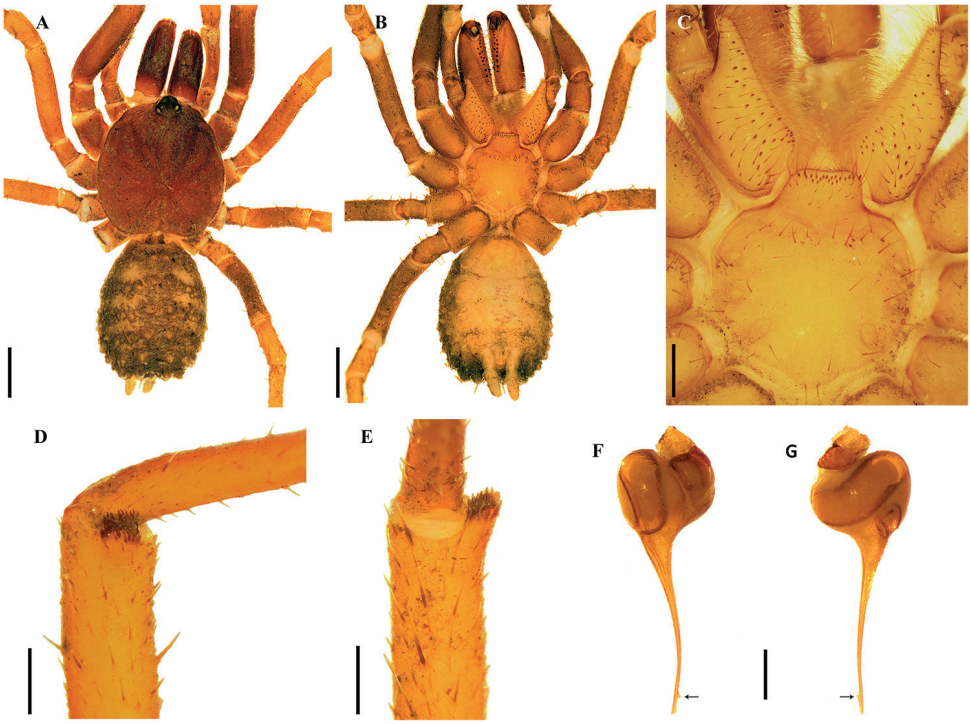

Figure 9. *Stormtropis parvum* gen. n., sp. n., male. **A, B** *habitus* **A** dorsal view **B** ventral view **C** sternum, labium and maxillae **D, E** tibial apophysis on leg I **D** prolateral view **E** ventral view **F, G** palpal bulb **F** prolateral view **G** retrolateral view. Arrows point to the triangular tooth on the subapical region of the embolus. Scale bars: 1.0 mm (**A, B**); 0.5 mm (**C**); 0.25 mm (**D, E**); 0.25 mm (**F, G**).

Table 8. Length (in mm) of legs and palpal segments of the holotype male *Stormtropis parvum* sp. n.

	I	II	III	IV	Palp
Femur	2.6	2.1	1.8	2.5	1.4
Patella	1.3	1.1	0.9	1.0	0.8
Tibia	2.1	1.5	1.3	2.0	1.0
Metatarsus	1.9	1.7	1.5	2.1	–
Tarsus	1.1	1.1	1.1	1.2	0.5
Total	9.0	7.5	6.6	8.8	3.7

verse shallow fovea, straight, width 0.3 (Figure 9A). Eyes and ocular tubercle: tubercle length 0.5, width 0.6, very elevated (height 0.4) and forwardly directed, with few stout setae. Clypeus absent. Anterior eye row slightly procurved, posterior slightly recurved. Ocular sizes and interdistances: AME 0.15, ALE 0.18, PME 0.13, PLE 0.14, AME-AME 0.10, AME-ALE 0.03, PME-PME 0.25, PME-PLE 0.03, ALE-PLE 0.03, AME-PME 0.03, ALE-ALE 0.35, PLE-PLE 0.38. Chelicerae: dorsally with few plumose setae, short sparse bristles on dorsal and lateral areas, long fine bristles on ventral and anterior area. Rastellum absent. Cheliceral furrow narrow with two rows of teeth,

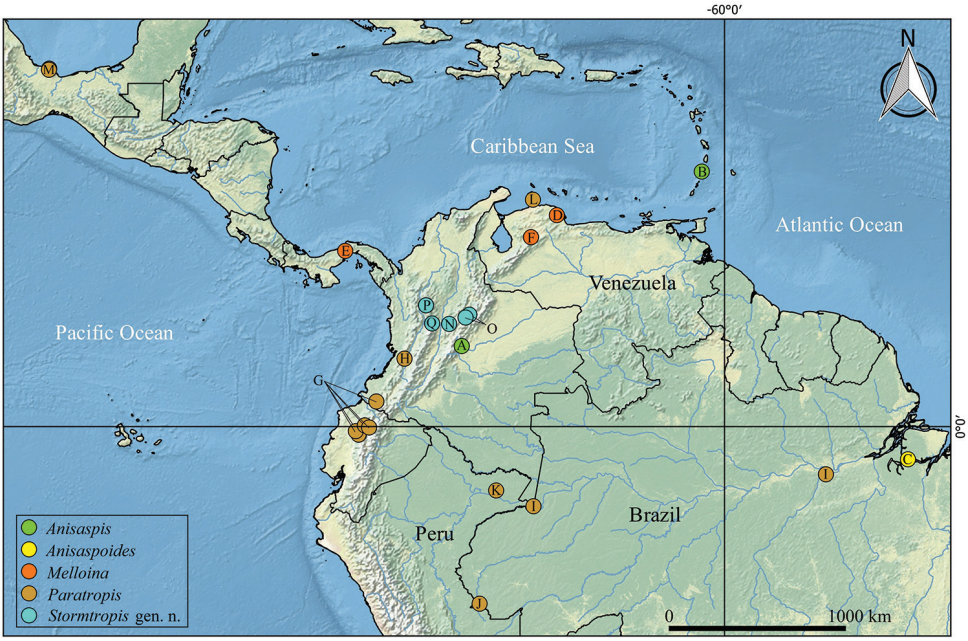

Figure 10. Distribution records of the entire family Paratropididae Simon, 1889; genera differentiated by color. **A** *Anisaspis camarita* sp. n. **B** *Anisaspis tuberculata* Simon, 1892 **C** *Anisaspoides gigantea* F.O. Pickard-Cambridge, 1896 **D** *Melloina gracilis* (Schenkel, 1953) **E** *Melloina rickwesti* Raven, 1999 **F** *Melloina santuario* Bertani, 2013 **G** *Paratropis elicioi* Dupérré, 2015 **H** *Paratropis florezi* sp. n. **I** *Paratropis papilligera* F.O. Pickard-Cambridge, 1896 **J** *Paratropis sanguinea* Mello-Leitão, 1923 **K** *Paratropis scruposa* Simon, 1889 **L** *Paratropis seminermis* Caporiacco, 1955 **M** *Paratropis tuxtlensis* Valdez-Mondragón, Mendoza & Francke, 2014 **N** *Stormtropis colima* gen. n., sp. n. **O** *Stormtropis muisca* gen. n., sp. n. **P** *Stormtropis paisa* gen. n., sp. n. **Q** *Stormtropis parvum* gen. n., sp. n.

7 teeth on promargin, on a discontinuous row (proximal-distal: 2-2-3); and 8/9 teeth on retromargin. Fang long. Labium subquadrate, length 0.25, width 0.65, with 20 elongated cuspules on anterior edge (Figure 9C). Labio-sternal groove narrower in the middle than laterally. Maxillae longer than wide, with the anterior prolateral lobe very elongated, conical; with 24/29 elongated cuspules widely distributed throughout the prolateral half of the maxillae; field of cuspules wider proximally (Figure 9C). Sternum heart shaped, length 1.15, width 1.53; three pairs of sigillae, anterior and median subcircular, submarginal; posterior sigillae oval, marginal (Figure 9C).

Legs: cuticle with soil particles encrusted. Leg and palpal segments measurements provided in Table 8. Leg I slightly stouter than II–IV. Clubbed plumose and thorn-like setae. Trichobothria: filiform, on central 2/3 of tarsi, palp and all legs 3; on distal 1/4 of metatarsi, all legs 2; and on proximal 1/3 of tibiae, palp and legs I–III two rows of 2 each, IV 3. Scopula absent, few and sparse pseudocopula setae on tarsi I and II. Claw tufts absent. Tarsal claws: ITC absent on all legs; STC long, with one tooth on all legs. Tibial apophysis on leg I present: only one flattened branch on distal prolateral side,

with spines on two parallel rows: 11 distal and 6 proximal (Figure 9D, E). Thorn-like setae mainly present on legs III and IV. Spines absent.

Palp: cymbium with two unequal lobes separated by a sclerotized groove; tibia with shallow distoventral groove. Palpal bulb pyriform elongated; embolus curved very long, tapering to the apex; a triangular translucent tooth on the subapical region (Figure 9F, G).

Abdomen: oval, with seven transverse dorsal rows of 4–6 small clubbed setae; lateral and dorsal area finely tuberculate, with smaller plumose clubbed setae, principally on posterior area (Figure 9A). Book lung apertures projected, oval, sclerotized (Figure 9B). Spinnerets: PMS length 0.20; PLS length 1.10, apical segment digitiform (Figure 9B).

Female: unknown.

Distribution. Only known from its type locality, in the Central Cordillera of Colombian Andes, eastern flank, at 2750 m altitude, Caldas Department, Pensilvania, Berlín (Figure 10).

Etymology. The species epithet *parvum* is a Latin adjective (neuter) which means little; *S. parvum* sp. n. is the smallest species of the genus known to date.

Discussion

Our examination of collections as well as field work revealed that paratropidids are very well represented among the aracnofauna of Colombia, currently represented by three genera and eight species. They are commonly present in diverse habitats, mainly in the soil, under stones, rotten logs and in burrows or crevices in ravines. Unexpectedly, and in spite of few unpublished data, the family was not formally reported for Colombia until now. However, de Mello-Leitão (1941) recorded *Paratropis scruposa* Simon, 1889 for Cúcuta (Colombia): this determination has not been included in the World Spider Catalog (2018); possibly this is a wrong identification, since the type locality of this species is in Peru. In this way, Paratropididae is here officially reported for Colombia as well as *Anisaspis*, *Paratropis*, and a new genus, *Stormtropis*.

Stormtropis gen. n. is described and represented only in Colombia, by *S. colima* sp. n., *S. muisca* sp. n., *S. paisa* sp. n., and *S. parvum* sp. n. The genus is distributed in the central Andean region of the country, between altitudes of 1377 and 3415 m. The altitudinal record of *S. muisca* sp. n. (above 3400 m) represents the highest of the family Paratropididae. *Anisaspis* is represented by *A. tuberculata* (St. Vincent) and *A. camarita* sp. n. (Colombia); the latter is distributed in the foothills of the eastern Colombian Andes, ca. 570–600 m altitude. *Paratropis* is distributed in Mexico, Antilles, and northern South America. It is represented by seven species, one of them described here as *P. florezi* sp. n., that inhabits in the south of western Cordillera of the Colombian Andes, at ca. 1800 m altitude. The geographic distributions of *P. elicioi* and *P. papilligera* are extended; the first to the south of the Colombian Andes and the second in the Colombian Amazon. *Paratropis* is widely distributed throughout Colombia and Ecuador and is present in almost all regions, from coasts and Amazonian lowlands reaching heights of ca. 2000 m in the Andean region. We have also records of the presence of the

genus *Melloina* in Colombia, but we did not include it here because we have molecular evidence that places it out of Paratropididae (Perafán et al. in preparation).

Although Colombian paratropidid species richness is the highest found in a country (WSC 2018), several undescribed species are expected to be found in the future, considering the enormous and unexplored ecological diversity of mygalomorph spiders in this region (Perafán 2017, Perafán and Valencia-Cuéllar 2018), coupled with the evidence of numerous specimens not yet studied.

Stormtropis gen. n. includes some species in which males have a tibial apophysis, a feature not found among paratropidids (except *Melloina*) until now. It is probably a recent acquisition of this group of species, which should be more closely related with *Paratropis*, but this hypothesis must be tested with a rigorous phylogenetic analysis. Another remarkable morphological characteristic of this genus is the sexual dimorphism in tarsal claws: ITC on leg I is only present in females. The presence of ITC on leg I was originally used to diagnose *Paratropis* from other paratropidids, but Valdéz-Mondragón et al. (2014) found that females of *Paratropis tuxtlensis* have ITC on legs I and II but males lack them. Likewise, Dupérré (2015) described *Paratropis elicioi*, lacking ITC in both sexes, and considered this character as ambiguous. We consider that there is a great inter- and intraspecific variation in this character, so this independent character should be carefully taken into account in the taxonomy of the family. Another sexual difference found in the Paratropidinae is related to the pseudoscopula, present in males and absent in females, as was reported for several Mygalomorphae (Pérez-Miles et al. 2017).

An important characteristic of Paratropididae, unique among Mygalomorphae, is the ability to adhere soil particles to their scaly cuticle. Although the natural history of the group is poorly known, paratropidids were considered cursorial spiders which hide themselves in the surface layers of the soil (West in Raven 1999). This condition should be compatible with the presence of soil encrusted on the cuticle, facilitating the camouflage of individuals on the ground. However, and unexpectedly in our field study, we found several females of *P. florezi* sp. n. and other undetermined species inhabiting tubular burrows on ravine walls or soil. Considering that burrowing paratropidids maintain the encrusted cuticle, burrowing habits could be a secondary adaptation in order to exploit different habitats.

Acknowledgments

We acknowledge Eduardo Flórez (ICN, Colombia) for his hospitality during our stays and his help in examination of the ICN collection. Thanks to Álvaro Barragán (QCAZ) and Janet Beccaloni (NHM) for the loan specimens, and the anonymous reviewers and the editors for their suggestions and corrections which markedly improved the paper. CP and FPM thank the Comisión Sectorial de Investigación Científica (CSIC, UDELAR) for travel facilities for the field studies in 2016. CP thanks Agencia Nacional de Investigación e Innovación (ANNI), Uruguay, for PhD scholarship, under POS_NAC_2011_1_3624 code.

References

Bertani R (2013) A new species of *Melloina* (Araneae: Paratropididae) from Venezuela. Zoologia (Curitiba) 30: 101–106. https://doi.org/10.1590/S1984-46702013000100013

Bond JE, Hedin M (2006) A total evidence assessment of the phylogeny of North American euctenizine trapdoor spiders (Araneae, Mygalomorphae, Cyrtaucheniidae) using Bayesian inference. Molecular Phylogenetics and Evolution 41: 70–85. https://doi.org/10.1016/j.ympev.2006.04.026

Bond JE, Hendrixson BE, Hamilton CA, Hedin M (2012) A reconsideration of the classification of the spider infraorder Mygalomorphae (Arachnida: Araneae) based on three nuclear genes and morphology. PLoS ONE 7(6): e38753. https://doi.org/10.1371/journal.pone.0038753

Brignoli PM (1985) On some generic homonymies in spiders (Araneae). Bulletin of the British Arachnological Society 6: 380.

Caporiacco L di (1955) Estudios sobre los aracnidos de Venezuela. 2a parte: Araneae. Acta Biologica Venezuelica 1: 265–448.

Dupérré N (2015) Description of the first visually cryptic species of *Paratropis* (Araneae: Paratropididae) from Ecuador. Journal of Arachnology 43(3): 327–330. https://doi.org/10.1636/arac-43-03-327-330

Fernández R, Kallal RJ, Dimitrov D, Ballesteros JA, Arnedo MA, Giribet G, Hormiga G (2018) Phylogenomics, Diversification Dynamics, and Comparative Transcriptomics across the Spider Tree of Life. Current Biology 28(9): 1489–1497. https://doi.org/10.1016/j.cub.2018.03.064

Flórez-D E, Sánchez-C H (1995) La diversidad de los arácnidos en Colombia, aproximación inicial. In: Rangel-Ch JO (Ed.) Colombia Diversidad Biótica I. Instituto de Ciencias Naturales-Universidad Nacional de Colombia-Inderena, Bogotá, 327–371.

Garrison NL, Rodriguez J, Agnarsson I, Coddington JA, Griswold CE, Hamilton CA, Hedin M, Kocot KM, Ledford JM, Bond JE (2016) Spider phylogenomics: untangling the spider tree of life. PeerJ 4: e1719. https://doi.org/10.7717/peerj.1719

Goloboff PA (1993) A reanalysis of mygalomorph spider families (Araneae). American Museum Novitates 3056: 1–32.

Hamilton CA, Lemmon AR, Moriarty Lemmon E, Bond JE (2016) Expanding anchored hybrid enrichment to resolve both deep and shallow relationships within the spider tree of life. BMC Evolutionary Biology 16: 212. https://doi.org/10.1186/s12862-016-0769-y

Hedin M, Derkarabetian D, Ramírez MJ, Vink C, Bond JE (2018) Phylogenomic reclassification of the world's most venomous spiders (Mygalomorphae, Atracinae), with implications for venom evolution. Scientific Reports 8: 1636. https://doi.org/10.1038/s41598-018-19946-2

Jocqué R, Dippenaar-Schoeman AS (2006) Spider Families of the World. Musée Royal de l'Afrique Central, Tervuren, 336 pp.

de Mello-Leitão CF (1923) Theraphosideas do Brasil. Revista do Museu Paulista 13: 1–438.

de Mello-Leitão CF (1941) Catalogo das aranhas da Colombia. Anais da Academia Brasileira de Ciências 13: 233–300.

Perafán C (2017) Distribución actual e histórica del infraorden Mygalomorphae (Araneae) en los Andes del norte. PhD Thesis, Facultad de Ciencias, Universidad de la República, Montevideo.

Perafán C, Valencia-Cuéllar D (2018) *Proshapalopus marimbai*, a new tarantula species (Mygalomorphae, Theraphosidae) and first genus record from Colombia. Tropical Zoology 31(4): 200–213. https://doi.org/10.1080/03946975.2018.1493181

Perafán C, Sabogal A, Moreno-González JA, García-Rincón A, Luna-Sarmiento D, Romero-Ortíz C, Flórez E (2013) Diagnóstico del estado actual de la fauna de arácnidos y de su gestión en Colombia. In: Rueda-Ramírez D, Torrado-León E, Becerra EH (Eds) Memorias 40 Congreso Colombiano de Entomología, Bogotá (Colombia), July 2013. Sociedad Colombiana de Entomología (Socolen), DVD, Bogotá, 479 pp.

Pérez-Miles F, Guadanucci JPL, Jurgilas JP, Becco R, Perafán C (2017) Morphology and evolution of scopula, pseudoscopula and claw tufts in Mygalomorphae (Araneae). Zoomorphology 136(4): 345–459. https://doi.org/10.1007/s00435-017-0364-9

Pickard-Cambridge, FO (1896) On the Theraphosidae of the lower Amazons: being an account of the new genera and species of this group of spiders discovered during the expedition of the steamship "Faraday" up the river Amazons. Proceedings of the Zoological Society of London 64(3): 716–766. [pls XXXIII–XXXV] https://doi.org/10.1111/j.1096-3642.1896.tb03076.x

Raven RJ (1985) The spider infraorder Mygalomorphae (Araneae): Cladistics and systematics. Bulletin of the American Museum of Natural History 182: 1–180.

Raven RJ (1999) Review of the mygalomorph genus *Melloina* Brignoli (Paratropididae: Araneae). Memoirs of the Queensland Museum 43: 819–825.

Schenkel E (1953) Bericht über einige Spinnentiere aus Venezuela. Verhandlungen der Naturforschenden Gesellschaft in Basel 64: 1–57.

Simon E (1889) Arachnides. Voyage de M.E. Simon au Venezuela (décembre 1887-avril 1888). 4e Mémoire. Annales de la Société Entomologique de France 69: 169–220.

Simon E (1892) On the spiders of the island of St. Vincent. Part 1. Proceedings of the Zoological Society of London 59(4, for 1891): 549–575. [pl. XLII]

Valdez-Mondragón A, Mendoza JI, Francke OF (2014) First record of the mygalomorph spider family Paratropididae (Arachnida, Araneae) in North America with the description of a new species of *Paratropis* Simon from Mexico, and with new ultramorphological data for the family. ZooKeys 416: 1–21. https://doi.org/10.3897/zookeys.416.7253

Wheeler WC, Coddington JA, Crowley LM, Dimitrov D, Goloboff PA, Griswold CE, Hormiga G, Prendini L, Ramírez MJ, Sierwald P, Almeida-Silva LM, Álvarez-Padilla F, Arnedo MA, Benavides LR, Benjamin SP, Bond JE, Grismado CJ, Hasan E, Hedin M, Izquierdo MA, Labarque FM, Ledford J, Lopardo L, Maddison WP, Miller JA, Piacentini LN, Platnick NI, Polotow D, Silva-Dávila D, Scharff N, Szűts T, Ubick D, Vink C, Wood HM, Zhang JX (2017) The spider tree of life: phylogeny of Araneae based on target-gene analyses from an extensive taxon sampling. Cladistics 33(6): 576–616. https://doi.org/10.1111/cla.12182

World Spider Catalog (2018) World Spider Catalog. Version 19.5. Natural History Museum Bern. http://wsc.nmbe.ch [Accessed on 22 Oct 2018]

ZooKeys 830: 33–51 (2019)
doi: 10.3897/zookeys.830.33060
http://zookeys.pensoft.net

RESEARCH ARTICLE

A peer-reviewed open-access journal
ZooKeys
Launched to accelerate biodiversity research

A new species of the genus *Arrup* from a limestone cave in Akiyoshi-dai, Western Japan (Chilopoda, Geophilomorpha, Mecistocephalidae)

Sho Tsukamoto[1], Satoshi Shimano[2], Takashi Murakami[3], Shimpei F. Hiruta[4], Takeshi Yamasaki[1], Katsuyuki Eguchi[1]

1 *Systematic Zoology Laboratory, Graduate School of Science, Tokyo Metropolitan University, Minami-osawa 1-1 Hachioji-shi, Tokyo, 192-0397, Japan* **2** *Science Research Center, Hosei University, Fujimi 2-17-1 Chiyo-da-ku, Tokyo, 102-8160, Japan* **3** *Cultural Property Protection Division, Board of Education, Mine City Office, Akiyoshi 5353-1 Shuho-cho, Yamaguchi, 754-0511, Japan* **4** *Center for Molecular Biodiversity Research, National Museum of Nature and Science, Tokyo, Amakubo 4-1-1 Tsukuba-shi, Ibaraki, 305-0005, Japan*

Corresponding author: *Sho Tsukamoto* (esutukamoto153@gmail.com)

Academic editor: *M. Zapparoli* | Received 13 January 2019 | Accepted 24 January 2019 | Published 14 March 2019

http://zoobank.org/04BFCAE4-6B9A-4B87-AEB9-7E871E46AAB2

Citation: Tsukamoto S, Shimano S, Murakami T, Hiruta SF, Yamasaki T, Eguchi K (2019) A new species of the genus *Arrup* from a limestone cave in Akiyoshi-dai, Western Japan (Chilopoda, Geophilomorpha, Mecistocephalidae). ZooKeys 830: 33–51. https://doi.org/10.3897/zookeys.830.33060

Abstract

Arrup akiyoshiensis Tsukamoto & Shimano, **sp. n.** is described from a limestone cave, Kagekiyo-ana, in Akiyoshi-dai, one of the largest karst regions in Japan, Yamaguchi prefecture. It is distinguishable from 14 valid named congeners by some unique characteristics including entire areolation on the cephalic pleurite, elongation of distal part of female gonopod, and a tubercle on forcipular segment II. In addition, the 18S rRNA gene sequences of *A. akiyoshiensis* Tsukamoto & Shimano, **sp. n.** and *A. ishiianus,* one of the most morphologically similar species, differed by four bp out of 1821 bp. The fact that only troglobionts and troglophilic species are found in the collection site suggests that this new species might be a cave-dweller.

Keywords

Arrupinae, Chilopoda, Kagekiyo-ana, limestone, taxonomy, 18S rRNA gene

Introduction

Centipedes are for the most part soil-dwellers, and common in various habitats such as forests, grasslands, coastal areas and so on (Lewis 1981). Although the most of soil-dwelling animal taxa have troglobionts species, few troglobiotic centipedes have so far been recorded (Chagas-Jr and Bichuette 2018). Especially, despite high adaptation for subterranean habitats, only two troglobionts species are hitherto known in Geophilomorpha: *Geophilus persephones* Foddai & Minelli, 1999 and *Geophilus hadesi* Stoev, Akkari, Komerički, Edgecombe & Bonato, 2015. Both of them have unusual traits, which are common among troglobiotic arthropods (exceptionally elongated antennae, legs, and claws) (Foddai and Minelli 1999, Stoev et al. 2015). In Japan, several centipede species can be found in both the inside and outside cave, and Shinohara (1966) referred two species were considered to be troglobiotic centipedes; *Brachygeophilus polyporus* Takakuwa, 1942 (Geophilomorpha) and *Monotarsobius minor* Takakuwa, 1942 (Lithobiomorpha). Commonly, the troglobiotic fauna has a high proportion of endemic species in each cave or cave group (Gibert and Deharveng 2002; Christman et al. 2005). Many endemic species with small geographic ranges may occur in isolated caves (Barr Jr and Holsinger 1985); therefore, the inventory of the troglobiotic fauna is important to clarify the formulation of endemism.

Akiyoshi-dai, where is a one of the largest karst regions in Japan, has a spread of 16 km in northeast direction and 6 km northwest direction, with more than 400 limestone caves (Fujii 2009). Thirteen invertebrate species are endemic to the area (Kuramoto 1980). For Chilopoda, 13 species are recorded from Akiyoshi-dai, but all of them are not endemic species (Kuramoto 1980). In the course of our recent survey of cave invertebrates in Kagekiyo-ana cave of Akiyoshi-dai, six individuals belonging to the genus *Arrup* Chamberlin, 1912 were collected, and later confirmed as a new species based on our careful morphological examination and comparison with 14 valid named congeners (Uliana et al. 2007, Bonato et al. 2016) by using cephalic capsule, mandible, maxillae, the number of coxal pore and genital segments. We herein describe this species as *A. akiyoshiensis* sp. n.

Materials and methods

Two adult female specimens and four juvenile specimens of *A. akiyoshiensis* sp. n. were collected by hand under rocks inside Kagekiyo-ana cave (a limestone cave; 34°17.50'N, 131°20.00'E), in Akiyoshi-dai (a karst region), Mitou-cho, Mine-shi, Yamaguchi Prefecture, Japan. The exact position of the collection site is shown in Fig. 1. This was 130 m below the surface, 500 m from the northern entrance, and 900 m from the southern entrance of the cave. In addition, one specimen of *A. ishiianus* Uliana, Bonato & Minelli, 2007 from Imperial Palace, Tokyo was used for comparing morphology

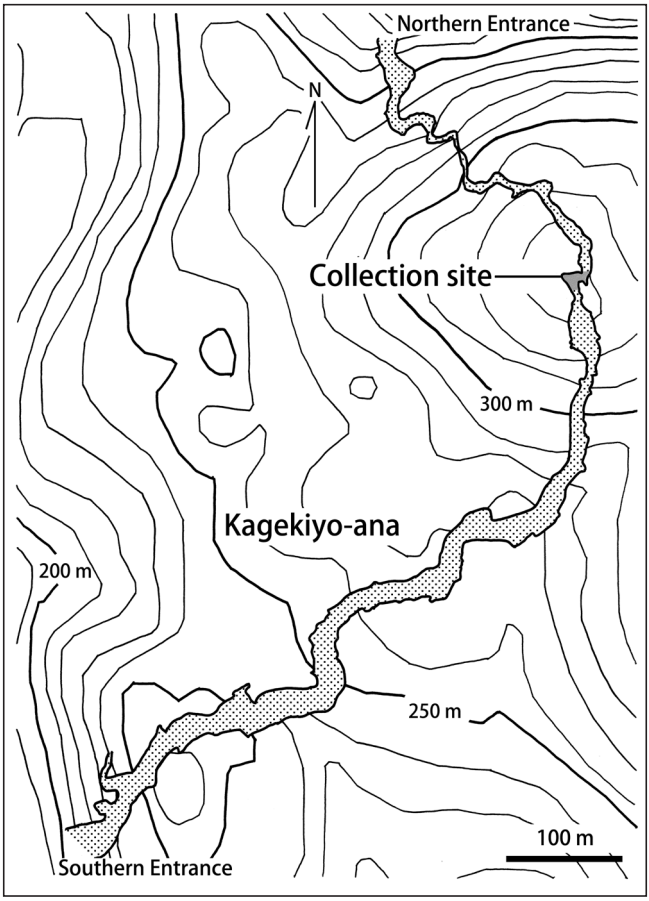

Figure 1. A map of Kagekiyo-ana cave. Contour lines are shown with altitudes every 50 m.

and 18S rRNA gene sequence with *A. akiyoshiensis* sp. n. Each specimen examined in the present study is specified by its specimen identification number, in the form "TS-YYYYMMDD-XX"; where TS is an abbreviation of the first author, Tsukamoto Sho; YYYYMMDD designates the date on which the specimen was collected; and XX is the identification number given to each specimen collected on that date (e.g., TS-20180330-01). All specimens are deposited at the Collection of Myriapoda, Department of Zoology, National Museum of Nature and Science, Tokyo (**NMST**).

Specimens were observed and drawn in lactic acid on temporary cavity slides using a Nikon Eclipse E600 microscope, and were then mounted with Hoyer's medium (gum arabic, chloral hydrate and glycerol). Some characters were photographed by using Panasonic LUMIX DMC-GX8 and Canon EOS Kiss X9, and focus stack images were produced from a series of pictures at different focal planes by Helicon Focus Pro version 6.6.1 on a desktop PC. Note that the external shape might be slightly distorted

when immersed in lactic acid because of expansion of internal tissue. Besides, specimens were measured with their each part mounted with Hoyer's medium in order to avoid distortion of the external shape. The morphological terminology used below is mainly based on Bonato et al. (2010).

Genomic DNA was extracted from part of the appendage using a DNeasy Blood & Tissue Kit (Qiagen), with modifications from Johnson et al. (2004). An appendage of each specimen was incubated at 55 °C for 48 h to lyse the tissue. Before each lysis mixture was pipetted into a spin column, the exoskeleton was retrieved and preserved in 100% Ethanol.

Table 1 lists all primers used in this study. Partial sequences of 18S rRNA gene were amplified by polymerase chain reactions (PCR) using the primer sets, 18S-F1 and 18S-R9 (Yamaguchi and Endo 2003). The PCR amplification was performed in a Thermal Cycler Dice (Takara) in a 10 µl volume containing 0.5 µl of template solution, 2 mM $MgCl_2$, 2.5 mM each dNTP, 10 pmol each primer, and 0.25 U Ex Taq polymerase Hot Start version (Takara) in 1× buffer provided by the manufacturer. Amplification conditions were 95 °C for 2 min; 35 cycles of 95 °C for 30 sec, 50 °C for 30 sec, and 72 °C for 2 min; and 72 °C for 7 min.

Amplification products were purified with the ExoSAP-IT kit (Thermo Fisher Scientific). All nucleotide sequences were determined by direct sequencing using a BigDye Terminator Cycle Sequencing Kit ver. 3.1 with an ABI 3500XL automated sequencer (Thermo Fisher Scientific). The amplification primers and internal primers were used in sequencing 18S rRNA gene. Nucleotide sequences were assembled and edited with MEGA7 (Kumar et al. 2016). Sequences have been deposited in DDBJ/EMBL/GenBank database under accession numbers LC460298–LC460301 (Table 2).

Table 1. Primers used in this study.

Gene	Name	Sequence (5'–3')	Direction	Source	Used for PCR
18S rRNA	18S-F1	TACCTGGTTGATCCTGCCAG	forward	Yamaguchi and Endo (2003)	*
	18S-F2	CCTGAGAAACGGCTRCCACAT	forward	Yamaguchi and Endo (2003)	
	18S-F3	GYGRTCAGATACCRCCSTAGTT	forward	Yamaguchi and Endo (2003)	
	18S-F4	GGTCTGTGATGCCCTYAGATGT	forward	Yamaguchi and Endo (2003)	
	18S-R6	TYTCTCRKGCTBCCTCTCC	reverse	Yamaguchi and Endo (2003)	
	18S-R7	GYYARAACTAGGGCGGTATCTG	reverse	Yamaguchi and Endo (2003)	
	18S-R8	ACATCTRAGGGCATCACAGACC	reverse	Yamaguchi and Endo (2003)	
	18S-R9	GATCCTTCCGCAGGTTCACCTAC	reverse	Yamaguchi and Endo (2003)	*

Table 2. GenBank accession numbers of *Arrup* sequence data.

Species	Collection site	Specimen identification no.	Accession no.
Arrup akiyoshiensis	Kagekiyo-ana, Yamaguchi	TS-20180330-01 (holotype)	LC460298
Arrup akiyoshiensis	Kagekiyo-ana, Yamaguchi	TS-20180418-01 (paratype)	LC460299
Arrup akiyoshiensis	Kagekiyo-ana, Yamaguchi	TS-20180418-02	LC460300
Arrup ishiianus	Imperial Palace, Tokyo	TS-20090729-01	LC460301

Taxonomy

Family Mecistocephalidae Bollmann, 1893
Genus *Arrup* Chamberlin, 1912

***Arrup akiyoshiensis* Tsukamoto & Shimano, sp. n.**
http://zoobank.org/6B8C8441-CD7C-4F1C-9280-1DF1D5EDB994
Figs 2–9, Tables 3–6
Japanese name: Kagekiyo-tsumejimukade

Type Material. Holotype 1 female, Kagekiyo-ana, Mitou Town (Mitou-cho), Mine City (Mine-shi), Yamaguchi Prefecture, Japan, 30th of March 2018, coll. Takashi Murakami (labeled as TS-20180330-01). **Paratype** 1 female, Kagekiyo-ana, Mitou Town (Mitou-cho), Mine City (Mine-shi), Yamaguchi Prefecture, Japan, 18th of April 2018, coll. Takashi Murakami (labeled as TS-20180418-01).

Etymology. The species name is derived from the name of Akiyoshi-dai Karst region, which includes the type locality.

Diagnosis. *Arrup akiyoshiensis* sp. n. can be distinguished from the all named congeners by a combination of the following morphological characteristics: frontal line curved; seven pectinate lamellae in mandible; comma-shaped distal lobe of coxal projection in first maxillae; a tiny tubercle on outer-distal corner of each article of the telopodite; distal article of the telopodite of the second maxillae without claw; the well-developed tooth of forcipular article I; the triangular basal tooth in tarsungulum; the poison calyx overreaching forcipular article I; 31–35 pores on lateral and ventral sides on coxopleura.

Description. Measurements of the holotype (adult female, TS-20180330-01) are followed by those of 1 paratype (adult female, TS-20180418-01) in parentheses. Body length 36.0 (34.5) mm, maximum body width 1.0 (0.95) mm, cephalic plate length 1.45 (1.30) mm, maximum cephalic plate width 0.92 (0.78) mm.

Antenna (Figs 2A–E, 3A–F, 7D, Tables 3–5) length 3.4 times as long as cephalic plate length. All articles weak areolate, except anterior margin; anterior margin of articles I to IV well areolate. Articles I to V slightly asymmetrical, with internal margin longer than external margin. Articles VI to XIV symmetrical. Setae on articles I to XIV spiniform, arranged uniformly (Figs 2A–D, 3A–D, Table 3). Distodorsal and distoventral surfaces of articles II, V, IX, and XIII with 1–7 small pointed sensilla (Fig. 2E, Table 5). Article XIV with 96–101 claviform sensilla on outer-lateral and inner-lateral sides (Figs 3A–E, triangle in Fig. 3A, Table 4), with 6–9 pointed sensilla on the tip (Figs 3A–D, F, arrow in Fig. 3A, Table 5).

Cephalic plate (Figs 4A, 8A) 1.5 times as long as wide. Transverse suture present. Paramedian sulci present. Lateral margins almost straight and convergent backwards; anterior margin convex; posterior margin straight. Surface areolated; proximal and distal scutes clearly marked. Setae arranged nearly symmetrically.

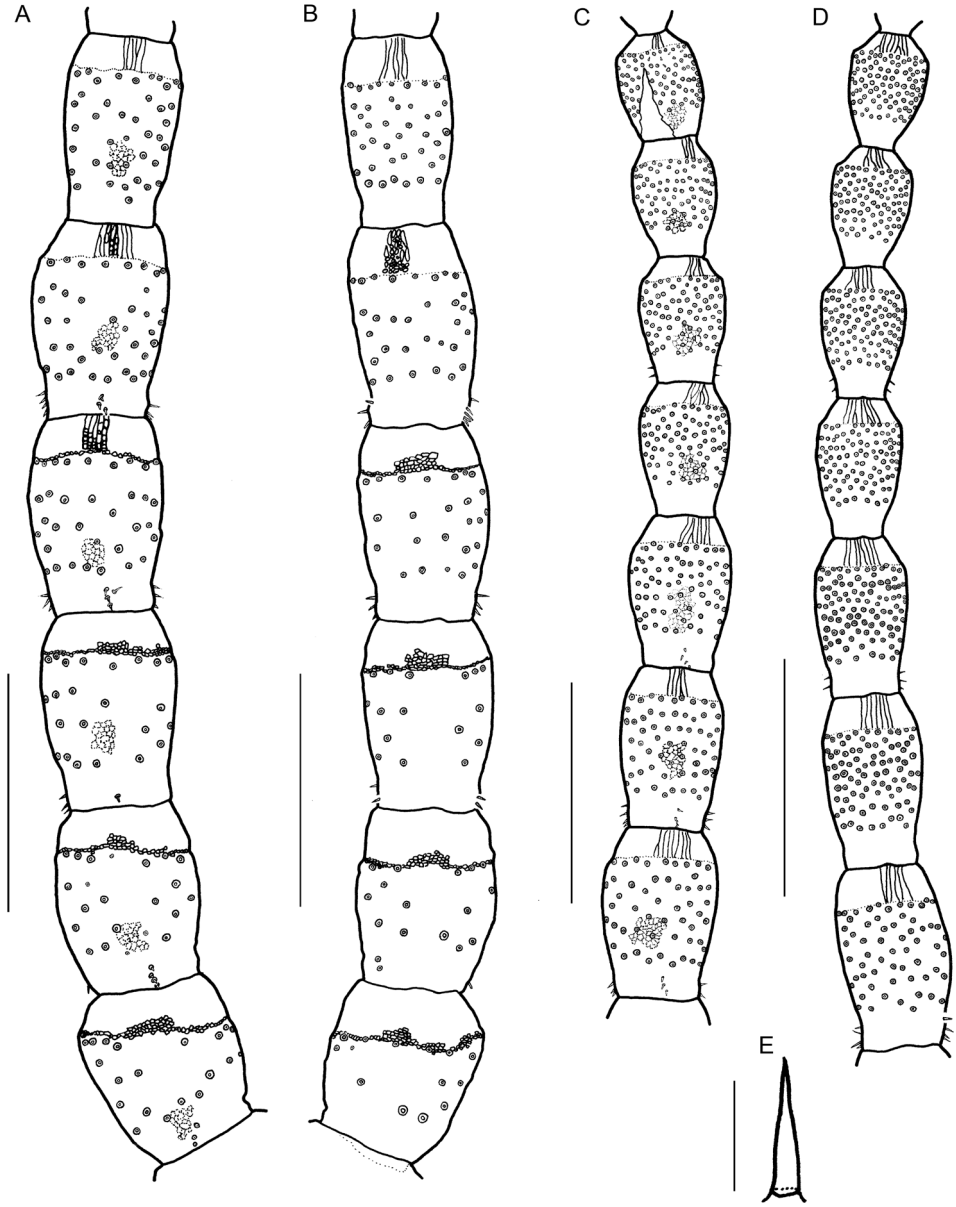

Figure 2. *Arrup akiyoshiensis* sp. n., holotype (TS-20180330-01), **A** right antennal article, I–VI, dorsal **B** right antennal article, I–VI, ventral **C** right antennal article, VII–XIII, dorsal **D** right antennal article, VII–XIII, ventral **E** a pointed sensillum on the dorsal side of article XIII. Setae are not drawn, only their sockets. Scale bars: 500 μm (**A–D**); 10 μm (**E**).

Clypeus (Figs 4B, 8B) 1.5 times as wide as long. Clypeal area absent. Paraclypeal sutures complete, strongly convergent backwards. Two clypeal plagulae not contacting with the paraclypeal sutures; remaining clypeal parts uniformly areolate, with setae arranged in two groups.

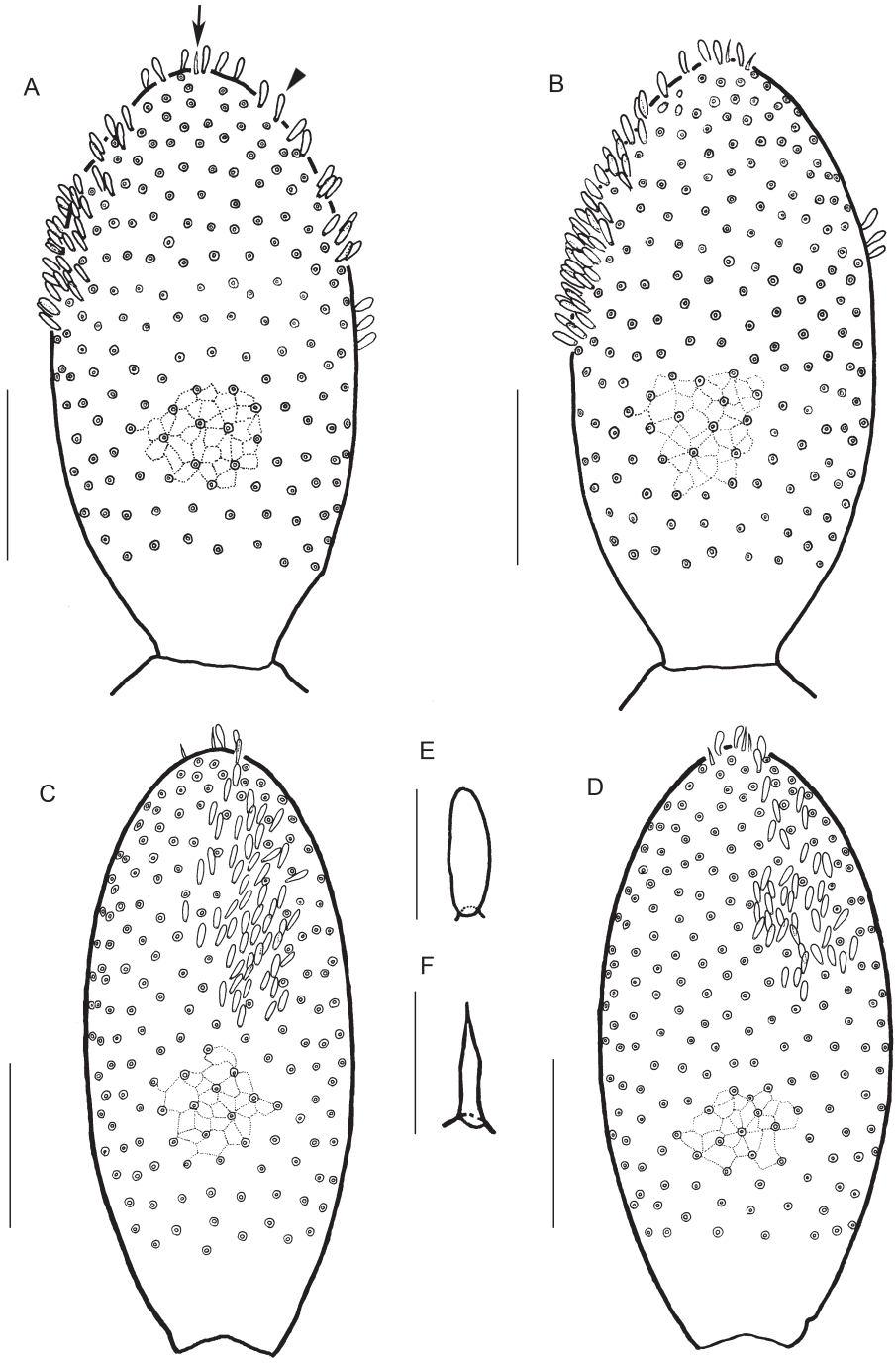

Figure 3. *Arrup akiyoshiensis* sp. n., holotype (TS-20180330-01), **A** right antennal article, XIV, dorsal **B** right antennal article, XIV, ventral **C** right antennal article, XIV, outer-lateral **D** right antennal article, XIV, inner-lateral **E** a claviform sensillum on the antennal article XIV (triangle in fig. 9) **F** a pointed sensillum on the antennal article XIV (arrow in fig. 9). Setae are indicated only with sockets. Scale bars: 100 µm (**A–D**); 25 µm (**E**); 12.5 µm (**F**).

Table 3. Number of right antennal setae of *Arrup akiyoshiensis* sp. n., holotype (TS-20180330-01).

Antennal article	I	II	III	IV	V	VI	VII	VIII	IX	X	XI	XII	XIII	XIV
Number of Setae	45	53	57	73	98	102	140	155	207	201	215	207	194	343

Table 4. Number of claviform sensilla on antennal article XIV of *Arrup akiyoshiensis* sp. n., holotype (TS-20180330-01), paratype (TS-20180418-01).

Side of antenna	Right		Left	
	Inner-lateral	Outer-lateral	Inner-lateral	Outer-lateral
Holotype (TS-20180330-01)	43	58	36	60
Paratype (TS-20180418-01)	38	61	n/a	n/a

Note n/a: Antennal article XIV left was lost.

Table 5. Number of antennal pointed sensilla of *Arrup akiyoshiensis* sp. n., holotype (TS-20180330-01).

Antennal article	I	II	III	IV	V	VI	VII	VIII	IX	X	XI	XII	XIII	XIV
Right, dorsal	0	3	0	0	8	0	0	0	4	0	0	0	3	6
Right, ventral	0	2	0	0	5	0	0	0	4	0	0	0	3	
Left, dorsal	0	1	0	0	7	0	0	0	7	0	0	0	3	9
Left, ventral	0	2	0	0	5	0	0	0	5	0	0	0	3	

Labrum (Fig. 4C) consisted of three pieces. Side pieces divided into anterior and posterior alae with convexed chitinous line. Longitudinal stripes on the posterior alae absent. Anterior margin of side pieces almost straight. Internal margins of side pieces convergent backward, but not bordered directly with each other. Posterior margin of side pieces convex. Mid-piece 1.1 times as long as wide.

Cephalic pleurite (Figs 4B, 8C) with areolation entirely except a part of anterior region; scutes clearly marked along anterior margin, lateral margin, and paraclypeal suture. Spicula absent. Setae absent. Stilus well chitinized.

Mandible (Fig. 4D, Table 6) with seven pectinate lamellae. Lamellar teeth sharp; 2–15 teeth present in each lamella (Table 6); anterior tooth gradually longer than posterior one in each lamella.

First maxillae (Figs 4E, 8D) undivided, without mid-longitudinal suture in coxosternite, convergent forward; anterior corners not projecting; ventral surface areolate, except for anterior and lateral margins; setae absent. Coxal projection well developed, with six spines on each internal margin and 4–5 setae at the each middle position. Basal part of medial projection round, with distal lobe; distal lobe clavate as comma-shaped. Basal part 1.7 times as long as distal lobe.

Second maxillae (Figs 4E, 8D) undivided, without mid-longitudinal suture in coxosternite; 5 + 5 setae arranged along the anterior margin, 3 + 3 setae on lateral side. Isthmus areolate. Anterior and posterior margins concave. Lateral margins

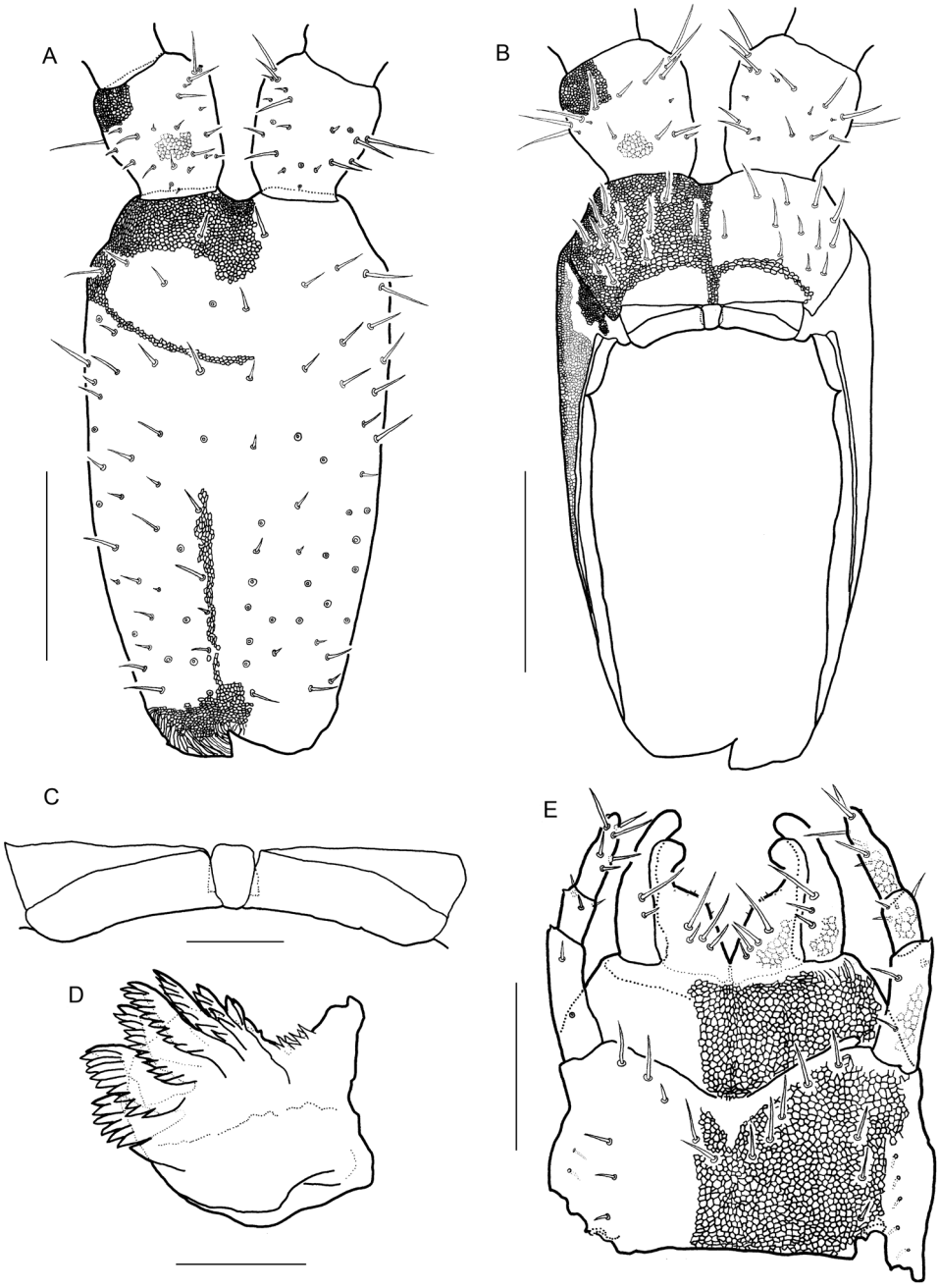

Figure 4. *Arrup akiyoshiensis* sp. n., holotype (TS-20180330-01), **A** cephalic plate, dorsal **B** clypeus and clypeal pleurite, ventral **C** labrum, ventral **D** right mandible, dorsal **E** maxillae complex, ventral. Note that **A–C** are distorted by the effects of lactic acid. Scale bars: 500 µm (**A, B**); 100 µm (**C, D**); 250 µm (**E**).

Table 6. Number of the pectinate lamellae of *Arrup akiyoshiensis* sp. n., holoype (TS-20180330-01) and paratype (TS-20180418-01).

Pectinate lamellae	Right							Left						
	I	II	III	IV	V	VI	VII	I	II	III	IV	V	VI	VII
Holotype (TS-20180330-1)	6	11	11	11	8	5	2	6	11	11	11	8	5	2
Paratype (TS-20180418-1)	6	11	15	12	8	4	2	6	11	13	9	3	4	–*

* pectinate lamella VII of paratype was broken.

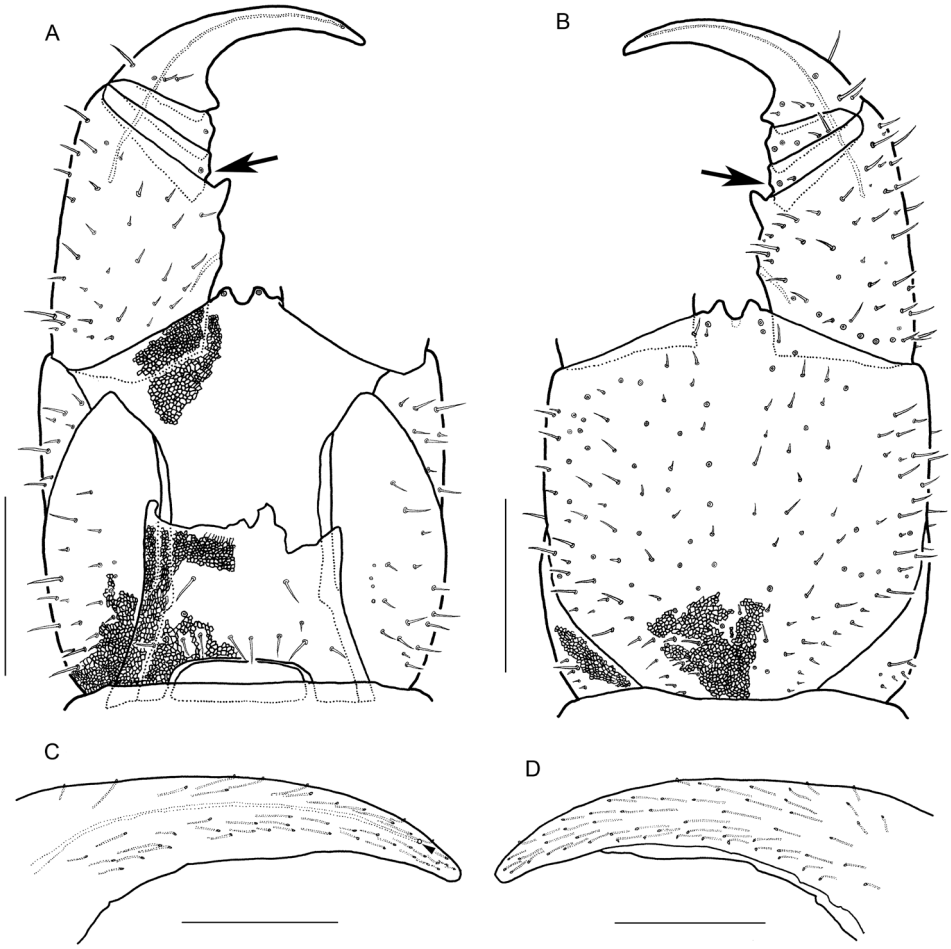

Figure 5. *Arrup akiyoshiensis* sp. n., **A, B** paratype (TS-20180418-01) **C, D** holotype (TS-20180330-01) **A** forcipular segment and left forcipule, dorsal **B** forcipular segment and left forcipule, ventral **C** claw of left tarsungulum, dosral **D** claw of left tarsungulum, ventral. Scale bars: 500 μm (**A, B**); 200 μm (**C, D**).

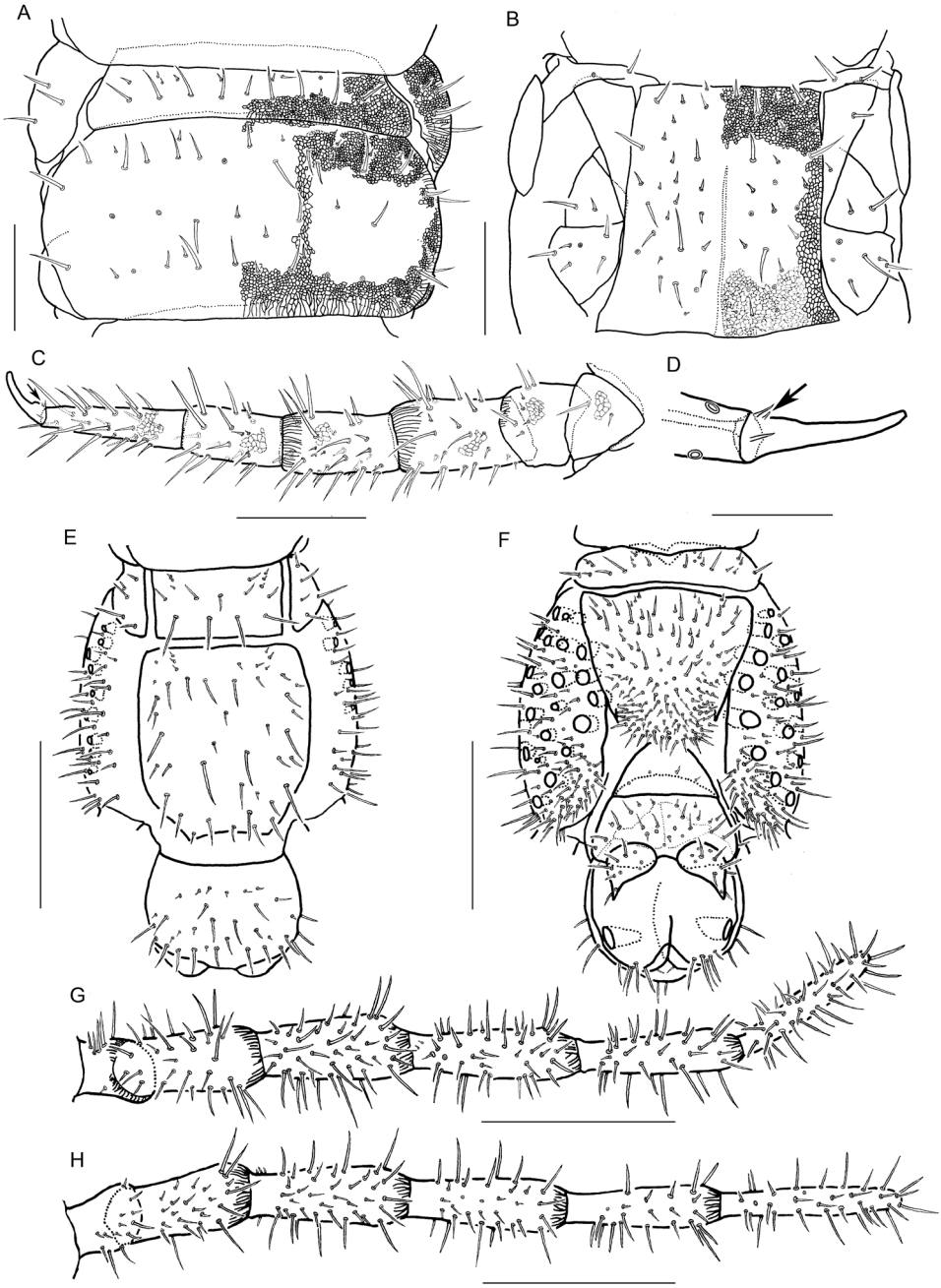

Figure 6. *Arrup akiyoshiensis* sp. n., holotype (TS-20180330-01), **A** four leg-bearing segments, dorsal **B** four leg-bearing segments, ventral **C** left leg (pair 4), ventral **D** claw of right leg (pair 4), lateral **E** last leg-bearing and postpedal segments, dorsal **F** last leg-bearing and postpedal segments, ventral **G** right telopodite of last leg-bearing segment, dorsal **H** right telopodite of last leg-bearing segment, ventral. Scale bars: 300 μm (**A–C**); 100 μm (**D**); 500 μm (**E–H**).

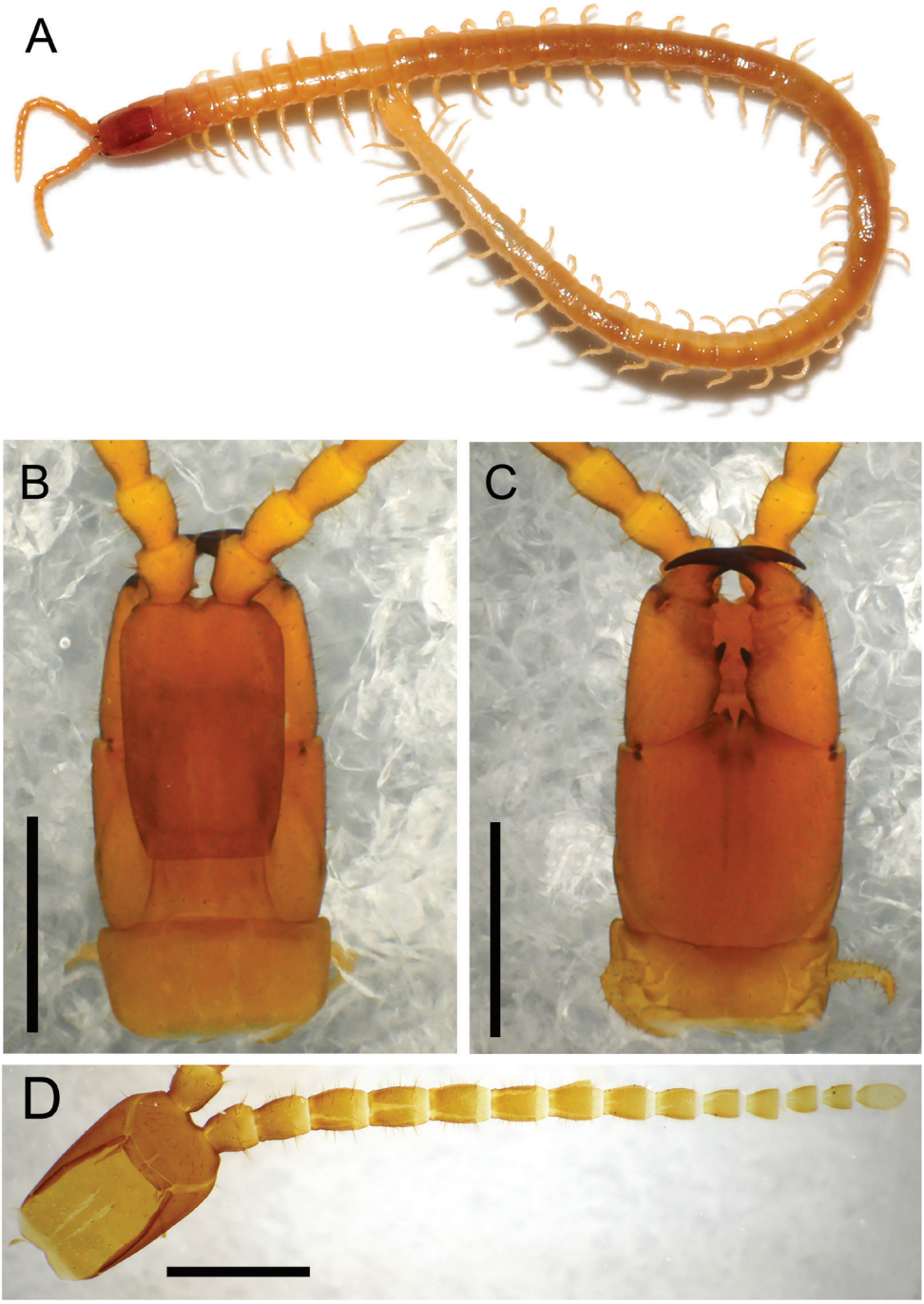

Figure 7. *Arrup akiyoshiensis* sp. n., **A–C** paratype (TS-20180418-01) **D** holotype (TS-20180330-01) **A** whole body, dorsal **B** head and forcipular segment, dorsal **C** head and forcipular segment, ventral **D** head and left antenna, ventral. Scale bar: 1 mm (**B–D**).

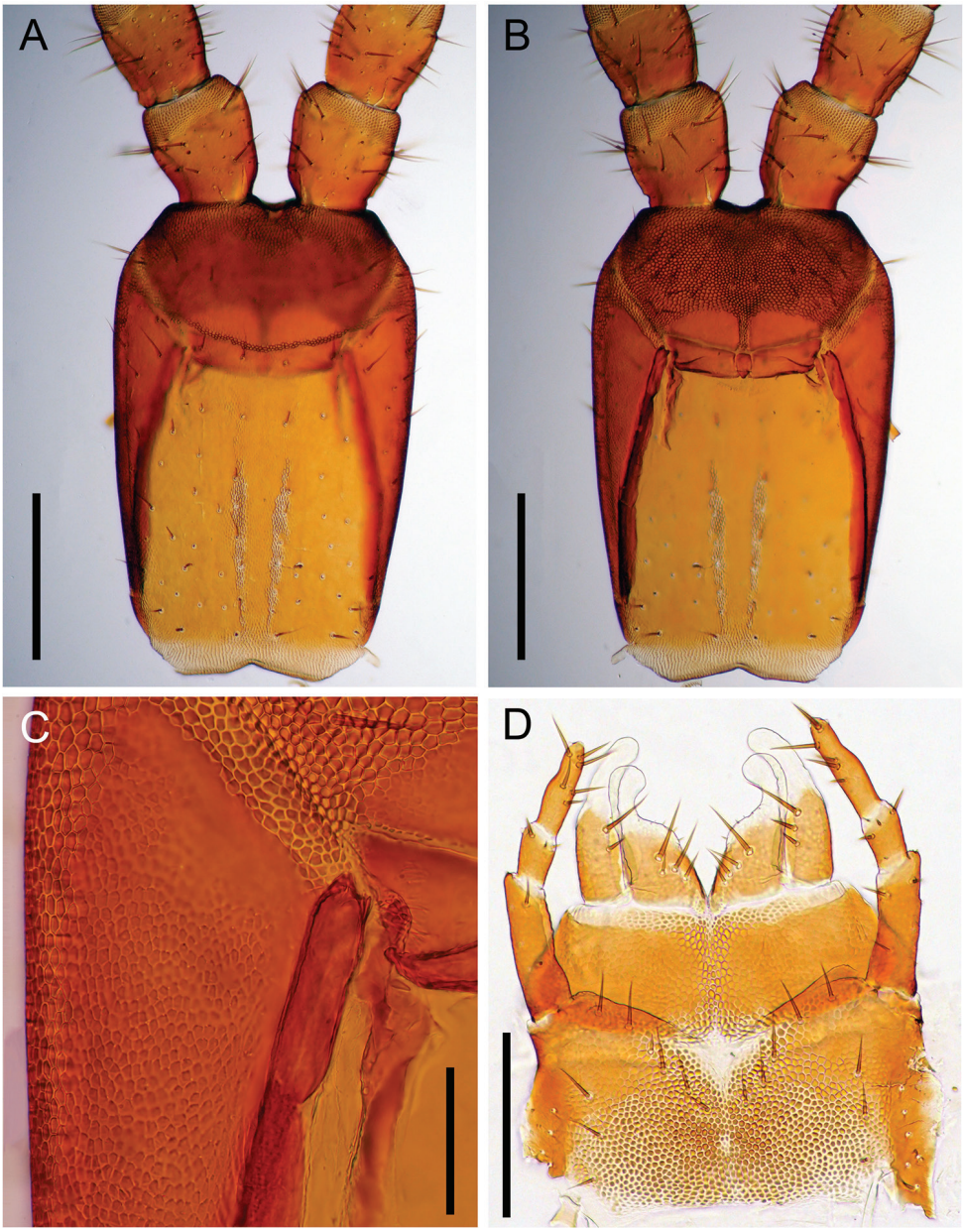

Figure 8. *Arrup akiyoshiensis* sp. n., holotype (TS-20180330-01), **A** cephalic plate, dorsal **B** clypeus and clypeal pleurite, ventral **C** anterior part of cephalic pleurite, ventral **D** maxillae complex, ventral. Scale bars: 500 µm (**A, B**); 100 µm (**C**); 250 µm (**D**).

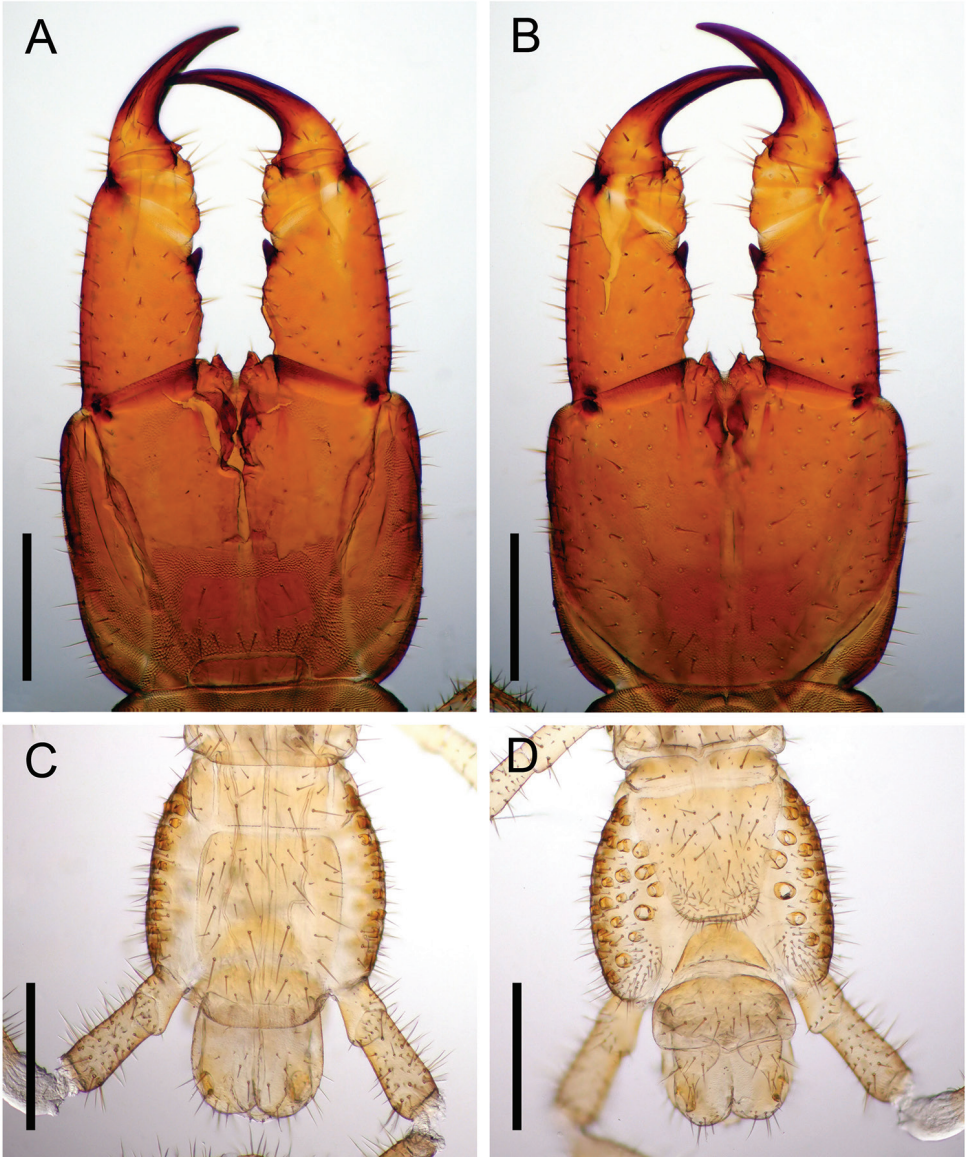

Figure 9. *Arrup akiyoshiensis* sp. n., **A, B** paratype (TS-20180418-01) **C, D** holotype (TS-20180330-01) **A** forcipular segment, dorsal **B** forcipular segment, ventral **C** last leg-bearing and terminal segments, dorsal **D** last leg-bearing and postpedal segments, ventral. Scale bars: 500 μm.

parallel. Telopodites triarticulated, reaching the telopodite of first maxillae. Claw of the telopodite absent. A tiny tubercle present on outer-distal corner of each article. Article I 2.8 times as long as wide; article II 1.6 times as long as wide; article III 3.2 times as long as wide.

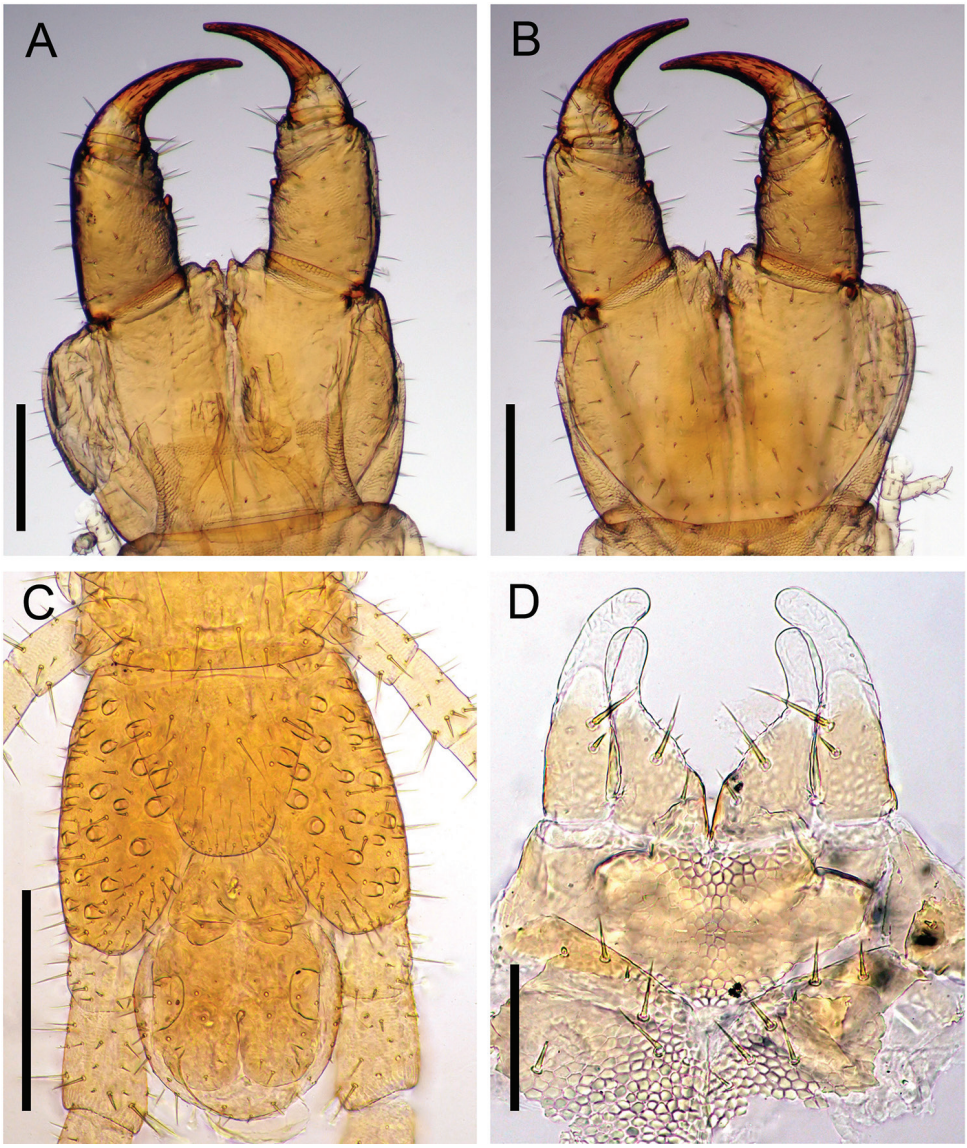

Figure 10. *Arrup ishiianus* Uliana, Bonato & Minelli, 2007 (TS-20090729-01) **A** forcipular segment, dorsal **B** forcipular segment, ventral **C** last leg-bearing and postpedal segments, ventral **D** maxillae complex, ventral (telopodites of second maxilla broken). Scale bars: 300 µm (**A–C**); 100 µm (**D**).

Forcipular segment (Figs 5A–D, 7B, C, 9A, B) with setae both on dorsal and ventral surface; setae arranged almost symmetrically. Coxosternite with distinct 1 + 1 projections in anterior margin. Chitinous lines absent. Forcipular tergite trapeziform. When telopodites closed, tarsungulum reaching anterior margin of

cephalic plate. Article I 1.9 times as long as wide, with a well-developed pointed tooth at the distal internal corner. Article II 0.40 times as long as wide, with a tubercle at the internal margin (arrows in Fig. 5A, B). Article III 0.37 times as long as wide, with a tubercle at the internal margin. Tarsungulum with a triangular basal denticle. Claw of tarsungulum with numerous tiny sensilla. Calyx of poison gland overreaching article I. Duct opening of poison gland on dorsal tip of tarsungulum (triangle in Fig. 5C).

Leg-bearing segments (excepting last leg-bearing segment) (Fig. 6A–D) without pore field on sternites. Median longitudinal sulcus present on sternites I–XVII. Forty-one leg-bearing segments in both the holotype and paratype. All legs weakly areolate. First pair of legs much shorter than the others. All leg claws with anterior and posterior accessory spines; posterior one with a subsidiary spine at its bottom (arrows in Fig. 6C, D).

Last leg-bearing segment (Figs 6E–H, 9C, D) with numerous setae both on tergite and sternite; setae arranged almost symmetrically. Sternite as long as wide, sub-triangular, with posterior margin round. Tergite sub-pentagonal. Coxopleura with 31–35 pores on lateral and ventral sides. Telopodite having six articles, but without claw.

Postpedal segment (Figs 6E, F, 9C, D) with setae on each segment; setae arranged almost symmetrically. Female gonopod uniarticulate; distal part elongate. Anal pore opened laterally.

Coloration (Fig. 7A). Head and forcipular segment pale ocher; other body segments whitish yellow, without dark patches.

Distribution. Known from only the type locality.

Type locality. Kagekiyo-ana, Mitou Town (Mitou-cho), Mine City (Mine-shi), Yamaguchi Prefecture, Japan (34°17.50'N, 131°20.00'E).

Remarks. *Arrup akiyoshiensis* sp. n. is morphologically similar to several other congeners, especially *A. holstii* (Pocock, 1895) and *A. ishiianus* Uliana, Bonato & Minelli, 2007 (Fig. 10), but can be easily distinguished from them by a combination of the characteristics shown in Table 7.

Table 7. Morphological comparison between *A. akiyoshiensis* sp. n. and other similar congeners based on Uliana et al. (2007).

Characteristics	*A. akiyoshiensis* sp. n.	*A. holstii*	*A. ishiianus*	*A. obtusus*	*A. kyushuensis*	*A. longicalix*
Body length	approx. 3.5 cm	approx. 2 cm	4–5 cm	approx. 2 cm	1.5–3 cm	approx. 2 cm
Shape of the distal lobe of medial projection	clavate at the top	clavate at the top	slightly clavate	–*	slightly clavate	very elongate
distal tooth of forcipular article I	well developed, pointed	sharp and short	well developed, rounded	well developed	large and subtriangular	pointed, medium sized
basal tooth of forcipular tarsungulum	triangular	sharp	rounded or slightly pointed	shallow and rounded	well developed	very shallow and obtuse
Sternite of ultimate leg-bearing segment	as long as wide	as long as wide	wider than long	wider than long	as long as wide	wider than long
Number of coxal pore	31–35	around 12	around 35	around 40	–*	around 15

* no data in Uliana et al. (2007).

Discussion

The two adult female specimens examined were morphologically almost identical (except for the body size), and were therefore concluded to be conspecific. Male characteristics are unknown at present.

Arrup akiyoshiensis sp. n. exhibits unique characteristics which are not observed in other valid named congeners, i.e., the entire areolation of the crypeal pleurite, elongation of distal part of female gonopod, and tiny tubercle on forcipular article II. It is most similar to *A. holstii* (Pocock, 1895) and *A. ishiianus* Uliana, Bonato & Minelli, 2007 (Fig. 10) known from Japan, but can be easily distinguished from them by clearly developed, outwardly pointed tooth of the forcipular segment I (sharp and short tooth in *A. holstii*; well developed, rounded tooth in *A. ishiianus*), and triangular basal tooth of forcipular tarsungulum (sharp basal tooth in *A. holstii*; rounded or slightly pointed basal tooth in *A. ishiianus*). It is also easily distinguished from other similar congeners (Uliana et al. 2007) by a combination of the characteristics shown in Table 7. In addition, the 18S rRNA gene sequences of *A. akiyoshiensis* sp. n. and *A. ishiianus* differed by four bp out of 1821 bp (sequence of three individuals of *A. akiyoshiensis* sp. n. are all identical). Therefore, the undetermined species is herein concluded to be new species, named *A. akiyoshiensis*.

Arrup akiyoshiensis sp. n. and *A. holstii* can be found in the same area, Akiyoshi-dai. However, it is unclear whether the both species occur in the same cave or not, because the cave where *A. holstii* was found is not clearly mentioned (Kuramoto 1980). At least, *A. holstii* was not collected in our survey of Kagekiyo-ana, where *A. akiyoshiensis* sp. n. was collected. Many endemic species with small geographic ranges may occur in isolated caves (Barr Jr and Holsinger 1985). For further understanding of endemism of Akiyoshi-dai, a thorough inventory of cave invertebrates is needed.

Arrup akiyoshiensis sp. n. has no troglomorphic traits such as exceptionally long antennae, legs, and claws (Stoev et al. 2015). In the collection site (shown in Fig. 1), four troglobionts species *Nesticus akiyoshiensis akiyoshiensis* (Uyemura, 1941) (Araneae); *Coecobrya akiyoshiana* (Yosii, 1956) (Collembola); *Trechiama pluto kanekiyo* Ueno, 1958 (Coleoptera); an undescribed species of Campodeidae (Diplura), and one troglophiles species: *Epanerchodus etoi etoi* Miyosi, 1955 (Polydesmida) can be found. *Thereuopoda clunifera* (Wood, 1862) (Scutigeromorpha) and species of Rhaphidophorid (Orthoptera), both of which have strongly indicated epigeal ecology, cannot be found (T Murakami pers. obs.). Considering the above facts, the habitat of *A. akiyoshiensis* sp. n. seems to be confined to cave environments. Further surveys are needed to consider adaptations of its ecology for cave environment.

Acknowledgements

We are grateful to Dr Manabu Hori (Yamaguchi University) for helpful support. We also thank Mr Tatsumi Suguro (Keio Yochisha Elementary School), Ms Mari Ishida

(Akiyoshi-dai Museum of Natural History), Mr Keisuke Kawano (The Firefly Museum of Toyota Town), Dr Kiyoshi Ishii (Professer Emeritus, Dokkyo University), and Dr Makiko Hasegawa (Showa University) for much support and advice. A part of this study was supported by Nippon Life Insurance Foundation (Leader: Takeshi Yamasaki, FY2017–FY2018), Asahi Glass Foundation (Leader: Katsuyuki Eguchi; FY2017–FY2020) and JSPS KAKENHI Grant Numbers 15H02858 for Satoshi Shimano.

References

Barr Jr TC, Holsinger JR (1985) Speciation in cave faunas. Annual Review of Ecology and Systematics 16: 313–337. https://doi.org/10.1146/annurev.es.16.110185.001525

Bollman CH (1893) Classification of the Syngnatha. In: Underwood LM (Ed) The Myriapoda of North America by Charles Harvey Bollman. Bulletin of the United States National Museum, No. 46. Washington, Government Printing Office, 163–167. https://doi.org/10.5962/bhl.title.2787

Bonato L, Edgecombe GD, Lewis JG, Minelli A, Pereira LA, Shelley RM, Zapparoli M (2010) A common terminology for the external anatomy of centipedes (Chilopoda). ZooKeys 69: 17–51. https://doi.org/10.3897/zookeys.69.737

Bonato L, Chagas-Jr A, Edgecombe GD, Lewis JGE, Minelli A, Pereira LA, Shelley RM, Stoev P, Zapparoli M (2017) ChiloBase 2.0. A World Catalogue of Centipedes (Chilopoda). http://chilobase.biologia.unipd.it [Accessed 23 January 2019]

Chagas-Jr A, Bichuette ME (2018) A synopsis of centipedes in Brazilian caves: hidden species diversity that needs conservation (Myriapoda, Chilopoda). ZooKeys 737: 13–56. https://doi.org/10.3897/zookeys.737.20307

Chamberlin RV (1912) The Chilopoda of California. III. Pomona College Journal of Entomology 4: 651–672.

Christman MC, Culver DC, Madden MK, White D (2005) Pattern of endemism of the eastern North American cave fauna. Journal of Biogeography 32: 1441–1452. https://doi.org/10.1111/j.1365-2699.2005.01263.x

Fujii A (2009) A Report on the Public Symposium "Mammal fossils in the Cenozoic Era preserved in limestone caves of the Akiyoshi-dai plateau" at the Annual Meeting of the Mammalogical Society of Japan (2008): Cave of Akiyoshi-dai Plateau and their chronology based on the rate of downward erosion of the Koto-gawa River. Mammalian Science 49(1): 91–95.

Foddai D, Minelli A (1999) A troglomorphic geophilomorph centipede from southern France (Chilopoda: Geophilomorpha: Geophilida). Journal of Natural History 33: 267–287. https://doi.org/10.1080/002229399300416

Gibert J, Deharveng L (2002) Subterranean ecosystems: a truncated functional biodiversity. BioScience 52: 473–481. https://doi.org/10.1641/0006-3568(2002)052[0473:SEATFB]2.0.CO;2

Johnson KP, Yoshizawa K, Smith VS (2004) Multiple origins of parasitism in lice. Proceedings of the Royal Society B: Biological Sciences. 271: 1771–1776. https://doi.org/10.1098/rspb.2004.2798

Kumar S, Stecher G, Tamura K (2016) MEGA7: Molecular Evolutionary Genetics Analysis version 7.0. Molecular Biology and Evolution 33(7): 1870–1874. https://doi.org/10.1093/molbev/msw054

Kuramoto T (1980) A limestone cave and creatures. In: Kawano M (Ed.) Limestone cave of Akiyoshi-dai Science of limestone cave. Kisui-kai, Yamaguchi, 173–184.

Lewis JGE (1981) The biology of centipedes. Cambridge University Press, Cambridge, 476 pp. https://doi.org/10.1017/CBO9780511565649

Pocock RI (1895) Report upon the Chilopoda and Diplopoda obtained by PW Bassett-Smith, Esq, Surgeon RN and JJ Walker Esq, RN, during the cruise in the Chinese seas of HMS "Penguin", Commander WU Moore commanding. Annals and Magazine of Natural History (6)15: 346–372. https://doi.org/10.1080/00222939508677895

Shinohara K (1966) Chilopoda. In: Uchida T, Yamada M, Yamaguchi H, Nagao Z, Kato K, Morikawa K (Eds) Systematic Zoology, vol 7. Nakayama-shoten, Tokyo, 82–124.

Stoev P, Akkari N, Komerički A, Edgecombe GD, Bonato L (2015) At the end of the rope: *Geophilus hadesi* sp. n. – the world's deepest cave-dwelling centipede (Chilopoda, Geophilomorpha, Geophilidae). In: Tuf IH, Tajovský K (Eds) Proceedings of the 16th International Congress of Myriapodology, Olomouc, Czech Republic. ZooKeys 510: 95–114. https://doi.org/10.3897/zookeys.510.9614

Takakuwa Y (1942) Die Myriopoden aus Formosa, Philippinien usw. Transactions of the Natural History Society of Formosa 32(231): 359–367.

Uliana M, Bonato L, Minelli A (2007) The Mecistocephalidae of the Japanese and Taiwanese islands (Chilopoda: Geophilomorpha). Zootaxa 1396: 1–84. https://doi.org/10.11646/zootaxa.1396.1.1

Yamaguchi S, Endo K (2003) Molecular phylogeny of Ostracoda (Crustacea) inferred from 18S ribosomal DNA sequences: implication for its origin and diversification. Marine Biology 143(1): 23–38. https://doi.org/10.2108/zs150103

ZooKeys 830: 53–61 (2019)
doi: 10.3897/zookeys.830.31147
http://zookeys.pensoft.net

RESEARCH ARTICLE

A peer-reviewed open-access journal
ZooKeys
Launched to accelerate biodiversity research

A new species of the ant genus *Recurvidris* Bolton, 1992 (Hymenoptera, Formicidae, Myrmicinae) from Thailand

Weeyawat Jaitrong[1], Yuppayao Tokeeree[2], Piyaporn Pitaktunsakul[3,4]

1 *Thailand Natural History Museum, National Science Museum, Technopolis, Khlong 5, Khlong Luang, Pathum Thani, 12120 Thailand* **2** *Program of Environmental Science, Faculty of Science and Technology, Surindra Rajabhat University, Muang, Surin, 32000 Thailand* **3** *Department of General Science, Faculty of Science and Technology, Kanchanaburi Rajabhat University, Kanchanaburi, 71190 Thailand*

Corresponding author: *Piyaporn Pitaktunsakul* (ppiyaporn@kru.ac.th)

Academic editor: *Marek Borowiec* | Received 4 November 2018 | Accepted 26 January 2019 | Published 14 March 2019

http://zoobank.org/6DC52738-5598-491C-AA02-068C81DE85A2

Citation: Jaitrong W, Tokeeree Y, Pitaktunsakul P (2019) A new species of the ant genus *Recurvidris* Bolton, 1992 (Hymenoptera, Formicidae, Myrmicinae) from Thailand. ZooKeys 830: 53–61. https://doi.org/10.3897/zookeys.830.31147

Abstract

Recurvidris Bolton, 1992 is a small myrmicine genus of the tribe Crematogastrini. Until now, eleven species are known in this genus from Asia. A new species, *Recurvidris lekakuli* **sp. n.**, is here described from Thailand based on the worker caste. The type series of the new species was collected from leaf litter in a dry evergreen forest. A key to the Asian species of *Recurvidris* based on the worker caste is provided.

Keywords

Formicidae, ants, *Recurvidris*, new species, taxonomy, Thailand

Introduction

Recurvidris Bolton, 1992 is a small myrmicine genus of the tribe Crematogastrini (Bolton 2003, Ward et al. 2015). Members of the genus are characterized by the propodeal spine curving upwards and forwards from its base; antenna with 11 segments and 3-segmented club; a mandible with 4–5 teeth on the masticatory margin, and the basal margin with or without tooth; and the petiole low and pedunculate (see Bolton

1992). They are distributed in Asia from India and Sri Lanka in the south and west; Japan, China and Taiwan in the north; various countries in Southeast Asia; and eastwards to Sulawesi in Indonesia (Bolton 1992, Xu and Zheng 1995, Zhou 2000, Zettel 2008, Terayama 2009, Jaitrong and Wiwatwitaya 2015, Antweb 2018). Currently, eleven species are recognized in the genus. Among them, Jaitrong and Wiwatwitaya (2015) recorded only three species, *Recurvidris browni* Bolton, 1992; *R. chanapaithooni* Jaitrong & Wiwatwitaya, 2015 and *R. recurvispinosa* (Forel, 1890) from Thailand.

Surveys of ants in Kanchanaburi province, western Thailand under the project "Conservation and economic assessment at Kanchanaburi limestone community forest for sustainable uses", led to the discovery of a few unidentified *Recurvidris* specimens belonging to the *R. kemneri* species group (sensu Bolton 1992). Having carefully compared them with the type material of closely related species, we concluded that this species is new to science. We here describe and name it *Recurvidris lekakuli* sp. n. based on the worker caste.

Materials and methods

The material was collected from western Thailand, Kanchanaburi province, Thong Phaphum district, Sahakhon Nikhom village (14.76255556N, 98.80966667E). The area was covered with a dry evergreen forest. The holotype and paratypes of *Recurvidris lekakuli* sp. n. are pin-mounted dry specimens. The type material of the new species was compared with the holotype and paratypes of the most closely related species, *Recurvidris chanapaithooni* Jaitrong & Wiwatwitaya, 2015 (in Natural History Museum of the National Science Museum, Thailand). Most morphological observations were made with a ZEISS Discovery V12 stereoscope.

Multi-focused montage images were produced using NIS-Elements-D from a series of source images taken by a Nikon Digital Sight-Ri1 camera attached to a Nikon AZ100M stereoscope. The holotype and paratypes were measured for the following parts using a micrometer (accurate to 0.01 mm).

The abbreviations used for the measurements and indices are as follows (edited from Bolton (1987)):

DPW Dorsal Petiole Width. Maximum width of petiole in dorsal view.

ED Eye Diameter. Maximum diameter of eye with head positioned in profile view, such that anterior and posterior eye margins are in same plane of focus.

HL Head length. Length of head capsule, excluding mandibles, measured by a straight line from anterior clypeal margin to mid-point of a line drawn across posterior margin of head.

HW Head width. Maximum width of head, in full-face view, measured behind eyes (excluding eyes).

ML Mesosomal length. Maximum diagonal length of mesosoma in profile view, measured from posterodorsal border of pronotal flange to posterior basal angle of metapleuron.

PW Pronotal width. Maximum width of pronotum in dorsal view.
SL Scape length. Maximum length of antennal scape excluding basal constriction and condylar bulb.
TL Total length. Roughly measured from anterior margin of head to tip of gaster in stretched specimens.
CI Cephalic index. HW/HL × 100.
DPI Dorsal petiole index. DPW/PL × 100.
OI Ocular Index. ED/HW × 100.
SI Scape index. SL/HW × 100.

Abbreviations of the type depositories are as follows:

MHNG Muséum d'histoire naturelle, Geneva, Switzerland.
SKYC Seiki Yamane's Collection at Kitakyushu Museum of Natural History and Human History, Japan.
THNHM Natural History Museum of the National Science Museum, Thailand.

Results

***Recurvidris lekakuli* sp. n.**
http://zoobank.org/80A6A0F0-9D84-4B4C-865C-6831C7C7239B
Figures 1–5

Type. Holotype: worker (THNHM-I-01219, THNHM), West Thailand, Kanchanaburi Province, Thong Phaphum District, Ban Sahakhon Nikhom, dry evergreen forest (DEF), 14.76255N, 98.80966E, 13.VII.2018, W. Jaitrong leg., WJT130718-07. **Paratypes:** three workers (THNHM-I-01220 to THNHM-I-01222, THNHM), same data as holotype; one worker (THNHM-I-01249, THNHM), West Thailand, Kanchanaburi Province, Thong Phaphum District, Ban Sahakhon Nikhom, dry evergreen forest (DEF), 14.76255N, 98.80966E, 26.VIII.2018, C. Sathiandee leg.; five workers (THNHM-I-02617, MHNG, SKYC, THNHM), West Thailand, Kanchanaburi Province, Thong Phaphum District, Ban Sahakhon Nikhom, dry evergreen forest (DEF), 14.76255N, 98.80966E, 6.XI.2018, W. Jaitrong leg., WJT061118-12; one worker (THNHM-I-02618, THNHM), West Thailand, Kanchanaburi Province, Thong Phaphum District, Ban Sahakhon Nikhom, dry evergreen forest (DEF), 14.76255N, 98.80966E, 6.XI.2018, C. Sathiandee leg., WJT1/5.

Measurements and indices. Holotype and four paratype workers (n = 5): DPW 0.10–0.12, ED 0.12–0.13, HL 0.50–0.56, HW 0.50–0.56, PW 0.23–0.26, ML 0.69–0.73, SL 0.53–0.56, TL 2.28–2.34, CI 97–100, DPI 30–35, OI 22–27, SI 100–107.

Diagnosis. Head in full-face view round, almost as long as broad; masticatory margin of mandible with four sharp teeth, fourth (basal) tooth almost as large as third

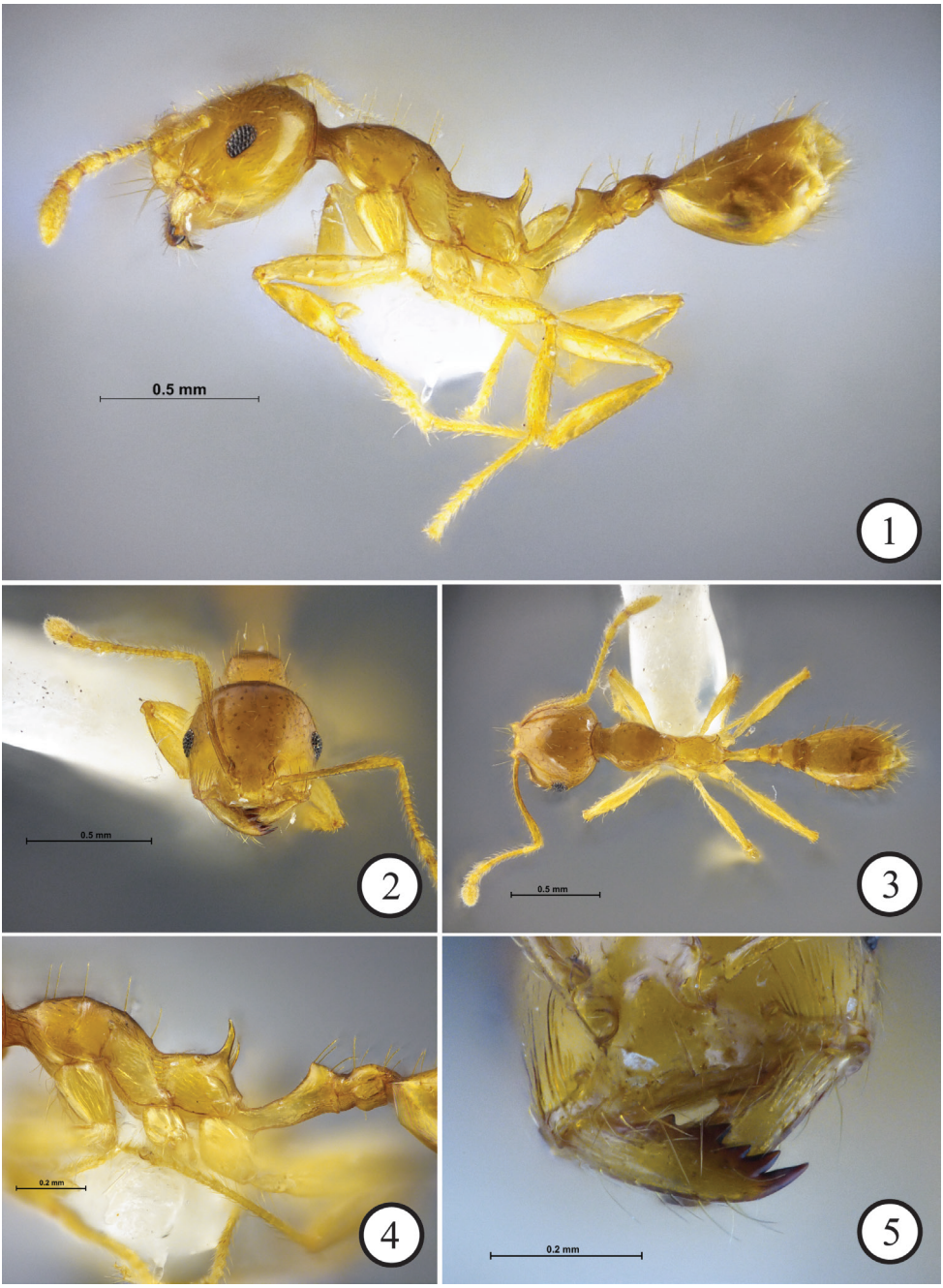

Figures 1–5. *Recurvidris lekakuli* sp. n., holotype worker (THNHM-I-01219) **1** body in profile **2** head in full-face view **3** body in dorsal view **4** mesosoma, petiole and postpetiole in profile **5** right mandible showing mandibular dentition.

tooth; basal margin with a small tooth; propodeal declivity lacking infradental lamella or ridge linking propodeal spine to metapleural lobe; head, promesonotum, propodeum, petiolar node, postpetiole and gaster entirely smooth and shiny; mesopleuron and peduncle of petiole superficially reticulate with slightly smooth and shiny interspaces; propodeal dorsum with a pair of very short appressed hairs in front of spiracles.

Description (Holotype and paratypes). Head in full-face view round and almost as long as broad, with posterior margin convex. Eye with seven ommatidia along longest axis. Antennal scape extending posteriorly slightly beyond posterolateral corner of head. Masticatory margin of mandible with four sharp teeth, fourth (basal) tooth as large as third tooth; basal margin with a small tooth. Clypeus without paired carinae, its anterior margin almost straight. Promesonotum in profile strongly convex dorsally and sloping gradually to metanotal groove. Propodeum in profile with almost straight dorsal outline; propodeal spines very slender, divergent, and in posterior view very narrow. Propodeal declivity lacking infradental lamella or ridge linking propodeal spine to metapleural lobe. Peduncle of petiole in profile relatively long, with its dorsal outline concave and ending posteriorly in right angle; its ventral outline convex with long acute subpetiolar process.

Head entirely smooth and shiny, lacking sculpture except some short longitudinal rugulae near mandiblular base. Antennal scape smooth and shiny. Promesonotum smooth and shiny; mesopleuron superficially reticulate with smooth and shiny interspaces; entire propodeum including propodeal spine smooth and shiny. Peduncle of petiole superficially reticulate with smooth and shiny interspaces; petiolar node entirely smooth and shiny; postpetiole entirely smooth and shiny; legs smooth and shiny. Gaster smooth and shiny.

Head with relatively dense short hairs; promesonotum with sparse longer hairs (8–10 hairs); longest pronotal hairs 0.13–0.15 mm long; propodeum dorsally with a pair of very short decumbent or appressed hairs (these hairs missing in two paratypes). Petiole with two dorsal pairs of long hairs. Postpetiole with two dorsal pairs of long hairs. Body colour yellow.

Etymology. The specific name is dedicated to the late Dr. Boonsong Lekakul, who was the most excellent specialist in zoological sciences in Thailand and helped and inspired many young biologists.

Comparative notes. *Recurvidris lekakuli* is closely related to *R. chanapaithooni* Jaitrong & Wiwatwitaya, 2015; *R. kemneri* Bolton, 1992; *R. nigrans* Zettel, 2008 and *R. proles* Bolton, 1992 in having the following characteristics: masticatory margin of mandible with a series of four sharp teeth (acute basal tooth), basal margin of mandible with a small tooth; propodeum without infradental lamella or ridge linking the propodeal spine to metapleural lobe; head smooth and shining. Among them *R. lekakuli* is more similar in general appearance to *R. chanapaithooni* and *R. kemneri* than to *R. nigrans* and *R. proles*, the former two sharing the clear yellow body that is unicolorous (black to dark brown in *R. nigrans* and *R. proles*). *Recurvidris lekakuli* is easily separated

Figure 6. Type locality of *R. lekakuli* sp. n. at Ban Sahakhon Nikhom, Kanchanaburi Province, Thong Phaphum District, West Thailand, dry evergreen forest.

from *R. chanapaithooni* by the following characteristics: clearly larger body (TL 2.28–2.34 mm, HW 0.50–0.56 mm in *R. lekakuli*; TL 2.00–2.10 mm, HW 0.38–0.41 mm in *R. chanapaithooni*); mesopleuron largely smooth and shiny, only partly superficially reticulate (strongly reticulate in *R. chanapaithooni*); petiole relatively longer (DPI 30–35 in *R. lekakuli*; 42–43 in *R. chanapaithooni*); petiolar node clearly smooth and shiny (petiole entirely reticulate in *R. chanapaithooni*); propodeal dorsum with a pair of very short appressed hairs (with 2 pairs of standing hairs in *R. chanapaithooni*). *Recurvidris lekakuli* differs from *R. kemneri* by the clypeus clearly smooth and shiny (median portion of clypeus weakly bicarinate in *R. kemneri*) and having a pair of very short appressed hairs on propodeal dorsum (without hairs in *R. kemneri*). The new species is also similar to *R. glabriceps* Zhou, 2000 from China, but the latter lacks a small tooth on basal margin of mandible.

Bionomics. The type series was collected from leaf litter on the forest floor in a dry evergreen forest (Figure 6) near a stream.

Distribution. *Recurvidris lekakuli* has been known only from the type locality. The most closely related species, *R. chanapaithooni* was recorded from eastern and southern Thailand (Jaitrong and Wiwatwitaya 2015). This species is very probably sympatric with *R. lekakuli* in at least the dry evergreen forest in western and/or southern Thailand.

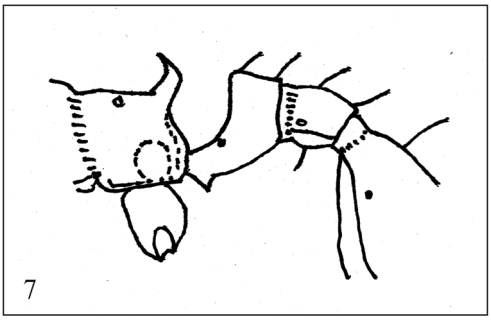

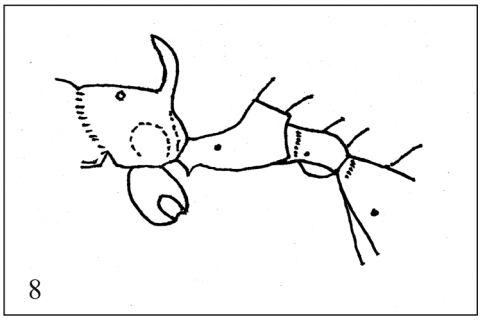

Figures 7–8. Propodeal spine and petiolar peduncle, edited from Bolton (1992) **7** *R. recurvispinosa* (Forel, 1890) **8** *R. hebe* Bolton, 1992.

Key to Asian species of the genus *Recurvidris* based on worker caste

1 Masticatory margin of mandible with 4 or 5 teeth, basal (fourth or fifth) tooth distinctly larger than preceding tooth, acute to bidenticulate; head behind level of frontal lobes sculptured (opaque, reticulate, reticulate-punctate); propodeal declivity with narrow infradental lamella or ridge linking propodeal spine to metapleural lobe **2**

– Masticatory margin of mandible with 4 teeth, basal (fourth) tooth at most only slightly larger than third; head behind level of frontal lobes unsculptured; propodeal declivity lacking infradental lamella or ridge linking propodeal spine to metapleural lobe..... **7**

2 Masticatory margin of mandible with 5 teeth..... **3**

– Masticatory margin of mandible with 4 teeth..... **4**

3 Dorsum of head finely and densely reticulate-punctate everywhere, dull and opaque; disc of pronotum finely and densely sculptured; subpetiolar process as a short tooth; small species (HW 0.39, see Bolton 1992)..... ***R. williami* Bolton, 1992**

– Dorsum of head only with very fine superficially reticulate patterning, glossy; disc of pronotum glassy smooth; subpetiolar process as a long spine; large species (HW 0.45–0.56, see Bolton 1992; Jaitrong and Wiwatwitaya 2015)..... ..... ***R. browni* Bolton, 1992**

4 Basal tooth of mandible acute apically..... **5**

– Basal tooth of mandible bidenticulate apically, may appear as abruptly truncated in worn mandible..... **6**

5 Propodeal dorsum with only faint superficial sculpture and with a pair of short decumbent hairs..... ***R. pickburni* Bolton, 1992**

– Propodeal dorsum with fine dense reticulate-rugulae and without a pair of short decumbent hairs..... ***R. nuwa* Xu & Zheng, 1995**

6 In profile view, propodeal spine and petiolar peduncle relatively short and stout (Figure 7); with head in full-face view, occipital corner narrowly rounded; postpetiole in dorsal view 1.6–1.8 times as broad as petiolar node (Bolton, 1992).... ..... ***R. recurvispinosa* Forel, 1890**

– In profile view, propodeal spine and petiolar peduncle relatively long and narrow (Figure 8); with head in full-face view, occipital corner broadly rounded; postpetiole in dorsal view 1.3–1.4 times as broad as petiolar node (Bolton, 1992) ....***R. hebe*** **Bolton, 1992**

7 Propodeal dorsum with 1–2 standing (erect) hairs.....**8**

– Propodeal dorsum with 1–2 pairs of very short decumbent or appressed hairs, without standing hairs. **10**

8 Head and gaster dark brown, much darker than the yellowish mesosoma ....***R. proles*** **Bolton, 1992**

– Body color uniformly yellow.....**9**

9 Basal margin of mandible unarmed; head relatively long (CI < 90) .... ***R. glabriceps*** **Zhou, 2000**

– Basal margin of mandible armed with a small tooth which is widely separated from basal tooth; head relatively short and broad (CI ≥ 100) ....***R. chanapaithooni*** **Jaitrong & Wiwatwitaya, 2015**

10 Body color uniformly blackish brown; in profile propodeal spine broad at base .. ..***R. nigrans*** **Zettel, 2008**

– Body yellowish brown; in profile propodeal spine narrow at base.....**11**

11 Entire propodeum and dorsum of petiolar peduncle smooth and shiny; propodeal spine long, slightly longer than longest pronotal hairs.....***R. lekakuli*** **sp. n.**

– Dorsum of propodeum superficially sculptured; dorsum of petiolar peduncle finely reticulate; propodeal spine short, shorter than longest pronotal hairs .. ..***R. kemneri*** **(Wheeler & Wheeler, 1954)**

Acknowledgements

This study was supported by Office of the Higher Education Commission and Centre of Excellence on Biodiversity (project no. BDC-PG2-16009) and partly by the National Science and Technology Development Agency (Funding contract no. FDA-CO2561-5851-TH). We thank Miss Chatsarin Sathiandee (Kanchanaburi Rajabhat University), who donated us a paratype.

References

Antweb (2018) Genus: *Recurvidris* Bolton, 1992. https://www.antweb.org/browse.do?subfamily=myrmicinae&genus=recurvidris&rank=genus&project=allantwebants [Accessed on: 2018–8–24]

Bolton B (1987) A review of the *Solenopsis* genus-group and revision of Afrotropical *Monomorium* Mayr (Hymenoptera: Formicidae). Bulletin of the British Museum (Natural History), Entomology 54: 263–452.

Bolton B (1992) A review of the ant genus *Recurvidris* (Hymenoptera: Formicidae), a new name for *Trigonogaster* Forel. Psyche 99: 35–48.

Bolton B (1995) A New General Catalogue of the Ants of the World. Harvard University Press, Cambridge, 504 pp.

Bolton B (2003) Synopsis and classification of Formicidae. Memoirs of the American Entomological Institute 71: 1–370.

Jaitrong W, Wiwatwitaya D (2015) The species of the ant genus *Recurvidris* Bolton, 1992 (Hymenoptera: Formicidae: Myrmicinae) in Thailand. Halteres 6: 104–112.

Terayama M (2009) A synopsis of the family Formicidae of Taiwan. Research Bulletin of Kanto Gakuen University 17: 81–266.

Ward SP, Brady SG, Fisher BL, Schultz TR (2015) The evolution of myrmicine ants: phylogeny and biogeography of a hyperdiverse ant clade (Hymenoptera: Formicidae). Systematic Entomology 40: 61–81.

Xu Z, Zheng Z (1995) Two new species of the ant genera *Recurvidris* Bolton and *Kartidris* Bolton (Hymenoptera: Formicidae: Myrmicinae) from Southwestern China. Entomotaxomomia 17(2): 143–146.

Zettel H (2008) On the ants (Hymenoptera: Formicidae) of the Philippine Islands: III. The genus *Recurvidris* Bolton, 1992. Linzer Biologische Beitraege 40(1): 891–895.

Zhou S (2000) A taxonomic study of the ant genus *Recuruidris* [sic] Bolton (Hymenoptera: Formicidae) from China, with description of a new species. Entomotaxomomia 22 (4): 301–303.

ZooKeys 830: 63–73 (2019)
doi: 10.3897/zookeys.830.32463
http://zookeys.pensoft.net

RESEARCH ARTICLE

A peer-reviewed open-access journal
ZooKeys
Launched to accelerate biodiversity research

Calixomeria, a new genus of Sceliotrachelinae (Hymenoptera, Platygastridae) from Australia

Zachary Lahey[1], Lubomír Masner[2], Norman F. Johnson[1]

1 *Department of Evolution, Ecology, and Organismal Biology, The Ohio State University, 1315 Kinnear Road, Columbus, Ohio 43212, USA* **2** *Agriculture and Agri-Food Canada, K.W. Neatby Building, Ottawa, Ontario K1A 0C6, Canada*

Corresponding author: *Zachary Lahey* (lahey.18@osu.edu)

Academic editor: *M. Ohl* | Received 15 December 2018 | Accepted 12 February 2019 | Published 14 March 2019

http://zoobank.org/B5B3AB6F-2E7D-44E3-8266-19BE914B7BF9

Citation: Lahey Z, Masner L, Johnson NF (2019) *Calixomeria*, a new genus of Sceliotrachelinae (Hymenoptera, Platygastridae) from Australia. ZooKeys 830: 63–73. https://doi.org/10.3897/zookeys.830.32463

Abstract

Calixomeria lasallei **gen. n. et sp. n.** is described as a new genus and species of Sceliotrachelinae. *Calixomeria* most closely resembles genera of the *Aphanomerus*-cluster but possesses several characters that readily separate it from other sceliotracheline genera. The key of Masner and Huggert (1989) is modified to accommodate *Calixomeria*, and the relationship of the genus to other members of the subfamily is discussed.

Keywords

Parasitoid, Platygastroidea, taxonomy

Introduction

Platygastroidea is well represented in Australia. Approximately 10% (740 species in 80 genera) of all described species occur there, with an estimated 1800 species left to be described (ABRS 2015). A disproportionate amount of that diversity, however, has been described in the family Scelionidae, one of two families that classically comprise the superfamily Platygastroidea (Talamas and Buffington 2015). Much less attention has been paid to Platygastridae, and even less to the subfamily Sceliotrachelinae, due to their small size (most species < 1 mm) and rarity in collections (Masner and Huggert 1989).

The first Australian sceliotrachelines were described by Robert C. L. Perkins during his search for natural enemies of leafhoppers as an entomologist with the Hawaiian Sugar Planters' Association (Perkins 1905). Shortly thereafter, Alan P. Dodd, then an

assistant entomologist with the Bureau of Sugar Experiment Stations, added two genera, *Aphanomerella* Dodd and *Platygastoides* Dodd (Dodd 1913a, b). Following Dodd, descriptions of Australian sceliotrachelines all but stopped until the landmark work of Masner and Huggert (1989), who erected 13 new genera, including several known only from Australasia. The purpose of our research is to follow in the footsteps of Perkins and Dodd by describing an unusual new genus of Sceliotrachelinae from southern Australia.

The contributions of the authors are as follows: Z. Lahey: character definition and coding, generic concept development, species concept development, imaging, key development, manuscript preparation; L. Masner and N. F. Johnson: character definition, generic concept development, species concept development.

Materials and methods

The numbers prefixed with "OSUC" or "USNMENT" are unique identifiers for the individual specimens (note the blank space after some acronyms). Details of the data associated with these specimens may be accessed at the following link: https://hol.osu.edu, and entering the identifier in the form.

Abbreviations and morphological terms used in the text: sensillar formula of clavomeres: distribution of the large papillary sensilla on the ventral clavomeres of the adult female (Bin et al. 1989; Yang et al. 2016), with the segment interval specified followed by the number of papillary sensilla (PS) per segment (e.g., A10–A8/1-2-2) (Bin 1981); T1, T2, ... T6: metasomal tergite 1, 2, ... 6; S1, S2, … S6: metasomal sternite 1, 2, … 6. Morphological terminology generally follows Masner and Huggert (1989), Mikó et al. (2007), and Talamas and Masner (2016). Morphological terms were matched to concepts in the Hymenoptera Anatomy Ontology (Yoder et al. 2010) using the text analyzer function.

Images were captured with a Leica MC170 HD digital camera attached to a Leica Z16 APOA microscope using Leica Application Suite (version 4.12.0), or with a Canon EOS 70D attached to an Olympus BX51. Image stacks were combined into a single montage image using Zerene Stacker (version 1.04). Montage images were post-processed with Adobe Photoshop CS6 Extended and are archived at https://specimage.osu.edu, the image database at The Ohio State University.

Scanning electron micrographs were produced with a Thermo Fisher Scientific Apreo Scanning Electron Microscope. The specimen was disarticulated with a minuten probe on a 0.5-inch slotted aluminum mounting stub using carbon adhesive tabs. The specimen was not coated.

Collections

This work is based on specimens deposited in the following repositories:

ANIC Australian National Insect Collection, Canberra, ACT, Australia
CNCI Canadian National Collection of Insects, Ottawa, Ontario, Canada

OSUC C.A. Triplehorn Collection, The Ohio State University, Columbus, Ohio, USA
USNM National Museum of Natural History, Washington, DC, USA

Abbreviations and characters annotated in the figures:

apT2 anterior setal patch on T2 (Fig. 19)
atp anterior tentorial pit (Fig. 9)
auc axillular carina (Fig. 12)
ax axilla (Fig. 12)
axu axillula (Fig. 12)
cly clypeus (Fig. 9)
Cu cubital vein (Fig. 17)
fed femoral depression (Fig. 13)
fp foamy structures on propodeum (Fig. 19)
mkT1 median keel on T1 (Fig. 19)
lpa lateral pronotal area (Fig. 14)
lpc lateral propodeal carina (Fig. 22)
M+Cu fusion of medial and cubital veins (Fig. 17)
metp metapleural pit (Fig. 13)
mgps multiporous grooved peg sensillum (Figs 6, 7)
mnt metanotal trough (Figs 15, 16)
msc mesoscutum (Fig. 11)
mtpc metapleural carina (Fig. 15)
mtps metapleural sulcus (Fig. 13)
pxcs paracoxal sulcus (Fig. 13)
ppd propodeum (Fig. 15)
prcs pronotal cervical sulcus (Fig. 13)
ps papillary sensillum (Figs 6, 8)
psu posterior mesoscutellar sulcus (Fig. 20)
R submarginal vein (Fig. 17)
RS+M basal vein (Fig. 17)
scu mesoscutellum (Fig. 11)
sss scutoscutellar sulcus (Figs 11, 12)
tel transepisternal line (Fig. 21)
tsa transcutal articulation (Fig. 12)

Taxonomy

Calixomeria lasallei **Lahey & Masner, gen. n. et sp. n.**
http://zoobank.org/B02021B7-DBBB-4C18-8231-42B6C09C6033
http://zoobank.org/55B75102-179B-4F0D-9376-DB5E8F6013A7
Figures 1–18

Description. Body length 0.71–0.85 mm (n = 20). Squat, dorsoventrally flattened.

Head. Color of head: light to dark brown. Shape of head in anterior view: nearly triangular. Shape of head in dorsal view: ovoid to semicircular. Shape of vertex: flat anteriorly, sharply angled posteriorly. Setation of compound eye: present. Occipital pit: absent. Position of lateral ocellus: remote from inner orbit, OOL > 3 ocellar diameters. Length of LOL: equal to OOL. Shape of frons: sharply angled anterior to anterior ocellus. Sculpture of gena: alutaceous. Shape of gena: strongly receding behind compound eye. Median sulcus of postgenal bridge: setose. Malar sulcus: absent. Epistomal sulcus: absent. Shape of clypeus: convex. Anteclypeus: undifferentiated. Orientation of mandibular teeth: transverse. Mandibular dentition: bidentate. Number of maxillary palpomeres: 1. Number of labial palpomeres: 1. Number of antennomeres: 10. A7:

fused to clavomere A8. Shape of A7: 1.5× as wide as long, distinctly wider and longer than A6. Number of clavomeres: 3. Sensillar formula of clavomeres: A10–A8/1-2-2.

Mesosoma. Color of mesosoma: light to dark brown. Epomium: absent. Lateral pronotal area: strongly excavate below anterior margin of pronotal shoulders. Form of pronotal cervical sulcus: indicated as narrow groove dorsally. Setation of pronotal cervical sulcus: absent. Sculpture of pronotal shoulders: imbricate. Pronotal shoulders: visible in dorsal view. Anterior margin of mesoscutum: not reflexed, on same plane as posterior margin of pronotum. Sculpture of mesoscutum: imbricate. Shape of mesoscutum: pentagonal, curved along anterior margin. Anterior admedian line: absent. Median mesoscutal line: absent. Notaulus: absent. Parapsidal line: absent; present. Netrion: absent. Axilla: present, almost hidden in dorsal view. Sculpture of mesoscutellum: imbricate. Length of mesoscutellum: nearly equal to maximum width. Shape of mesoscutellum: semielliptical. Metascutellum: weakly carinate medially, undifferentiated from metanotal trough. Sculpture of metanotal trough: smooth. Sculpture of mesopleuron posterior to femoral depression: transversely striate. Sculpture of femoral depression: sometimes with faint traces of transverse striation. Sculpture of ventral mesopleuron: reticulate. Mesofemoral depression: present. Mesopleural carina: absent. Metapleural carina: present. Metapleural pit: present, located at anterior margin; Paracoxal sulcus: present as a smooth furrow below metapleural pit. Sculpture of propodeum: mostly smooth, weakly carinate medially, weakly rugose anterolaterally. Shape of legs: laterally compressed, especially hind coxae. Protibial spur: simple, curved, without comb. Tibial spur formula: 1-1-1. Tarsal formula: 5-5-5.

Metasoma. Color of metasoma: light to dark brown. Shape of metasoma: distinctly longer than wide, narrowed apically. Number of visible terga: 6. Number of visible sterna: 6. Sculpture of T1: mostly smooth, weakly carinate along anterior margin. Sculpture of terga: T2–T5 weakly reticulate laterally, smooth medially. Setation of terga: present. Shape of setae on terga: stout, straight. Number of setae on terga: increasing in number from T2–T5. Setation of T2–T4: present laterally, absent medially. Setation of T5–T6: present across tergite. Sculpture of sterna: not apparent. Laterotergites: present. Sculpture of laterotergites: absent. Setation of laterotergites: present. Laterosternites: absent. Shape of T1: trapezoidal, widening posteriorly. Longest tergite: T2, 2.5× as long as T3. Transverse furrow on anterior margin of T2: present. Shape of T6: triangular. Transverse felt field on anterior S2: absent. Pilosity of S2: dense.

Wings. Wing development: macropterous. Length of fore wing: extending to apex of metasoma. Marginal cilia of fore wing: present, longest along apical margin. Color of wings: hyaline basally, fuscous distally. Length of fore wing submarginal vein: 1/3 to greater than 1/2 fore wing length. Submarginal vein of fore wing: tubular basally, gradually becoming a tessellated line of cells medially, terminating in a nebulous knob. Shape of fore wing submarginal vein: straight. Shape of knob of submarginal vein: circular, with a single spine-like seta emerging from anterodorsal margin. Basal vein of fore wing: nebulous. Cubital vein of fore wing: nebulous basally, weaker distally. Marginal cilia of hind wing: present, longest along posteroapical margin. Submarginal vein of hind wing: present.

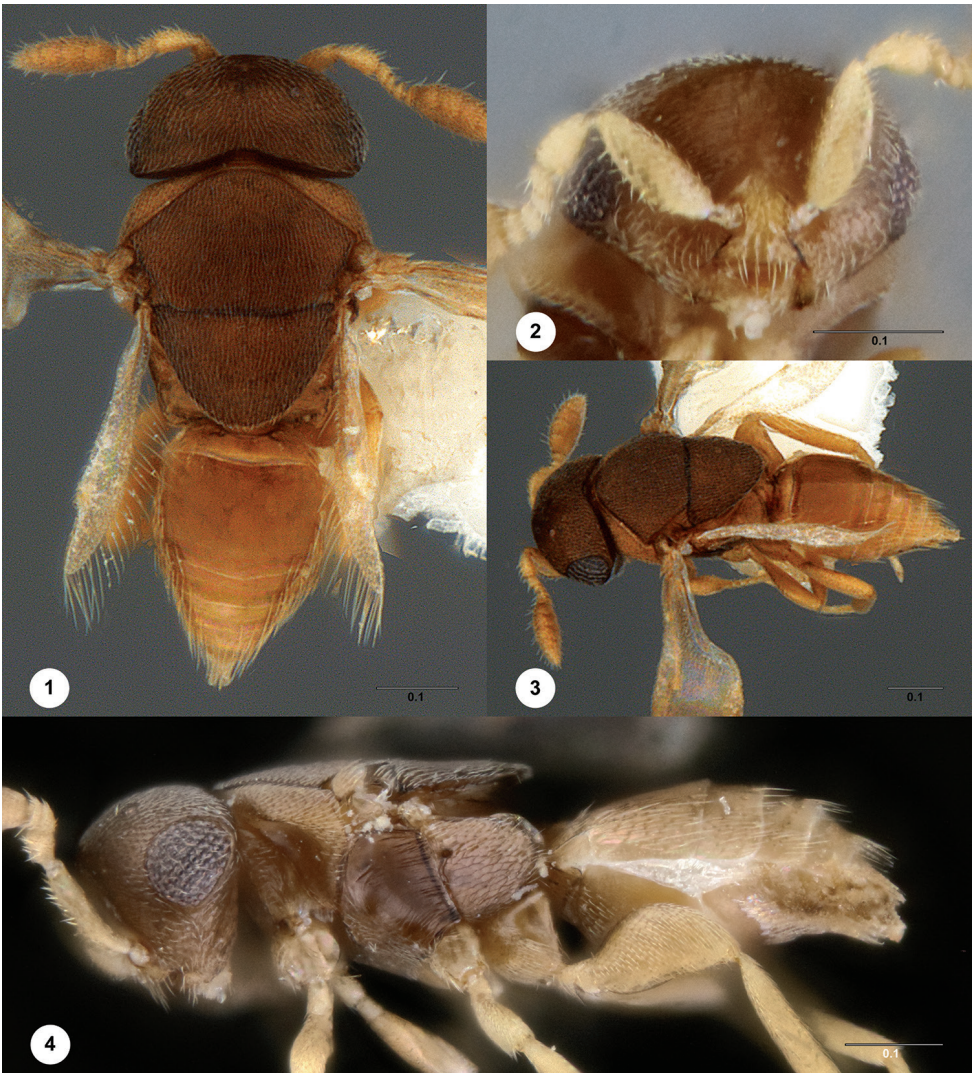

Figures 1–4. *Calixomeria lasallei* **1** female holotype (OSUC 711133), head, mesosoma, metasoma, dorsal view **2** female (USNMENT01197947), head, anterior view **3** female holotype (OSUC 711133), head, mesosoma, metasoma, dorsolateral view **4** female (USNMENT01197947), head, mesosoma, metasoma, lateral view. Scale bar: in millimeters.

Male. Unknown.

Biology. Unknown.

Etymology. The genus name is derived from the Latin word for 'cup' (*calix*) in reference to the shape of the mesoscutellum in dorsal view. The gender is feminine. This species is named in memory of Dr John La Salle for his lifetime of achievements that have advanced our knowledge of the parasitic Hymenoptera and biodiversity of Australia.

Link to Distribution Map. [http://hol.osu.edu/map-large.html?id=410778]

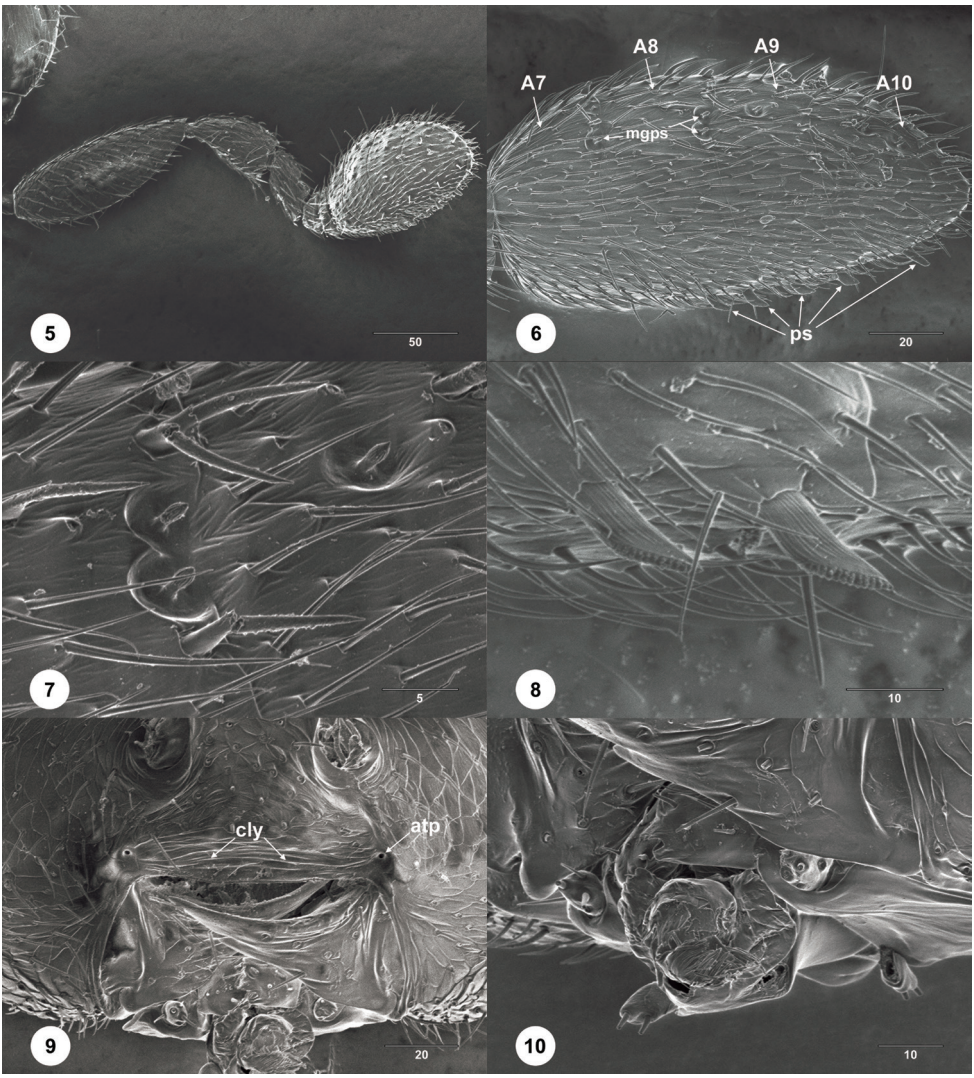

Figures 5–10. *Calixomeria lasallei* female (USNMENT01197947) **5** antenna, lateral view **6** clavomeres, lateral view **7** multiporous grooved peg sensilla, dorsal view **8** papillary sensilla, dorsolateral view **9** mouthparts, anterior view **10** maxillary and labial palps, anterolateral view. Scale bar: in micrometers.

Material examined. Holotype, female: **AUSTRALIA**: ACT, Blundells Creek, 35°22'S, 148°50'E, 850 m, 3 km E Piccadilly Circus, March 1985, flight intercept trap/window trough trap, Lawrence, Weir, & Johnson, OSUC 711133 (deposited in ANIC). *Paratypes*: **AUSTRALIA**: 31 females, OSUC 711124–711132, 711134–711149 (ANIC); OSUC 711150–711153 (CNCI); OSUC 711154–711155 (OSUC). *Other material*: **AUSTRALIA**: 1 female, USNMENT01197947 (ANIC).

Diagnosis. *Calixomeria* possesses several autapomorphic characters that readily separate it from the rest of Sceliotrachelinae, the most salient of which are: LOL and

OOL equal in length; knob of submarginal vein with a single, long, spine-like seta; the well-defined paracoxal sulcus; the large mesoscutellum, the posterior margin of which overhangs the metascutellum and most of the propodeum; and the presence of long, stout setae on tergites T2–T6.

In the key to world genera of Sceliotrachelinae (Masner and Huggert 1989), *Calixomeria* keys to couplet 31 separating *Helava* from *Alfredella* Masner & Huggert and *Aphanomerus* based on the pilosity of T1 and T2, and the presence or absence of foamy structures and median keels on the propodeum. *Calixomeria* lacks both setae that medially obscure the junction of T1 and T2 and foamy structures on the propodeum, thereby distinguishing it from *Helava*. Additionally, the propodeum is flat and lacks keels or protuberances, reliably separating *Calixomeria* from both *Alfredella* and *Aphanomerus*. The key of Masner and Huggert (1989) is modified to accommodate *Calixomeria*:

31 Anterior margin of T2 densely setose; T1 with keel; propodeum with foamy structures (Fig. 19)..... ***Helava* Masner & Huggert**

– Anterior margin of T2 glabrous or finely setose; T1 without keel; propodeum without foamy structures **32**

32 Female antennae appearing 8-merous; A8–A10 cylindrical, subcompact (Fig. 20); posterior mesoscutellar sulcus clearly indicated (Fig. 20)..... ..... ***Alfredella* Masner & Huggert**

– Female antennae appearing 7-merous; A7–A10 ovoid, compact (Figs 1–3, 5, 7, 8); posterior mesoscutellar sulcus not defined **32a**

32a Mesoscutellum distinctly wider than long, not obscuring medial portion of propodeum in dorsal view (Fig. 22); transepisternal line present (Fig. 21); OOL less than 1 ocellar diameter from inner margin of compound eye (Fig. 22); propodeum with subparallel median keels or bulges (Fig. 22)..... ..... ***Aphanomerus* Perkins**

– Mesoscutellum approximately as wide as long, nearly as long as mesoscutum (Fig. 1); posterior portion of mesoscutellum obscuring medial portion of propodeum in dorsal view (Fig. 1); transepisternal line absent (Fig. 4); OOL more than 3 ocellar diameters from inner margin of compound eye (Fig. 1); propodeum without median keels or bulges (Figs 11, 15) ....***Calixomeria* Lahey & Masner**

Discussion. *Calixomeria* is a highly apomorphic genus within Sceliotrachelinae. In the generic cluster concepts of Masner and Huggert (1989), *Calixomeria* falls within the *Aphanomerus*-cluster due to its compact, ovoid clava with distinct sutures, a character shared with *Aphanomerella* Dodd, *Parabaeus* Kieffer, *Tetrabaeus* Kieffer, and some species of *Aphanomerus* Perkins (Fig. 11) and *Helava* Masner & Huggert (Talamas and Masner 2016). The remaining genera within the *Aphanomerus*-cluster have a subcompact (*Austromerus* Masner & Huggert and some *Helava*) or compact antennal clava without sutures (*Calomerella* Masner & Huggert, *Pseudaphanomerus* Szelényi, and most *Aphanomerus*).

Clavomeres are defined by the presence of papillary sensilla on the ventral surface of antennomeres of female platygastroids (Bin 1981). The apical four antennomeres (A7–

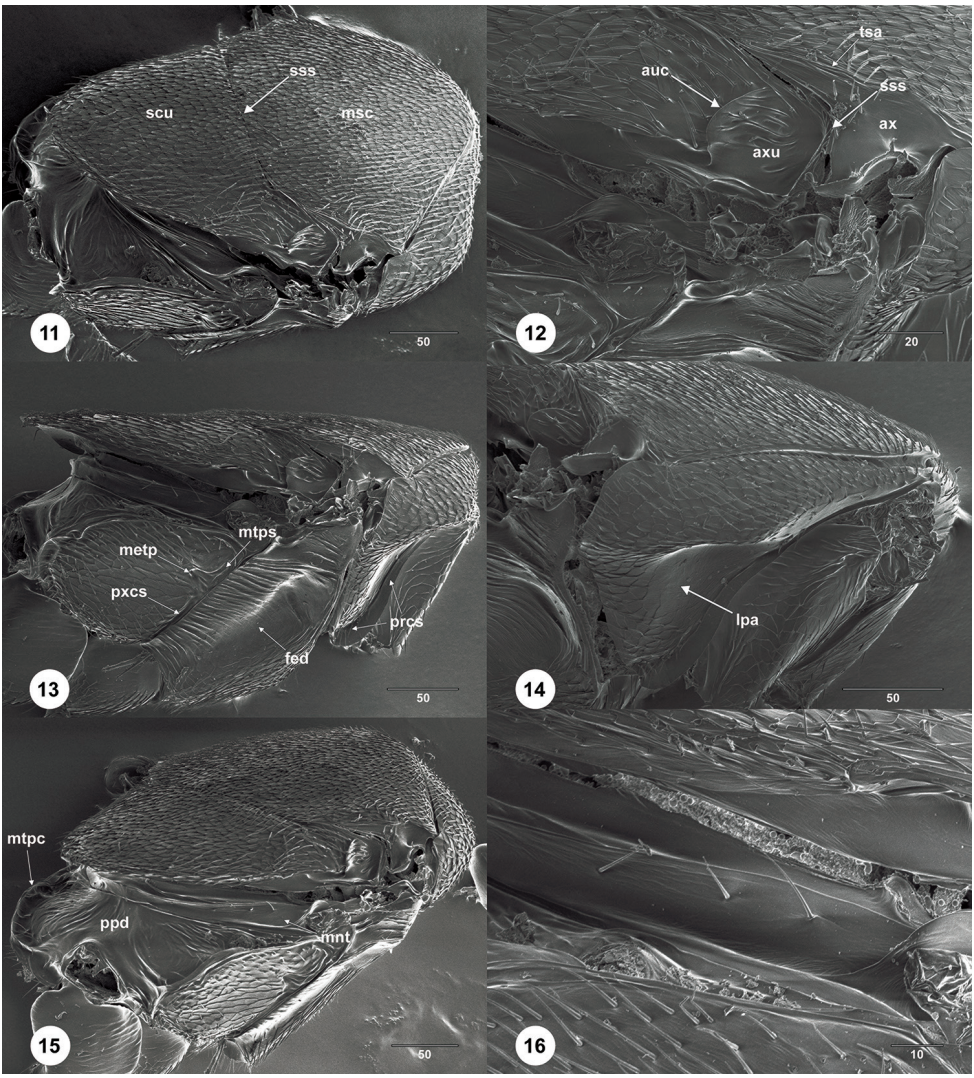

Figures 11–16. *Calixomeria lasallei* female (USNMENT01197947) **11** mesosoma, dorsolateral view **12** axillar complex, dorsolateral view **13** mesosoma, lateral view **14** pronotum, anterolateral view **15** mesosoma, posterodorsal view **16** metanotal trough, posterodorsal view. Scale bar: in micrometers.

A10) of *Calixomeria* females are enlarged, and A7 is fused to A8; however, A7 lacks papillary sensilla (Fig 6). The only sceliotracheline hypothesized to have lost papillary sensilla on one or more of its antennomeres is *Pseudaphanomerus*, but in this genus sutures between the clavomeres are absent, resulting in a 1-merous clava with a claval formula of 3, presumably from the loss of papillary sensilla on A7 and A8 (Masner and Huggert 1989). *Aleyroctonus* Masner & Huggert may be another example of this reductive trend:

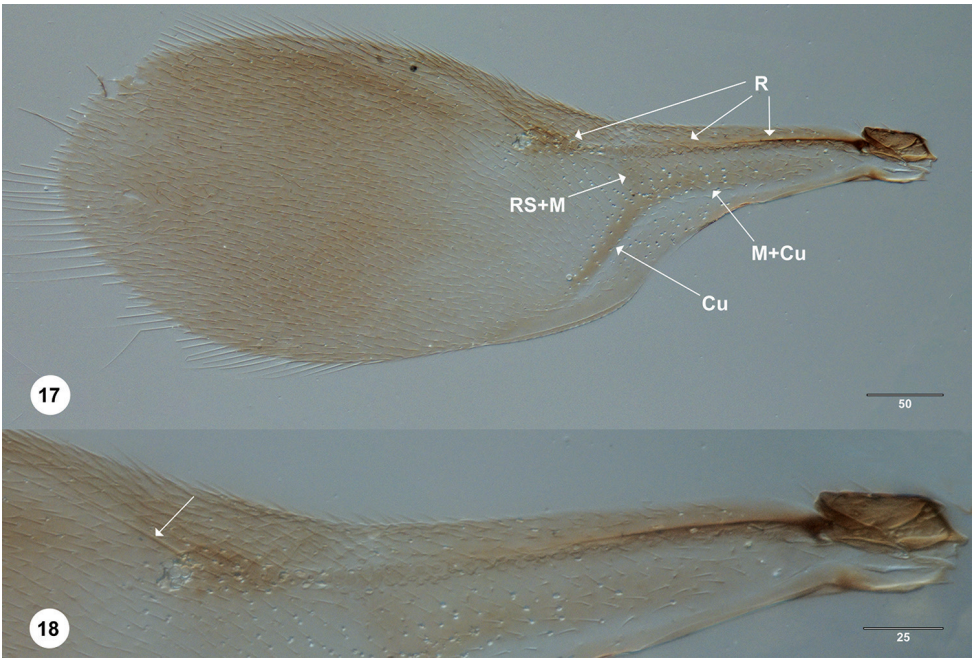

Figures 17, 18. *Calixomeria lasallei* female (OSUC 711154) **17** fore wing, dorsal view **18** close-up of R vein, with the arrow indicating the elongate seta emerging from the knob, dorsal view. Scale bar: in micrometers.

its claval formula is 1-2-2 and A7 is enlarged relative to A6; however, A7 is clearly separated from the clava by a deep suture, which is faintly indicated in *Calixomeria*.

The elongate marginal cilia of the fore wing are found in relatively few taxa within Platygastroidea (e.g., *Dyscritobaeus* Perkins, *Embioctonus* Masner, *Encyrtoscelio* Dodd, *Eumicrosoma* Gahan, *Exon* Masner, *Idris* Förster). Sceliotrachelines that possess this character are *Errolium* Masner & Huggert and *Neobia* Masner & Huggert, but in these genera the apex of the submarginal vein nearly touches the anterior margin of the fore wing, whereas it is distant from the margin in *Calixomeria* (Fig. 3). In addition, there is a single, long, spine-like seta near the anterodorsal margin of the knob of the submarginal vein in *Calixomeria*, a character not known to us elsewhere in Platygastroidea.

Calixomeria is most easily recognized by its cup-shaped mesoscutellum that overhangs the metascutellum and most of the propodeum (Figs 1, 3, 4, 13). This character is not encountered elsewhere within Sceliotracheline, but is expressed to varying degrees in certain scelionids, some of which possess a mesoscutellum very similar in appearance to *Calixomeria* (e.g. *Gryon* Haliday). Convergence in the character systems mentioned above may reflect biological (i.e., host choice) or environmental (i.e., habitat) similarities between these genera. Unfortunately, host associations are known for just a fraction of the superfamily. Molecular data from additional, freshly collected specimens would greatly facilitate the placement of this taxon within the framework of Sceliotrachelinae.

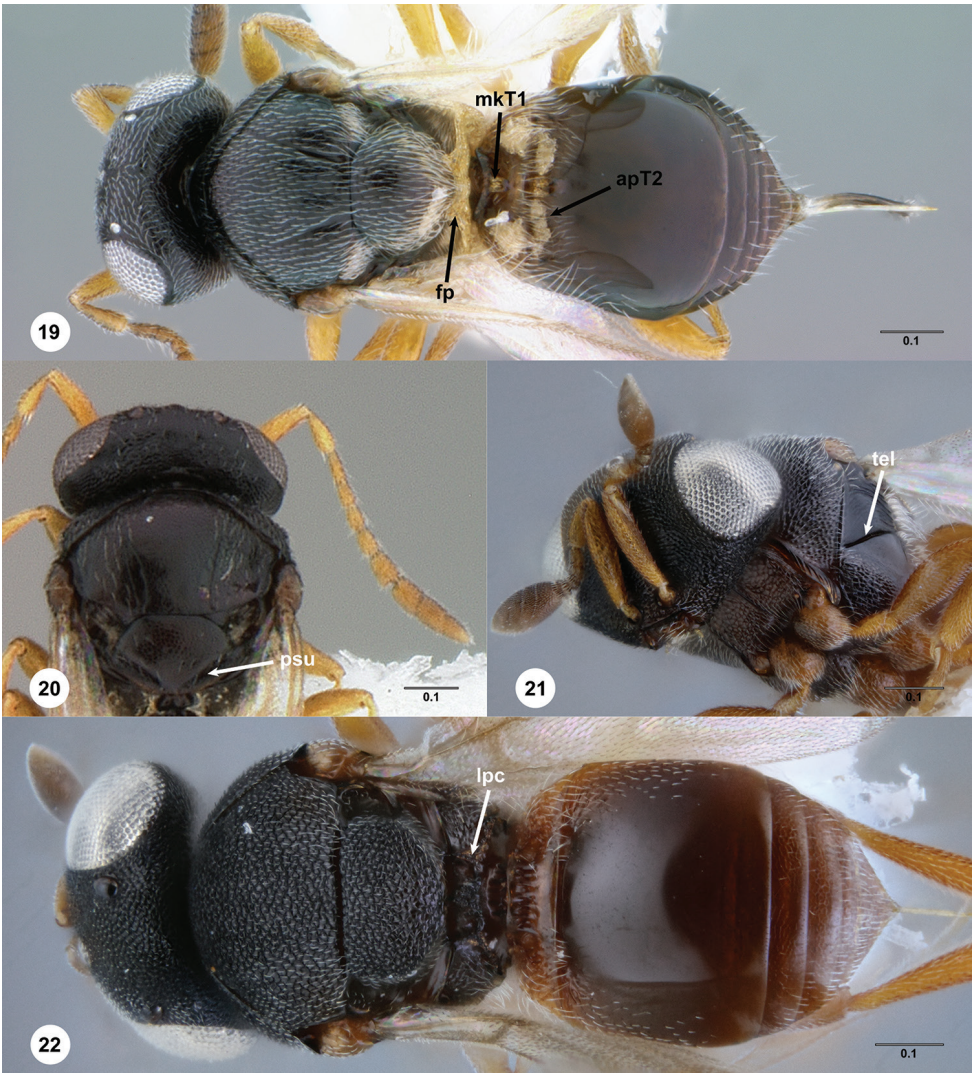

Figures 19–22. 19 *Helava aureipes* Masner & Talamas female holotype (USNMENT00989205), head, mesosoma, metasoma, dorsal view **20** *Alfredella* sp. female (USNMENT00916677), head, mesosoma, dorsal view **21** *Aphanomerus* sp. female (USNMENT01109890), head, mesosoma, ventrolateral view **22** *Aphanomerus* sp. female (USNMENT01109890), head, mesosoma, metasoma, dorsal view. Scale bar: in millimeters.

Acknowledgements

We thank Elijah Talamas (Florida State Collection of Arthropods, Gainesville, FL) and Amy Cutler (formerly of USNM) for providing most of the images in this publication. Elijah Talamas also provided useful comments on the manuscript. We also thank L. Musetti and S. Hemly (OSUC) for critical assistance with specimen handling and databasing.

References

ABRS (2015) Australian Faunal Directory. Platygastroidea. Australian Biological Resources Study, Canberra. https://biodiversity.org.au/afd/taxa/PLATYGASTROIDEA [Accessed on 2018-7-8]

Austin AD, Field SA (1997) The ovipositor system of scelionid and platygastrid wasps (Hymenoptera: Platygastroidea): comparative morphology and phylogenetic implications. Invertebrate Systematics 11: 1–87. https://doi.org/10.1071/IT95048

Bin F (1981) Definition of female antennal clava based on its plate sensilla in Hymenoptera Scelionidae Telenominae. Redia 64: 245–261.

Bin F, Colazza S, Isidoro N, Solinas M, Vinson SB (1989) Antennal chemosensilla and glands, and their possible meaning in the reproductive behavior of *Trissolcus basalis* (Woll.) (Hym.: Scelionidae). Entomologica 24: 33–97.

Dodd AP (1913a) Some south Queensland Proctotrypoidea. Memoirs of the Queensland Museum 2: 335–339.

Dodd AP (1913b) A remarkable new platygasterid genus from Australia. The Canadian Entomologist 45: 346–347. https://doi.org/10.4039/Ent45346-10

Masner L, Huggert L (1989) World review and keys to genera of the subfamily Inostemmatinae with reassignment of the taxa to the Platygastrinae and Sceliotrachelinae (Hymenoptera: Platygastridae). Memoirs of the Entomological Society of Canada 147: 1–214. https://doi.org/10.4039/entm121147fv

Mikó I, Vilhelmsen L, Johnson NF, Masner L, Pénzes Z (2007) Skeletomusculature of Scelionidae (Hymenoptera: Platygastroidea): head and mesosoma. Zootaxa 1571: 1–78. https://doi.org/10.11646/zootaxa.1571.1

Perkins RCL (1905) Leaf-hoppers and their natural enemies (Pt. VI. Mymaridae, Platygasteridae). Bulletin of the Experiment Station of the Hawaiian Sugar Planters' Association 1: 187–205.

Polaszek A, Agosti D, Alonso-Zarazaga M, Beccaloni G, de Place Bjørn P, Bouchet P, Brothers DJ,Earl of Cranbrook, Evenhuis NL, Godfray HCJ, Johnson NF, Krell FT, Lipscomb D, Lyal CHC, Mace GM, Mawatari SF, Miller SE, Minelli A, Morris S, Ng PKL, Patterson DJ, Pyle RL, Robinson N, Rogo L, Taverne J, Thompson FC, van Tol J, Wheeler QD, Wilson EO (2005) A universal register for animal names. Nature 437: 477. https://doi.org/10.1038/437477a

Talamas EJ, Buffington ML (2015) Fossil Platygastroidea in the National Museum of Natural History, Smithsonian Institution. Journal of Hymenoptera Research 47: 1–52. https://doi.org/10.3897/JHR.47.5730

Talamas EJ, Masner L (2016) Revision of New World *Helava* Masner & Huggert (Platygastridae, Sceliotrachelinae). Journal of Hymenoptera Research 53: 1–24. https://doi.org/10.3897/jhr.53.10217

Yang SY, Zhong YZ, Zhang JP, Wang XP, Zhang F (2016) A Comparative scanning electron microscopy study on antennal sensilla of *Trissolcus japonicus* and *Trissolcus plautiae*, egg parasitoids of stink bugs (Pentatomidae). Annals of the Entomological Society of America 109: 112–120. https://doi.org/10.1093/aesa/sav104

Yoder MJ, Mikó I, Seltmann K, Bertone MA, Deans AR (2010) A gross anatomy ontology for Hymenoptera. PLoS ONE 5 (12): e15991. https://doi.org/10.1371/journal.pone.0015991

ZooKeys 830: 75–98 (2019)
doi: 10.3897/zookeys.830.32188
http://zookeys.pensoft.net

RESEARCH ARTICLE

A peer-reviewed open-access journal
ZooKeys
Launched to accelerate biodiversity research

Molecular and morphological characterisation of *Longidorus polyae* sp. n. and *L. pisi* Edward, Misra & Singh, 1964 (Dorylaimida, Longidoridae) from Bulgaria

Stela S. Lazarova[1], Milka Elshishka[1], Georgi Radoslavov[1], Lydmila Lozanova[1], Peter Hristov[1], Alexander Mladenov[1], Jingwu Zheng[2], Elena Fanelli[3], Francesca De Luca[3], Vlada K. Peneva[1]

1 *Institute of Biodiversity and Ecosystem Research, Bulgarian Academy of Sciences, 2 Y. Gagarin Street, 1113 Sofia, Bulgaria* **2** *Laboratory of Plant Nematology, Institute of Biotechnology, College of Agriculture and Biotechnology, Zhejiang University, Hangzhou 310058, China* **3** *Istituto per la Protezione Sostenibile delle Piante, Consiglio Nazionale delle Ricerche (CNR), Bari, Italy*

Corresponding author: *Vlada K. Peneva* (vpeneva@ecolab.bas.bg)

Academic editor: *S. Subbotin* | Received 5 December 2018 | Accepted 7 February 2019 | Published 14 March 2019

http://zoobank.org/802300DF-1283-4852-B60A-0F883605CF42

Citation: Lazarova SS, Elshishka M, Radoslavov G, Lozanova L, Hristov P, Mladenov A, Zheng J, Fanelli E, De Luca F, Peneva VK (2019) Molecular and morphological characterisation of *Longidorus polyae* sp. n. and *L. pisi* Edward, Misra & Singh, 1964 (Dorylaimida, Longidoridae) from Bulgaria. ZooKeys 830: 75–98. https://doi.org/10.3897/zookeys.830.32188

Abstract

Longidorus polyae **sp. n.**, a bisexual nematode species found in the rhizosphere of pear tree (*Pyrus communis* L.), is described and characterised using an integrative approach. The new species has a female body length of 6.8–9.1 mm; a comparatively long odontostyle (114.0–127.5 µm); a narrow lip region (14.0–15.5 µm), anteriorly flattened and almost continuous with the body profile; pocket-like amphidial pouches long, deeply bilobed, and slightly asymmetrical, a guide ring at 37–42 µm from the anterior end; normal arrangement of pharyngeal glands; and a short bluntly rounded to hemispherical tail. Four juvenile stages identified: the first stage with a digitate tail, and the second and subsequent stages with a bluntly rounded tail. Males have one adcloacal pair and a row of 10 or 11 single ventromedian supplements; spicules 71.0–74.5 µm long. Based on morphometric data, the new species belongs to a group of species spread over Europe (*L. arthensis*, *L. silvae*, *L. uroshis*,), Iran (*L. kheirii*), and Syria (*L. pauli*), which share common

characters such as amphidial fovea, lip region and tail shapes, similar odontostyle and body length, and similar first-stage juvenile tail shape. Codes for identifying the new species are A5, B2, C34, D3, E3, F45, G12, H1, I2, J1, K7. The phylogenetic analysis based on D2-D3 expansion domains of the rRNA gene revealed that the new species has the closest relationships with *L. athesinus* from Italy and three unidentified *Longidorus* spp. from USA (*Longidorus* sp. 1, *Longidorus* sp. 2, and *Longidorus* sp. 6). New morphometric and molecular data (18S rRNA gene, ITS1-5.8S-ITS2 regions and D2-D3 28S rRNA gene sequences) for three populations of *L. pisi* from Bulgaria were obtained and variations between populations are discussed.

Keywords
18S rDNA, Bayesian inference, croplands, D2-D3 28S rDNA, ITS1-5.8S-ITS2, morphology, phylogeny

Introduction

Longidorus Micoletzky, 1922 is the second most diverse genus within family Longidoridae (Thorne, 1935) Meyl, 1961 occurring in all continents except Antarctica. At present, it contains 170 species (Barsalote et al. 2018; Gharibzadeh et al. 2018; Xu et al. 2018). So far, 16 species have been recorded in Bulgaria (Peneva et al. 2012, 2013). During the study of longidorids in croplands with organic and conventional management, an unknown species was recovered from the rhizosphere of a pear tree in north-central Bulgaria. Further, several populations of *L. pisi* Edward, Misra & Singh, 1964 were found in a tobacco field and two vineyards from the southwestern part of the country. *Longidorus pisi* was originally described from the rhizosphere of *Pisum sativum* L. growing at the Allahabad Agricultural Institute (now Sam Higginbottom University of Agriculture) in Uttar Pradesh, India (Edward et al. 1964). It was subsequently reported from various countries in Asia and Africa. *Longidorus latocephalus* Lamberti, Choleva & Agostinelli, 1983, a very similar species to *L. pisi*, was described from southwestern part of Bulgaria where it was associated with various crops. Choleva et al. (1991) proposed that *L. latocephalus* is a junior synonym of *L. pisi*. However, Navas et al. (1993), using the same data and those of Brown et al. (1982), carried out comprehensive analyses and distinguished two separate groups of *L. latocephalus* (8 populations from Bulgaria) and *L. pisi* (3 populations from India, 2 from South Africa, and 1 from Malawi). As a result, the taxonomic status of these two species has been debated in several subsequent studies (Robbins et al. 1995; Lamberti et al. 1996, 1997; Chen et al. 1997). Although there are observed differences in certain metrical data and amphid shape, Loof and Chen (1999) accepted the synonymy of *L. latocephalus* and *L. pisi* in their revised polytomous key. In three recent studies, sequences of D2-D3 28S rRNA or the *cox*I gene for populations from Greece, South Africa, and Iran have been provided, but, only the last population was characterised with morphological and morphometric data (He et al. 2005; Pedram et al. 2012; Palomares-Rius et al. 2017).

The present study aims to characterise morphologically and molecularly: i) an unknown species of genus *Longidorus* and ii) populations of *L. pisi* from Bulgaria, and iii) to evaluate these species' phylogenetic relationships by using 18S rRNA and D2-D3 expansion domains of the 28S rRNA genes.

Materials and methods

Sampling, nematode isolation and processing

The *Longidorus* specimens examined originated from various croplands in Bulgaria: Balgarene village (private garden, *Pyrus communis* L. tree), Petrich (a small field of *Nicotiana tabacum* L.), and two vineyards, near Sandanski (Polenitsa village, small-scale management) and Kromidovo village (organic farm). Nematodes were isolated from soil samples by a decanting and sieving technique (Cobb 1918). The recovered *Longidorus* specimens were heat killed at 55 °C for 2 minutes, fixed in a 4% formalin/1% glycerol mixture, processed to anhydrous glycerol (Seinhorst 1959), and mounted on glass microscope slides. Drawings were prepared using an Olympus BX51 compound microscope with differential interference contrast (DIC). Microphotographs and selected measurements were taken with an Axio Imager.M2 Carl Zeiss microscope, digital camera (ProgRes C7), and CapturePro 2.8 software (Jenoptic). Measurements were made using a system of a light microscope (Olympus BX41), digitising tablet (CalComp Drawing Board III) and Digitrak 1.0f programme (Philip Smith, the John Hutton Institute, Dundee, UK). The alpha-numeric codes of polytomous identification key of the genus *Longidorus* (Chen et al. 1997) and modified partial polytomous key (Peneva et al. 2013) were used for the morphological species delimitation.

DNA extraction, amplifications and sequencing

The genomic DNA extraction, amplification, and sequencing of single female specimens from three populations of *L. pisi* were carried out independently in two laboratories: one at the Institute for Sustainable Plant Protection, Bari, Italy and two at the Institute of Biodiversity and Ecosystem Research, Sofia, Bulgaria (IBER-BAS). Protocols used in both laboratories are presented previously (Groza et al. 2017). DNA analyses of *L. polyae* sp. n. were done in the IBER-BAS. One female, one male, and two first-stage juveniles were used for DNA extraction, amplification, and sequencing. The amplified products were sequenced by Eurofins MWG Operon, Germany. Sequences were deposited in GenBank with the following accession numbers: MK172047 and MK172049 for 18S rRNA gene of *L. polyae* sp. n. and *L. pisi*, respectively, MK172046 for D2-D3 expansion domains of 28S rDNA of the new species, and MK172048 and LR032064-65 for *L. pisi*. The partial 18S-ITS1-5.8S-ITS2 ribosomal segment was also sequenced for one population of *L. pisi* (LR032063, Petrich).

Sequence and phylogenetic analyses

The 18S and D2–D3 expansion segments of the 28S rRNA gene sequences were compared with those of other nematode species deposited in the GenBank database using

the BLASTn similarity search tool. The homologous sequences nearest to those of the new species were aligned using the GUIDANCE2 Server (http://guidance.tau.ac.il/) with default parameters (Sela et al. 2015) and manually trimmed and edited in Mega 6 (Tamura et al. 2013). Pairwise sequence identities/similarities were computed using the Sequence Manipulation Suite online (http://www.bioinformatics.org/sms2/) (Stothard 2000). The Bayesian Inference (BI) algorithm implemented in MrBayes 3.2.5 was used for phylogenetic relationships reconstructions (Huelsenbeck and Ronquist 2001; Ronquist et al. 2012). For further details, see Lazarova et al. (2016).

Results

Longidorus polyae **Lazarova, Elshishka, Radoslavov & Peneva, sp. n.**
http://zoobank.org/7BE5AED3-2352-4039-AFC5-4E0D2AB42C49

Description. (for measurements see Table 1, Figs 1–7)

Female. Body assuming a spiral shape. Lip region narrow, 5–6 µm high, continuous with body profile, anteriorly flattened. Labial papillae, especially second circle, prominent, changing slightly the body contour. Cuticle 4–5 µm thick at postlabial region, 4–5 µm along the body, and 9–10 µm on tail posterior to anus. Guide ring 4–6 µm wide. Body pores conspicuous, 1 lateral pore anterior to or at the level of guide ring, 2 or 3 along odontostyle, 1 or 2 along odontophore, 3–5 in narrow part of the pharynx and 2–4 in bulb region as well as none dorsal and 5–6 ventral in pharyngeal region; numerous lateral pores observed along the rest of body. Amphidial fovea prominent, deeply bilobed, lobes long, slightly asymmetrical, amphidial aperture assumed to be a minute pore, hardly visible under light microscope. Odontostyle very slender, 1.5–2 µm wide at base. Two nerve rings observed, the first at some distance behind the odontophore and at 246.3 ± 11.1 (230–254) µm from anterior end, the second, more prominent, behind the first one at 354.8 ± 48.1 (327–440) µm from anterior end. Pharyngo-intestinal valve broadly rounded. Normal arrangement of pharyngeal glands: nuclei of the dorsal and ventrosublateral glands situated at 22.7–28.5 % and 54.3–58.5 % (n = 5) of the distance from anterior end of the bulb. Dorsal gland nuclei 2–2.5 µm in diameter, subventral gland nuclei 3–4 µm in diameter. In odontophore area of one female a small rudimentary odontostyle tip (vestigium) observed pointing forward. Peculiar crystalloid bodies of various sizes and shapes (mostly rod-like) found in the intestine of all females. Prerectum 465–497.5 µm long and rectum 33–42 µm or 0.6–0.8 of body diameter at anus. Tail bluntly conoid, rounded to hemispherical. Two pairs of lateral caudal pores. Vagina extending to *ca.* half the corresponding body width. *Pars distalis vaginae* 20–26 µm long; *pars proximalis vaginae* 21–27 µm long, thick walled. Uterus bipartite, moderately long, anterior uterus 230–406, posterior uterus 235–394 µm long, respectively; well-developed sphincter between uterus and *pars dilatata oviductus*, *pars dilatata*, and uteri containing numerous sperm cells; ovary small.

Table 1. Measurements of adults and juveniles of *Longidorus polyae* sp. n. (mean ± standard deviation, with range). All measurements in micrometers except body length (mm).

Character	Holotype	Females n = 10	Males n = 4	J4 n = 8	J3 n = 3	J2 n = 7	J1 n = 8
L	7.87	7.98 ± 0.82 6.81–9.12	6.90 ± 0.590 6.15–7.53	6.28 ± 0.476 5.87–6.87	4.10, 4.12, 4.43	2.80 ± 0.21 2.51–3.13	2.19 ± 0.19 1.9–2.4
a	119.5	105.5 ± 8.4 95.7–119.5	115.3 ± 9.8 101.9–125.1	102.3 ± 11.2 89.4–116.6	93.8, 96.9, 99.3	83.1 ± 3.4 77.1–87.2	77.1 ± 5.8 70.4–88.2
b	14.0	14.7 ± 1.5 2.3–17.3	12.2 ± 0.8 11.1–13.1	11.5 ± 0.4 11.2–12.0	8.8, 8.8, 9.0	7.6 ± 0.5 6.9–8.6	6.6 ± 0.9 5.5–8.0
c	206.9	211.3 ± 21.5 184.8–260.0	171.4 ± 25.4 146.3–197.4	155.0 ± 9.2 145.0–166.4	100.2, 96.7, 102.1	77.2 ± 4.3 70.8–83.3	48.0 ± 8.1 38.0–65.0
c'	0.7	0.7 ± 0.04 0.7–0.8	0.8 ± 0.1 0.8–0.9	0.8 ± 0.0 0.8–0.9	1.1, 1.1, 1.1	1.3 ± 0.0 1.3–1.4	2.3 ± 0.3 1.8–2.6
V (%)/ Spicules	51	50.9 ± 0.9 49.2–52.6	72.8 ± 1.9 71–74.5				
G1 (%)	8.1	8.0 ± 1.0 6.7–10.3					
G2 (%)	8.2	7.8 ± 1.0 6.0–9.6					
d	2.71	2.8 ± 0.1 2.7–2.9	2.4, 2.8				
d'	2.04	2.1 ± 0.1 2.0–2.2	1.8, 2.0				
Odontostyle	124	121.8 ± 3.9 114–127.5	117.6 ± 5.0 112–123	108.8 ± 3.6 105–113	98, 95, 98	80.2 ± 2.1 78–83	75.6 ± 2.1 71–78.5
Replacement odontostyle				120.8 ± 2.0 119–123.5	113, 106, 115	93.4 ± 2.5 90–98	81.4 ± 2.2 77–83
Odontophore	79	79.8 ± 5.2 68–84	80.2 ± 3.8 76–84	71.2 ± 8.2 65–77	54.5, 64, 68	56.7 ± 3.9 51–61	
Anterior end to guide ring	40	40.4 ± 1.4 37–42	39.4 ± 2.5 37–42	34.5 ± 2.6 32–38	32, 29.5, 31	25.4 ± 1.5 23–27	21.2 ± 0.9 20–23
Pharyngeal bulb length	155	152 ± 10.2 132–167	145.5 ± 3.0 142–148	139.6 ± 1.1 138–141	128, 115, 113	99.5 ± 2.8 95–102	84.1 ± 6.0 78–94
Pharyngeal bulb width	29	26 ± 1.1 25–28	24.8 ± 1.7 23–27	23.6 ± 1.3 22–25	23, 19, 20	18.25 ± 0.5 17–19	14.7 ± 1.2 14–17
Developing gonad	–	–	–	73.7 ± 9.9 7–85	35, 33, 35	26.6 ± 1.6 22–30	19.6 ± 2.4 17–23
Pharynx	562	553.5 ± 54.1 481–646	565.0 ± 36.5 518–601	554.6 ± 26.1 524.5–571	468, 466, 494	367.9 ± 16.7 342–387	328.9 ± 20.9 298–359.5
Tail	38	37.9 ± 3.0 33–43	41.0 ± 7.3 1–47	40.6 ± 3.5 37.5–45.5	41, 43, 43	36.2 ± 1.5 35–38	46.4 ± 6.2 2–52
Length of hyaline part of tail	12	12.3 ± 0.7 12–13	12.5 ± 2.5 11–14				
Body diameter at:							
– lip region	14.5	14.6 ± 0.5 4–15.5	14.8 ± 0.6 14–15	12.2 ± 1.0 11–13	11, 11	8.2 ± 0.6 7–9	6.8 ± 0.2 6.5–7
– guide ring	30	30.3 ± 1.0 29–32	29.4 ± 2.0 27–32				
– base of pharynx	61	63.1 ± 4.7 59–75	56.0 ± 2.7 52–58	54.2 ± 1.2 52.5–55	43, 42, 44	33.5 ± 1.6 31–35.5	27.1 ± 2.0 24.5–30
– mid-body/ vulva	66	76.0 ± 8.6 66–92.5	60.0 ± 5.5 53–66.5	61.8 ± 6.1 55–68	44, 42.5, 45	33.6 ± 1.5 32–36	28.6 ± 3.6 24–34
– anus	53	53.1 ± 3.6 49– 61	48.2 ± 5.5 41–53	51.3 ± 1.7 49–53	36.5, 39, 40	27.1 ± 1.5 25–29	20.6 ± 2.2 18–24
– hyaline part	35	37.4 ± 3.1 35–42	26.5 ± 1.2 26–27				

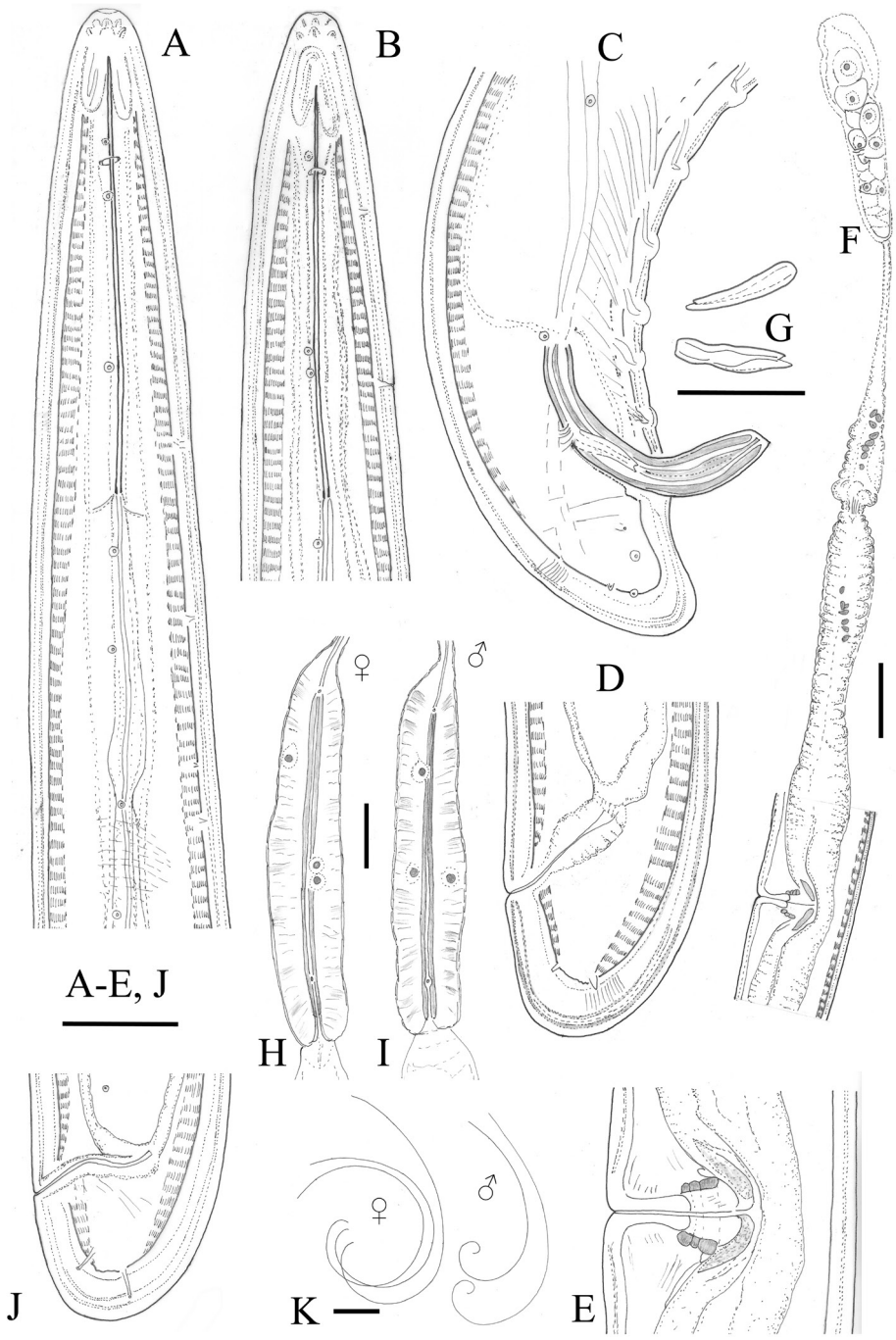

Figure 1. *Longidorus polyae* sp. n. **A, B** anterior region **C** posterior region **D, J** variations in tail shape **E** vagina **F** anterior genital branch **G** lateral pieces **H, I** female and male pharyngeal bulb **K** variations in female and male habitus shapes. Female: all except **C, G** and **I**. Scale bars: 25 µm (**A–E, J, G**); 50 µm (**F**); 1 mm (**K**).

Figure 2. *Longidorus polyae* sp. n., female **A** anterior region **B, C** variations in vagina **D, E** variations in tail shape **F–H** intestine inclusions **I** posterior genital branch **J** part of reproductive system. Scale bars: 20 µm (**A–H**); 100 µm (**I, J**).

Figure 3. *Longidorus polyae* sp. n., holotype **A** anterior end **B** pharyngeal region, arrows point to at nerve ring, pharyngeal bulb and cardia **C** intestine, posterior part with inclusions **D** anterior genital branch **E** vagina and part of the posterior genital branch **F** sphincter **G** intestine inclusion at higher magnification **H** tail **I** vagina **J** posterior ovary. Scale bars: 20 µm (**A, F–I**); 40 µm (**E, J**); 100 µm (**B–D**).

Figure 4. *Longidorus polyae* sp. n., male **A** anterior region **B** amphidial fovea **C** labial region **D** junction of two testes **E** distal part of testis **F** sperm cells **G** nerve ring **H, I** posterior end, different magnifications **J** tail and spicules **K** supplements. Scale bars: 20 µm (**A–C, F, G, J, K**); 40 µm (**D, E, H**); 100 µm (**I**).

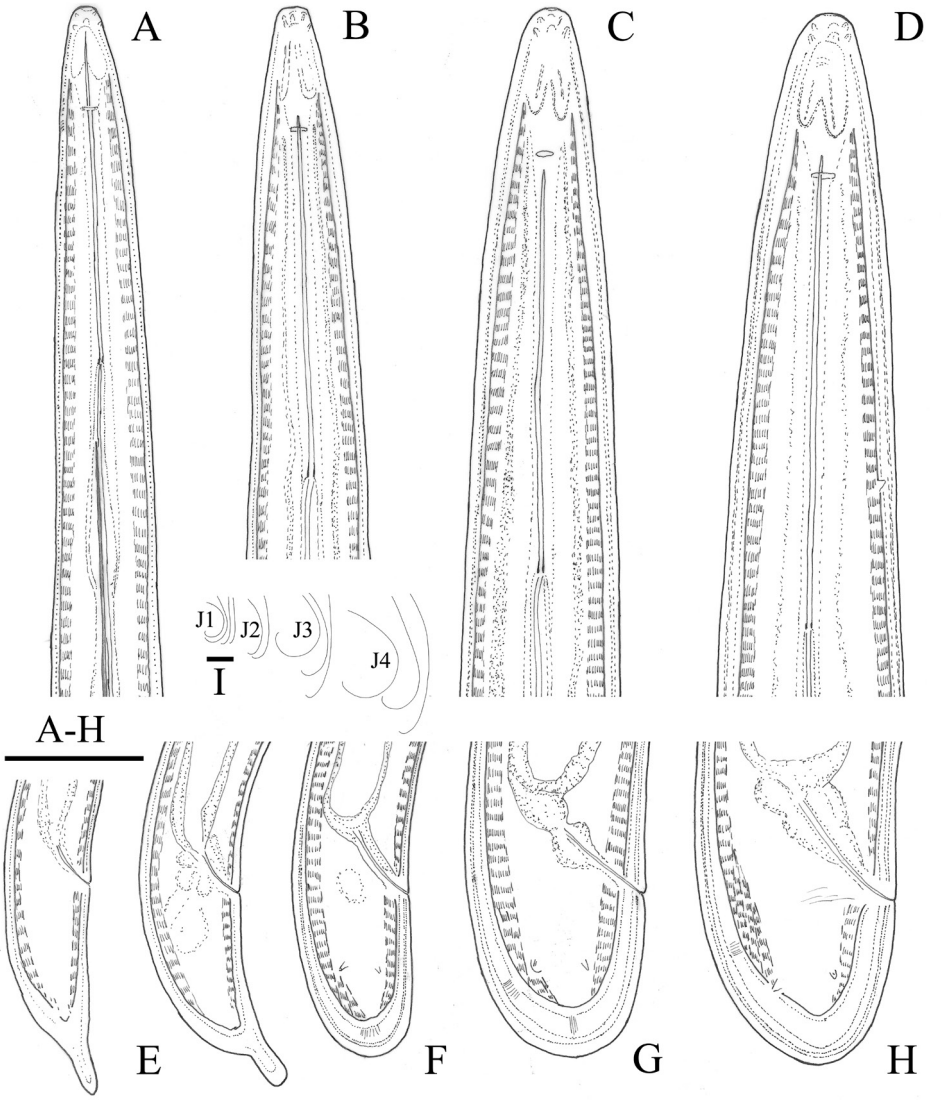

Figure 5. *Longidorus polyae* sp. n. **A–D** anterior end of first- (J1) to fourth- (J4) stage juveniles **E–H** tail of first to fourth juvenile stages **I** variations in J1-J4 habitus shapes. Scale bars: 25 µm (**A–H**); 1 mm (**I**).

Male. Rarer than females. Habitus as in females, posterior part more strongly coiled ventrally. Shape of lip region similar to that in females. Cuticle 4.0–4.5 µm thick at postlabial region, 4 µm along the body and 5 µm on tail posterior to cloaca. One lateral pore anterior to or at the level of guide ring, 2 along odontostyle, 1 or 2 along odontophore, 3 or 4 in narrow part of the pharynx and 2 or 3 in pharyngeal bulb region, no dorsal and 6 ventral pores; numerous lateral pores present along the rest of the body.

Two nerve rings observed, the first just behind the odontophore at a distance of 240.7 ± 12.0 (229–253) µm from anterior end, the second, more prominent behind the first one at 324 ± 12.7 (307.5–333) µm from anterior end. A small rudimentary odontostyle tip (vestigium) pointing forward observed in all males; in odontophore area (in 2 specimens) and in the slender part of pharynx (in 2 specimens). Pharyngo-intestinal valve broadly rounded. Tail short, bluntly conoid, dorsally convex, ventrally first straight then slightly concave. Three pairs of lateral pores on tail. One adclocal pair preceded by a row of 10 or 11 ventromedian supplements. Spicules slender, curved ventrally, lateral guiding piece sigmoid, 20–22 µm long. Spermatozoids oval (6–8 µm long).

Juveniles. Four juvenile stages can be differentiated based on the body, odontostyle, and replacement odontostyle length (Figs 5–7, Table 1). Habitus more or less an open C-shape, tail of the first stage juvenile digitate, with 9–11 µm long ventral peg, whereas in the subsequent developmental stages, bluntly rounded, **c'** decreasing.

Type locality and plant association. Balgarene village, Pre-Balkan zone of the Balkan Mountains, north-central Bulgaria (43°2'48.08"N; 24°46'24.53"E), 386 m a.s.l., private orchard, rhizosphere of *Pyrus communis* L.

Type material. The holotype (PNT 42), 20 paratype females, 2 males, and 92 juveniles (overall PNT 43-101) from all stages are deposited in the nematode collection of the Institute of Biodiversity and Ecosystem Research, BAS, Sofia, Bulgaria; 1 female, 1 male and 6 juveniles in the USDA Nematode Collection, Beltsville, Maryland, USA; 1 female, 1 male and 6 juveniles in the Wageningen Nematode Collection (WANECO), Wageningen, the Netherlands; 1 female and 8 juveniles in the Nematode Collection of the Institute of Sustainable Plant Protection, Bari, Italy.

Molecular characterisation. The NCBI BLASTn search of D2-D3 expansion segments of the 28S rRNA gene sequence showed highest similarity (93–94%) to several *Longidorus* species (*L. attenuatus* Hooper, 1961; *L. dunensis* Brinkmam, Loof & Barbez, 1987; *L. athesinus* Lamberti, Coiro & Agostinelli, 1991; *L. persicus* Esmaeili, Heydari, Archidona-Yuste, Castillo & Palomares-Rius, 2017; *L. euonymus* Mali & Hooper, 1974; *Longidorus* sp. 1, and *Longidorus* sp. 3). The highest identity (93.0–93.1%) was calculated with populations identified as *L. attenuatus* and *L. dunensis* (accessions KT755457 and AY593057, respectively). However, in the 28S rDNA phylogenetic analyses *L. polyae* sp. n. grouped in a clade with four *Longidorus* spp. (*L. athesinus*, Italy; *Longidorus* sp. 1, *Longidorus* sp. 2, and *Longidorus* sp. 6 from USA) with intermediate to high PP support (0.7–1.0) depending of the applied MSA algorithm (Fig. 9). The phylogenetic position of the new species based of 18S rRNA gene remained unresolved (Fig. 10) and was changing when different MSA algorithms and outgroups were tested. The pairwise sequence comparisons revealed highest identity (99.2%) with 18S rDNA sequences of *L. attenuatus* (AY687994), *L. elongatus* (de Man, 1876) Micoletzky, 1922 (EU503141), *L. piceicola* Liskova, Robbins & Brown, 1997 (AY687993), and *L. uroshis* Krnjaić, Lamberti, Krnjaić, Agostinelli & Radicci, 2000 (EF538760) (or 1564 identical residues of 1577 MSA length).

Diagnosis and relationships. *Longodorus polyae* sp. n. is a comparatively large bisexual species average 7.98 (6.81–9.12 mm) with the odontostyle over 100 µm (114.0–127.5

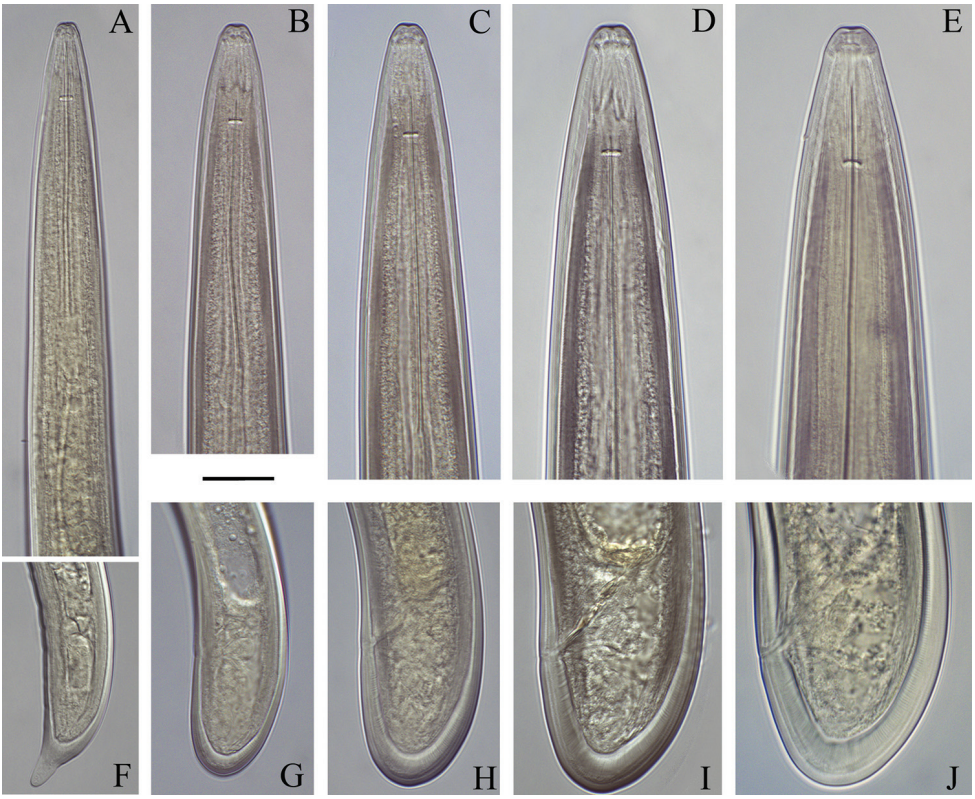

Figure 6. *Longidorus polyae* sp. n. **A–E** anterior end of first- to fourth-stage juveniles and female **F–J** tail of first- to fourth- stage juvenile and female. Scale bar: 20 µm.

µm) long; the lip region narrow (14.0–15.5 µm), almost continuous with body profile, anteriorly flat; amphidial fovea long, pocket-shaped, deeply bilobed, and lobes slightly asymmetrical; normal arrangement of pharyngeal glands; and tail short, bluntly rounded to hemispherical, four juvenile stages present, with the tail of the first-stage juvenile digitate.

The alpha-numeric codes for *L. polyae* sp. n. to be applied to the polytomous identification key for *Longidorus* species by Chen et al. (1997) and partial polytomous key proposed by Peneva et al. (2013) are: A5, B2, C34, D3, E3, F45, G12, H1, I2, J1, K7 (Table 2).

The group of large *Longidorus* species (code F34) with a moderately long odontostyle (code A45), pocket-shaped amphidial fovea, bilobed, symmetrical (code E2) or asymmetrical (code E3), normal arrangement of pharyngeal glands nuclei, short rounded tail (code H1) and digitate tail or tail with mucro (code K7) (according to Peneva et al. 2013) consists of a few species, namely: *L. arthensis*; *L. pauli* Lamberti, Molinari, De Luca, Agostinelli & Di Vito, 1999; *L. kheirii* Pedram, Niknam, Robbins, Ye & Karegar, 2008; *L. silvae* Roca, 1993; and *L. uroshis* (Table 2). The new species differs from these by the presence of peculiar inclusions in the intestine. Furthermore, it differs from:

Table 2. A partial polytomous key to the species of *Longidorus* species close to *L. polyae* sp. n., based on the key by Chen et al. (1997) and Peneva et al. (2013) incorporating species described after 1997.

***Longidorus* species**	**A**	**B**	**C**	**D**	**E**	**F**	**G**	**H**	**I**	**J**	**K**
***L. polyae* sp. n.**	**5**	**2**	**34**	**3**	**3**	**45**	**12**	**1**	**2**	**1**	**7**
L. arthensis	4	23	3	1	2	3	12	12	2	1	67
L. pauli	4	23	23	3	23	4	3	1	2	1	7
L. silvae	45	23	34	1**3***	3	34	2(3)	11	1	1	7
L. kheirii	45	345	34	1**3***	2	34	12	1	2	1	7
L. uroshis	56	24	34	3	23	34	2	1	2	1	7

Note: A – odontostyle length; B – lip region width; C – distance of guide ring to anterior body length; D – shape of anterior region; E – amphidial fovea shape; F – body length; G – index "**a**"; H – tail shape; I – presence/absence of male; J – number of juvenile stages; K – tail shape in first stage juvenile. *Changes in code D proposed.

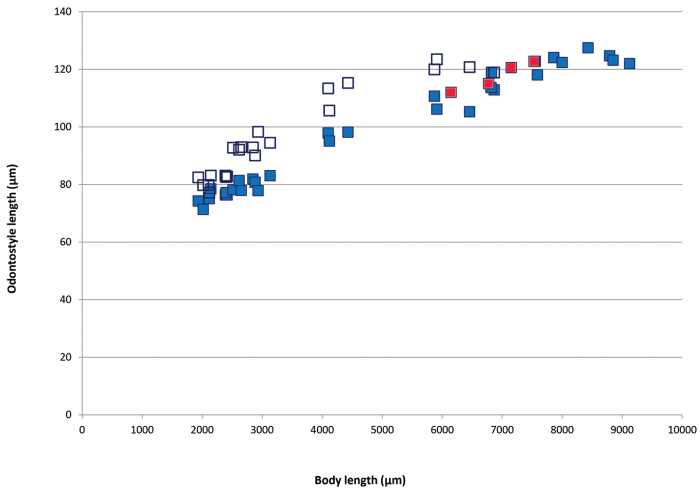

Figure 7. Scatter plot of functional odontostyle (blue square) and replacement odontostyle (white square) against body length of *Lonigidorus polyae* sp. n. juveniles (J1-J4) and females (blue), and male odontostyle (red).

L. pauli by females having differently shaped amphidial pouches (asymmetrically vs symmetrically bilobed); plumper body (**a** = 95.7–119.5 vs 120.3–143.5); more posterior guide ring position (37–42 vs 27–36 µm); longer spicules (71.0–74.5 vs 61–69 µm); guiding piece in male sigmoid vs straight; different shape of tail in second- and third-stage juveniles (bluntly rounded vs conical) (Lamberti et al. 1999);

L. uroshis by females having a longer body (6.81–9.12 vs 5.6–7.6 mm); narrower lip region (average 14.6 (14.0–15.5) vs average 17 (15.0–20.5) µm), higher **c** (184.8–260.0 vs 120.4–162.0) and lower **c'** values (0.7–0.8 vs 0.9–1.0) (Krnjaić et al. 2000);

L. kheirii by females having a narrower lip region (14.0–15.5 vs 19.5–23.0 µm) and pharyngeal bulb (25–29 vs 39.5–48 µm), higher **c** values (184.8–260.0 vs 119.0–167.8),

Table 3. Morphometric comparisons of *Longidorus polyae* sp. n. and related *Longidorus* spp. with similar morphological characters and DNA sequences.

Species	L (mm)	a	c'	Odontostyle length (µm)	Lip region width (µm)	Guide ring position (µm)
L. polyae	**6.81–9.12**	**95.7–119.5**	**0.7–0.8**	**114–127.5**	**14–15.5**	**37–42**
L. arthensis	5.14–6.74	74.5–110	0.8–1.1	102–111	14–17	30–38
L. athesinus	3.7–5.8	56.2–88.1	0.7–1.1	83.5–94	14–18	32–38
L. kheirii	6.7–9.0	60.3–82	0.6–0.9	113–130	19.5–23	36.5–45
L. pauli	6.5–8.6	120.3–143.5	0.8–1.0	102–118	14–17	27–36
L. silvae	5.9–8.0	87.5–123.5	0.72–0.84	113.5–133.0	14.0–17.0	37.0–44.0
L. uroshis	5.6–7.6	96.9–108.9	0.9–1.0	125–144	15–20.5	38–47

Note: Decimals are omitted for measurements in µm.

amphidial pouches deeply bilobed *vs* not to slightly bilobed; differently shaped tail of the first- and second-stage juvenile and different ovarium structure (Pedram et al. 2008).

L. arthensis by females having longer body (6.81–9.12 vs 5.14–6.74 mm) and odontostyle (114.0–127.5 vs 102.0–111.0 µm); asymmetrically vs evenly bilobed amphidial pouches, lower **c'** values (0.7–0.8 vs 1.0); males with longer spicules (71.0–74.5 vs 60.0–66.0 µm) (Brown et al. 1994);

L. silvae by females having two vs one nerve rings, differently shaped tail of the first-stage juvenile (subcylindrical, rarely cylindrical part/mucro with ventral position vs cylindrical mucro with central position), mucro shorter (9–11 vs 20–27 µm), higher **c** values (average 211.3 (184.8–260.0) vs average 166.7 (132.0–189.0) and posteriorly located vulva (50.9 (49.2–52.6) vs 48.6 (44.9–50.7) (Roca 1993). Males common vs absent (Roca 1993) or rare (Barsi and Lamberti 2004; Barsi et al. 2007).

Additionally, it can be differentiated from *L. athesinus*, a phylogenetically related species (Fig. 9), by females having longer body (6.81–9.12 vs 3.7–5.8 mm) and odontostyle (114.0–127.5 vs 83.5–94.0 µm); higher **a** value (95.7–119.5 vs 56.2–88.1); differently shaped tail in first-stage juvenile (digitate vs bluntly conoid) (Lamberti et al. 1991);

Morphometrical data of the most similar species are presented in Table 3.

Etymology. Named after the first author's sister Mrs Polya Kadiyska, a school teacher of art and iconography at the "Nikola Obretenov" Primary school in Rousse, Bulgaria.

Longidorus pisi Edward, Misra & Singh, 1964

= *Longidorus latocephalus* Lamberti, Choleva & Agostinelli, 1983

Notes. Morphological and morphometric data for females and juvenile stages are presented in Table 4 and in Figure 8. The morphometric data obtained in this study agreed with those of *L. latocephalus* from its type locality (Lamberti et al. 1983) and several additional populations studied by Lamberti et al. (1997). Furthermore, when compared to the type population of *L. pisi* (Edward et al. 1964), specimens from our populations

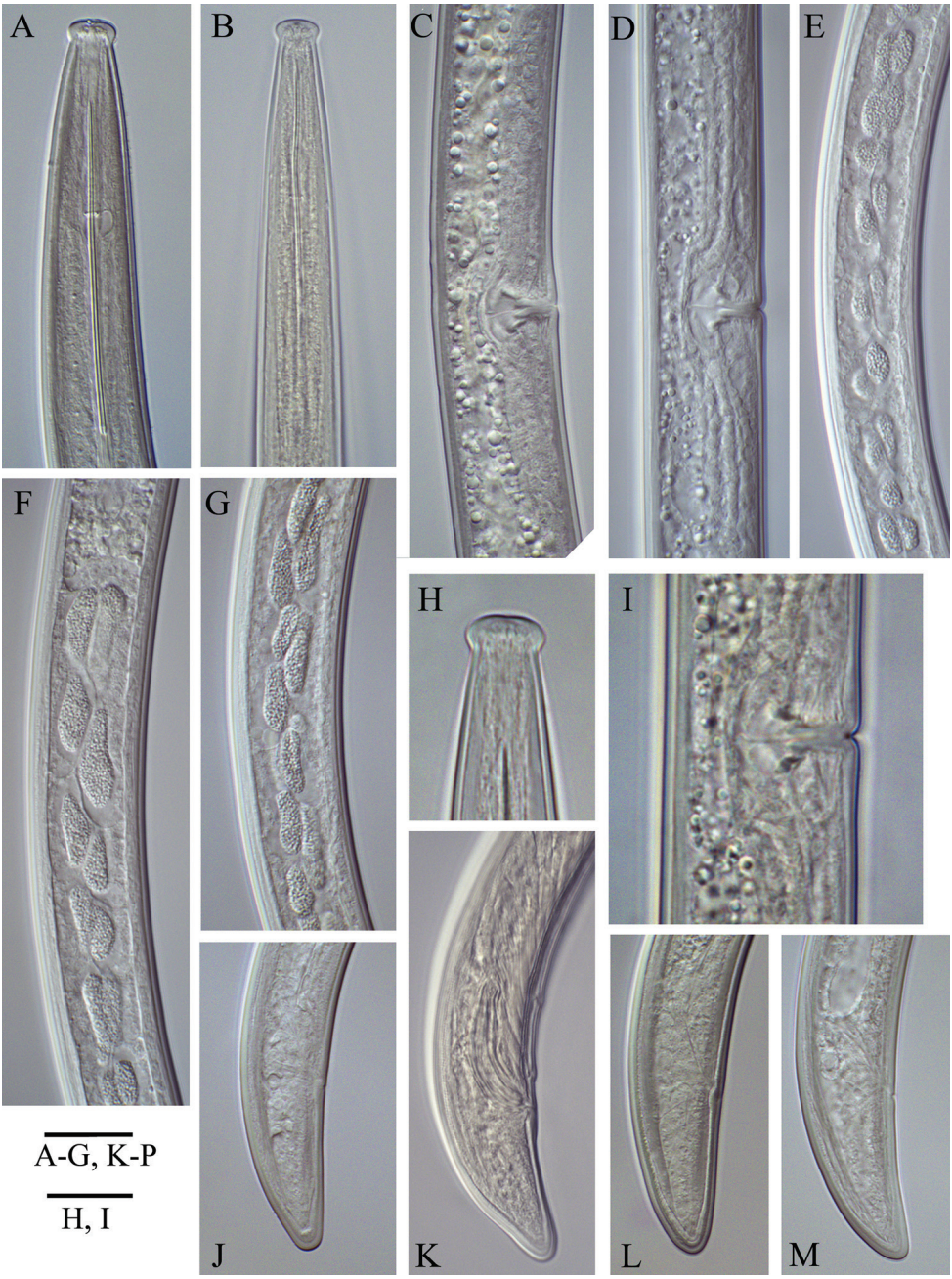

Figure 8. Bulgarian populations of *Longidorus pisi* Edward, Misra & Singh, 1964, anterior end of female (**A**) and male (**B**) female **C, D** vagina and part of reproductive system (different populations) **E–G** prerectum inclusions **H** labial region **I** vagina **J–M** variations in tail shape, female (**J, L, M**) and male (**K**). Populations: **A, L** Petrich **C, E–G, M** Sandanski **D, H, I, J** Kromidovo **B, K** male specimens from a tobacco field, Petrich region. Scale bars: 20 µm (**A–G, J–M**); 12 µm (**H, I**).

Table 4. Measurements of adults and juveniles of *Longidorus pisi* (mean ± standard deviation, with range) from different crops in Bulgaria. All measurements in micrometers except body length (mm).

Character \ Host	Petrich *Nicotiana tabacum*	Sandanski *Vitis vinifera*	Kromidovo *Vitis vinifera*	Petrich *Nicotiana tabacum*		
	female n = 9	female n = 6	female n = 2	J1 n = 2	J2 n = 9	J3 n = 2
L	4.02 ± 0.2 (3.77–4.28)	3.73 ± 0.2 (3.37–3.91)	3.17, 3.91	1.10, 1.21	1.8 ± 0.2 (1.55–2.07)	2.71, 2.65
a	125.2 ± 6.3 (117.2–132.1)	127.3 ± 5.2 (119.8–132.9)	113.7, 129.5	68.7, 68.6	82.2 ± 4.7 (75.8–88.6)	104.0, 99.1
b	12.1 ± 0.9 (10.9–13.4)	11.8 ± 1.2 (10.3–13.2)	8.8, 11.9	5.0, 5.7	6.8 ± 0.7 (5.9–8.2)	9.5, 9.1
c	102.8 ± 4.2 (96.7–111.3)	95.5 ± 5.7 (87.2–102.0)	80.9, 94.7	34.1, 38.2	46.2 ± 3.2 (41.2–50.3)	54.6, 63.7
c'	1.7 ± 0.1 (1.5–1.8)	1.9 ± 0.11 (1.7–2.0)	2.0, 2.0	3.0, 2.6	2.7 ± 0.2 2.5–2.9)	2.4, 2.2
V (%)	48.4 ± 0.9 (47.0–49.7)	50.9 ± 0.6 (50.2–51.7)	51.4, 51.4			
G1 (%)	5.3 ± 0.6 (4.9–6.2)					
G2 (%)	5.7 ± 0.6 (5.2–6.6)					
Odontostyle	74.8 ± 2.3 (72–79)	76.1 ± 1.7 (74–78)	75, 78	47.5, 46.5	52.9 ± 1.3 (50–55)	59, 59
Replacement odontostyle				53, 53	63.2 ± 1.5 (61–65)	76, 77
Odontophore	49.8 ± 2.8 (45–53)	49.4 ± 2.8 (46–53)	50		39.3 ± 2.1 (37–42)	
Anterior end to guide ring	44.1 ± 1.6 (42–46)	43.6 ± 0.9 (43–45)	44, 42	25, –	31.7 ± 1.4 (30–34)	36, 36
Pharyngeal bulbus length	69.1 ± 2.9 (65–73)	71.3 ± 1.4 (69.5–74)	76, 74	45, 37	51.5 ± 3.3 (47–56)	63, 62
Anterior to nerve ring	147.4 ± 5.0 (138–151)	141.4 ± 6.2 (132–150)	–, 153		115.4 ± 4.4 (110–121)	130, 138
Pharynx	330.9 ± 20.8 (292–368)	310.7 ± 23.3 (291–342)	361, 328	222, 212	263.4 ± 14.8 (242–285)	286, 292
Tail	38.7 ± 2.0 (36–43)	39.1 ± 1.8 (37–42)	39, 41	32, 32	39 ± 2.5 (35–43)	50, 42
Body diameter at:						
– lip region	11.0 ± 0.5 (10–12)	10.3 ± 0.3 (10–11)	10, 11	7, 7	8.5 ± 0.9 (8–9)	10.5, 9
– base of pharynx	27.9 ± 0.8 (27–29)	25.6 ± 0.5 (25–26)	27, 26.5	16, 17	20.5 ± 0.7 (19.5–22)	26, 24.5
– mid-body	31.9 ± 1.1 (30–34)	29.3 ± 0.8 28–30)	28, 30	16, 18	21.7 ± 0.9 (20–23.5)	26, 27
– anus	22.9 ± 1.2 (21–24.5)	20.5 ± 0.8 (20–22)	20, 21	11, 12	14.5 ± 0.5 (14–15)	21, 19

revealed longer odontostyle (average 75 (72–79) and average 76 (74–78) vs 58 (56–61) µm) and odontophore (average 50 (45–53) and average 49 (46–53) vs average 42.7 (35–43) µm); longer distances anterior end to guide (average 44 (42–46) vs average 32 (31–35) µm) and nerve ring (average 147 (138–151) and 141 (132–150) vs average 133 µm); wider (average 10.6 vs 7.5 µm) and higher (5–6 vs 3.5 µm) lip region and lower

c' ratio (average 1.9 (1.5–2.0) and average 1.7 (1.5–1.8) vs average 2.5 (2.4–2.6). The morphometrics of our populations were more similar to the Iranian population of *L. pisi* (Saveh, Markazi province) for which a D2-D3 expansion domain of 28S rRNA gene sequence identical to ours is available (Pedram et al. 2012). Differences in a few characters were observed, e.g. smaller **a** (average 125.2 (117.2–132.1) and 127.3 (119.8–132.9) vs 139.4 (134.8–144.6) and **c'** (average 1.9 (1.5–2.0) and average 1.7 (1.5–1.8) vs average 2.5 (2.3–2.9) values, larger diameter at anus level (average 22.9 (21–24.5) and average 20.5 (20–22) vs average 18.1 (16–19) μm) and slightly shorter tail (average 38.9 (36–43) and average 39.1 (37–42) vs average 45 (43–47) μm) compared to the latter population.

Sequence and phylogenetic analyses. Three ribosomal DNA regions (D2-D3 expansion segments of 28S rRNA gene, 18S rRNA gene, and ITS1-5.8S-ITS2 regions) of *L. pisi* were amplified and sequenced. The D2-D3 expansion segments of 28S rRNA gene sequences from all populations were identical to that of the Iranian population (JQ240274, Pedram et al. 2012) and differed slightly (1 and 3 bp) from those of other populations (Greece (AY601569) and South Africa (AY601568), respectively) identified as *L. latocephalus* (He et al. 2005). In the phylogenetic analysis, all aforementioned sequences formed a clade with maximal Bayesian posterior probability (1.0) and showed a close relationship with *L. mindanaoensis*. The BLASTn search using 18S rRNA gene sequence revealed highest identity (99%) with five accessions (two *Longidorus* (HQ735099 *L. mindanaoensis* Coomans, Tandingan De Ley, Angsinco Jimenez & De Ley, 2012 and AY283163 *L. ferrisi* Robbins, Ye & Pedram, 2009) and three *Paralongidorus* species (JN032586 *P. bikanerensis* (Lal & Mathur, 1987) Siddiqi, Baujard & Mounport, 1993; AJ875152 *P. maximus* (Bütschli, 1874) Siddiqi, 1964 and KJ427794 *P. rex* Andrássy, 1986). A pairwise comparison of *L. pisi* sequence with the closest sequences (AY283163, HQ735099, JN032586, AJ875152 and KJ427794) revealed 14–22 different nucleotides. The 18S rDNA phylogenetic tree is presented in Figure 10.

Discussion

Longidorus polyae Lazarova, Elshishka, Radoslavov & Peneva sp. n.

The new species belongs to a group of large *Longidorus* species having a moderately long odontostyle, a bilobed pocket-shaped amphidial fovea, a short rounded tail in adults, and a digitate tail with mucro in first-stage juveniles. The group contains just a few species occurring in Europe (*L. arthensis*, *L. silvae*, *L. uroshis*), Syria (*L. pauli*), and Iran (*L. kheirii*). A very specific character observed in all female specimens of *L. polyae* sp. n. were the crystalloid structures of various shapes and sizes present in the intestinal lumen, especially in the posterior gut region. To our knowledge, the presence of similar crystalloid structures has been rarely observed in plant-parasitic species (e.g. *L. perangustus* (Roshan-Bakhsh et al. 2016) and *Hirschmanniella kwazuna* (Van den Berg et al. 2009)), and more often in non-parasitic nematodes (Heyns and Coomans 1983; Bird et al. 1991; Tahseen 2012; Abebe et al. 2013).

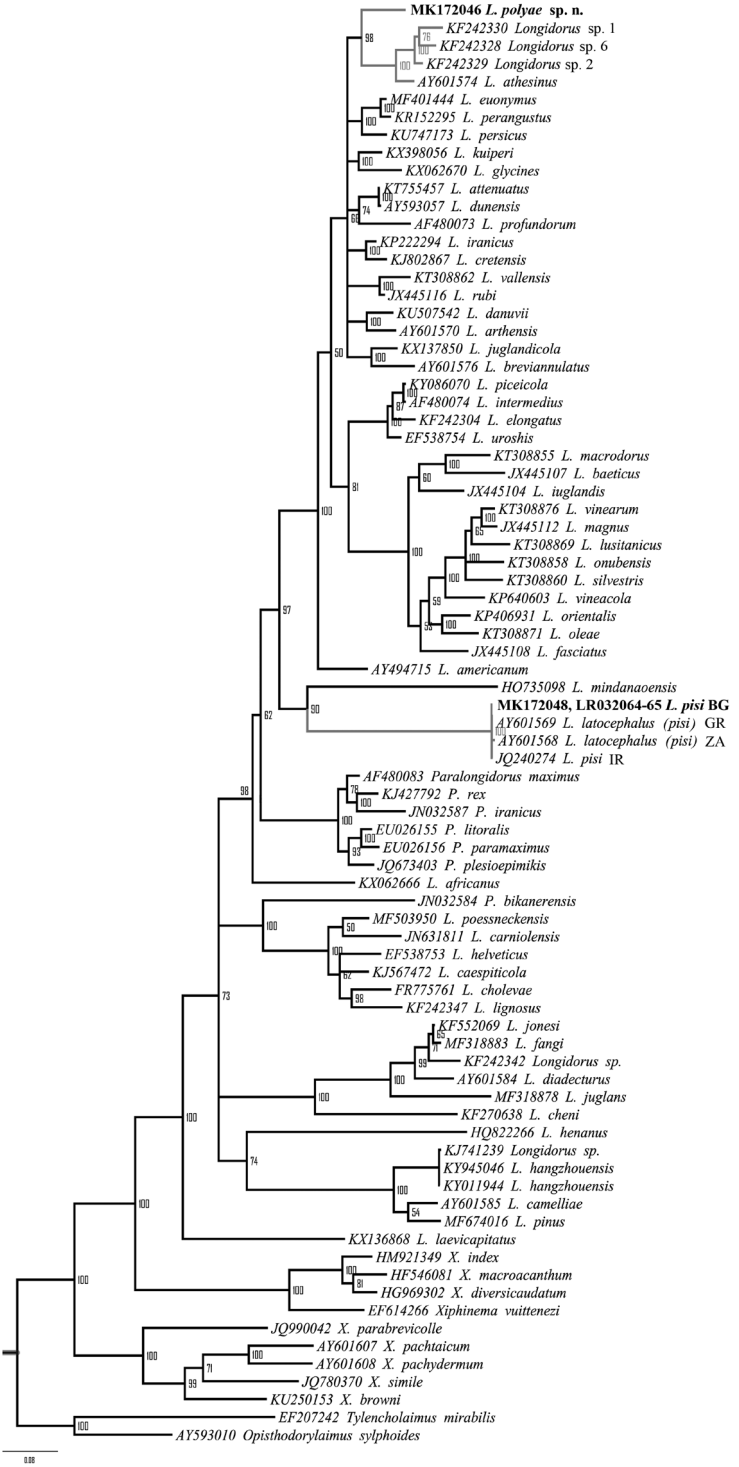

Figure 9. Phylogenetic tree using D2-D3 expansion segments of the 28S rRNA gene inferred from a Bayesian analysis with GTR+I+G model. Numbers represent the Bayesian posterior probabilities.

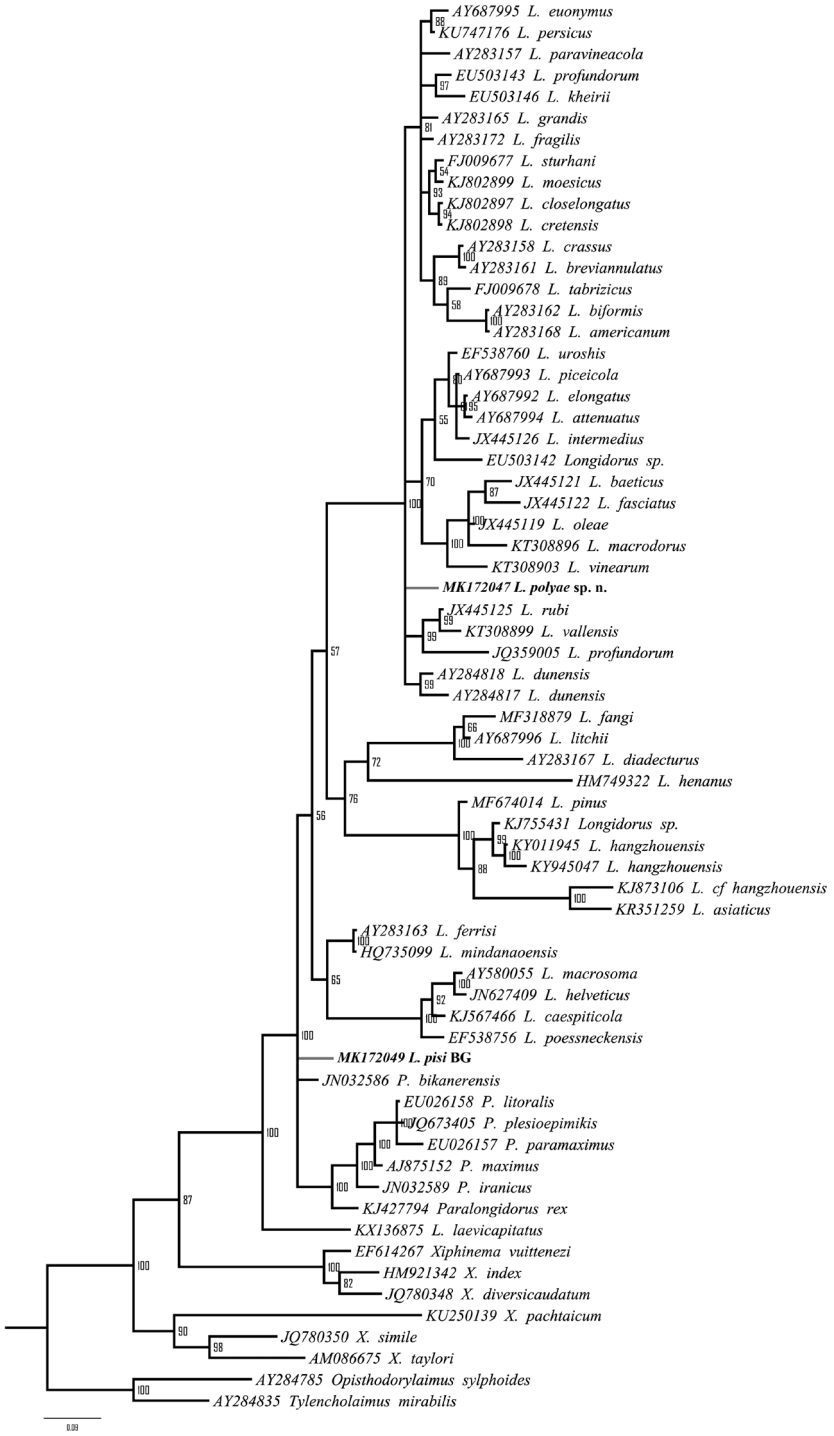

Figure 10. Phylogenetic tree using 18S rRNA gene inferred from a Bayesian analysis with GTR+I+G model. Numbers represent the Bayesian posterior probabilities.

DNA data were available for all species except *L. pauli*. However, different ribosomal fragments have been deposited in the GenBank database, which limit the reconstruction of phylogenetic relationships within the group. Moreover, the D2-D3 expansion segments of 28S rDNA sequences of the new species showed highest similarity (93%) to two other species of *Longidorus*, *L. attenuatus* and *L. dunensis*, with sequences revealing a very high inter-species similarity (or 1–3 nucleotides difference). One population of *L. silvae* from Serbia, characterised molecularly by three sequences of D3 segment of 28S rDNA (AM412367-AM412369, Barsi et al. 2007), was very similar to *L. polyae* sp. n. comparing the same fragment (2 nucleotides difference at the 3' end, overall multiple sequence alignment of 300 characters). Likewise, a very high level of similarity for the same ribosomal segment of 28S rDNA are known for other *Longidorus* species, e.g. the multiple alignment of 10 *L. aetnaeus* Roca, Lamberti, Agostinelli & Vinciguerra, 1986 and five *L. leptocephalus* Hooper, 1961 sequences revealed one indel for an alignment length of 237 characters. However, both species showed higher inter-species dissimilarity in D2-D3 expansion segments of 28S rDNA (0.7–1.6%) and the *cox*1 mtDNA region (3.2%) (Palomares-Rius et al. 2017).

In comparing the morphology of *L. polaye* sp. n. to the most closely related species, inaccuracies in code D values (related to the shape of anterior regions) were identified. In the original description of *L. silvae*, the lip region was described as "subacute, flattened frontally and continuous with the rest of the body" (Roca 1993: 211), which rather corresponds to D3 code description ("body tapering distinctly, lip region flattened, continuous, or slightly offset by depression") than to D1 ("body tapering distinctly, lip region rounded, continuous") according to Chen et al. (1997: 18). Similarly, in the diagnosis of *L. kheirii*, a D1 code was assigned instead of D3 ("head continuous with the contour of the rest of body, a truncate and slightly concave" Pedram et al. 2008: 206).

Logidorus pisi Edward, Misra, & Singh, 1964

Morphological and molecular data of three Bulgarian populations of *L. pisi* have been presented within the framework of this study. Some differences in morphometrics between these populations and the original description have been observed; however, a more comprehensive integrative study on materials from the type area would help to evaluate the divergences. New sequences for two ribosomal DNA regions (18S rRNA gene and ITS1-5.8S-ITS2) were obtained for *L. pisi* for the first time. The D2-D3 expansion segments of 28S rRNA gene sequences of all populations from Bulgaria were identical. In the phylogenetic analysis (Fig. 9), our populations and all populations of *L.pisi* (= *L. latocephalus*) from Greece, Iran, and South Africa clustered together with *L. mindanaoensis* and thus supports their evolutionary relationship as revealed by a previous study (Coomans et al. 2012). However, in the phylogenetic tree based on the 18S rRNA gene (Fig. 10), the position of *L. pisi* was not resolved. Both phylogenetic trees showed incongruent evolutionary relationships between *L. pisi* and *L. mindanaoensis*. The ITS sequence of *L. pisi* showed no similarity with the corresponding region of *Longidorus* species present in the database and no phylogenetic analyses were carried out.

The species appears to have a wide distribution, having been reported from three continents and numerous countries: Asia (India, Pakistan, Iran, China), Africa (Botswana, Egypt, Malawi, Mozambique, Cameroon, Libya, Namibia, Senegal, South Africa, Sudan), and Europe (Bulgaria, Macedonia, Greece). It was associated mainly with cultivated plants (pea, grapevine, mint and other medical plants, maize, potato, apple, pear, sugarcane) and rarely with natural vegetation (Marais and Swart 2002; Bohra and Baqri 2005). In Bulgaria and other Balkan countries, it was found in soils from agricultural habitats, associated with annual and perennial crops (tobacco, tomato, sweet pepper, black currant, grapevine, apple, peach, kiwifruit walnut, sweet chestnut, *Pinus nigra* J.F. Arnold, etc.) (Lamberti et al. 1983; Choleva et al. 1991, 1997), which suggest its probable introduction to Europe.

Acknowledgements

The study was supported by the Sino-Bulgaria government cooperation project (project number 01/3-2014) and the project ANIDIV3, funded by the Bulgarian Academy of Sciences. We thank Thomas Prior (Plant Pest and Disease Programme, FERA, Sand Hutton, UK) for providing images of a *L. silvae* paratype and both reviewers for their constructive comments and feedback on the manuscript.

References

Abebe E, Ferebee B, Taylor T, Mundo-Ocampo M, Mekete T, De Ley P (2013) *Neotobrilus nicsmolae* n. sp. (Tobrilidae: Nematoda) and *Chronogaster carolinensis* n. sp. (Chronogasteridae: Nematoda) from Lake Phelps, North Carolina. Journal of Nematology 45(1): 66–77.

Barsalote EM, Pham HT, Lazarova S, Peneva V, Zheng J (2018) Description of *Longidorus cheni* sp. n. (Nematoda, Longidoridae) from China. ZooKeys 744: 1–18. https://doi.org/10.3897/zookeys.744.23265

Barsi L, Lamberti F (2004) *Longidorus silvae* Roca, 1993 (Nematoda: Longidoridae): a first record from the former territory of Yugoslavia and the description of a male specimen. Russian Journal of Nematology 12: 97–105.

Barsi L, Lamberti F, De Luca F (2007) Morphological and molecular characterisation of *Longidorus danuvii* sp. n. and *L. silvae* Roca, 1993 (Nematoda: Dorylaimida) from Serbia. Nematology 9(4): 585–598. https://doi.org/10.1163/156854107781487279

Bird AF, McClure SG, Nicholas WL (1991) Observations on crystalloid bodies in the pseudocoelom of *Eutobrilus heptapapillatus*. Journal of Nematology 23(1): 39–47.

Brinkman H, Loof PAA, Barbez (1987) *Longidorus dunensis* n. sp. and *L. kuiperi* n. sp. from the Sand dune coastal region of the Netherlands (Nematoda: Longidoridae). Revue de Nématologie 10(3): 299–308.

Brown DJF, Grunder J, Hooper DJ, Klingler J, Kunz P (1994) *Longidorus arthensis* sp. n. (Nematoda: Longidoridae), a vector of cherry rosette disease caused by a new nepovirus in cherry trees in Switzerland. Nematologica 40: 133–149. https://doi.org/10.1163/003525994X00094

Brown DJ, Hooper DJ, Saka VW (1982) A description of a male *Longidorus pisi* (Nematoda: Dorylaimoidea) from Malawi with observations of females and the taxonomic status of the species. Nematologia Mediterranea 10(1): 101–106.

Bohra P, Baqri QH (2005) Plant and soil nematodes from Ranthambhore National Park, Rajasthan, India. Zoos' Print Journal 21(1): 2126. https://doi.org/10.11609/JoTT.ZPJ.1340.2126

Chen Q, Hooper DJ, Loof PA, Xu J (1997) A revised polytomous key for the identification of species of the genus *Longidorus* Micoletzky, 1922 (Nematoda: Dorylaimoidea). Fundamental and Applied Nematology 20(1): 15–28. https://doi.org/10.1163/156854199507974

Choleva B, Peneva V, Brown DJ (1991) *Longidorus latocephalus* Lamberti, Choleva & Agostinelli, 1983, a junior synonym of *L. pisi* Edward, Misra & Singh, 1964 (Nematoda: Dorylaimida). Revue de Nématologie 14(4): 505–509.

Cobb NA (1918) Estimating the nema population of the soil. Agricultural Technology Circular I. Bureau of Plant Industry, U.S. Government Printing Office, Washington, 48 pp.

Coomans A, Tandingan De Ley I, Angsinco Jimenez L, De Ley P (2012) Morphological, molecular characterization and phylogenetic position of *Longidorus mindanaoensis* n. sp. (Nematoda: Longidoridae) from a Philippine *Avicennia* mangrove habitat. Nematology 14(3): 285–307. https://doi.org/10.1163/156854111X594974

Edward JC, Misra SL, Singh GR (1964) *Longidorus pisi* n. sp. (Nematoda, Dorylaimoidea) associated with the rhizosphere of *Pisum sativum*, from Uttar Pradesh, India. Japanese Journal of Applied Entomology and Zoology 8: 310–312. https://doi.org/10.1303/jjaez.8.310

Esmaeili M, Heydari R, Archidona-Yuste A, Castillo P, Palomares-Rius JE (2017) A new needle nematode, *Longidorus persicus* n. sp. (Nematoda: Longidoridae), from Kermanshah province, western Iran. European Journal of Plant Pathology 147: 27–41. https://doi.org/10.1007/s10658-016-0976-9

Gharibzadeh F, Pourjam E, Pedram M (2018) Description of *Longidorus azarbaijanensis* n. sp. (Dorylaimida: Longidoridae) from Iran Journal of Nematology 50(2): 207–218. https://doi.org/10.21307/jofnem-2018-009

Groza M, Lazarova S, De Luca F, Fanelli E, Elshishka M, Radoslavov G, Hristov P, Coman M, Peneva V (2017) The morphological and molecular identity of *Longidorus piceicola* Lišková, Robbins & Brown, 1997 from Romania (Nematoda, Dorylaimida). ZooKeys 667: 1–19. https://doi.org/10.3897/zookeys.667.12011

Palomares-Rius JE, Cantalapiedra-Navarrete C, Archidona-Yuste A, Subbotin SA, Castillo P (2017) The utility of mtDNA and rDNA for barcoding and phylogeny of plant-parasitic nematodes from Longidoridae (Nematoda, Enoplea). Scientific Reports 7(1): 10905. https://doi.org/10.1038/s41598-017-11085-4

He Y, Subbotin SA, Rubtsova TV, Lamberti F, Brown DJF, Moens M (2005) A molecular phylogenetic approach to Longidoridae (Nematoda: Dorylaimida). Nematology 7: 111–124. https://doi.org/10.1163/1568541054192108

Heyns J, Coomans A (1983) New and known species of *Chronogaster* Cobb, 1913 (Nematoda: Leptolaimidae). Nematologica 29(3): 245–265. https://doi.org/10.1163/187529283X00014

Hooper D (1961) A redescription of *Longidorus elongatus* (de Man, 1876) Thorne & Swanger, 1936, (Nematoda, Dorylaimidae) and descriptions of five new species of *Longidorus* from Great Britain. Nematologica 6: 237–257. https://doi.org/10.1163/187529261X00072

Huelsenbeck JP, Ronquist F (2001) MRBAYES: Bayesian inference of phylogeny. Bioinformatics 17: 754–755. https://doi.org/10.1093/bioinformatics/17.8.754

Krnjaić D, Lamberti F, Krnjaić S, Agostinelli A, Radicci V (2000) Three new longidorids (Nematoda: Dorylaimida) from Montenegro. Nematologia Mediterranea 28: 235–248.

Lamberti F, Agostinelli A, Radicci V (1996) Longidorid nematodes from northern Egypt. Nematologia Mediterranea 24(2): 307–339.

Lamberti F, Choleva B, Agostinelli A (1983) Longidoridae from Bulgaria (Nematoda, Dorylaimida) with description of three new species of *Longidorus* and two new species of *Xiphinema*. Nematologia Mediterranea 11(1): 49–72.

Lamberti F, Coiro MI, Agostinelli A (1991) *Longidorus athesinus* sp.n. (Nematoda: Dorylaimida) From Northern Italy. Nematologia Mediterranea 19: 163–167.

Lamberti F, Iovev T, Choleva B, Brown DJ, Agostinelli A, Radicci V (1997) Morphometric variation and juvenile stages of some longidorid nematodes from Bulgaria with comments on the number of juvenile stages of *Longidorus africanus*, *L. closelongatus* and *Xiphinema santos*. Nematologia Mediterranea 25: 213–237.

Lamberti F, Molinari S, De Luca F, Agostinelli A, Di Vito M (1999) Longidorids (Nematoda: Dorylaimida) from Syria with a description of *Longidorus pauli* sp. n. and *Paralongidorus halepensis* sp. n. with sod isozymes and PCR RLFP profiles. Nematologia Mediterranea 27: 63–78.

Lazarova S, Peneva V, Kumari S (2016) Morphological and molecular characterisation, and phylogenetic position of *X. browni* sp. n., *X. penevi* sp. n. and two known species of *Xiphinema americanum*-group (Nematoda, Longidoridae). ZooKeys 574: 1–42. https://doi.org/10.3897/zookeys.574.8037

Loof PAA, Chen Q (1999) A revised polytomous key for the identification of species of the genus *Longidorus* Micoletzky, 1922. Supplement 1. (Nematoda: Dorylaimida). Nematology 1: 55–59. https://doi.org/10.1163/156854199507974

Marais M, Swart A (2002) Plant nematodes in South Africa. Modimolle area. Limpopo Province. African Plant Protection 8: 25–32.

Micoletzky H (1922) Die freilebenden Erd-Nematoden. Archiv für Naturgeschichte Berlin 89: 1–650.

Navas A, Baldwin JG, Lamberti F (1993) Contributions to the taxonomy status of *Longidorus latocephalus* Lamberti, Choleva & Agostinelli, 1983 and *L. pisi* Edward, Misra & Singh, 1964 (Nematoda: Longidoridae). Nematologia Mediterranea 21: 117–122.

Palomares-Rius JE, Cantalapiedra-Navarrete C, Archidona-Yuste A, Subbotin SA, Castillo P (2017) The utility of mtDNA and rDNA for barcoding and phylogeny of plant-parasitic nematodes from Longidoridae (Nematoda, Enoplea). Scientific Reports 7(1): 10905. https://doi.org/10.1371/journal.pone.0165412

Pedram M, Niknam G, Robbins RT, Ye W, Karegar A (2008) *Longidorus kheirii* n. sp. (Nematoda: Longidoridae) from Iran. Systematic Prasitology 71: 199–211. https://doi.org/10.1007/s11230-008-9148-4

Pedram M, Pourjam E, Palomares-Rius JE, Ghaemi R, Cantalapiedra-Navarrete C, Castillo P (2012) Molecular and morphological characterisation of *Xiphinema granatum* n. sp. and *Longidorus pisi* Edward, Misra & Singh, 1964 (Dorylaimida: Longidoridae) from Iran. Nematology 14: 949–960. https://doi.org/10.1163/156854112X638406

Peneva V, Urek G, Lazarova S, Širca S, Knapič M, Elshishka M, Brown DJF (2012) Longidoridae and nepoviruses in Bulgaria and Slovenia. Helminthologia 49(1): 49–56. https://doi.org/10.2478/s11687-012-0008-z

Peneva VK, Lazarova SS, De Luca F, Brown DJF (2013) Description of *Longidorus cholevae* n. sp. (Nematoda, Dorylaimida) from a riparian habitat in the Rila Mountains, Bulgaria. ZooKeys 330: 1–26. https://doi.org/10.3897/zookeys.330.5750

Robbins RT, Brown DJ, Halbrendt JM, Vrain TC (1995) Compendium of *Longidorus* juvenile stages with observations on *L. pisi*, *L. taniwha* and *L. diadecturus* (Nematoda: Longidoridae). Systematic Parasitology 32(1): 33–52. https://doi.org/10.1007/BF00009466

Roca F (1993) *Longidorus silvae* sp. n. (Nematoda: Longidoridae) from Italy. Nematologia Mediterranea 16: 211–214.

Ronquist F, Teslenko M, van der Mark P, Ayres DL, Darling A, Höhna S, Larget B, Liu L, Suchard MA, Huelsenbeck JP (2012) MrBayes 3.2: efficient Bayesian phylogenetic inference and model choice across a large model space. Systematic Biology 61: 539–542. https://doi.org/10.1093/sysbio/sys029

Sela I, Ashkenazy H, Katoh K, Pupko T (2015) GUIDANCE2: accurate detection of unreliable alignment regions accounting for the uncertainty of multiple parameters. Nucleic Acids Research 43(Web Server issue): 7–14. https://doi.org/10.1093/nar/gkq443

Seinhorst W (1959) A rapid method for the transfer of nematodes from fixitive to anhydrous glycerin. Nematologica 4: 67–69. https://doi.org/10.1163/187529259X00381

Stothard P (2000) The sequence manipulation suite: JavaScript programs for analyzing and formatting protein and DNA sequences. Biotechniques 28: 1102–1104. https://doi.org/10.2144/00286ir01

Tamura K, Stecher G, Peterson D, Filipski A, Kumar S (2013) MEGA6: molecular evolutionary genetics analysis version 6.0. Molecular Biology and Evolution 30(12): 2725–2729. https://doi.org/10.1093/molbev/mst197

Tahseen Q (2012) Nematodes in aquatic environments: adaptations and survival strategies. Biodiversity Journal 3(1): 13–40.

Xu Y, Ye W, Wang J, Zhao Z (2018) Morphological and molecular characterisation of *Longidorus pinus* sp. n. (Nematoda: Longidoridae) from China and a key to known species of *Longidorus* in China. Nematology 20(7): 619–639. https://doi.org/10.1163/15685411-00003165

Van den Berg E, Subbotin SA, Handoo ZA, Tiedt LR (2009) *Hirschmanniella kwazuna* sp. n. from South Africa with notes on a new record of *H. spinicaudata* (Schuurmans Stekhoven, 1944) Luc & Goodey, 1964 (Nematoda: Pratylenchidae) and on the molecular phylogeny of *Hirschmanniella* Luc & Goodey, 1964. Nematology 11(4): 523–540. https://doi.org/10.1163/138855409X12465362560430

ZooKeys 830: 99–109 (2019)
doi: 10.3897/zookeys.830.31974
http://zookeys.pensoft.net

RESEARCH ARTICLE

A peer-reviewed open-access journal
ZooKeys
Launched to accelerate biodiversity research

Cryptopimpla (Hymenoptera, Ichneumonidae, Banchinae) of South Korea, with description of two new species

Gyu-Won Kang[1], Janko Kolarov[2], Jong-Wook Lee[1]

1 *Department of Life Sciences, Yeungnam University, Gyeongsan, South Korea* **2** *Faculty of Pedagogy, University of Plovdiv, 24 Tsar Assen Str., 4000 Plovdiv, Bulgaria*

Corresponding author: *Jong-Wook Lee* (jwlee1@ynu.ac.kr)

Academic editor: *B. Santos* | Received 28 November 2018 | Accepted 9 February 2019 | Published 14 March 2019

http://zoobank.org/839C42E7-B4CC-487A-AFAA-0525DFBC9FAE

Citation: Kang G-W, Kolarov J, Lee J-W (2019) *Cryptopimpla* (Hymenoptera, Ichneumonidae, Banchinae) of South Korea, with description of two new species ZooKeys 830: 99–109. https://doi.org/10.3897/zookeys.830.31974

Abstract

The genus *Cryptopimpla* Taschenberg is recorded for the first time in South Korea. Four species are recognized; among these, two species, *C. aspeculosus* Kang & Lee, **sp. n.** and *C. pentagonalis* Kang & Lee, **sp. n.**, are described as new to science. For the other two species, *C. brevigena* Kuslitzkii and *C. carinifacialis* Sheng, the males were hitherto unknown and are described here. An illustrated identification key is provided for the species of *Cryptopimpla* known from South Korea.

Keywords

Atrophini, Eastern Palearctic, ichneumon wasp, species description, new records, taxonomy

Introduction

Cryptopimpla Taschenberg is a moderately large genus with a worldwide distribution, containing 57 species (Reynolds Berry and van Noort 2016; Yu et al. 2016). Among these, 15 species are from the Eastern Palearctic region. Additionally, the Oriental, and Western Palearctic regions contain 15 species each, only one from the Neotropical region, and eight from the Nearctic region (Yu et al. 2016). Recently, Sheng (2011)

described five new species from China. As a member of the tribe Atrophini, the genus can be distinguished by the following combination of traits: occipital carina joining hypostomal carina; dorsal tooth of mandible longer than ventral tooth; epomia absent; ventral half of mesopleuron weakly convex; forewing with areolet; hindwing vein 1/cu slightly longer than cu-a; ovipositor sheath 0.5–1.0 times as long as hind tibia; ovipositor tip with subapical dorsal notch (Townes 1970). *Cryptopimpla* species are parasitoids of leaf-rolling larvae of Lepidoptera (Yu et al. 2016). Unfortunately, the hosts from the species of *Cryptopimpla* that occur in South Korea remain unknown. This work aims to provide a taxonomic account of the *Cryptopimpla* from South Korea, recording the genus for the first time, and describing two new species to sciences.

Materials and methods

Specimens were collected by sweeping and Malaise traps, and are deposited in the animal systematic laboratory of Yeungnam University (Gyeongsan, South Korea). Morphological terminology follows that of the American Entomological Institute website (http://www.amentinst.org/GIN/morphology.php), wing vein nomenclature is based on Ross (1936). Specimens were examined using an AxioCam MRc5 camera attached to a stereo microscope (Zeiss SteREO Discovery V20; Carl Zeiss, Göttingen, Germany), processed using AxioVision SE64 software (Carl Zeiss), and optimized with a Delta imaging system (i-solution, IMT i-Solution Inc. Vancouver, Canada).

Abbreviations used in this paper are as follows: **CN**, Chungcheongnam-do; **GB**, Gyeongsangbuk-do; **GG**, Gyeonggi-do; **GW**, Gangwon-do; **JB**, Jeollabuk-do; **JN**, Jeollanam-do; **TL**, Type Locality and **TD**, Type depository. Abbreviations for collections are as follows: **MF**, Ministry of Forestry, General Station of Forestry Pest and Management, Shenyang, Lioning, China; **YNU**, Laboratory of Animal Systematics and Taxonomy, Department of Life Sciences, Yeungnam University, Gyeongsan, South Korea and **ZI**: Zoological Institute, Academy of Sciences, St. Petersburg, Russia.

Results

Systematics
Genus *Cryptopimpla* Taschenberg, 1863

Cryptopimpla Taschenberg, 1863: 292. Type species: *Phytodietus blandus* Gravenhorst, 1829
Aphanodon Förster, 1869: 166. Type species: *Phytodietus errabundus* Gravenhorst, 1829
Xenacis Förster, 1869: 167. Type species: *Lissonota caligata* Gravenhorst, 1829
Xenocornia Schmiedeknecht, 1900: 334. Type species: *Xenocornia solitaria* Schmiedeknech, 1900
Harrimaniella Ashmead, 1900: 52. Type species: *Harrimaniella yukakensis* Ashmead, 1900

Key to species of the genus *Cryptopimpla* from South Korea

1 Malar space shorter than 0.3 times basal width of mandible. Tarsal claws simple. Propodeum without pleural and posterior transverse carina (Fig. 2C) .... ***C. brevigena***

– Malar space longer than 0.3 times basal width of mandible. Tarsal claws simple or pectinate. Propodeum with pleural and posterior transverse carina (Fig. 4C) **2**

2 3rs-m vein present only basal, vestigial (Fig. 1E). Antenna with less than 40 flagellomeres ..... ***C. aspeculosus* sp. n.**

– 3rs-m vein complete (Fig. 3E). Antenna with more than 40 flagellomeres... **3**

3 Areolet narrowly petiolate (Fig. 3E). Face with strong median carina on dorsal half. Tergites with yellow apical band (Fig. 3A) ..... ***C. carinifacialis***

– Areolet pentagonal (Fig. 4E). Face without strong median carina on dorsal half. Tergites without yellow apical band (Fig. 4A).... ***C. pentagonalis* sp. n.**

Cryptopimpla aspeculosus Kang & Lee, sp. n.

http://zoobank.org/08018962-545B-40D6-93D6-3F1D13D68D97
Fig. 1

Male. Forewing 7.6 mm (7.6–7.7 mm, n = 2), body 10.3 mm (10.3–10.5 mm, n = 2) long (Fig. 1A).

Head. In dorsal view, 2.3 times as wide as long, and distinctly narrowed behind, densely and coarsely punctate with coriaceous between punctures. Diameter of median ocellus 0.6 times as long as distance between lateral ocellus and compound eye. Flagellum with 38 elongated flagellomeres; 1st flagellomere 3.5 times as long as wide. Occipital carina narrowly curved from above, reaching hypostomal carina above the base of mandible. Face weakly convex medially, 1.7 times as wide as long, densely and rather coarsely punctate, without carina between antennal sockets (Fig. 1B). Clypeus weakly convex; 2.3 times as wide as long, with sparse punctures and blunt fore ridge. Malar space 0.7 times as long as basal width of mandible.

Mesosoma. Coarsely and densely punctate on the coriaceous surface; 1.6 times as long as high. Notaulus long and shallow. Epicnemial carina reaches near the ventral hind margin of pronotum, but does not join it. Propodeum slightly straight in lateral view, with posterior transverse, pleural carinae and weak median longitudinal carina; propodeal spiracle moderately large, oval (Fig. 1C). Legs very slender; hind femur 7.1 times as long as wide; hind inner tibial spur 0.42 times as long as 1st tarsal segment; ratio of hind tarsal segments are 5.2:2.3:1.5:1.0:1.3; all tarsal claws simple. Forewing with incomplete 3rs-m; 2m-cu with a single bulla; 1cu-a vein weakly postfurcal; vein 2-Cu as long as 2cu-a. Hindwing with 8 distal hamuli; vein 1/cu about 1.5 times as long as cu-a (Fig. 1E).

Metasoma. 1st tergite 1.7 times as long as wide, with prominent spiracle at basal 0.45 (Fig. 1D). 2nd tergite square. All tergites finely coriaceous. 4th and apical third of 3rd tergite with sparse punctures.

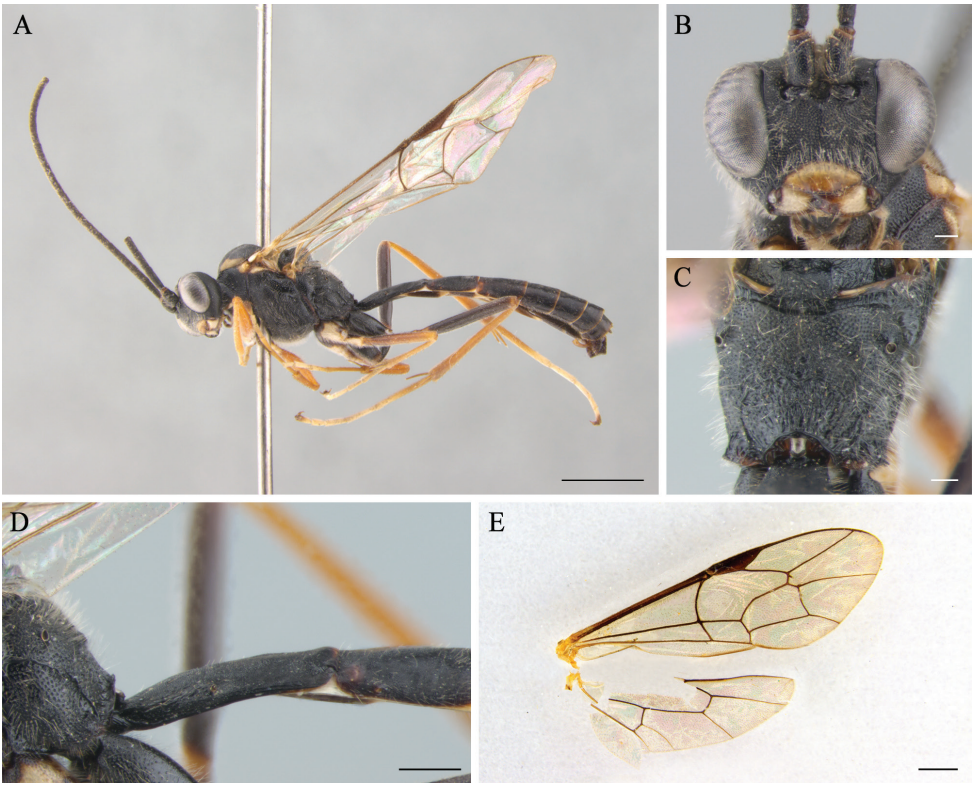

Figure 1. *Cryptopimpla aspeculosus* sp. n. (holotype, male) **A** habitus in lateral view **B** head in frontal view **C** propodeum **D** first tergite in lateral view **E** wings. Scale bars: 2.0 mm (**A**); 0.2 mm (**B, C**); 0.5 mm (**D**); 1.0 mm (**E**).

Color. Body black; basal half of clypeus and mandible, palpi, collar, hind ventral and dorsal angle of pronotum, wide lateral stripe on mesonotum from tegula to mid lobe, tegula, subtegular ridge, fore and mid coxa, fore trochanter from below and hind tarsus, except basal 3/4 of basitarsus and apical half of last tarsal segment yellow; fore and mid femora, tibiae and tarsi reddish, hind tibia and hind basitarsus (except apical 1/4) red; apical half of last tarsal segment of hind leg dark brown.

Female. Unknown.

Specimens examined: Holotype. male, South Korea, Icheon, Mt. Seolbongsan, 1 April 1984, Y.S. Kim (YNU);

Paratype. 1 male, South Korea, GG, Namyangju-si, Bogwangsa, 13 April 1984, J.W. Lee (YNU).

Distribution. South Korea (new record).

Etymology. The name comes from Latin "speculo", *aspeculosus* meaning "without areolet".

Remarks. The species is similar to *C. brevigena*, from which it differs by the presence of pleural and posterior transverse carinae and the entirely black face. Further-

more, the malar space in *C. brevigena* is 0.3 times as long as the basal width of the mandible while in *C. aspeculosus* it is 0.7 times. Additionally, this species is easily separated from other two species (*C. carinifacialis* and *C. pentagonalis*) as follows: the 3rs-m vein in *C. aspeculosus* is only present in the basal part, while in the other two species have a complete 3rs-m vein.

Cryptopimpla brevigena **Kuslitzkii, 2007**
Fig. 2

Cryptopimpla brevigena Kuslitzkii, 2007: 453. Type: ♀, TL: Russia – Primorsky Kray; TD: ZI.

Male. Forewing 7.7 mm (7.4–8.0 mm, n = 42), body 9.5 mm (9.3–9.7 mm, n = 42) long (Fig. 2A).

Head. In dorsal view, 2.0 times as wide as long, narrowed behind, round, densely punctate with coriaceous between punctures. Diameter of median ocellus 0.64 times as long as distance between compound eye and lateral ocellus. Flagellum with 46 (43–48, n = 40) elongated flagellomeres; 1st flagellomere 3.8 times as long as wide. Occipital carina evenly curved from above, meeting hypostomal carina near base of mandible. Face convex medially, 1.7 times as wide as long, densely and coarsely punctate (Fig. 2B). Clypeus strongly convex; 2.5 times as wide as long, with more sparse punctures and blunt fore ridge. Malar space 0.28 times as long as basal width of mandible.

Mesosoma. Moderately coarsely and densely punctate, 1.5 times as long as high. Notaulus short and very shallow. Epicnemial carina ends near middle of epicnemium and does not reach frontal ridge of mesopleuron. Propodeum convex in lateral view, without posterior transverse and pleural carinae (Fig. 2C); propodeal spiracle moderately small, oval. Legs slender; hind femur 6.5 times as long as wide; hind inner tibial spur 0.5 times as long as basitarsus; ratio of hind tarsal segments 4.4:2.2:1.6:1.0:1.1; all tarsal claws simple. Areolet petiolate; 2m-cu with two bullae; 1cu-a vein weakly postfurcal; vein 2-Cu slightly longer than 2cu-a. Hindwing with 9 distal hamuli; vein 1/cu about 1.6 times as long as cu-a, reclivous (Fig. 2E).

Metasoma. 1st tergite 2.2 times as long as wide, with spiracles before its middle (Fig. 2D); lateral carina developed on entire length of tergite. 2nd tergite 1.4 times as long as its apical width. All tergites coriaceous with fine punctures.

Color. Body black. Scape and pedicel from below, a large triangular spot on face centrum, clypeus entirely, mandible except teeth, palpi, hind dorsal corner of pronotum, tegula, subtegular ridge, fore and mid coxa and trochanters, and hind trochanters from below yellow. Fore and mid legs orange yellow, basal hind tibia faint whitish.

Female. Flagellum with 40–44 segments (n=17). Hindwing with 7 distal hamuli.

Specimens examined. South Korea: 1 male, CN, Seosan-si, Haemi-myeon, Daegok-ri, Hanseo Univ., 30 April–9 May 2006; 1 male, CN, Taean-gun, Geunheung-myeon, 18 July 1994, M.J. Shin; 1 female, GB, Uiseong-gun, Danchon-myeon,

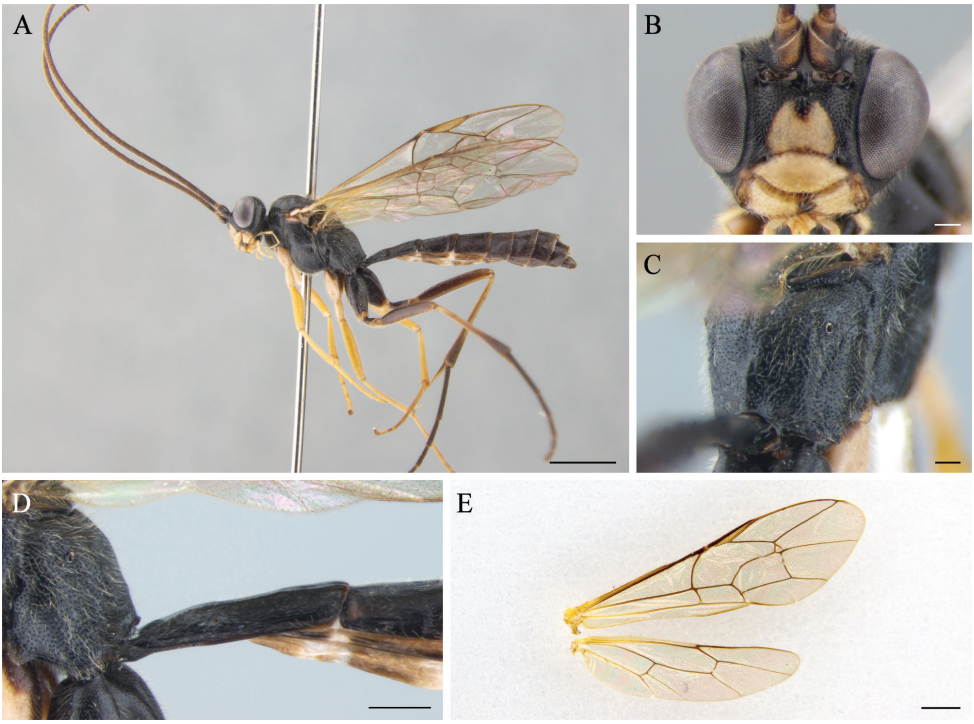

Figure 2. *Cryptopimpla brevigena* (male) **A** habitus in lateral view **B** head in frontal view **C** propodeum **D** first tergite in lateral view **E** wings. Scale bars: 2.0 mm (**A**); 0.2 mm (**B**, **C**); 0.5 mm (**D**); 1.0 mm (**E**).

Sanghwa-ri, 7 May 2016, J.W. Lee; 1 male, GB, Ulleung-gun, Buk-myeon, Naribunji, 27 May 2016, G.H. Ko; 1 male, GB, Yeongju-si, Punggi-eup, Jungnyeong, 12–22 June 2009; 1 female, ditto, 22 June–3 July 2009, C.J. Kim; 1 female, GG, Geumgok, 11 June 1983, H.I. J.; 1 male, GG, Namyangju-si, Choan-myeon, Songchon-ri, Mt. Ungilsan, 27 May–10 June 2009, J.O. Lim; 1 female, GG, Namyangju-si, Sudong-myeon, Mt. Chungnyeongsan, 12 July 1980, J.I. Kim; 1 female, GG, Namyangju-si, Mt. Cheonmasan, 18 June 1983, J.W. Lee; 1 female, GW, Goheung-gun, Yeongam-myeon, Paryeong-ro, Geumsa-ri, Mt. Paryeongsan Forest Resort, 13 April 2012; 3 females, GW, Pyeongchang-gun, Yongpyeong-myeon, Mt. Gyebangsan, 28 June–12 August 2012, J.Y. Park; 1 female, GW, Wonju-si Maeji-ri Yonsei Univ. Campus, 1 August 1999, S.W. Kim, D.W. Kim, and D.Y. Kim; 3 females and 31 males, GW, Wonju-si, Panbu-myeon, Mt. Baegunsan, 25 May–26 July 2012, H.Y. Han; 1 female, JB, Jangsu-gun, Jangsu-eup, Daeseong-ri, San 258-1, Mt. Palgongsan, 17 June–2 July 2015, J.W. Lee; 4 males, JB, Namwon-si, Sanneae-myeon, Dalgung valley (M.T.), 1–9 July 2001, J.W. Lee; 1 female and 1 male, JN, Gwangyang-si, Daap-myeon, Hacheon-ri, San123, Mt. Baegunsan, 17 June–2 July 2015, J.W. Lee; 1 female, Seoul, Gwanak-gu, Mt. Gwanaksan, 19 June 1983, J.H. Han; 1 female, Seoul, Nowon-gu, Mt. Suraksan, 25 May 1997, H.C. Lim; 1 male,

Seoul, Seocho-gu, Wonji-dong, Mt. Cheonggyesan, 4 June 1989, J.W. Lee; 1 female, ditto, 17 June 1998, Y.G. Park.

Distribution. South Korea (new record), Russia (Primorsky Kray, Sakhalin Oblast)

Remarks. This species is recorded for the first time from South Korea. It is easily distinguished from other South Korean species by having simple tarsal claws and the absence of posterior transverse and pleural carinae. The male is newly described from South Korea in this study.

Cryptopimpla carinifacialis **Sheng, 2011**

Fig. 3

Cryptopimpla carinifacialis Sheng, 2011: 32. Type: ♀, TL: China-Jiangxi; TD: MF.

Male. Forewing 7.8 mm, body 9.3 mm long (Fig. 3A).

Head. In dorsal view, 2.0 times as wide as long, narrowed behind roundly, densely and finely punctate, coriaceous between punctures. Diameter of median ocellus 0.9 times as long as distance between lateral ocellus and compound eye. Flagellum with 49 elongated segments; 1st flagellomere 4.0 times as long as wide. Occipital carina complete entirely, reaching hypostomal carina above base of mandible. Inner profile of basal half of flagellum without a strong longitudinal carina (present only in female). Face convex medially, 1.3 times as wide as long, coriaceous and densely punctate, with short, distinct median longitudinal carina just between and below antennal sockets (Fig. 3B). Clypeus 2.4 times as wide as long; sparsely punctured at basal half. Malar space 0.5 times as long as basal width of mandible.

Mesosoma. Densely punctate on the coriaceous surface, 1.5 times as long as high. Notaulus short and very shallow. Epicnemial carina reaches near the ventral hind, not reaching frontal ridge of mesopleuron. Propodeum slightly straight in lateral view, posterior transverse carina weak, more evident in the middle (Fig. 3C); propodeal spiracle moderately large, oval. Legs moderately slender, hind femur 5.6 times as long as wide. Ratio of hind tarsal segments 4.8:2.3:1.6:1.0:1.2. Tarsal claws pectinate. Forewing with complete areolet narrowly petiolate; 2m-cu connects areolet in its outer angle, with two bullae; 1cu-a vein weakly postfurcal; vein 2-Cu slightly longer than 2cu-a. Hindwing with 10 distal hamuli; vein 1/cu about 3.0 times as long as cu-a, weakly reclival (Fig. 3E).

Metasoma. 1st tergite 2.0 times as long as wide, without median dorsal and lateral carinae; spiracle prominent laterally, situated well before mid tergite (Fig. 3D). Anterior three tergites punctured on coriaceous surface, matt; following tergites with fine punctures and shiny.

Color. Body black, with numerous yellow marks; scape and pedicel from below, 11th to 18th flagellomeres, facial orbit, face, clypeus, mandible, malar space, ventral 2/3 of outer eye orbit, palpi, fore margin of pronotum widely and hind dorsal angle, two antero-lateral spots and two spots on mid mesonotum, scutellum except basally and apically,

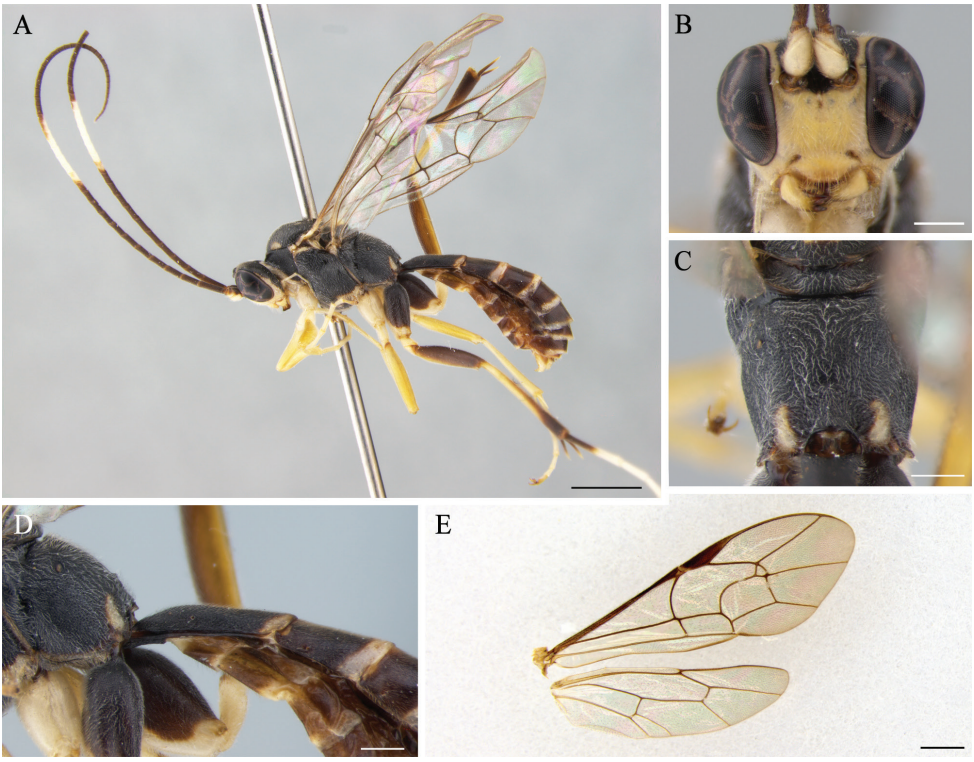

Figure 3. *Cryptopimpla carinifacialis* (male) **A** habitus in lateral view **B** head in frontal view **C** propodeum **D** first tergite in lateral view **E** wings. Scale bars: 2.0 mm (**A**); 0.5 mm (**B,C, D**); 1.0 mm (**E**).

subtegular ridge, a spot on hind low ventral part of mesopleuron above mid coxa to near epicnemial carina, two spots on propodeum apically, fore and mid legs, all trochanters, hind coxa apically, basal half of hind tibia, hind tarsal segments except basal half of 1st one, all tergites apically yellow; hind femur darkened from above, red-yellow from below.

Female. Flagellum with 46 segments. Hindwing with 9 distal hamuli. There is some variation in coloration from the original description: scape and pedicel entirely black; inner eye orbit and ventral half of outer orbit, apical half of clypeus, mandible except basally and teeth yellow; meso – and metapleuron entirely black, but propodeum with two yellow spots apically; apical part of hind basitarsus, and 2nd to 4th tarsal segments entirely yellow; 1st and 2nd tergites with two latero-apical yellow spots.

Specimens examined. South Korea: 1 male, GG, Gapyeong-gun, Sangtan-ri, 14 June 1992, Y.H. Baek; 1 female, GW, Samcheok-si, Hajang-myeon, Mt. Jungbongsan, 19 October 2008, H.S. Lee.

Distribution. South Korea (new record), China (Jiangxi).

Remarks. Only the female of the species has been described to date (Sheng 2011; Sheng et al. 2013). The male is newly described in this study.

Cryptopimpla pentagonalis **Kang & Lee, sp. n.**
http://zoobank.org/68DA02AF-17A7-4DAD-8C5D-112C57EDB8B3
Fig. 4

Female. Forewing 9.3 mm (8.8–9.3 mm, n = 7), body 9.8 mm (9.5–9.8 mm, n = 7), ovipositor sheath 2.6 mm (2.4–2.6 mm, n = 7) long (Fig. 4A).

Head. In dorsal view, 3.4 times as wide as long, narrowed behind distinctly, densely punctate between punctures. Diameter of median ocellus 0.77 times as long as distance between lateral ocellus and compound eye. Flagellum with 42 (in paratypes 41–43, n = 6) elongated segments; 1st flagellomere 5.0 times as long as wide. Occipital carina weakly curved from above, reaching hypostomal carina at base of mandible. Face slightly convex medially, 1.4 times as wide as long, densely and rather coarsely punctate (Fig. 4) without carina between antennal sockets (Fig. 4B). Clypeus convex; 1.8 times as wide as long with sparse punctures and blunt fore ridge. Malar space 0.6 times as long as basal width of mandible.

Mesosoma. Densely and coarsely punctate on the coriaceous surface, 1.6 times as long as high. Notaulus short and very weak. Epicnemial carina reaching near ventral hind margin of pronotum. Propodeum convex in lateral view, with only posterior transverse and pleural carinae; spiracle moderately large, oval (Fig. 4C). Legs slender; hind femur 6.5 times as long as wide; hind inner tibial spur 0.42 times as long as basitarsus; ratio of hind tarsal segments 6.0:2.7:1.8:1.0:1.3; tarsal claws fully pectinate. Forewing with pentagonal areolet; vein 3rs-m distinctly present; 2m-cu with two bullae; 1cu-a vein weakly postfurcal; vein 2-Cu slightly longer than 2cu-a. Hindwing with 9 distal hamuli; vein 1/cu about 2.0 times as long as cu-a, reclivous (Fig. 4E).

Metasoma. 1st tergite 2.5 times as long as wide apically, without median and lateral carinae; spiracle situated before middle (Fig. 4D). 2nd tergite 1.0 times as long as apical width. Ovipositor sheath 0.63 times as long as hind tibia. Ovipositor straight and compressed, with subapical dorsal notch.

Color. Black. Inner face of orbit, ventral part of frontal orbit, spot on top of eye orbit opposite to lateral ocellus, facial orbit, fore ridge of pronotum medially, thin lateral stripe on antero-lateral portion of mesonotum and 2nd to 4th tarsal segments of hind leg yellow. Apical half of clypeus, fore tibia, and tarsus reddish-brown.

Male. Unknown.

Specimens examined. Holotype: South Korea: female, GW, Jeongseon-gun, Gohan-eup, Haiwongil, Mountain condo, 9 July 2010 (YNU).

Paratypes. 2 females, GW, Jeongseon-gun, Gohan-eup, Haiwongil, Mountain condo, 9 July 2010 (YNU); 3 females, GW, Jeongseon-gun, Gohan-eup, Mt. Baegunsan, 9 July 2010 (YNU); 1 female, GW, Wonju-si, Panbu-myeon, Mt. Baegunsan, 25 May–26 July 2012, H.Y. Han (YNU).

Distribution. South Korea (new record).

Etymology. The name comes from Latin "Pentagonum", *pentagonalis* means "pentagon areola".

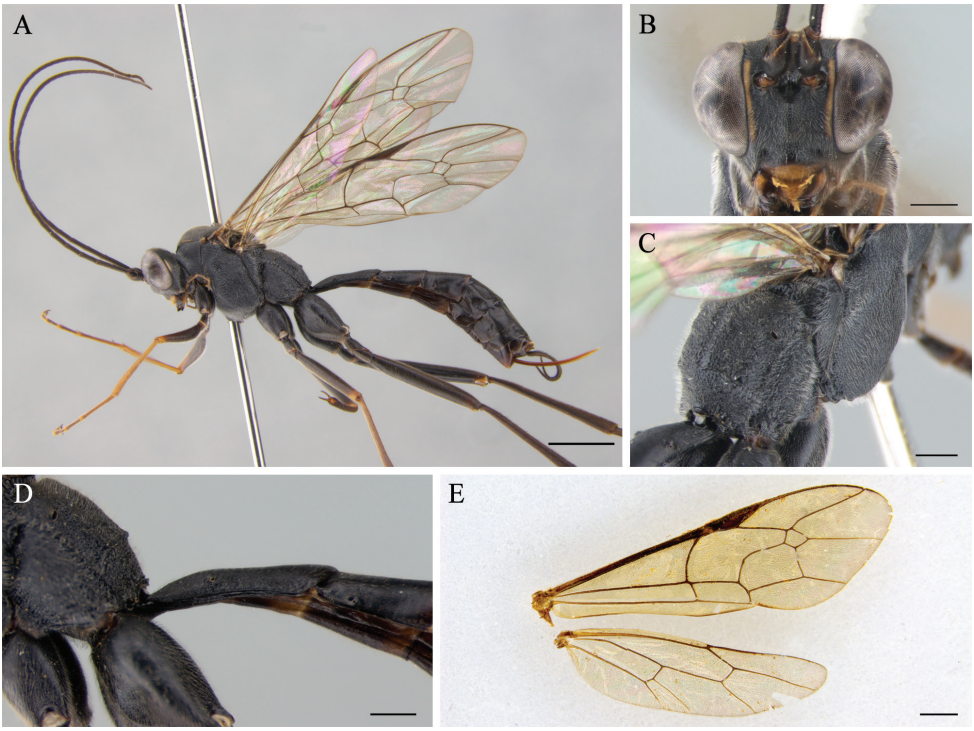

Figure 4. *Cryptopimpla pentagonalis* sp. n. (female) **A** habitus in lateral view (holotype) **B** head in frontal view (holotype) **C** propodeum (holotype) **D** first tergite in lateral view (holotype) **E** wings (paratype). Scale bars: 2.0 mm (**A**); 0.5 mm (**B, C, D**); 1.0 mm (**E**).

Remarks. With the pentagonal areolet, black metasoma, hind coxa and femur, this species is similar to *Cryptopimpla henanensis* Sheng, but differs in the propodeum structure and body coloration; in *C. pentagonalis* the mesosoma is entirely black while in *C. henanensis* it has more yellow spots. The latter species also has more flagellomeres; in *C. henanensis* with 46 segments while in *C. pentagonalis* with an average of 42 segments.

Acknowledgements

We are grateful to the anonymous reviewers for editing this manuscript. This work was supported by a grant from the National Institute of Biological Resources (NIBR), funded by the Ministry of Environment (MOE) of the Republic of Korea (NIBR201801201).

References

Ashmead WH (1900) Classification of the Ichneumon flies, or the superfamily Ichneumonoidea. Proceedings of the United States National Museum 23: 1–220. https://doi.org/10.5479/si.00963801.23-1206.1

Förster A (1869) Synopsis der Familien und Gattungen der Ichneumonen. Verhandlungen des Naturhistorischen Vereins der Preussischen Rheinlande und Westfalens 25: 135–221.

Gravenhorst JLC (1829) Ichneumonologia Europaea. Pars II. Vratislaviae, 989 pp.

Kuslitzky WS (2007) Banchinae. In: Lelej AS (Ed.) Key to the insects of Russia Far East. Vol. IV. Neuropteroidea, Mecoptera, Hymenoptera. Pt 5. Dalnauka, Vladivostok, 433–472. [in Russian]

Reynolds Berry T, van Noort S (2016) Review of Afrotropical *Cryptopimpla* Taschenberg (Hymenoptera, Ichneumonidae, Banchinae), with description of nine new species. ZooKeys 640: 103–137. https://doi.org/10.3897/zookeys.640.10334

Ross HH (1936) The ancestry and wing venation of the Hymenoptera. Annals of the Entomological Society of America 29: 99–111. https://doi.org/10.1093/aesa/29.1.99

Schmiedeknecht O (1900) Die palaarktischen Gattungen und Arten der Ichneumonidentribus der Lissonotinen. Zoologische Jahrbucher Abteilung fur Systematik 13: 299–398.

Sheng ML (2011) Five new species of the genus *Cryptopimpla* Taschenberg (Hymenoptera, Ichneumonidae) with a key to species known from China. ZooKeys 117: 29–49. https://doi.org/10.3897/zookeys.117.1302

Sheng ML, Sun SP, Ding DS, Luo JG (2013) [Ichneumonid fauna of Jianxi (Hymenoptera: Ichneumonidae)]. Science Press, Beijing, 569 pp. [in Chinese with English summary]

Takasuka K, Watanabe K, Konishi K (2011) Genus *Cryptopimpla* Taschenberg new to Sulawesi, Indonesia, with description of a new species (Hymenoptera, Ichneumonidae, Banchinae). Journal of Hymenoptera Research 23: 65–75. https://doi.org/10.3897/jhr.23.1595

Taschenberg EL (1863) Die Schlupfwespenfamilie Pimplariae der deutschen Fauna, mit besonderer Rucksicht auf die Umgegend von Halle. Zeitschrift fur die Gesammten Naturwissenschaften 21: 245–305.

Townes H (1969) The genera of Ichneumonidae, Part 1. Memoirs of the American Entomological Institute 11: 1–300. https://doi.org/10.1007/BF02027741

Townes H (1970) The genera of Ichneumonidae, Part 3. Memoirs of the American Entomological Institute13[1969]: 1–307.

Yu DS, Van Achterberg C, Horstmann K (2016) Taxapad (2016) Ichneumonoidea 2015. Database on flash-drive. Dicky Sick Ki Yu, Ottawa. http://www.taxapad.com [accessed 1 January 2016]

ZooKeys 830: 111–125 (2019)
doi: 10.3897/zookeys.830.31490
http://zookeys.pensoft.net

CHECKLIST

A peer-reviewed open-access journal
ZooKeys
Launched to accelerate biodiversity research

Diversity and conservation of amphibians and reptiles of a protected and heavily disturbed forest of central Mexico

Aníbal H. Díaz de la Vega-Pérez[1], Víctor H. Jiménez-Arcos[2,3], Eric Centenero-Alcalá[4], Fausto R. Méndez-de la Cruz[4], Andre Ngo[5]

1 *Consejo Nacional de Ciencia y Tecnología-Centro Tlaxcala de Biología de la Conducta, Universidad Autónoma de Tlaxcala. Carretera Tlaxcala-Puebla km 1.5, C.P. 90062, Tlaxcala, Mexico* **2** *Laboratorio de Ecología, UBIPRO, FES Iztacala Universidad Nacional Autónoma de México. Av. de los Barrios No. 1, Los Reyes Iztacala, C.P. 54090, Tlalnepantla, Mexico* **3** *Naturam Sequi A.C. 16 de septiembre 43, Ciudad de los niños, C.P. 53450, Naucalpan, Mexico* **4** *Laboratorio de Herpetología, Departamento de Zoología, Instituto de Biología, Universidad Nacional Autónoma de México, Ciudad Universitaria, C.P. 04510, Coyoacán, Ciudad de México, Mexico* **5** *Little Ray's Reptile Zoo, 869 Barton St E, Hamilton, ON L8L 3B4, Canada*

Corresponding author: *Aníbal H. Díaz de la Vega-Pérez* (anibal.helios@gmail.com)

Academic editor: *A. Herrel* | Received 8 November 2018 | Accepted 21 January 2019 | Published 14 March 2019

http://zoobank.org/14295BC3-41A3-408F-B99A-CA748037B703

Citation: Díaz de la Vega-Pérez AH, Jiménez-Arcos VH, Centenero-Alcalá E, Méndez-de la Cruz FR, Ngo A (2019) Diversity and conservation of amphibians and reptiles of a protected and heavily disturbed forest of central Mexico. ZooKeys 830: 111–125. https://doi.org/10.3897/zookeys.830.31490

Abstract

The high loss rate of forest ecosystem by deforestation in the Trans-Mexican Volcanic Belt is one of the principal ecological problems of central Mexico, even in natural protected areas. We compiled a checklist and determined β-diversity indexes of amphibians and reptiles of the highly disturbed protected area, La Malinche National Park (LMNP) in Mexico, to determine the principal habitats for herpetofaunal conservation. After our extensive eight-year field sampling, we documented 28 species (nine amphibians and 19 reptiles), representing 11 families and 18 genera; four of these species are new records for LMNP. Of the species, 89% are endemic to Mexico. The IUCN Red List considers 22 species as Least Concern, one as Near Threatened, and four as Vulnerable. Meanwhile, the Environmental Viability Scores categorize three species as low vulnerability, 15 as medium, and 10 as high. According to the Mexican list of protected species, eight species are under Special Protection and nine are considered Vulnerable. The dissimilarity index between habitat types (βsør) in both groups is high, principally due to the environmental gradient generated by the altitudinal range. *Abies* and Pine forest are high diversity areas for amphibians and rep-

tiles, respectively, and must be considered for special protection. LMNP hosts more than 60% of the herpetofauna of Tlaxcala and is the principal "conservation island" for this state. Therefore, based on the percentage of state species represented, endemism and the current social and ecological problems, additional efforts that involve the local communities to protect the biodiversity of this National Park are necessary.

Keywords

Herpetofauna, natural protected area, high mountain ecosystem, β-diversity

Introduction

Mexico presents the highest richness of amphibians and reptile species in Mesoamerica (Mexico, Belize, Guatemala, El Salvador, Honduras, Nicaragua, Costa Rica, and Panama) not solely due to the sheer size of the country (Wilson and Johnson 2010). The orography of Mexico is one of the factors that contributes to the high biodiversity of these groups of vertebrates. According to Flores-Villela et al. (2010), 131 reptiles and 217 amphibian species inhabit the central mountains of Mexico, including a southern region of the central plain, the Sierra Madre del Sur, and the Trans-Mexican Volcanic Belt (TMVB). The TMVB crosses from the west to the east coast through the center of Mexico, and is formed by many active and inactive volcanoes (Ferrari 2000). This region hosts a high diversity of species, is one of the most important transition zones between two biogeographic regions (Neotropical and Nearctic) and is where the biotas overlap (Morrone 2010). The TMVB holds about 50% of the microendemic amphibian species reported for the whole country (Ochoa-Ochoa et al. 2011). Worryingly, approximately 1% of the original forests of the TMVB disappear every year, and 70% of the natural ecosystems have been transformed into agrosystems and settlements (Toledo et al. 1989, Challenger 1998, Arriaga et al. 2000, Sánchez-Cordero et al. 2005). Within the TMVB lies La Malinche (also called Matlalcuéyatl) which, at 4461 m elevation is the 6th highest peak and the most isolated volcano in Mexico (Fig. 1).

This volcano and the surrounding area were designated La Malinche National Park (LMNP) in 1938. Despite this designation, this protected natural area is still subject to numerous ecological and social problems; nearly 60% of its original vegetation has been removed by local communities for crops and to expand their urban settlements (Villers-Ruiz and López-Blanco 2004). The habitat from 2400 to 2800 m elevation is deteriorated by human activity, such as agriculture, open cattle grazing, farming, fire, and induced grassland (Villers-Ruiz et al. 2006). These human activities are considered the greatest threat to the conservation of biodiversity in high mountain ecosystems, and LMNP is no exception. Because of these activities, this national park presents a high rate of deforestation (20 ha per year) and 77% of the vegetation has deteriorated since it was designated a national park (Díaz-Ojeda 1992, Vargas-Márquez 1997, SEMARNAT 2013). In addition, misinformation and the local beliefs of the people inhabiting the lowlands of LMNP promote the death of many amphibians and reptiles every day.

Previous studies in LMNP have documented 23 reptile and amphibian species (15 and eight species, respectively) in the area. In 1978, Sánchez-de Tagle performed the first herpetofaunal assessment of LMNP, reporting two amphibian species and seven reptile

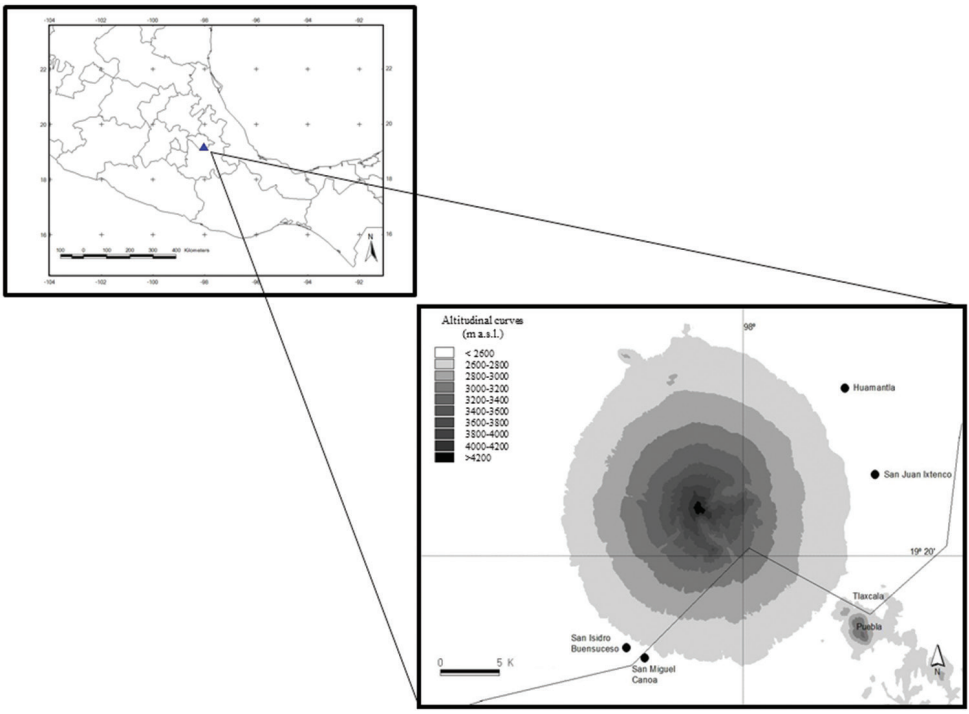

Figure 1. Study area. Geographic delimitation and altitudinal curves of the volcano La Malinche, between the Mexican states of Tlaxcala and Puebla.

species. Two years later, in a study of Tlaxcala´s herpetofauna, Sánchez-Herrera (1980) determined that 12 species occur in LMNP (two amphibians and 10 reptiles) and four additional species in the surrounding areas. Subsequently, Sánchez-Herrera and López-Ortega (1987) added one lizard species (*Aspidoscelis costata*) to the documented herpetofauna of LMNP. This species had been previously misidentified and reported as *Cnemidophorus gularis* by Sánchez-Herrera (1980). Afterwards, Sánchez-Aguilar (2005), based on a year of fieldwork combined with an analysis of the literature, published a further list of herpetofauna for LMNP identifying 21 species: seven amphibians (two without specific identification) and 14 reptiles; five of these species were new records (*Pseudoeurycea bellii* [*Isthmura bellii*], *Eumeces lynxe* [*Plestiodon lynxe*], *Sceloporus megalepidurus*, *S. scalaris* and *Storeria storerioides*). A year later, Gómez-Álvarez and Reyes-Gómez (2006) documented 15 species of herpetofauna (four amphibians and 11 reptiles) from nine years in a single transect, from 2600 to 3500 m elevation on the north-facing slope of LMNP in Tlaxcala. They found three species not previously reported from the area (*Hyla eximia* [*Dryophytes eximius*], *Ambystoma altamiranoi* and *Thamnophis eques*), eight species in common with the first herpetofaunal list of Sánchez-de Tagle (1978) and 12 with that of Sánchez-Aguilar (2005). Nevertheless, *Ambystoma altamiranoi* was a misidentification by Gómez-Álvarez and Reyes-Gómez (2006) and was correctly identified as *A. velasci* by Ramírez-Bautista et al. (2009). Later, Fernández et al. (2006) identified two presumed

new species records for LMNP (*Chiropterotriton* sp. and *Storeria storerioides*); however, these two species had been previously published by Sánchez-Aguilar (2005) (Table 1).

Amphibians and reptiles are ideal bio-indicators of the ecosystem health due to their high sensitivity to environmental change; nevertheless, they are not the most common study groups (Welsh and Droege 2001, Siddig et al. 2016). Additionally, the absence of recent biodiversity studies in natural protected areas, like LMNP, and the high rate of habitat change, necessitate the urgent compilation of information that allows assessment of the status of the herpetofauna of these conservation areas. Therefore, our objective is to provide an analysis of amphibian and reptile species richness and a biodiversity analysis of LMNP, to identify high-diversity areas on which to focus conservation efforts. Moreover, we perform a dissimilarity analysis among habitat types, as an indicator of β-diversity, in order to evaluate the herpetofaunal community. This effort promotes their study and provides a guide to future conservation strategies, by providing accurate information to government agencies.

Materials and methods

Study site

LMNP is found between the Mexican states of Tlaxcala (70%) and Puebla (19.240195N; -98.034472W). It covers an area of 46,112 ha, ranges in elevation from 2400 to 4461 m, and is largest national park in the TMVB (SEMARNAT 2013). LMNP is a high mountain ecosystem, and the climate and the vegetation community changes according to altitude, air temperature, and humidity. Villers-Ruiz et al., 2006 analyzed the vegetation of LMNP according to elevation gradient and proposed that from 2400 to 2800 m elevation, is the most deteriorated habitat, affected by activities such as agriculture, cattle grazing, fire, and induced grassland, presenting a semiarid climate with a temperature between 14 and 16 °C (SEMARNAT 2013). Above that, from 2800 to 3000 m, there are patches of Oak and Pine forest, agriculture, cattle grazed land, and induced grassland, presenting a sub-humid climate with a temperature between 12 and 18 °C. Between 3000 and 4000 m is a semi-cold climate, with temperatures ranging from 5 to 12 °C, where abundant communities of Pine, *Alnus*, and *Abies* forest exist. Above 4000 m, only a few patches of *Juniperus monticola* are present as shrubs and alpine grassland dominates in a cold climate with temperatures ranging from 2 to 5 °C.

Data collection

We generated this list of the amphibians and reptiles of the LMNP from: 1) available herpetofaunal literature: Sánchez-de Tagle (1978), Sánchez-Herrera (1980), Sánchez-Herrera and López-Ortega (1987), Sánchez-Aguilar (2005), Gómez-Álvarez and Reyes-Gómez (2006), Fernández et al. (2006); 2) databases from national scientific collections to which we had access: Colección Herpetológica, Museo de Zoología "Alfonso L. Herrera",

Facultad de Ciencias UNAM (MZFC-UNAM); Colección Nacional de Anfibios y Reptiles, Instituto de Biología UNAM (CNAR); 3) Global Biodiversity Information Facility (GBIF, http://doi.org/10.15468/dl.n4pvrm); and, most importantly; 4) through eight years of fieldwork in LMNP (2010–2018).

We performed an average of seven-field visits per year for five days (four to five people per visit). We included dry and wet seasons all around the volcano slopes and in eight different habitat types (community vegetation and human modification types, see Results section). We made at least one visit to each community vegetation and human modification type each season every year. The sampling was homogeneous among slopes and vegetation types. We used direct capture methods with diurnal and nocturnal searching (nocturnal surveys were less frequent because LMNP is highly insecure). All species previously reported in the literature from field sampling efforts were included in the present list, even if we could not confirm the record by direct observation or by vouchers in a scientific collection. We deposited images of vouchers of new species records in the Instituto de Biología, UNAM (CNAR-IB) scientific collection.

Threatened status of species and β-diversity analysis

We included the conservation status of each species according to: 1) the IUCN Red List 2018; 2) environmental viability scores (EVS) from Wilson et al. (2013a, b); and 3) the Mexican species´ protection list (SEMARNAT, NOM 059-2010). Vegetation type (presence/absence) was identified for all species following Villers-Ruiz et al. (2006). We also include human constructions as a habitat type.

We use the Sørensen dissimilarity index ($\beta_{sør}$) as our approach to determine beta-diversity (Sørensen 1948). The $\beta_{sør}$ quantifies the proportion of species shared between two communities incorporating both true spatial turnover (i.e. taxonomic turnover) and differences in richness by nesting (Koleff et al. 2003, Baselga 2010). We performed the $\beta_{sør}$ analysis for amphibians, reptiles, and both groups together (herpetofauna). To estimate $\beta_{sør}$ we performed a dissimilitude linkage matrix using the software R ver. 3.5.0 (R Development Core Team, 2008) with the 'betapart' package (Baselga and Orme 2012). Because $\beta_{sør}$ is composed of the sum of the component of the net taxonomic turnover (β_{sim}) and the difference between communities by nesting in the species composition (β_{nes}), we present both components in the Suppl. material 1: Tables S1–S6). In addition, we analyzed the proportion of the LMNP´s herpetofauna against that found in the states of Tlaxcala and Puebla, and Mexico as a whole.

Results

Species richness

The herpetofauna of LMNP includes 28 species: nine amphibians (six caudates and three anurans) and 19 reptiles (11 lizards and eight snakes). These taxa represent 11

families (four amphibians and seven reptiles) and 18 genera (seven amphibians and 11 reptiles). All the species of the present list were found in Tlaxcala, and eight of these species were only recorded from this state (one amphibian and seven reptiles) (Table 1).

We added four previously undocumented species from LMNP. Three of these new records, the frog, *Dryophytes plicatus* (CNAR-IB-RF 515-516), the lizard, *Sceloporus spinosus* (CNAR-IB-RF 517-518), and the snake *Salvadora bairdi* (observation), were made by direct capture or observations in the field (Table 1). The fourth new record, the snake *Pituophis deppei*, was not directly observed. However, resident people have seen this species sporadically; moreover, there are precise records of this species in the agricultural fields close to the lowest region of LMNP (~6 km straight line distance, Santa Ana Chiautempan Municipality). Because of this, we included *P. deppei* in the LMNP herpetofaunal list. Additionally, we corroborated the presence of *Conopsis lineata* (CNAR-IB-RF 519-520) that has been recorded with imprecise locality near to LMNP (ENCB, 0.5 km S, 6.5 km E San Francisco Tetlanhocan). There were five species, previously reported from LMNP, that we could not verify through fieldwork, photographs, or in scientific collections. These were the amphibian, *Isthmura bellii*, and the reptiles, *Sceloporus megalepidurus, S. scalaris, Plestiodon lynxe,* and *Thamnophis eques.* Because they were previously documented from LMNP, they are included in our final LMNP herpetofaunal list and included in the analyses where possible.

Threatened status of species

Four of the reptile and amphibian species found in LMNP are considered Vulnerable according to the IUCN Red List (three amphibians and one reptile); one Near Threatened (the salamander *Aquiloeurycea cephalica*); and 23 Least Concern (five amphibians and 18 reptiles) (Table 1). Using Wilson et al.'s (2013a, b) EVS score, three species are considered to have low vulnerability (one amphibian and two reptiles); 15 with medium vulnerability (five amphibians and 10 reptiles); and 10 are highly vulnerable to extinction (three amphibians and seven reptiles) (Table 1). However, according to the Mexican Species Protection List (SEMARNAT 2010), nine species are Threatened (four amphibians and five reptiles), eight are Subject to Special Protection (two amphibians and six reptiles), and 11 are not listed under any protection category (three amphibians and eight reptiles) (Table 1).

β-diversity analysis

We identified eight different habitats (community vegetation and human modification types) occupied by amphibians and reptiles in LMNP: Oak forest (OF), Pine forest (PF), *Abies* forest (AF), Pine-Oak forest (POF), Pine-*Alnus* forest (PAF), Alpine grassland (AG), Human constructions (HC), and Cropland (C). We excluded the AG habitats from amphibian $\beta_{sør}$ analysis, because, no species were recorded at those

Table 1. Checklist of amphibians and reptiles of La Malinche National Park, Mexico. We provide the state presence, habitat type (Cropland = C, Pine-Oak forest = POF, Pine forest = PF, *Abies* forest = AF, Alpine grassland = AG, Oak forest = OF, Human constructions = HC, Pine-*Alnus* forest = PAF), IUCN status (Least Concern = LC, Near Threatened = NT, Vulnerable = V, Endangered = E, Critically Endangered = CE) according to the IUCN Red List, the Environmental Vulnerability Score (The EVS range is broken into the following three categories: low (3–9), medium (10–13), and high vulnerability (14–19) from Wilson et al. (2013a, b), and the conservation status in Mexico (subject to special protection = Pr, Threatened =A, Danger of extinction = P, and Not listed = NL) according to SEMARNAT (NOM 059-2010). Source refers to the origin of the information: 1) Sánchez-de Tagle (1978); 2) Sánchez-Herrera (1980); 3) Sánchez-Herrera and López-Ortega (1987); 4) Sánchez-Aguilar (2005); 5) Fernández et al. (2006); 6) Gómez-Álvarez and Reyes-Gómez (2006); 7) This study.

	State	Habitat type	IUCN status	EVS score	NOM 059 2010	Source
Class Amphibia						
Order Caudata						
Family Ambistomatidae						
*Ambystoma velasci**	P/T	C, HC	LC	10	Pr	6,7
Family Plethodontidae						
*Aquiloeurycea cephalica**	P/T	AF	NT	14	A	4, 7
*Chiropterotriton orculus**	P/T	AF	VU	18	NL	4,5,7
*Isthmura bellii**	T	–	VU	12	A	4
*Pseudoeurycea gadovii**	P/T	AF	VU	13	Pr	1,2,4,7
*Pseudoeurycea leprosa**	P/T	POF, PF, AF, PAF	LC	16	A	1,2,4,6,7
Order Anura						
Family Hylidae						
Dryophytes eximius *	P/T	C, POF, PF, PAF	LC	10	NL	6,7
*Dryophytes plicatus**	P/T	C, PF, HC	LC	11	A	7
Family Scaphiopodidae						
Spea multiplicata	P/T	C, OF, PF, HC, PAF	LC	6	NL	4,6,7
Class Reptilia						
Order Squamata						
Suborder Lacertilia						
Family Anguidae						
*Barisia imbricata**	P/T	C, POF, PF, AF, AG, OF, PAF	LC	14	Pr	1,4,6,7
Family Phrynosomatidae						
*Phrynosoma orbiculare**	P/T	C, POF, PF, AG	LC	12	A	1,4,6,7
*Sceloporus aeneus**	P/T	C, POF, PF, AG, HC, PAF	LC	13	NL	2,4,6,7
*Sceloporus bicanthalis**	P/T	PF, AG, PAF	LC	13	NL	1,4,6,7
Sceloporus grammicus	P/T	C, POF, PF, AF, AG, OF, HC, PAF	LC	9	Pr	1,2,4,6,7
*Sceloporus megalepidurus**	T	C	VU	14	Pr	2,4
*Sceloporus scalaris**	T	AG	LC	12	NL	4,6
*Sceloporus spinosus**	T	C, HC	LC	12	NL	7
Family Scincidae						
*Plestiodon brevirostris**	P/T	C, POF, PF, AF, HC	LC	11	NL	2,4,6,7
*Plestiodon lynxe**	T	–	LC	10	Pr	4
Family Teiidae						
*Aspidoscelis costata**	T	C, OF, HC	LC	11	Pr	2,3,7
Order Squamata						
Suborder Serpentes						
Family Colubridae						
*Conopsis lineata**	P/T	C, POF, PF	LC	13	NL	7
*Pituophis deppei**	P/T	C	LC	14	A	7
*Salvadora bairdi**	T	C	LC	15	Pr	7
Family Natricidae						
*Storeria storerioides**	P/T	C, POF, OF, PF	LC	11	NL	4,5,7
Thamnophis eques	T	C, PF	LC	8	A	6
*Thamnophis scalaris**	P/T	C, POF, PF, AF, AG, OF, HC, PAF	LC	14	A	1,2,4,6,7
Family Viperidae						
*Crotalus ravus**	P/T	C, POF, PF, AG, HC, PAF	LC	14	A	1,2,4,6,7
*Crotalus triseriatus**	P/T	POF, PF, AF, AG, OF, PAF	LC	16	NL	1,2,4,6,7

* endemic of Mexico, – no information.

elevations. The vegetation communities inhabited by the most amphibians were *Abies* forest, Pine forest, and croplands (four species each). While, the most commonly occupied habitats for reptiles were croplands (15 species), Pine forest (13), and Pine-Oak forest (10) (Fig. 2).

The average dissimilarity for amphibians, was 0.60±0.29 (mean ± 1SD). The highest average of taxonomic replacement was recorded in AF (0.86±0.16), where three plethodontid salamander species were found exclusively in this habitat. In contrast, PF had the lowest dissimilarity (0.42±0.23) among habitat types, with no species unique to the habitat (Table 2). The average dissimilarity for reptiles was lower than that for amphibians (0.40±0.13). The highest dissimilarity value for reptiles was in HC (0.47±0.07), and the lowest in POF (0.30±0.11; Table 3). Croplands had the highest number of unique reptile species (3), followed by AG with a single unique species. The average taxonomic turnover for reptiles and amphibians together (herpetofauna) was 0.46±0.13, and the highest and lowest herpetofaunal turnover rates by habitat type (AF and PF respectively) were the same as found for amphibians alone (Table 4).

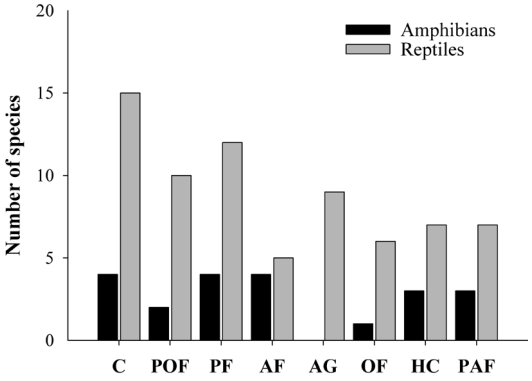

Figure 2. Species richness. Number of amphibian and reptile species by habitat type (Cropland = C, Pine-Oak forest = POF, Pine forest = PF, *Abies* forest = AF, Alpine grassland = AG, Oak forest = OF, Human constructions = HC, Pine-*Alnus* forest = PAF).

Table 2. Sørensen pairwise dissimilarity (β_{sor}) among vegetation types for the amphibians of LMNP. The average β_{sor} for vegetation types and regional β_{sor} values are shown with one standard deviation. Note that the Alpine grassland was excluded because no amphibian species were recorded in this habitat.

Habitat (unique species)	Pine-Oak forest	Pine forest	*Abies* forest	Oak forest	Human constructions	Pine-*Alnus* forest	Cropland
Pine-Oak forest (0)							
Pine forest (0)	0.33						
Abies forest (3)	0.67	0.75					
Oak forest (0)	1.00	0.60	1.00				
Human constructions (0)	1.00	0.43	1.00	0.50			
Pine-*Alnus* forest (0)	0.20	0.14	0.71	0.50	0.67		
Cropland (0)	0.67	0.25	1.00	0.60	0.14	0.43	
Average β_{sor}	0.64 (±0.33)	0.42 (±0.23)	0.86 (±0.16)	0.70 (±0.24)	0.62 (±0.34)	0.44 (±0.24)	0.51 (±0.31)
Regional β_{sor}	0.60 (±0.29)						

Table 3. Sørensen pairwise dissimilarity ($\beta_{sør}$) among vegetation types for the reptiles of LMNP. The average $\beta_{sør}$ for vegetation types and regional $\beta_{sør}$ values are showed with one standard deviation.

Habitat (unique species)	Pine-Oak forest	Pine forest	*Abies* forest	Alpine grassland	Oak forest	Human constructions	Pine-*Alnus* forest	Cropland
Pine-Oak forest (0)								
Pine forest (0)	0.09							
Abies forest (0)	0.33	0.41						
Alpine grassland (1)	0.26	0.24	0.43					
Oak forest (0)	0.38	0.44	0.27	0.47				
Human constructions (0)	0.41	0.47	0.50	0.50	0.54			
Pine-*Alnus* forest (0)	0.38	0.33	0.45	0.20	0.50	0.54		
Cropland (3)	0.28	0.26	0.60	0.50	0.52	0.36	0.62	
Average $\beta_{sør}$	0.30 (±0.11)	0.32 (±0.14)	0.43 (±0.11)	0.37 (±0.13)	0.45 (±0.09)	0.47 (±0.07)	0.43 (±0.14)	0.45 (±0.15)
Regional $\beta_{sør}$	0.40 (±0.13)							

Table 4. Sørensen pairwise dissimilarity ($\beta_{sør}$) among vegetation types for the herpetofauna of LMNP. The average $\beta_{sør}$ for vegetation types and regional $\beta_{sør}$ values are showed with one standard deviation.

Habitat (unique species)	Pine-Oak forest	Pine forest	*Abies* forest	Alpine grassland	Oak forest	Human constructions	Pine-*Alnus* forest	Cropland
Pine-Oak forest (0)								
Pine forest (0)	0.14							
Abies forest (3)	0.43	0.52						
Alpine grassland (1)	0.33	0.36	0.56					
Oak forest (0)	0.47	0.48	0.50	0.50				
Human constructions (0)	0.55	0.46	0.68	0.58	0.53			
Pine-*Alnus* forest (0)	0.33	0.28	0.56	0.33	0.50	0.58		
Cropland (1)	0.35	0.26	0.71	0.57	0.54	0.31	0.57	
Average β_{sim}	0.37 (±0.13)	0.36 (±0.14)	0.56 (±0.10)	0.46 (±0.11)	0.50 (±0.02)	0.53 (±0.12)	0.45 (±0.13)	0.47 (±0.17)
Regional β_{sim}	0.46 (±0.13)							

Discussion

Mexico has 864 species of reptiles and 376 species of amphibians (Flores-Villela and García-Vázquez 2014, Parra-Olea and Flores-Villela 2014). The central mountain region is highly biodiverse and hosts 217 reptiles and131 amphibians; this represents 29% of the Mexican herpetofauna (Flores-Villela et al. 2010). According to our results, 2.3% of the total Mexican herpetofauna and 6.8% of that of the central mountain region is found in LMNP. Most importantly, 89% of the herpetofauna (17 species of reptiles and eight amphibians) in LMNP are endemic to Mexico, and *Pseudoeurycea gadovii* is endemic to this specific volcanic region (Wilson and Johnson 2010). According to Flores-Villela and García-Vázquez (2014), Tlaxcala is the state with the lowest diversity of reptiles in Mexico (31 species), and only 16 amphibian species have been reported in this state (Parra-Olea and Flores-Villela 2014). This

means that LMNP is home to more than 56% and 61% of the amphibian and reptile species, respectively, that have been documented in entire state of Tlaxcala. The state of Puebla is different due to the high diversity of herpetofauna there, combined with a larger overall area and wider diversity of ecosystems than Tlaxcala. For that reason, the reptile and amphibian species inhabiting LMNP represent only 9.3% and 12.5%, respectively, of Puebla's herpetofauna in accordance with the hypotheses of Flores-Villela and García-Vázquez (2014) and Parra-Olea and Flores-Villela (2014). Additionally, it has been proposed by distribution models that *Crotalus intermedius* could inhabit LMNP (Paredes-García et al. 2011), nevertheless this hypothesis has been not corroborated by field work or *in situ* observations, and the nearest records to LMNP are more than 13 km of straight line in a xerophytic scrub habitat (Sánchez-Herrera 1980, Sánchez-Herrera and López-Ortega 1987, Campbell and Lamar 2004).

LMNP plays an important role in Tlaxcala's herpetofaunal preservation. First, this small area (~8.3% of the total length of the state) hosts more than 60% of the herpetofauna known from the entire state. Second, it is the largest protected area in the state (CONANP 2018). Third, it is a refuge for biodiversity because it is an isolated volcano surrounded primarily by croplands, cattle fields, and human constructions (Villers-Ruiz et al. 2006, Castro-Pérez and Tucker 2009). Therefore, we believe that LMNP has to be considered the most important "conservation island" of Tlaxcala. Despite the protected designation of LMNP, 60% of the protected area has been disturbed and the biodiversity is affected by such activities as deforestation, illegal logging, extraction of moss, cattle, induced fire, and agriculture (Díaz-Ojeda 1992, Vargas-Márquez 1997, Villers-Ruiz and López-Blanco 2004, Rojas-García and Villers-Ruíz 2008). All of these activities endanger the permanence of LMNP's herpetofauna. Moreover, global reptile diversity is already imperiled due to the rise of environmental temperature (Sinervo et al. 2010). Warmer temperatures restrict the activities (compromise fitness) of reptiles and could cause species extinction and promote distributional shifts. Montane and viviparous species will be most affected by rising temperature. High elevation taxa with lower thermal requirements may become compromised due to the impossibility of expanding their altitudinal distribution interval to less hot areas. Conversely species of lower elevations may expand their altitudinal distribution to cooler areas (Sinervo et al. 2010).

Analysis of herpetofaunal habitat use provides insight to determine high diversity sites in LMNP that may warrant special attention. *Abies* forest has the highest level of taxonomic replacement in addition to hosting the greatest diversity of plethodontid species (four) in LMNP, highlighting the importance of this forest in future conservation plans. Also, the protection of Pine-Oak forest, Pine forest, and Oak forest communities is very important, due to presented high taxonomic turnovers in the two groups of organisms and in the interaction as herpetofaunal analysis. In addition, these habitats are under degradation and pressure from illegal logging, cattle grazing, and fire. According to Koleff and Soberón (2008), amphibians demonstrate a level of endemism and geographical rarity far higher than other vertebrate groups in Mexico,

followed by reptiles, with both groups showing the highest β-diversity values of terrestrial vertebrates. Similarly, we found the patterns of taxonomic turnover (β-diversity) of amphibians and reptiles in LMNP to be high and mirroring the general patterns of Mexican fauna (see Espinosa et al. 2008, Koleff and Soberón 2008, Morrone 2014). The high taxonomic turnover of these two groups at LMNP, can be explained by the environmental gradient generated by the altitudinal range, more than the size of the area *per se*. Altitudinal and climatic variation shapes the physiological tolerances of the species (Janzen 1967, Koleff and Soberón 2008), which may restrict some herpetofauna to specific biomes, and these dispersal restrictions can result in small distribution areas. These patterns have important implications for the understanding of the structure of the herpetofaunal community, and should be used to inform and improve conservation strategies. Because of the limited distribution of some species in LMNP (e.g. the three salamanders exclusive to *Abies* forest), small areas that do not include all the habitat types might under-represent the species richness of this protected area.

Conclusion

This study evaluates the richness and diversity of both protected and disturbed areas in the highly diverse central Mexico region; it provides valuable information on biodiversity to determine priority areas to consider for future management protection. More than 17% of the species (five) registered in LMNP are listed in the IUCN Red List, and 35% have a high EVS vulnerability score (10); despite this, only 60% of these amphibians and reptiles are protected by Mexican law. Paradoxically, 88% of amphibians and 89% of reptiles inhabiting this heavily disturbed and protected area are endemic to Mexico.

In addition, after three studies focusing on the herpetofauna of LMNP since 1978, we found four species previously unreported from the protected area; but, were unable to find another five species previously reported from there. The absence of vouchers, photos, or precise information makes it difficult to determine if these are legitimate records or if it was a case of misidentification of these five species. The worst-case scenario would be that these are incidents of short-term local extinctions (40 years) in a natural protected area. LMNP was decreed a protected area 80 years ago; nevertheless, the issues mentioned previously still have an impact on the biodiversity and the natural environment. In addition, the lack of security in LMNP limits research activities in the most important "conservation island" in Tlaxcala. Urgent actions to promote protection and preservation of the diversity in LMNP are necessary. We feel that these protective actions must involve the lowland communities, offering options to stop the high exploitation of natural resources and to demystify and promote the ecological importance of these two groups of vertebrates. Also, any policies should preserve the geographical connectedness of protected areas (biological corridors) to increase the possibility of exchange of the different vertebrates and vegetation from area to area.

Acknowledgements

We are grateful to Cátedras CONACyT program (project 883), Volkswagen-Por amor al planeta, project: "Estación Científica La Malinche: Investigación integrativa para la conservación y la Educación Ambiental", and the Mohamed Bin Zayed Conservation Fund (project 162513838) for supporting financially this work. We are grateful to Martínez-Gómez M. and La Malinche Scientific Station for logistical support and to Secretaría de Medio Ambiente y Recursos Naturales for providing the collecting permits (SGPA/DGVS/15396/15 and SEMARNAT FAUT-074). We also thank to García-Vázquez U. and Lemos-Espinal J. for comments that greatly improved the manuscript.

References

Arriaga L, Espinoza JM, Aguilar C, Martínez E, Gómez L, Loa E (2000) Regiones terrestres prioritarias de México. Comisión Nacional para el Conocimiento y uso de la Biodiversidad, México. http://www.conabio.gob.mx/conocimiento/regionalizacion/doctos/Tmapa.html

Baselga A (2010) Partitioning the turnover and nestedness components of beta diversity. Global Ecology and Biogeography 19: 134–143. https://doi.org/10.1111/j.1466-8238.2009.00490.x

Baselga A, Orme CDL (2012) betapart: an R package for the study of beta diversity. Methods in Ecology and Evolution 808–812. https://doi.org/10.1111/j.2041-210X.2012.00224.x

Campbell JA, Lamar WW (2004) The venomous reptiles of the Western Hemisphere. New York. Cornell University, 976 pp.

Castro-Pérez F, Tucker TM (2009) Matlalcuéyetl: Visiones plurales sobre cultura, ambiente y desarrollo. El Colegio de Tlaxcala-CONACYT-Mesoamerican Research Foundation, 355 pp.

Challenger A (1998) Utilización y conservación de los ecosistemas terrestres de México: pasado, presente y futuro CONABIO, Instituto de Ecología, UNAM y Agrupación Sierra Madre S.C., México, 847 pp.

CONANP (2018) Comisión Nacional de Áreas Naturales Protegidas. https://www.gob.mx/conanp/documentos/areas-naturales-protegidas-region-centro-y-eje-neovolcanico?state=published

Díaz-Ojeda EV (1992) Informe del Parque Nacional Malinche. Jefatura del Programa Forestal de Tlaxcala. Oficio 729-03.03.-0040.1, Dirigido al Ing. Jaime González Hernández. 21 de septiembre.

Espinosa D, Ocegueda S, Aguilar C, Flores O, Llorente-Bousquets J, Vázquez B (2008) El conocimiento biogeográfico de las especies y su regionalización natural. In: Capital natural de México, vol. I: Conocimiento actual de la biodiversidad. CONABIO, México, 33–65. http://www.biodiversidad.gob.mx/pais/pdf/CapNatMex/Vol%20I/I01_Elconocimiento-biog.pdf

Fernández J, Sánchez O, Flores-Villela O (2006) New records of amphibians and reptiles from Tlaxcala, México. Acta Zoológica Mexicana 22: 159–162. http://www.scielo.org.mx/scielo.php?script=sci_arttext&pid=S0065-17372006000300015

Ferrari L (2000) Avances en el conocimiento de la Faja Volcánica Transmexicana durante la última década. Boletín de la Sociedad Geológica Mexicana 53: 84–92. http://boletinsgm.igeolcu.unam.mx/bsgm/vols/epoca03/5301/5301-(5)Ferrari.pdf

Flores-Villela O, Canseco-Márquez L, Ochoa-Ochoa LM (2010) Geographic distribution and conservation of the Mexican central highlands herpetofauna. In: Wilson LD, Townsend JH, Johnson JJ (Eds) Conservation of Mesoamerican Amphibians and Reptiles. Eagle Mountain Publications, China, 302–321.

Flores-Villela O, García-Vázquez U (2014) Biodiversidad de reptiles en México. Revista Mexicana de Biodiversidad 85: 467–475. https://doi.org/10.7550/rmb.43236

Gómez-Álvarez G, Reyes-Gómez S (2006) Anfibios y reptiles del Parque Nacional "Malinche", Estado de Tlaxcala. In: Ramírez-Bautista A, Canseco-Márquez L, Mendoza-Quijano F (Eds) Inventarios herpetofaunísticos de México: Avances en el conocimiento de su biodiversidad. Publicaciones de la Sociedad Herpetológica Mexicana, 241–250.

IUCN (2018) The IUCN Red List of Threatened Species. Version 2018-2. http://www.iucnredlist.org

Janzen DH (1967) Why mountain passes are higher in the tropics. The American Naturalist 101: 233–249. https://doi.org/10.1086/282487

Koleff P, Gaston KJ, Lennon JJ (2003) Measuring beta diversity for presence – absence data. Journal of Animal Ecology 72: 367–382. https://doi.org/10.1046/j.1365-2656.2003.00710.x

Koleff P, Soberón J (2008) Patrones de diversidad espacial en grupos selectos de especies. In: Capital natural de México, vol. I: Conocimiento actual de la biodiversidad. CONABIO, México, 323–364. http://www.biodiversidad.gob.mx/pais/pdf/CapNatMex/Vol%20I/I12_Patronesdiv.pdf

Morrone JJ (2010) Fundamental biogeographic patterns across the Mexican Transition Zone: an evolutionary approach. Ecography 33: 355–361. https://doi.org/10.1111/j.1600-0587.2010.06266.x

Morrone JJ (2014) Biogeographical regionalisation of the Neotropical region. Zootaxa 3782: 1–110. https://doi.org/10.11646/zootaxa.3782.1.1

Ochoa-Ochoa LM, Bezaury-Creel JE, Vázquez LB, Flores-Villela O (2011) Choosing the survivors? A GIS-based triage support tool for micro-endemics: application to data for Mexican amphibians. Biological Conservation 144: 2710–2718. https://doi.org/10.1016/j.biocon.2011.07.032

Paredes-García DM, Ramírez-Bautista A, Martínez-Morales MA (2011) Distribución y representatividad de las especies del género *Crotalus* en las áreas naturales protegidas de México. Revista Mexicana de Biodiversidad 82: 689–700. http://www.scielo.org.mx/scielo.php?script=sci_arttext&pid=S1870-34532011000200026

Parra-Olea G, Flores-Villela O, Mendoza-Almerálla (2014) Biodiversidad de anfibios en México. Revista Mexicana de Biodiversidad 85: 460–466. https://doi.org/10.7550/rmb.32027

R Development Core Team (2016) R: A language and environment for statistical computing. Vienna. http://www. R-project. org

Ramírez-Bautista A, Hernández-Salinas U, García-Vázquez UO, Leyte A, Canseco-Márquez L (2009) Herpetofauna del Valle de México, diversidad y conservación. CONABIO, Universidad Autónoma de Hidalgo, México, 213 pp.

Rojas-García F, Villers-Ruíz L (2008) Estimación de la biomasa forestal del Parque Nacional Malinche Tlaxcala-Puebla. Revista de Ciencia Forestal en México 33: 59–86.

Sánchez-Aguilar C (2005) Anfibios y reptiles. In: Fernández-Fernández J, López-Domínguez J (Eds) Biodiversidad del Parque Nacional Malinche, Tlaxcala México. Coordinación General de Ecología Estado de Tlaxcala, México, 101–113.

Sánchez-Cordero V, Illoldi-Rangel P, Linaje M, Sarkar S, Peterson AT (2005) Deforestation and extant distributions of Mexican endemic mammals. Biological Conservation 126: 465–473. https://doi.org/10.1016/j.biocon.2005.06.022

Sánchez-de Tagle (1978) Contribución al conocimiento de la fauna herpetológica del Parque Nacional La Malinche. Bachelor thesis, Mexico City: Universidad Nacional Autónoma de México.

Sánchez-Herrera O (1980) Diagnosis preliminar de la herpetofauna de Tlaxcala, México. Bachelor Thesis, Universidad Nacional Autónoma de México, Mexico City.

Sánchez-Herrera O, López-Ortega G (1987) Noteworthy records of amphibians and reptiles from Tlaxcala, México. Herpetological Review 18: 41.

SEMARNAT [Secretaría de Medio Ambiente y Recursos Naturales] (2010) Norma Oficial Mexicana NOM-059-SEMARNAT-2010, protección ambiental de especies nativas de México de flora y fauna silvestre categorías de riesgo y especificaciones para su inclusión, exclusión, o cambio-Lista de especies en riesgo. Diario Oficial de la Federación (Segunda Sección, 30-dic), 77 pp. http://www.profepa.gob.mx/innovaportal/file/435/1/NOM_059_SEMARNAT_2010.pdf

SEMARNAT [Secretaría de Medio Ambiente y Recursos Naturales] (2013) Acuerdo por el 217 que se da a conocer el Resumen del Programa de Manejo del Parque Nacional 218 La Montaña Malinche o Matlalcuéyatl. Diario Oficial de la Federación (Segunda Sección, 03-abr), 15–43. http://dof.gob.mx/nota_detalle_popup.php?codigo=5294346

Siddig AA, Ellison AM, Ochs A, Villar-Leeman C, Lau MK (2016) How do ecologists select and use indicator species to monitor ecological change? Insights from 14 years of publication in Ecological Indicators. Ecological Indicators 60: 223–230. https://doi.org/10.1016/j.ecolind.2015.06.036

Sinervo B, Mendez de la Cruz F, Miles DB, Heulin B, Bastiaans E, Cruz MVS, Lara Resendiz R, Martinez Mendez N, Calderon Espinosa ML, Meza Lazaro RN, Gadsden H, Avila LJ, Morando M, De la Riva IJ, Sepulveda PV, Rocha CFD, Ibargüengoytía N, Puntriano CA, Massot M, Lepetz V, Oksanen TA, Chapple DG, Bauer AM, Branch WR, Clobert J, Sites JW (2010) Erosion of lizard diversity by climate change and altered thermal niches. Science 328: 894–899. https://doi.org/10.1126/science.1184695

Sørenson T (1948) A method of establishing groups of equal amplitudes in plant sociology based on similarity of species content and its application to analyses of the vegetation on Danish commons. Kongelige Danske Videnskabernes Selskab, Biologiske Skrifter 5: 1–34.

Toledo VM, Carabias J, Toledo C, González-Pacheco C (1989) La producción rural en México: alternativas ecológicas. Fundación Universo Veintiuno, México, 402. http://www.revistas.unam.mx/index.php/pde/article/view/34785/31717

Vargas-Márquez F (1997) Parques Nacionales de México. Aspectos físicos, sociales, legales, administrativos, recreativos, biológicos, culturales, situación actual y propuestas en torno a los parques nacionales de México. SEMARNAP, Instituto Nacional de Ecología, México, 261 pp. http://www.paot.mx/centro/ine-semarnat/anp/AN07.pdf

Villers-Ruiz L, López-Blanco J (2004) Comportamiento del fuego y evaluación de riesgos a incendios en áreas forestales de México: Un estudio en el volcán La Malinche. In: Villers-Ruiz L, López-Blanco J (Eds) Incendios forestales en México: Métodos de evaluación. Centro de Ciencias de la Atmósfera, Universidad Nacional Autónoma México, Consejo Nacional de Ciencia y Tecnología, 60–78.

Villers-Ruiz L, Rojas-García F, Tenorio-Lezama P (2006) Guía botánica del Parque Nacional Malinche, Tlaxcala-Puebla. Centro de Ciencias de la Atmósfera, Instituto de Biología, UNAM, 184 pp.

Welsh Jr HH, Droege S (2001) A case for using plethodontid salamanders for monitoring biodiversity and ecosystem integrity of North American forests. Conservation Biology 15: 558–569. https://www.fs.fed.us/psw/publications/welsh/welsh13.pdf

Wilson LD, Johnson JJ (2010) Distributional patterns of the herpetofauna of Mesoamerica, a biodiversity hotspot. In: Wilson LD, JH Townsend, JJ Johnson (Eds) Conservation of Mesoamerican Amphibians and Reptiles. Eagle Mountain Publications, China, 31–235.

Wilson LD, Johnson JD, Mata-Silva V (2013a) A conservation reassessment of the amphibians of Mexico based on the EVS measure. Amphibian & Reptile Conservation 7: 97–127. http://amphibian-reptile-conservation.org/pdfs/Volume/Vol_7_no_1/Special_Mexico_Issue_ARC_7_1_97-127_e69_high_res.pdf

Wilson LD, Mata-Silva V, Johnson JD (2013b) A conservation reassessment of the reptiles of Mexico based on the EVS measure. Amphibian & Reptile Conservation 7: 1–47. http://amphibian-reptile-conservation.org/pdfs/Volume/Vol_7_no_1/Special_Mexico_Issue_ARC_7_1_1-47_e61_high_res.pdf

Supplementary material 1

Tables S1–S6

Authors: Aníbal H. Díaz de la Vega-Pérez, Víctor H. Jiménez-Arcos, Eric Centenero-Alcalá, Fausto R. Méndez-de la Cruz, Andre Ngo

Data type: measurement

Link: https://doi.org/10.3897/zookeys.830.31490.suppl1

ZooKeys 830: 127–144 (2019)
doi: 10.3897/zookeys.830.30586
http://zookeys.pensoft.net

RESEARCH ARTICLE

A peer-reviewed open-access journal
ZooKeys
Launched to accelerate biodiversity research

Population genetic structure of Marbled Rockfish, *Sebastiscus marmoratus* (Cuvier, 1829), in the northwestern Pacific Ocean

Lu Liu[1], Xiumei Zhang[1,2], Chunhou Li[3], Hui Zhang[4], Takashi Yanagimoto[5], Na Song[1], Tianxiang Gao[6]

1 *The Key Laboratory of Mariculture (Ocean University of China), Ministry of Education, 266071 Qingdao, China* **2** *Laboratory for Marine Fisheries and Aquaculture, Qingdao National Laboratory for Marine Science and Technology, 266072 Qingdao, China* **3** *South China Sea Fisheries Research Institute, Chinese Academy of Fishery Sciences, 510003 Guangzhou, China* **4** *Key Laboratory of Marine Ecology and Environment Sciences, Institute of Oceanology, Chinese Academy of Sciences, 266071 Qingdao, China* **5** *National Research Institute of Fisheries Science, Japan Fisheries Research and Education Agency, 2368648 Yokohama, Japan* **6** *Fisheries College, Zhejiang Ocean University, 316000 Zhoushan, China*

Corresponding author: *Tianxiang Gao* (gaotianxiang0611@163.com)

Academic editor: *M.E. Bichuette* | Received 16 October 2018 | Accepted 2 February 2019 | Published 14 March 2019

http://zoobank.org/11C4F8F6-256F-4C41-A961-A2847CE94D4F

Citation: Liu L, Zhang X, Li C, Zhang H, Yanagimoto T, Song N, Gao T (2019) Population genetic structure of Marbled Rockfish, *Sebastiscus marmoratus* (Cuvier, 1829), in the northwestern Pacific Ocean. ZooKeys 830: 127–144. https://doi.org/10.3897/zookeys.830.30586

Abstract

Sebastiscus marmoratus is an ovoviviparous fish widely distributed in the northwestern Pacific. To examine the gene flow and test larval dispersal strategy of *S. marmoratus* in Chinese and Japanese coastal waters, 421 specimens were collected from 22 localities across its natural distribution. A 458 base-pair fragment of the mitochondrial DNA (mtDNA) control region was sequenced to examine genetic diversity and population structure. One-hundred-six variable sites defined 166 haplotypes. The populations of *S. marmoratus* showed high haplotype diversity with a range from 0.8587 to 0.9996, indicating a high level of intrapopulation genetic diversity. Low non-significant genetic differentiation was estimated among populations except those of Hyogo, Behai, and Niiigata, which showed significant genetic differences from the other populations. The demographic history examined by neutrality tests, mismatch distribution analysis, and Bayesian skyline analysis suggested a sudden population expansion dating to the late Pleistocene. Recent population expansion in the last glacial period, wide dispersal of larvae by coastal currents, and the homogeneity of the environment may have important influences on the population genetic pattern. Knowledge of genetic diversity and genetic structure will be crucial to establish appropriate fishery management of *S. marmoratus*.

Keywords
Genetic diversity, genetic structure, historical population demographics, mtDNA control region, *Sebastiscus marmoratus*

Introduction

The Marbled Rockfish, *Sebastiscus marmoratus* (Cuvier, 1829), valued for its high nutritional value and palatability (Zhu et al. 2011), is widely distributed in the coastal areas of the Northern Pacific Ocean, especially in China, Korea, and Japan (Higuchi and Kato 2002; Jin 2006; Nakabo 2013). In recent years, the number of *S. marmoratus* dramatically decreased due to overfishing, pollution, and habitat destruction , potentially influencing its genetic diversity and population structure.

The mitochondrial DNA (mtDNA) control region has been shown to be particularly effective in detecting population genetic structure and diversity, owing to its high polymorphism, maternal inheritance, high mutation rate, and nonrecombinant DNA (Bowen and Grant 1997; Whitehead et al. 2003; Dowling et al. 2008). Zhang et al. (2016) used mtDNA variation to determine that currents and larva dispersion with drifting seaweed influenced the phylogeographic pattern and genetic homogeneity of *Sebastiscus schlegelii* (Hilgendorf, 1880).

While *S. marmoratus* has been widely studied with respect to taxonomy (Hansen and Karlsbakk 2018), genetics (Deng et al. 2015; Cai et al. 2017; Xu et al. 2017), culture (Yin and Qian 2017; Watanabe et al. 2018), and breeding habitat (Chen et al. 2016; Guo et al. 2016), the genetic structure of its populations along the Chinese and Japanese coasts is not known. In view of the many genetic studies based on mtDNA (Zhao et al. 2017; Liu et al. 2018), we selected mtDNA markers to analyse the population genetics of *S. marmoratus*.

The goals of this study were to estimate genetic diversity, to characterize genetic structure, and to reconstruct the evolutionary relationships of *S. marmoratus* in its distribution range. Failure to characterize population units can lead to overfishing and severe decline (Waples 1998). Elucidation of *S. marmoratus* population genetic structure is crucial for its conservation management. The wide distribution of *S. marmoratus* throughout the NW Pacific, along with its short-distance migration life history, makes it an ideal candidate for investigating how the complex geological history of the Northwestern (NW) Pacific shapes intra-species diversity of the fish fauna.

Materials and methods

Sample collection

From June 2009 to August 2015, we collected 421 wild *S. marmoratus* from 22 locations in coastal China and Japan, 10–24 specimens per site (Fig. 1, Table 1). Muscle tissue samples were preserved in 95% ethanol for subsequent DNA extraction.

Table 1. Sampling information for *S. marmoratus*.

Region	Population	Abbreviation	Number size	Collection date
China coast	Weihai	WH	24	June, 2009
	Rushan	RS	23	June, 2009
	Qingdao	QD	24	July, 2009
	Zhoushan	ZS	24	January, 2015
	Wenzhou	WZ	14	September, 2010
	Xiamen	XM	24	March, 2014
	Shantou	ST	21	August, 2015
	Huizhou	HZ	21	September, 2010
	Guangzhou	GZ	18	September, 2010
	Hainan	HN	14	September, 2010
	Beihai	BH	24	February, 2015
Total			**231**	
Japan coast	Niigata	NI	15	June, 2015
	Ishikawa	IS	10	September, 2012
	Yokosuka	YK	22	November, 2011
	Tottori	TO	24	June, 2015
	Shizuoka	SH	12	September, 2012
	Awaji	AW	15	September, 2012
	Hyogo	HO	24	June, 2015
	Hakata Island	HA	14	November, 2011
	Kochi	KO	23	September, 2012
	Iki Island	IK	21	September, 2012
	Ariake-kai	AR	10	September, 2012
Total			**190**	

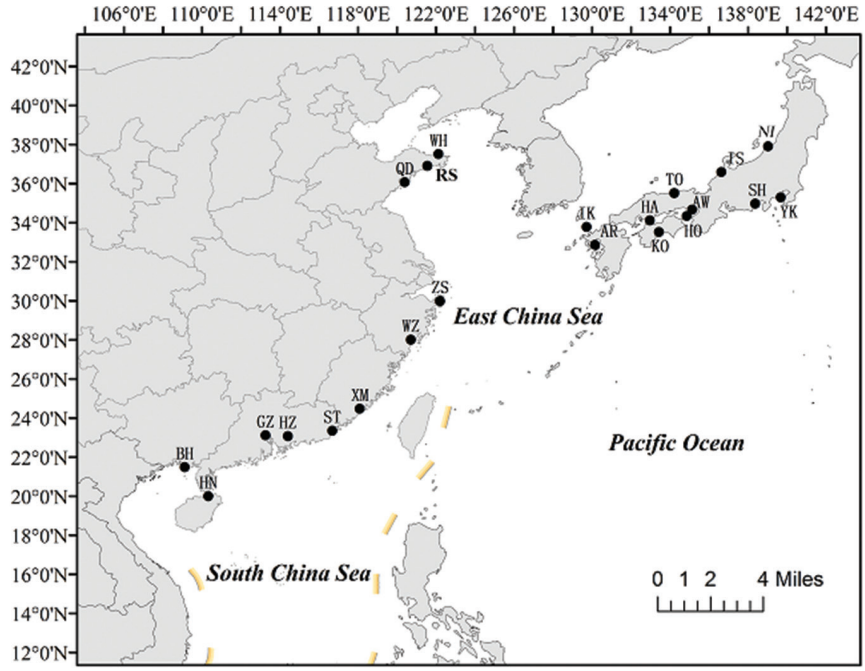

Figure 1. Sampling sites of *S. marmoratus*.

DNA extraction, amplification, and sequencing

Genomic DNA was extracted from muscle tissue by proteinase K digestion followed by a standard phenol-chloroform technique. Fragments of the mtDNA control region were amplified with primers referenced from Han et al. (2008): DL-S (5'-CCC ACC ACT AAC TCC CAA AGC-3'), DL-R (5'-CTG GAA AGA ACG CCC GGC ATG-3').

Polymerase chain reactions (PCR) were carried out in 25 μL of reaction mixture containing 10–100 ng template DNA, 0.1 μL (5 U/μL) Taq DNA polymerase (Takara Co., Dalian, China), 1.5 μL (10 pmol/μL) of each forward and reverse primer, and 2 μL (200 μmol/L) deoxy-ribonucleoside triphosphate (dNTP). The PCR amplification was conducted in a Biometra thermal cycler under the following conditions: 2 min initial denaturation at 95 °C; 40 cycles of 60 s at 94 °C for denaturation, 45 s at 52 °C for annealing, and 60 s at 72 °C for extension; and a final extension at 72 °C for 8 min. The PCR product was purified with a Gel Extraction Mini Kit (Watson BioTechnologies Inc., Shanghai, China). The purified product was used as the template DNA for cycle sequencing reactions performed using BigDye Terminator Cycle Sequencing Kit (v. 2.0, PE Biosystems, Foster City, CA, USA), and bi-directional sequencing was conducted on an Applied Biosystems Instrument Prism 3730 automatic sequencer (Sunny Biotechnology Co. Ltd, Shanghai, China) with both forward and reverse primers. The primers used for sequencing were the same as those used for PCR amplification.

Data analysis

All sequences were edited and aligned manually by DNAStar software (DNAStar Inc., Madison, WI, USA) using default settings and were manually corrected. The genetic diversity indices of *S. marmoratus*, including haplotype diversity (h), nucleotide diversity (π), mean number of pairwise differences (k), and number of polymorphic sites were calculated by ARLEQUIN v. 3.5 (Excoffier and Lischer 2010).

Nucleotide sequence evolution models were evaluated using likelihood-ratio tests implemented by Modeltest v. 3.06 (Posada and Crandall 1998). The neighbor-joining (NJ) tree of the haplotypes was rooted with the out-group *Sebastes schlegelii* (Zhang et al. 2016) using MEGA v.5.0 and evaluated with 1000 bootstrap replicates (Tamura et al. 2011) to reconstruct phylogenies of haplotypes. Among-site heterogeneity was corrected with the shape parameter of gamma distribution ($\gamma = 0.697$). The GenBank accession number of *S. schlegelii* is JX241455. Pairwise genetic divergence among populations were tested by the fixation index Fst (Excoffier et al. 1992), and the significance of the Fst was evaluated by 10,000 permutations for each pairwise comparison in ARLEQUIN v. 3.5 (Excoffier and Lischer 2010). The P values were adjusted by Bonferroni correction (Rice 1989). The Fst and P-value heatmaps with dendrograms were created with the R project 3.5.1 (www.r-project.org).

Characterization of population subdivisions and population structure were conducted using a hierarchical analysis of molecular variance (AMOVA) of different gene

pools (Excoffier et al. 1992). In addition to separate total population into the same gene pool analysis, AMOVA analyses were carried out on populations from the Chinese and Japanese coast; North China coast, South China and South Japan coast; North Yellow Sea, South Yellow Sea, East China Sea, South China Sea, and the Japanese coast. The haplotypes were assessed with 1000 permutations in AMOVA.

The Tajima *D* and Fu's F_S tests were examined for neutrality (Tajima 1989; Fu 1997). Historical demographic expansions were also investigated by examination of the frequency distribution of pairwise differences between sequences (mismatch distribution) based on three parameters: θ_0, θ_1 (θ before and after the population growth), and τ (time since expansion expressed in unit of mutational time) (Rogers and Harpending 1992). Historical pure demographic and range expansions were further investigated by the mismatch distributions using ARLEQUIN v. 3.5 (Excoffier and Lischer 2010). Unimodal distribution patterns reflect recent demographic or range expansion with a high level of migration between neighboring demes, while multimodal patterns indicate relatively stationary populations (Rogers and Harpending 1992; Ray et al. 2003). The sum of square deviations (SSD) and Harpending's raggedness index (HRI) were used to test goodness-of-fit of the observed unimodal mismatch distribution to that expected under the sudden expansion model. The time since population expansion was estimated using the equation $\tau = 2\mu t$, where μ is the mutation rate for the entire DNA sequence under study, and t is the time since expansion. We used the sequence divergence rate of 5%-10%/MY (Brunner et al. 2001) for the control region sequences.

Bayesian skyline analyses, implemented in BEAST v. 1.7.4 (Drummond and Rambaut 2007), were performed to estimate changes in effective population size through time, which can indicate past demographic changes by comparison with current patterns of genetic diversity within a population (Drummond et al. 2005). To check for convergence, we executed multiple independent runs for 300,000,000 iterations under an HKY+I+G nucleotide substitution model and a strict molecular clock, with individual parameters estimated from the data with a piecewise constant skyline model of 10 groups. Genealogies and model parameters were sampled every 10,000 generations with the first 10% discarded as burn-in. Trace plots were inspected to assess mixing, convergence, and stationary distribution of the MCMC process in Tracer v. 1.5 (Rambaut and Drummond 2009). The effective population sizes were checked and confirmed as >200 for each parameter in order to avoid autocorrelation of parameter sampling.

Results

Genetic diversity

A 458 bp segment of the mtDNA control region was amplified, and 106 polymorphic sites were detected, including 89 transitions and 17 transversions. A total of 166 haplotypes were identified based on the sequence variation in 421 individuals from 22 locations. Among these, 84 haplotypes were shared. The most common haplotypes, Hap4

Table 2. Genetic diversity parameters among population of *S. marmoratus* from 22 locations.

Population code	Number of haplotypes	Haplotype diversity (*h*)	Nucleotide diversity (π)	Number of polymorphic sites (*S*)	Mean number of pairwise (*k*) *differences*
WH	23	0.9964±0.0133	0.0235±0.0123	46	10.753±5.072
RS	14	0.9526±0.0252	0.0216±0.0114	38	9.874±4.689
QD	23	0.9964±0.0133	0.0208±0.0110	38	9.532±4.531
ZS	16	0.9601±0.0238	0.0219±0.0116	36	10.024±4.748
WZ	12	0.978±0.0350	0.0167±0.0093	31	7.634±3.789
XM	18	0.9565±0.0311	0.0236±0.01244	42	10.795±5.090
ST	15	0.9524±0.0317	0.0194±0.0100	36	8.090±4.269
HZ	14	0.9524±0.0278	0.0173±0.0093	27	7.884±3.820
GZ	16	0.9804±0.0284	0.0221±0.0118	36	10.111±4.847
HN	13	0.9890±0.0314	0.0110±0.0063	26	9.050±4.435
BH	16	0.9638±0.0208	0.0140±0.0077	32	6.408±3.145
AR	9	0.9778±0.0540	0.0216±0.0122	31	9.878±4.943
IK	15	0.9571±0.0301	0.0239±0.0126	39	10.940±5.184
NI	10	0.9238±0.0530	0.0156±0.0089	30	7.130±3.544
IS	7	0.8667±0.1072	0.0224±0.0126	25	10.251±5.117
TO	19	0.9783±0.0187	0.0224±0.0118	39	10.275±4.859
SH	11	0.9848±0.0403	0.0224±0.0124	28	10.242±5.033
YK	19	0.9740±0.0276	0.0229±0.0121	45	10.471±4.963
KO	14	0.9368±0.0306	0.0251±0.0132	45	11.485±5.404
AW	15	0.9996±0.0243	0.0171±0.0095	26	7.846±3.869
HA	10	0.9560±0.0377	0.0179±0.0099	28	8.209±4.052
HO	7	0.8587±0.0337	0.0098±0.0056	13	4.520±2.304
Total	166	0.956±0.0035	0.022±0.011	106	9.952±4.561

and Hap5, were both shared by 40 individuals. Haplotype sequences were deposited in GenBank under accession numbers KY703229–KY703394.

The estimated nucleotide diversity (π) and haplotype diversity (*h*) for the locations are shown in Table 2. The mean value of π was 0.0220±0.0110 with highest in Kochi (0.0250±0.0132) and the lowest in Hyogo (0.0098±0.0056). The mean value of *h* was 0.9560±0.0035 with the highest in Awaji (0.9996±0.0243) and the lowest in Hyogo (0.8587±0.0337).

Population structure

An unrooted phylogenetic tree was reconstructed by neighbor-joining analysis using 166 haplotypes with the best nucleotide substitution mode (HKY+I+G) rooted with the outgroup *S. schlegelii*. There were no significant genealogical branches or clusters corresponding to sampling localities (Fig. 2). The relationships among 166 haplotypes were represented on the minimum spanning tree (MST). The minimum spanning network was generally star-like with several common and ancestral haplotypes shared by most populations (Fig. 3). The MST was connected and indicated recent population expansion. The Hyogo population showed an obvious haplotype branch and others exhibited no unique haplotype corresponding to geographic populations.

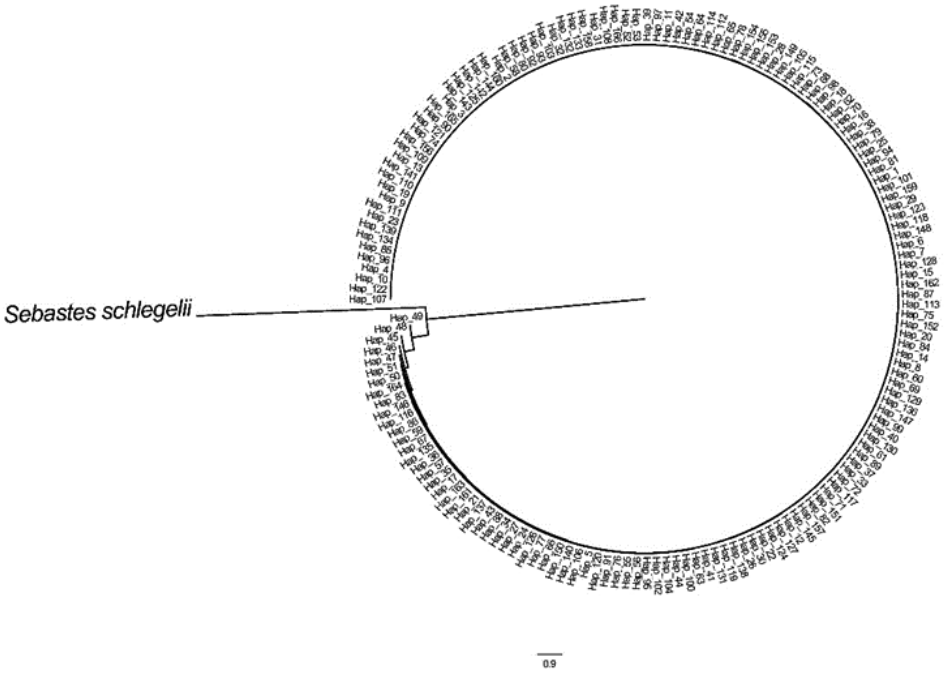

Figure 2. Phylogenetic tree of control region haplotypes constructed using neighbor-joining algorithms of *S. marmoratus* with *S. schlegelii* as outgroup.

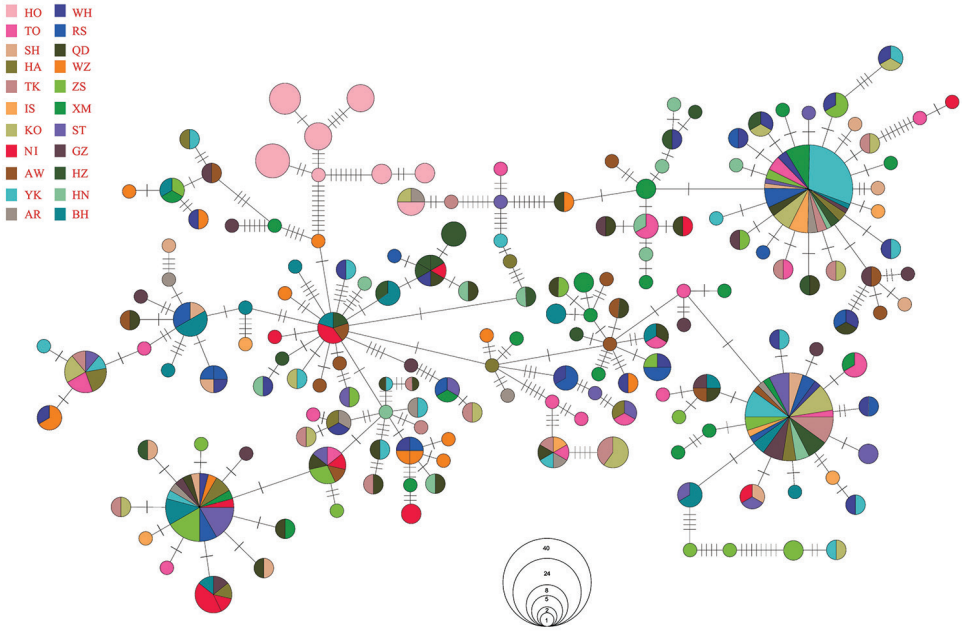

Figure 3. Median-joining network of *S. marmoratus* haplotypes.

Table 3. Pair-wise F_{ST} (below diagonal) sampling locations of *S. marmoratus*.

	BH	GZ	HA	HN	HO	HZ	IK	IS	KO	QD	RS	SH	ST	TO	WH	WZ	XM	NI	YK	ZS	AR	AW
BH																						
GZ	0.034																					
HA	0.006	-0.023																				
HN	0.147*	0.004	0.026																			
HO	0.674*	0.610*	0.657*	0.654*																		
HZ	0.085*	0.018	0.017	-0.001	0.649*																	
IK	0.081*	-0.003	-0.002	-0.001	0.611*	0.035																
IS	0.232*	0.036	0.096	-0.022	0.674*	0.079	0.012															
KO	0.143*	0.021	0.033	-0.022	0.604*	0.044	-0.023	-0.034														
QD	0.057*	-0.016	-0.020	-0.016	0.613*	0.001	0.003	0.028	0.018													
RS	0.054*	-0.014	-0.020	-0.011	0.613*	0.003	-0.005	0.027	0.005	-0.016												
SH	0.019	-0.036	-0.054	-0.007	0.633*	0.011	-0.008	0.037	0.010	-0.033	-0.039											
ST	-0.005	-0.015	-0.030	0.053	0.638*	0.038	0.017	0.107	0.059*	0.004*	0.003	-0.026										
TO	0.084*	-0.009	-0.004	-0.005	0.609*	0.028	-0.017	-0.005	-0.013	-0.012	-0.010	-0.017	0.020									
WH	0.092*	-0.007	0.004	-0.034	0.599*	-0.004	0.007	0.001	-0.003	-0.013	0.026	-0.017	0.027*	-0.009								
WZ	0.041	0.046	-0.018	0.109	0.664*	0.077	0.064*	0.200*	0.109*	0.042*	0.050	0.024	0.036	0.074	0.067							
XM	0.096*	-0.002	0.011	-0.018	0.602*	0.019	0.004	-0.016	-0.001	-0.064	-0.010	-0.012	0.021*	-0.008	-0.020	0.081*						
NI	0.081*	0.066	0.012	0.116	0.677*	0.094	0.100*	0.211*	0.136*	0.051*	0.083	0.042*	0.056	0.110	0.101	0.030	0.103*					
YK	0.034	-0.018	-0.029	0.005	0.608*	0.014	-0.012	0.042	0.007	-0.013	-0.009	-0.022	-0.011	-0.017	-0.012	0.030	-0.002	0.070*				
ZS	0.061*	-0.002	-0.016	0.015	0.610*	0.033	0.015	0.042	0.023	0.009	0.007	-0.016	-0.001	0.009	0.010	0.045	0.004	0.038	-0.010			
AR	0.030	-0.031	-0.060	-0.013	0.650*	0.006	-0.052	0.026	-0.016	-0.038	-0.038	-0.049	-0.020	-0.036	-0.022	0.002	-0.016	0.004	-0.047	-0.023		
AW	0.026	-0.029	-0.019	0.020	0.655*	0.010	0.012	0.074	0.033	-0.012	-0.023	-0.029	-0.070	0.002	-0.012	0.051	-0.010	0.097*	-0.020	0.008	0.029	

Table 4. AMOVA of *S. marmoratus* populations based on mtDNA control region sequences.

Source of variation	Observed partition			
	Variance components	Percentage variation	Φ Statistics	*P*
1. *Complete gene pool (WH, RS, QD, ZS, WZ, XM, ST, HZ, GZ, HN, BH, AR, IK, NI, IS, TO, SH, YK, KO, AW, HA, HO)*				
Among populations	0.6804	13.59	Φ_{ST}=0.1359	0.0000±0.0000
Within populations	4.3268	86.41		
2. *Two gene pools (WH, RS, QD, ZS, WZ, XM, ST, HZ, GZ, HN, BH) (AR, IK, NI, IS, TO, SH, YK, KO, AW, HA, HO)*				
Among groups	0.0224	0.45	Φ_{CT}=0.0045	0.1927±0.0038
Among populations within groups	0.6688	13.33	Φ_{SC}=0.1339	0.0000±0.0000
Within populations	4.3269	86.23	Φ_{ST}=0.1377	0.0000±0.0000
3. *Three gene pools (WH, RS, QD) (ZS, WZ, XM, ST, HZ, GZ, HN, BH) (AR, IK, NI, IS, TO, SH, YK, KO, AW, HA, HO)*				
Among groups	-0.0389	-0.78	Φ_{CT}=-0.0078	0.6663±0.0045
Among populations within groups	0.7059	14.14	Φ_{SC}=0.1403	0.0000±0.0000
Within populations	4.3268	86.64	Φ_{ST}=0.1336	0.0000±0.0000
4. Five gene pools (*WH*) (*RS, QD*) (*ZS, WZ*) (*XM, ST, HZ, GZ, HN, BH*) *(AR, IK, NI, IS, TO, SH, YK, KO, AW, HA, HO)*				
Among groups	-0.1703	-3.43	Φ_{CT}=-0.8840	0.8841±0.0032
Among populations within groups	0.8066	16.25	Φ_{SC}=0.0000	0.0000±0.0000
Within populations	4.3269	87.18	Φ_{ST}=0.0000	0.0000±0.0000

Genetic differentiation among the 22 locations was evaluated based on *F*st values (Table 3, Fig. 5) and AMOVA analyses (Table 4). In general, most of the pairwise *F*st values among populations showed non-significant differences after sequential Bonferroni correction. However, significant genetic differences were obtained among Hyogo, Behai, and Niigata populations and between Hyogo, Behai, and Niigata and the other populations. The largest difference was seen between Niigata and Hyogo (*F*st = 0.677, $P < 0.05$). Some pairwise *F*st estimates were negative, indicating that within-population variation was greater than that between populations. The global AMOVA showed about 13.59% of the genetic variation to be among populations. Other grouping methods also indicated most genetic variation to be within populations, rather than among groups and populations.

Population historical demography

Tajima's *D* (*D* = -1.027; $P > 0.05$) and *F*s test (*F*s = -23.917; $P < 0.01$) results were negative, indicating departure from selective neutrality (Table 5). Non-significant and low values of SSD and HRI were found for each population and for the overall population, suggesting a sudden expansion model. The sudden expansion model of mismatch distribution was unimodal and a valid goodness-of-fit was observed between observed and expected distributions (Fig. 4), indicating strong demographic expansion. The τ value, which reflects the location of the mismatch distribution crest, provides a rough estimate of the time of initiation of rapid population expansion. According to $t = \tau/2\mu$, based on τ values (τ = 12.305) and divergence rate of 5–10% per site per Myr (Brunner et al. 2001), the pure population expansion occurred 268,000–448,000 years ago. The ratio of estimated effective female population size after expansion to that before expansion (θ_1/θ_0) was 56.84 (Table 4). Results indicated that *S. marmoratus* underwent

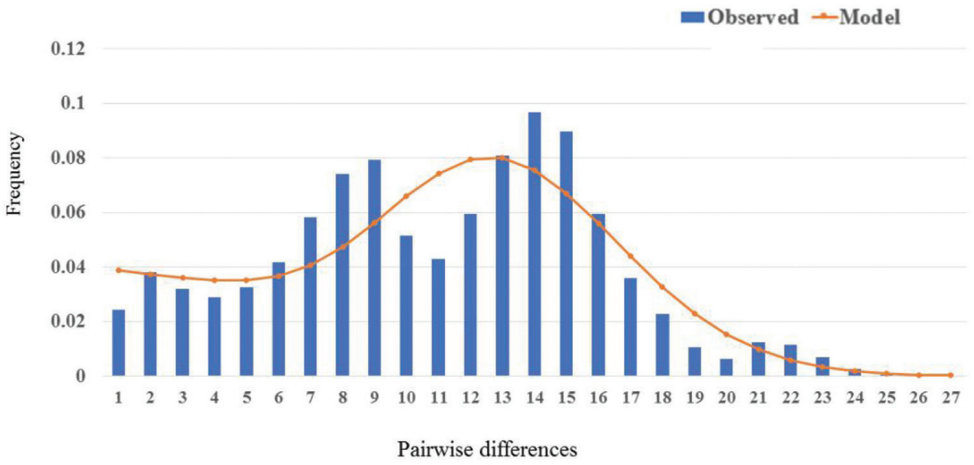

Figure 4. The observed pairwise difference (bars) and the expected mismatch distributions under the sudden-expansion model (solid line) of mtDNA control region haplotypes in *S. marmoratus*.

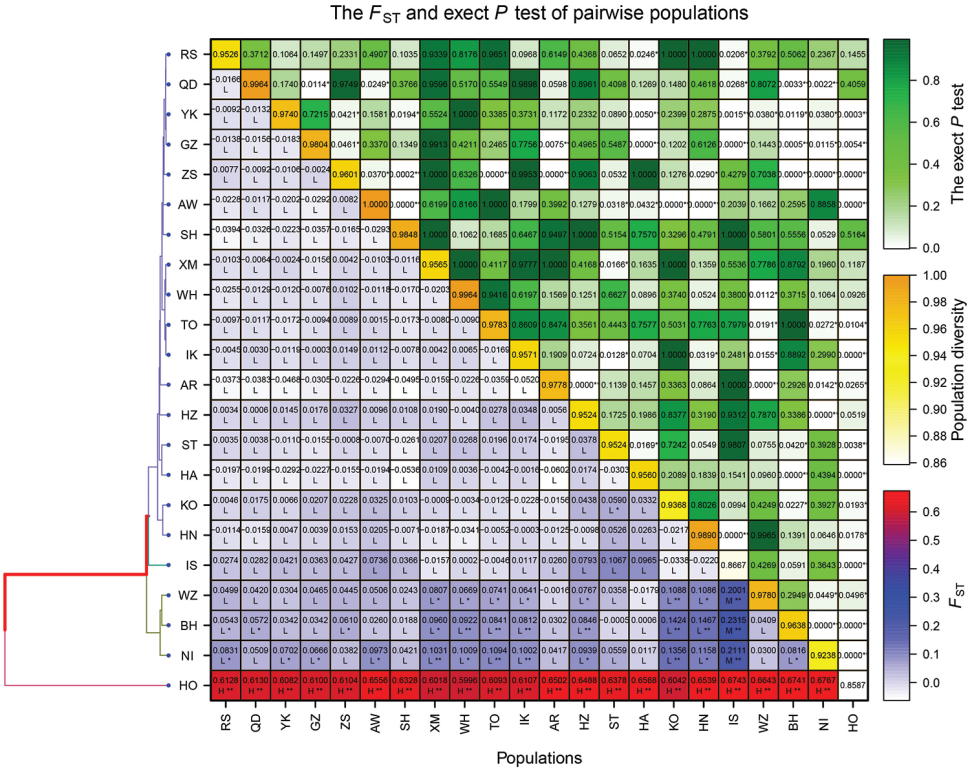

Figure 5. The heatmap of F_{st} genetic distances based on mtDNA control sequences of populations.

Table 5. Tajima's *D* and Fu's F_S, corresponding *P*-value, and mismatch distribution parameter estimates for each population of *S. marmoratus*.

Population	Tajima's *D*		Fu's *Fs*		Mismatch distribution				
	D	*P*	*Fs*	*P*	τ (95% CI)	θ_0	θ_1	*SSD*	*HRI*
BH	-1.089	0.149	-4.828	0.031	6.709 (4.043,10.332)	0.002	26.364	0.009ns	0.480ns
GZ	-0.291	0.442	-5.588	0.016	12.738 (5.533, 16.066)	0.000	48.730	0.018ns	0.027ns
HA	-0.508	0.333	-1.114	0.271	8.049(4.088,10.371)	0.009	66.982	0.058ns	0.124ns
HN	0.177	0.615	-4.933	0.015	12.803(5.627,19.664)	0.002	23.016	0.020ns	0.039ns
HO	0.878	0.832	1.688	0.782	5.467(0.803,10.469)	0.967	9.946	0.032ns	0.069ns
HZ	-0.034	0.542	-2.647	0.120	13.922(0.000,85.547)	0.000	13.865	0.011ns	0.016ns
IK	-0.224	0.450	-2.256	0.173	12.078(7.684,14.979)	0.000	99.219	0.023ns	0.051ns
IS	0.363	0.694	0.757	0.628	14.285(6.186,20.066)	0.005	29.102	0.046ns	0.084ns
KO	-0.405	0.372	-0.645	0.402	13.199(8.232,17.143)	0.000	83.906	0.032ns	0.060ns
QD	-0.457	0.351	-14.813	0.000	11.434(4.629,16.014)	0.139	29.270	0.016ns	0.022ns
RS	-0.404	0.369	-1.192	0.314	13.385(4.031,18.676)	0.002	23.507	0.034ns	0.035ns
SH	0.118	0.592	-3.022	0.050	8.398(1.467,91.398)	4.888	38.945	0.046ns	0.050ns
ST	-0.659	0.297	-3.169	0.092	6.348(1.977,22.352)	4.104	31.631	0.034ns	0.036ns
TO	-0.215	0.474	-5.824	0.025	11.219(5.793,13.742)	0.014	54.141	0.003ns	0.007ns
WH	-0.721	0.246	-13.615	0.000	13.646(5.686,18.615)	0.004	27.832	0.012ns	0.011ns
WZ	-1.115	0.133	-3.865	0.030	9.010(4.488,12.814)	0.021	24.199	0.010ns	0.030ns
XM	-0.417	0.384	-4.241	0.063	14.230(7.807,18.992)	0.000	33.264	0.025ns	0.026ns
NI	-1.142	0.116	-1.163	0.259	3.281(0.191,19.438)	4.706	18.687	0.028ns	0.064ns
YK	-0.743	0.242	-7.208	0.006	7.867(4.506,16.061)	3.841	90.938	0.018ns	0.023ns
ZS	-0.109	0.527	-2.516	0.174	13.576(5.086,18.025)	0.000	25.162	0.012ns	0.013ns
AR	-0.742	0.240	1.813	0.137	12.568(6.381,16.771)	0.004	47.383	0.029ns	0.061ns
AW	-0.151	0.478	-9.125	0.001	2.242(0.559,13.279)	7.604	99999	0.009ns	0.014ns
Pooled	-1.027	0.133	-23.917	0.005	12.305(8.693,15.988)	0.434	24.668	0.004ns	0.005ns

τ, time of initiation of population expansion, θ_0 and θ_1 are θ parameter before and after expansion, *SSD* and *HRI* are sum of squared deviations and raggedness index, respectively. $P > 0.05$

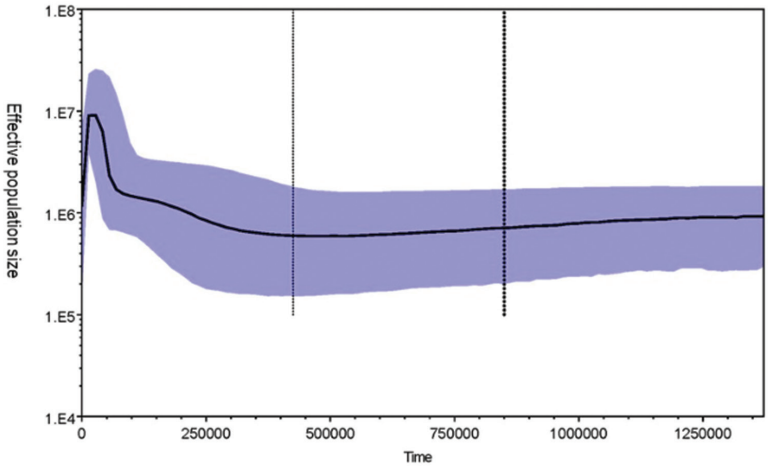

Figure 6. Bayesian skyline plot showing the effective female *S. marmoratus* population size through time. Black solid lines are median estimates of NeT (Ne=effective female population size; T=generation time); blue shading represents the 95% confidence interval of NeT. The y-axis was plotted on a logarithmic scale.

colonization and recent population expansion events along the Chinese and Japanese coasts during the Pleistocene.

The Bayesian skyline plot (Fig. 6) indicated an historic occurrence of a continual gradual increase in the effective size of *S. marmoratus* populations, dating to about 430,000 years BP at the end of the Pleistocene. These results are consistent with a process of historical expansion of *S. marmoratus* populations, as indicated by negative *D* and *F*s values and mismatch distributions.

Discussion

Inbreeding depression and other genetic problems impacted by human behavior can be monitored by assessing genetic diversity under natural conditions (Ryman 1991; Smith et al. 1991). The adaption of marine organisms to their surroundings and their evolutionary potential can be affected by genetic diversity (Templeton 2010). We found that, despite high haplotype diversity ($h = 0.9560 \pm 0.0035$) of *S. marmoratus* in the northwestern Pacific Ocean, its nucleotide diversity was low ($\pi = 0.0220 \pm 0.0110$). The high mutation rate of the D-loop region may be a factor in this phenomenon (Wan et al. 2004). Haplotype diversity with low nucleotide diversity may indicate population reduction or the existence of a genetic bottleneck and may result in extinction under environmental pressure. It can be observed in a population experiencing rapid expansion from a low effective population size, assuming adequate time for the increase in haplotypes through mutation but inadequate time for accumulation of large sequence differences (Lowe et al. 2004). The retention of new mutations in the population can be enhanced by rapid population growth (Grant and Bowen 1998). The phenomenon of high haplotype diversity and low nucleotide diversity has been reported in organisms such as *Glyptocephalus stelleri* (Xiao et al. 2010), *Trachurus japonicus* (Song et al. 2013) and *Circus spilonotus* (Nagai et al. 2018) that have undergone a rapid severe population reduction.

Compared with anadromous and freshwater fishes, marine species are generally expected to show a low degree of genetic differences among geographic regions owing to their high dispersal potential through planktonic drifting of eggs, larvae, or adults and the absence of physical barriers (Palumbi 1994; Hewitt 2000; Liu et al. 2018). Our AMOVA results and the neighbor-joining analysis did not show significant genetic structure among geographic populations. Ecological characteristics and marine currents may play important roles in shaping the contemporary phylogeographic pattern of marine fishes. For example, the rockfish *S. schlegelii* is typical of fish that congregate in drifting seaweed during early development (Ikehara 1977; Safran and Omori 1990; Zhang et al. 2016). *Sebastiscus marmoratus*, a species of rockfish with life history similar to *S. schlegelii*, is believed to exhibit the same behavior, dispersing with drifting seaweed during November and December and in the following year from February to April (Mitchell and Hunter 1970; Wu et al. 1999). The Kuroshio Current is one of the strongest currents in the world and can accelerate gene flow from the southern East China Sea to the coastal waters of Japan (Liu et al. 2007). Inflows from the Yellow Sea enter the Bohai Sea along the west coast of Korea via the Yellow Sea warm current and

the China Coastal Current (Jin et al. 2010). Waters also exchange between the warm Yellow Sea and Kuroshio currents. These strong currents might transport *S. marmoratus* larvae via drifting seaweed and promote exchange throughout its range.

Recent research reveals that the currently most common unintentional pathway for the transport of marine organisms is the ballast water of commercial vessels (Ruiz and Hines 1997; Wonham et al. 2000). As human activity becomes more frequent and extensive, trade between countries is strengthened, and commercial vessels traverse large area. Ballast water is usually taken from the harbor in one port and subsequently discharged in another port (Carlton and Geller 1993). Diverse organisms including protist, diatoms, invertebrate larvae, and copepods are collected and survive the voyage to the next port (Carlton 1985; Smith et al. 1999). Corrosion or other damage to protective grates or ballasting of water by gravitation, may provide access to the ballast for larger organisms such as post-larval fish (Springer and Gomom 1975; Wonham et al. 2000). Hansen and Karlsbakk (2018) reported *S. marmoratus* caught by bait in Norwegian waters and thus shown to be actively foraging, a strong indication that *S. marmoratus* may thrive in unfamiliar conditions.

We may conclude that transportation via ballast water may be a source of genetic homogeneity of *S. marmoratus*. It has been transported among ports and wharves along the NW Pacific Ocean and into rocky coastal areas with the release of ballast water, where it can easily survive (Hansen and Karlsbakk 2018). With adaptation to the same or similar environment, a number of invasive populations of *S. marmoratus* have been reported (Wonham et al. 2000). It is also possible that environmental factors such as salinity and temperature have brought about adaptive evolution of *S. marmoratus*. However, this is undetectable by the molecular markers we used in this study. It has been suggested that a genotyping-by-sequencing technique could reveal the occurrence of local adaptation (Xu et al. 2017).

Using genetics to understand biogeography is important to determine patterns influencing distribution of geographically distant populations. Genetic diversity, genetic distribution patterns, and effective population size were also influenced by paleogeological changes and fluctuations as well as life history and marine environment factors (Hewitt 1996). Following sea level falls in the glacial period (Wang 1999; Lambeck et al. 2002), *S. marmoratus* may have experienced a population contraction with the loss of genes of those dying out and the majority of survivors migrating to more suitable environments. A single branch from the star-like network representing the Hyogo population suggests a likely founder effect (Ramachandran et al. 2005).

Significant genetic differences were revealed between Hyogo and other populations based on the star-like network tree and *F*st value analysis, which suggests that the deep and semi-open area of inland waters might have an impact on the geographic isolation. Genetic differences among Hyogo, Behai, and Niigata populations and between Hyogo, Behai, and Niigata and the other populations were primarily significant, and possibly relate to convergence evolution (Wilkens and Strecker 2003) and the formation of a refuge (Consuegra et al. 2002). In addition, mutation-drift disequilibrium may exist among these populations, which are in an unstable state of genetic mutation-drift (Lacy 1987). Further molecular marker studies are required to evaluate this proposition.

Conclusions

Climate fluctuations caused by glacial-interglacial alternation, early life-history, and ecological characteristics, combined with transport via ballast water may play important roles in the extensive gene flow among populations and the current genetic distribution pattern of *S. marmoratus*. Information provided by the current study will facilitate its comprehensive management. Future studies should be based on informative nuclear markers to provide additional information on genetic structure and differentiation of populations of *S. marmoratus*.

Acknowledgments

This work was supported by the National Natural Science Foundation of China (grant numbers 41776171, 41176117, 31172447) and Fund of Key Laboratory of South China Sea Fishery Resources Exploitation & Utilization, Ministry of Agriculture and Rural Affairs, P. R. China (grant numbers FREU2018-04). The authors are very grateful to Dr Linlin Zhao, Dr Zhiqiang Han, Mr Yanping Wang, and Mr Long Yan forsample collection. The authors are also very grateful to Mr Wei Zhou and Dr Jiaguang Xiao for helping with data analysis.

References

Bowen BW, Grant WS (1997) Phylogeography of the sardines (*Sardinops* spp.): assessing biogeographic models and population histories in temperate upwelling zones. Evolution 51: 1601–1610. https://doi.org/10.1111/j.1558-5646.1997.tb01483.x

Brunner PC, Douglas MR, Osinov A, Wilson C, Bernatchez L (2001) Holarctic phylogeography of arctic charr (*Salvelinus alpinus* L.) inferred from mitochondrial DNA sequences. Evolution 55: 573–586. https://doi.org/10.1554/0014-3820(2001)055[0573:HPOACS]2.0.CO;2

Cai SS, Xu SY, Liu L, Gao TX, Zhou YD (2017) Development of genome-wide SNPs for population genetics and population assignment of *Sebastiscus marmoratus*. Conservation Genetic Resources. https://doi.org/10.1007/s12686-017-0868-0

Carlton JT, Geller JB (1993) Ecological roulette: the global transport of nonindigenous marine organisms. Science 261: 78–82. https://doi.org/10.1126/science.261.5117.78

Carlton JT (1985) Transoceanic and interoceanic dispersal of coastal marine organisms: the biology of ballast. Oceanography and Marine Biology Annual Review 23: 313–371.

Chen Y, Chen R, Mo ZP (2016) The effects of Cd and Pb on the levels of Hepatic HSPs mRNA in *Sebastiscus marmoratus*. Asian Journal of Ecotoxicology 11: 124–130. [In Chinese]

Consuegra S, García de Leániz C, Serdio A, González Morales M, Straus LG, Knox D, Verspoor E (2002) Mitochondrial DNA variation in Pleistocene and modern Atlantic salmon from the Iberian glacial refugium. Molecular Ecology 11: 2037–2048. https://doi.org/10.1046/j.1365-294X.2002.01592.x

Deng HW, Li ZB, Dai G, Yuan Y, Ning YF, Shangguan JB, Huang YS (2015) Isolation of new polymorphic microsatellite markers from the marbled rockfish *Sebastiscus marmoratus*. Genetic and Molecular Resources 14: 758–762. https://doi.org/10.4238/2015.January.30.19

Dowling DK, Friberg U, Lindell J (2008) Evolutionary implications of non-neutral mitochondrial genetic variation. Trends in Ecology and Evolution 23: 546–554. https://doi.org/10.1016/j.tree.2008.05.011

Drummond AJ, Rambaut A, Shapiro B, Pybus OG (2005) Bayesian coalescent inference of past population dynamics from molecular sequences. Molecular Biology and Evolution 22: 1185–92. https://doi.org/10.1093/molbev/msi103

Drummond AJ, Rambaut A (2007) BEAST: Bayesian evolutionary analysis by sampling trees. BMC evolutionary biology 7: 214. https://doi.org/10.1186/1471-2148-7-214

Excoffier L, Lischer HEL (2010) Arlequin suite ver. 3.5: a new series of programs to perform population genetics analyses under Linux and Windows. Molecular Ecology Resources 10: 564–567. https://doi.org/10.1111/j.1755-0998.2010.02847.x

Excoffier L, Smouse PE, Quattro JM (1992) Analysis of molecular variance inferred from metric distances among DNA haplotypes: application to human mitochondrial DNA restriction data. Genetics 131: 479–491.

Fu YX (1997) Statistical tests of neutrality of mutations against population growth, hitchhiking and background selection. Genetics 147: 915–925.

Grant WAS, Bowen BW (1998) Shallow population histories in deep evolutionary lineages of marine fishes: insights from sardines and anchovies and lessons for conservation. Journal of Heredity 89: 415–426. https://doi.org/10.1093/jhered/89.5.415

Guo CY, Lin SZ, Gong JH, Qiu CG, Zhao C, Xu SL (2016) Composition and variation of amino acid and fatty acid in fertilized eggs and larvae of *Sebastiscus marmoratus* in different developmental stages. Oceanologia Limnologia Sinica 47: 173–181. [in Chinese]

Han ZQ, Gao TX, Yanagimoto T, Yasunori S (2008) Genetic population structure of *Nibea albiflora* in Yellow Sea and East China Sea. Fisheries Science 74: 544–552. https://doi.org/10.1111/j.1444-2906.2008.01557.x

Han ZQ, Yanagimoto T, Zhang YP, Gao TX (2012) Phylogeography study of *Ammodytes personatus* in Northwestern Pacific: Pleistocene isolation, temperature and current conducted secondary contact. Plos One 7: e37425. https://doi.org/10.1371/journal.pone.0037425

Hansen H, Karlsbakk E (2018) Pacific false kelpfish, *Sebastiscus marmoratus* (Cuvier, 1829) (Scorpaeniformes, Sebastidae) found in Norwegian waters. Bioinvasions Records 7: 73–78. https://doi.org/10.3391/bir.2018.7.1.11

Hewitt GM (1996) Some genetic consequences of ice ages, and their role in divergence and speciation. Biological Journal of the Linnean Society 58: 247–276. https://doi.org/10.1111/j.1095-8312.1996.tb01434.x

Hewitt GM (2000) The genetic legacy of the Quaternary ice ages. Nature 405: 907. https://doi.org/10.1038/35016000

Higuchi M, Kato K (2002) Sequence variability in the mitochondrial DNA control region of five *Sebastes* species. Fisheries Science 68: 643–650. https://doi.org/10.1046/j.1444-2906.2002.00472.x

Ikehara K (1977) Studies on the fish eggs and larvae accompanied with drifting sea weeds in the Sado Strait and its vicinity. Bulletin of the Japan Sea Regional Fisheries Research Laboratory 28: 17–28.

Jin B, Wang G, Liu Y, Zhang R (2010) Interaction between the East China Sea Kuroshio and the Ryukyu Current as revealed by the self-organizing map. Journal of Geophysical Research-Oceans 115: C12047. https://doi.org/10.1029/2010JC006437

Jin XB (2006) Fauna Sincia: Ostichthyes, Scorpaeniformes. Beijing, China. Science Press [In Chinese]

Kong LF, Li Q (2009) Genetic evidence for the existence of cryptic species in an endangered clam *Coelomactra antiquata*. Marine Biology 156: 1507–1515. https://doi.org/10.1007/s00227-009-1190-5

Lacy RC (1987) Loss of genetic diversity from managed populations: interacting effects of drift, mutation, immigration, selection, and population subdivision. Conservation Biology 1: 143–158. https://doi.org/10.1111/j.1523-1739.1987.tb00023.x

Lambeck K, Esat TM, Potter EK (2002) Links between climate and sea levels for the past three million years. Nature 419: 199–206. https://doi.org/10.1038/nature01089

Liu JX, Gao TX, Wu SF, Zhang YP (2007) Pleistocene isolation in the Northwestern Pacific marginal seas and limited dispersal in a marine fish, *Chelon haematocheilus* (Temminck & Schlegel, 1845). Molecular Ecology 16: 275–288. https://doi.org/10.1111/j.1365-294X.2006.03140.x

Liu L, Liu LQ, Gao TX, Song N (2018) Phylogeographic pattern of *Liza affinis* populations in Chinese coastal waters: estimation of larval dispersal potential. Mitochondrial DNA Part A. https://doi.org/10.1080/24701394.2018.1444038

Lowe A, Harris S, Ashton P (2004) Ecological genetics: design, analysis, and application. Oxford, United Kingdom, Blackwell Science Ltd., 432pp.

Mitchell CT, Hunter JR (1970) Fishes associated with drifting kelp, *Macrocystis pyrifera*, off the coast of southern California and northern Baja California Calif Fish Game 56: 288–297.

Nagai K, Takahashi Y, Yamazaki S, Azuma A (2018) Analysis of the genetic diversity and structure of the Eastern Marsh Harrier in Japan using mitochondrial DNA. Journal of Ornithology 159: 73–78. https://doi.org/10.1007/s10336-017-1480-5

Nakabo T (2013) Fishes of Japan with pictorial keys to the species, 3nd ed. Kanagawa-ken, Japan. Tokai University Press [In Japanese]

Palumbi SR (1994) Genetic divergence, reproductive isolation, and marine speciation. Annual Review of Ecology Systematics 25: 547–572. https://doi.org/10.1146/annurev.es.25.110194.002555

Posada D, Crandall KA (1998) Modeltest: testing the model of DNA substitution. Bioinformatics (Oxford, England), 14: 817–818. https://doi.org/10.1093/bioinformatics/14.9.817

Ramachandran S, Deshpande O, Roseman CC, Rosenberg NA, Feldman MW, Cavalli-Sforza LL (2005) Support from the relationship of genetic and geographic distance in human populations for a serial founder effect originating in Africa. Proceedings of the National Academy of Sciences of the United States of America 102: 15942–15947. https://doi.org/10.1073/pnas.0507611102

Rambaut A, Drummond AJ (2009) Tracer: MCMC trace analysis tool, version 1.5. University of Oxford, Oxford.

Ray N, Currat M, Excoffier L (2003) Intra-deme molecular diversity in spatially expanding populations. Molecular Biology and Evolution 20: 76–86. https://doi.org/10.1093/molbev/msg009

Rice WR (1989) Analyzing tables of statistical tests. Evolution 43: 223–225. https://doi.org/10.1111/j.1558-5646.1989.tb04220.x

Rogers AR, Harpending H (1992) Population growth makes waves in the distribution of pairwise genetic differences. Molecular Biology and Evolution 9: 552–569.

Ruiz GM, Hines AH (1997) The risk of nonindigenous species invasion in Prince William Sound associated with oil tanker traffic and ballast water management: pilot study. Regional Citizens' Advisory Council of Prince William Sound, Valdez, Alaska.

Ryman N (1991) Conservation genetics considerations in fishery management. Journal of Fish Biology 39: 211–224. https://doi.org/10.1111/j.1095-8649.1991.tb05085.x

Safran P, Omori M (1990) Some ecological observations on fishes associated with drifting seaweed off Tohoku coast, Japan. Marine Biology 105: 395–402. https://doi.org/10.1007/BF01316310

Shen KN, Jamandre BW, Hsu CC, Tzeng WN, Durand JD (2011) Plio-Pleistocene sea level and temperature fluctuations in the northwestern Pacific promoted speciation in the globally-distributed flathead mullet *Mugil cephalus*. BMC Evolution Biology11: 83. https://doi.org/10.1186/1471-2148-11-83

Smith LD, Wonham MJ, Mcann LD, Ruiz GM (1999) Invasion pressure to a ballast-flooded estuary and an assessment of inoculant survival. Biological Invasions 1: 67–87. https://doi.org/10.1023/A:1010094527218

Smith PJ, Francis R, McVeagh M (1991) Loss of genetic diversity due to fishing pressure. Fisheries Research 10: 309–316. https://doi.org/10.1016/0165-7836(91)90082-Q

Song N, Jia N, Yanagimoto T, Lin L, Gao TX (2013) Genetic differentiation of *Trachurus japonicus* from the Northwestern Pacific based on the mitochondrial DNA control region. Mitochondrial DNA 24: 705–712. https://doi.org/10.3109/19401736.2013.773982

Springer VG, Gomon MF (1975) Revision of the blenniid fish genus *Omobranchus*, with descriptions of three new species and notes on other species of the tribe Omobranchini. Smithsonian Contributions to Zoology 112: 1–36. https://doi.org/10.5479/si.00810282.177

Tajima F (1989) Statistical method for testing the neutral mutation hypothesis by DNA polymorphism. Genetics 123: 585–595.

Tamura K, Peterson D, Peterson N, Stecher G, Nei M, Kumar (2011) MEGA5: molecular evolutionary genetic analysis using maximum likelihood, evolutionary distance, and maximum parsimony methods. Molecular Biology and Evolution 28: 2731–2739. https://doi.org/10.1093/molbev/msr121

Templeton AR (2010) Introduction to Conservation Genetics. Cambridge University Press.

Wan QH, Wu H, Fujihara T, Fang SG (2004) Which genetic marker for which conservation genetics issue? Electrophoresis 25: 2165–2176. https://doi.org/10.1002/elps.200305922

Wang P (1999) Response of Western Pacific marginal seas to glacial cycles: paleoceanographic and sedimentological features. Marine Geology 56: 5–39. https://doi.org/10.1016/S0025-3227(98)00172-8

Waples RS (1998) Separating the wheat from the chaff: patterns of genetic differentiation in high gene flow species. Journal of Heredity 89: 438–450. https://doi.org/10.1093/jhered/89.5.438

Watanabe M, Kakizaki H, Tsukamoto T, Fujiwara M, Fukusima H, Ueda M, Masumiya M (2018) Distribution of chitinolytic enzyme in the organs and molecular cloning of a novel chitinase gene from the kidney of marbled rockfish *Sebastiscus marmoratus*. Bioscience Biotechnology and Biochemistry 201: 68–78.

Whitehead A, Anderson SL, Kuivila KM, Roach JL, May B (2003) Genetic variation among interconnected populations of *Catostomus occidentalis*: implications for distinguishing impacts of contaminants from biogeographical structuring. Molecular Ecology 12: 2817–2833. https://doi.org/10.1046/j.1365-294X.2003.01933.x

Wilkens H, Strecker U (2003) Convergent evolution of the cavefish *Astyanax* (Characidae, Teleostei): genetic evidence from reduced eye-size and pigmentation. Biological Journal of Linnean Society 80: 545–554. https://doi.org/10.1111/j.1095-8312.2003.00230.x

Wonham MJ, Carlton JT, Ruiz GM, Smith LD (2000) Fish and ships: relating dispersal frequency to success in biological invasions. Marine Biology 136: 1111–1121. https://doi.org/10.1007/s002270000303

Wu CW, Wang WH, Li CD (1999) Preliminary study on the development of *Sebastiscus marmoratus* sex gland, embryo and fry. Journal of Zhejiang Ocean University (Natural Science) 18: 310–314. [in Chinese]

Xiao YS, Gao TX, Zhang Y, Yanagimoto T (2010) Demographic history and population structure of blackfin flounder (*Glyptocephalus stelleri*) in Japan revealed by mitochondrial control region sequences. Biochemical Genetics 48: 402–417. https://doi.org/10.1007/s10528-009-9321-8

Xu SY, Song N, Zhao LL, Cai SS, Han ZQ, Gao TX (2017) Genomic evidence for local adaptation in the ovoviviparous marine fish *Sebastiscus marmoratus* with a background of population homogeneity. Scientific Report 7: 1562. https://doi.org/10.1038/s41598-017-01742-z

Yin F, Qian D (2017) Transcriptomic analysis reveals the key immune-related signalling pathways of *Sebastiscus marmoratus* in response to infection with the parasitic ciliate *Cryptocaryon irritans*. Parasite Vector 10: 576. https://doi.org/10.1186/s13071-017-2508-7

Zhang H, Yanagimoto T, Zhang XM, Song N, Gao TX (2016) Lack of population genetic differentiation of a marine ovoviviparous fish *Sebastes schlegelii* in Northwestern Pacific. Mitochondrial DNA Part A 27: 1748–1754.

Zhao LL, Yi D, Li CH, Sun DR, Xu HX, Gao TX (2017) Phylogeography and population structure of *Johnius grypotus* (Richardson, 1846) as revealed by mitochondrial control region sequences. Zookeys 705: 143–158. https://doi.org/10.3897/zookeys.705.13001

Zhu AY, Xie JY, Jiang LH, Lou B (2011) The nutritional composition and evaluation in muscle of *Sebastiscus marmoratus*. Acta Nutrimenta Sinica 33: 621–623. [in Chinese]